



**29th World Congress on Ultrasound
in Obstetrics and Gynecology**
12-16 October 2019, Berlin, Germany

Certificate of fetal brain imaging

Suggested reading

1. Chaoui R, Nicolaidis KH. Detecting open spina bifida at the 11-13-week scan by assessing intracranial translucency and the posterior brain region: mid-sagittal or axial plane? *Ultrasound Obstet Gynecol.* 2011 Dec;38(6):609-12. doi:10.1002/uog.10128. PubMed PMID: 22411445.
2. Lerman-Sagie T, Prayer D, Stöcklein S, Malinge G. Fetal cerebellar disorders. *Handb Clin Neurol.* 2018;155:3-23. doi:10.1016/B978-0-444-64189-2.00001-9. Review: PubMed PMID: 29891067.
3. Choudhri AF, Cohen HL, Siddiqui A, Pande V, Blitz AM. Twenty-Five Diagnoses on Midline Images of the Brain: From Fetus to Child to Adult. *Radiographics.* 2018 Jan-Feb;38(1):218-235. doi:10.1148/rg.2018170019. Review. PubMed PMID: 29320328.
4. Davila I, Moscardo I, Yopez M, Sanz Cortes M. Contemporary Modalities to Image the Fetal Brain. *Clin Obstet Gynecol.* 2017 Sep;60(3):656-667. doi:10.1097/GRF.0000000000000307. PubMed PMID: 28742597.
5. Jakab A, Pogledic I, Schwartz E, Gruber G, Mitter C, Brugger PC, Langs G, Schöpf V, Kasprian G, Prayer D. Fetal Cerebral Magnetic Resonance Imaging Beyond Morphology. *Semin Ultrasound CT MR.* 2015 Dec;36(6):465-75. doi:10.1053/j.sult.2015.06.003. Epub 2015 Jun 14. Review. PubMed PMID: 26614130.

Sonographic examination of the fetal central nervous system: guidelines for performing the ‘basic examination’ and the ‘fetal neurosonogram’

INTRODUCTION

Central nervous system (CNS) malformations are some of the most common of all congenital abnormalities. Neural tube defects are the most frequent CNS malformations and amount to about 1–2 cases per 1000 births. The incidence of intracranial abnormalities with an intact neural tube is uncertain as probably most of these escape detection at birth and only become manifest in later life. Long-term follow-up studies suggest however that the incidence may be as high as one in 100 births¹.

Ultrasound has been used for nearly 30 years as the main modality to help diagnose fetal CNS anomalies. The scope of these guidelines is to review the technical aspects of an optimized approach to the evaluation of the fetal brain in surveys of fetal anatomy, that will be referred to in this document as a *basic examination*. Detailed evaluation of the fetal CNS (*fetal neurosonogram*) is also possible but requires specific expertise and sophisticated ultrasound machines. This type of examination, at times complemented by three-dimensional ultrasound, is indicated in pregnancies at increased risk of CNS anomalies.

In recent years fetal magnetic resonance imaging (MRI) has emerged as a promising new technique that may add important information in selected cases and mainly after 20–22 weeks^{2,3}, although its advantage over ultrasound remains debated^{4,5}.

GENERAL CONSIDERATIONS

Gestational age

The appearance of the brain and spine changes throughout gestation. To avoid diagnostic errors, it is important to be familiar with normal CNS appearances at different gestational ages. Most efforts to diagnose neural anomalies are focused around midgestation. Basic examinations are usually performed around 20 weeks’ gestation.

Some abnormalities may be visible in the first and early second trimesters^{6–11}. Even though these may represent a minority they usually are severe and deserve therefore special consideration. It is true that early examination requires special skills, however, it is always worthwhile to pay attention to the fetal head and the brain at earlier ages. The advantage of an early fetal neuroscan at 14–16 weeks is that the bones are thin and the brain may be evaluated from almost all angles.

Usually, a satisfying evaluation of the fetal CNS can always be obtained in the second and third trimesters of pregnancy. In late gestation, visualization of the intracranial structures is frequently hampered by the ossification of the calvarium

Technical factors

Ultrasound transducers

High frequency ultrasound transducers increase spatial resolution but decrease the penetration of the sound beam. The choice of the optimal transducer and operating frequency is influenced by a number of factors including maternal habitus, fetal position and the approach used. Most basic examinations are satisfactorily performed with 3–5-MHz transabdominal transducers. Fetal neurosonography frequently requires transvaginal examinations that are usually conveniently performed with transducers between 5 and 10 MHz^{12,13}. Three-dimensional ultrasound may facilitate the examination of the fetal brain and spine^{14,15}.

Imaging parameters

The examination is mostly performed with gray-scale bidimensional ultrasound. Harmonic imaging may enhance visualization of subtle anatomic details, particularly in patients who scan poorly. In neurosonographic studies, Color and power Doppler may be used, mainly to identify cerebral vessels. Proper adjustment of pulse repetition frequency (main cerebral arteries have velocities in the

range of 20–40 cm/s during intrauterine life)¹⁶ and signal persistence enhances visualization of small vessels.

BASIC EXAMINATION

Qualitative evaluation

Transabdominal sonography is the technique of choice to investigate the fetal CNS during late first, second and third trimesters of gestation in low risk pregnancies. The examination should include the evaluation of the fetal head and spine.

Two axial planes allow visualization of the cerebral structures relevant to assess the anatomic integrity of the brain¹⁷. These planes are commonly referred to as the *transventricular plane* and the *transcerebellar plane*. A third plane, the so-called *transthalamic plane*, is frequently added, mostly for the purpose of biometry (Figure 1). Structures that should be noted in the routine examination include the lateral ventricles, the cerebellum and cisterna magna, and *cavum septi pellucidi*. Head shape and brain texture should also be noted on these views (Table 1).

The transventricular plane

This plane demonstrates the anterior and posterior portion of the lateral ventricles. The anterior portion of the lateral ventricles (frontal or anterior horns) appears as two comma-shaped fluid filled structures. They have

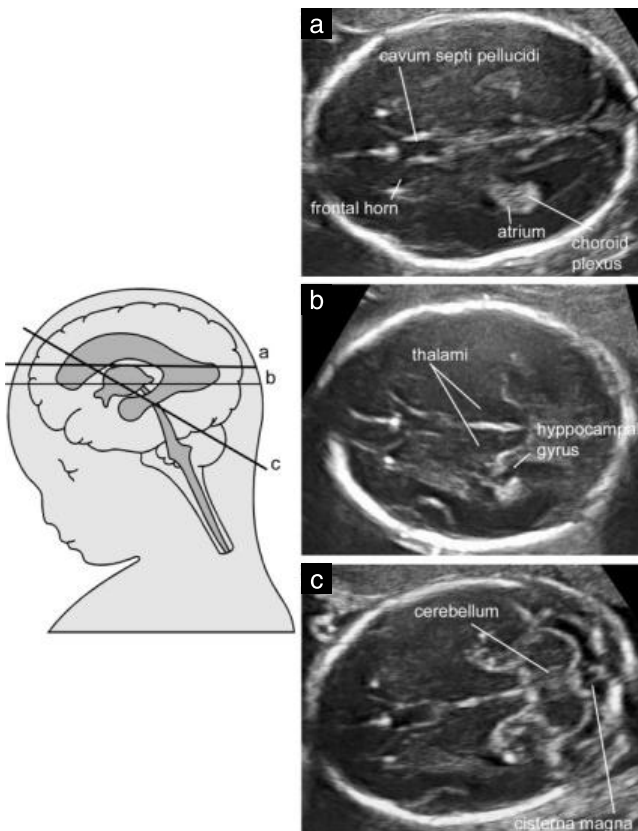


Figure 1 Axial views of the fetal head. (a) Transventricular plane; (b) transthalamic plane; (c) transcerebellar plane.

Table 1 Structures that are usually noted in a basic ultrasound examination of the fetal central nervous system

Head shape
Lateral ventricles
<i>Cavum septi pellucidi</i>
Thalami
Cerebellum
Cisterna magna
Spine

a well defined lateral wall and medially are separated by the *cavum septi pellucidi* (CSP). The CSP is a fluid filled cavity between two thin membranes. In late gestation or the early neonatal period these membranes usually fuse to become the *septum pellucidum*. The CSP becomes visible around 16 weeks and undergoes obliteration near term gestation. With transabdominal ultrasound, it should always be visualized between 18 and 37 weeks, or with a biparietal diameter of 44–88 mm¹⁸. Conversely, failure to demonstrate the CSP prior to 16 weeks or later than 37 weeks is a normal finding. The value of visualizing the CSP for identifying cerebral anomalies has been debated¹⁷. However, this structure is easy to identify and is obviously altered with many cerebral lesions such as holoprosencephaly, agenesis of the corpus callosum, severe hydrocephaly and septo-optic dysplasia¹⁹.

From about 16 weeks the posterior portion of the lateral ventricles (also referred to as posterior horns) is in reality a complex formed by the atrium that continues posteriorly into the occipital horn. The atrium is characterized by the presence of the glomus of the choroid plexus, which is brightly echogenic, while the occipital horn is fluid filled. Particularly in the second trimester of gestation both the medial and lateral walls of the ventricle are parallel to the midline and are therefore well depicted sonographically as bright lines. Under normal conditions the glomus of the choroid plexus almost completely fills the cavity of the ventricle at the level of the atrium being closely apposed to both the medial or lateral walls, but in some normal cases a small amount of fluid may be present between the medial wall and the choroid plexus^{20–23}.

In the standard transventricular plane only the hemisphere on the far side of the transducer is usually clearly visualized, as the hemisphere close to the transducer is frequently obscured by artifacts. However, most severe cerebral lesions are bilateral or associated with a significant deviation or distortion of the midline echo, and it has been suggested that in basic examinations symmetry of the brain is assumed¹⁷.

The transcerebellar plane

This plane is obtained at a slightly lower level than that of the transventricular plane and with a slight posterior tilting and includes visualization of the frontal horns of the lateral ventricles, CSP, thalami, cerebellum and cisterna magna. The cerebellum appears as a butterfly shaped structure formed by the round cerebellar hemispheres

joined in the middle by the slightly more echogenic cerebellar vermis. The cisterna magna or cisterna cerebello-medullaris is a fluid filled space posterior to the cerebellum. It contains thin septations, that are normal structures and should not be confused with vascular structures or cystic abnormalities. In the second half of gestation the depth of the cisterna magna is stable and should be 2–10 mm¹⁷. Early in gestation the cerebellar vermis has not completely covered the fourth ventricle, and this may give the false impression of a defect of the vermis. In later pregnancy such a finding may raise the suspicion of a cerebellar abnormality but prior to 20 weeks' gestation this is usually a normal finding²⁴.

Transthalamic plane

A third scanning plane, obtained at an intermediate level, is also frequently used in the sonographic assessment of the fetal head, and is commonly referred to as the *transthalamic plane* or *biparietal diameter plane*. The anatomic landmarks include, from anterior to posterior, the frontal horns of the lateral ventricles, the *cavum septi pellucidi*, the thalami and the hippocampal gyri²⁵. Although this plane does not add significant anatomic information to that obtained from the transventricular and transcerebellar planes, it is used for biometry of the fetal head. It has been proposed that, particularly in late gestation, this section plane is easier to identify and allows more reproducible measurements than does the transventricular plane²⁵.

The fetal spine

The detailed examination of the fetal spine requires expertise and meticulous scanning, and the results are heavily dependent upon the fetal position. Therefore, a full detailed evaluation of the fetal spine from every projection is not a part of the basic examination. The most frequent of the severe spinal abnormalities, open spina bifida, is usually associated with abnormal intracranial anatomy. However, a longitudinal section of the fetal spine should always be obtained because it may reveal, at least in some cases, other spinal malformations including vertebral abnormalities and sacral agenesis. Under normal conditions, a longitudinal section of the spine from about 14 weeks' gestation demonstrates the three ossification centers of the vertebrae (one inside the body, and one at the junction between the lamina and pedicle on each side) that surround the neural canal, and that appear as either two or three parallel lines depending upon the orientation of the sound beam. In addition, attempt should be made to demonstrate the intactness of the skin overlying the spine either on transverse or longitudinal views.

Quantitative evaluation

Biometry is an essential part of the sonographic examination of the fetal head. In the second trimester and third trimester, a standard examination usually

includes the measurement of the biparietal diameter, head circumference and internal diameter of the atrium. Some also advocate measurement of the transverse cerebellar diameter and cisterna magna depth.

Biparietal diameter and head circumference are commonly used for assessing fetal age and growth and may also be useful to identify some cerebral anomalies. They may be measured either in the transventricular plane or in the transthalamic plane. Different techniques can be used for measuring the biparietal diameter. Most frequently the calipers are positioned outside the fetal calvarium (so called outside to outside measurement)²⁶. However, some of the available charts have been produced using an outer to inner technique to avoid artifacts generated by the distal echo of the calvarium²⁵. The two approaches result in a difference of a few millimeters that may be clinically relevant in early gestation. It is important therefore to know the technique that was used while constructing the reference charts that one uses. If the ultrasound equipment has ellipse measurement capacity, then head circumference can be measured directly by placing the ellipse around the outside of the skull bone echoes. Alternatively, the head circumference (HC) can be calculated from biparietal diameter (BPD) and occipitofrontal diameter (OFD) by using the equation $HC = 1.62 \times (BPD + OFD)$. The ratio of the biparietal diameter over the occipitofrontal diameter is usually 75–85%. Moulding of the fetal head particularly in early gestation is however frequent, and most fetuses in breech presentation have some degree of dolicocephaly.

Measurement of the atrium is recommended because several studies suggest that this is the most effective approach for assessing the integrity of the ventricular system²², and ventriculomegaly is a frequent marker of abnormal cerebral development. Measurement is obtained at the level of the glomus of the choroid plexus, perpendicular to the ventricular cavity, positioning the calipers inside the echoes generated by the lateral walls (Figure 2). The measurement is stable in the second and early third trimesters, with a mean diameter of 6–8 mm^{20,22,27} and is considered normal when less than 10 mm^{27–32}. Most of the biometric studies on the size of the lateral ventricles have used ultrasound equipment that provided measurements in millimeters³³.

As, with modern equipment, measurements are given in tenths of millimeters, it is uncertain which is the most reasonable cut-off value. We believe that particularly at midgestation a value of 10.0 mm or greater should be considered suspicious.

The transverse cerebellar diameter increases by about one millimeter per week of pregnancy between 14 and 21 menstrual weeks. This measurement, along with the head circumference and the biparietal diameter is helpful to assess fetal growth. The depth of the cisterna magna measured between the cerebellar vermis and the internal side of the occipital bone is usually 2–10 mm³⁴. With dolicocephaly, measurements slightly larger than 10 mm may be encountered.

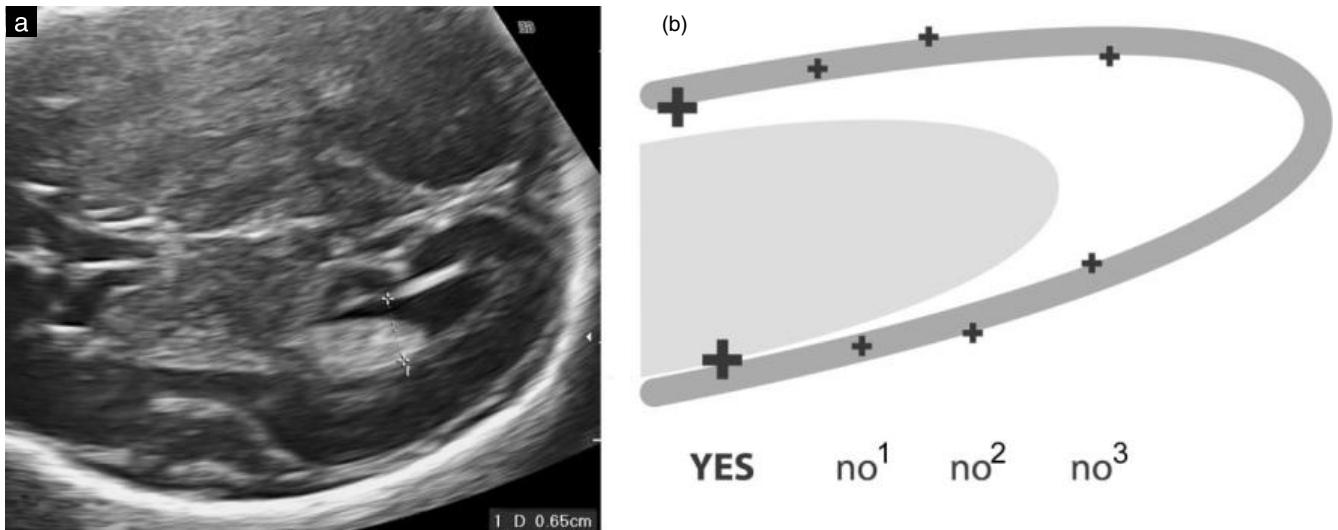


Figure 2 (a) Measurement of the atrium of the lateral ventricles. The calipers are positioned at the level of the glomus of the choroid plexus, inside the echoes generated by the ventricular walls; (b) diagram to illustrate correct caliper placement for ventricular measurement. Calipers are correctly placed touching the inner edge of the ventricle wall at its widest part and aligned perpendicular to the long axis of the ventricle (YES). Incorrect placements include middle–middle (no¹), outer–outer (no²), and placement that is too posterior in the narrower part of the ventricle or not perpendicular to the ventricle axis (no³).

FETAL NEUROSONOGRAM

It is commonly accepted that dedicated fetal neurosonography has a much greater diagnostic potential than that of the standard transabdominal examination, and is particularly helpful in the evaluation of complex malformations. However, this examination requires a grade of expertise that is not available in many settings and the method is not yet universally used. Dedicated fetal neurosonography is useful in patients with an increased risk of CNS anomalies, including cases in which the basic examination identifies suspicious findings.

The basis of the neurosonographic examination of the fetal brain is the multiplanar approach, that is obtained by aligning the transducer with the sutures and fontanelles of the fetal head^{12,13}. When the fetus is in vertex presentation, a transabdominal/transvaginal approach can be used. In fetuses in breech presentation, a transfundal approach is used, positioning the probe parallel instead of perpendicular to the abdomen. Vaginal probes have the advantage of operating at a higher frequency than do abdominal probes and therefore allow a greater definition of anatomical details. For this reason, in some breech presenting fetuses an external cephalic version may be considered in order to use the transvaginal approach.

Evaluation of the spine is a part of the neurosonographic examination and is performed using a combination of axial, coronal and sagittal planes.

The neurosonographic examination should include the same measurements that are commonly obtained in a basic examination: the biparietal diameter, head circumference and the atrium of the lateral ventricles. The specific measurements obtained may vary also depending upon the gestational age and the clinical setting.

Fetal brain

Whether the exam is performed transvaginally or transabdominally, proper alignment of the probe along the correct section planes usually requires gentle manipulation of the fetus. A variety of scanning planes can be used, also depending upon the position of the fetus¹². A systematic evaluation of the brain usually includes the visualization of four coronal and three sagittal planes. In the following, a description of the different structures that can be imaged in the late second and third trimesters is reported. Apart from the anatomic structures, fetal neurosonography should also include evaluation of the convolutions of the fetal brain that change throughout gestation^{35–38}.

Coronal planes (Figure 3)

The transfrontal plane or Frontal-2 plane. The visualization of this plane is obtained through the anterior fontanelle and depicts the midline interhemispheric fissure and the anterior horns of the lateral ventricles on each side. The plane is rostral to the genu of the corpus callosum and this explains the presence of an uninterrupted interhemispheric fissure. Other structures observed are the sphenoidal bone and the ocular orbits.

The transcavate plane or Mid-coronal-1 plane¹². At the level of the caudate nuclei, the genu or anterior portion of the corpus callosum interrupts the continuity of the interhemispheric fissure. Due to the thickness of the genu in coronal planes it is observed as a more echogenic structure than the body of the corpus callosum. The *cavum septi pellucidi* is depicted as an anechogenic triangular structure under the corpus callosum. The lateral ventricles are found at each side surrounded by the brain cortex. In a more lateral position the Sylvian fissures are clearly identified.

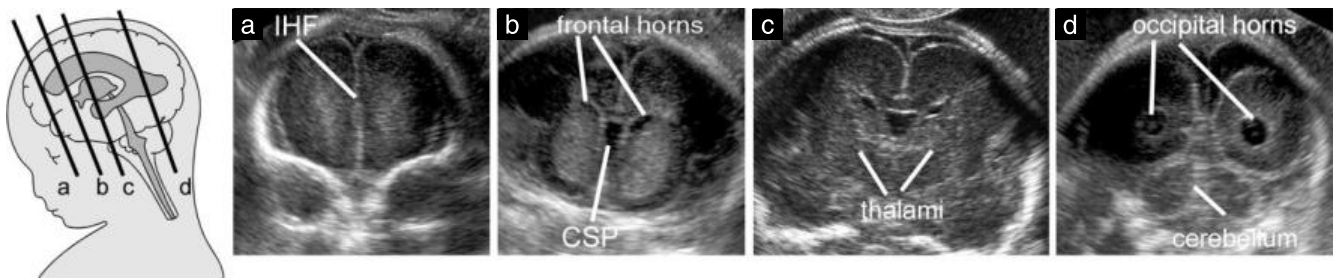


Figure 3 Coronal views of the fetal head. (a) Transfrontal plane; (b) transcaudate plane; (c) transthalamic plane; (d) transcerebellar plane. CSP, *cavum septi pellucidi*; IHF, *interhemispheric fissure*.

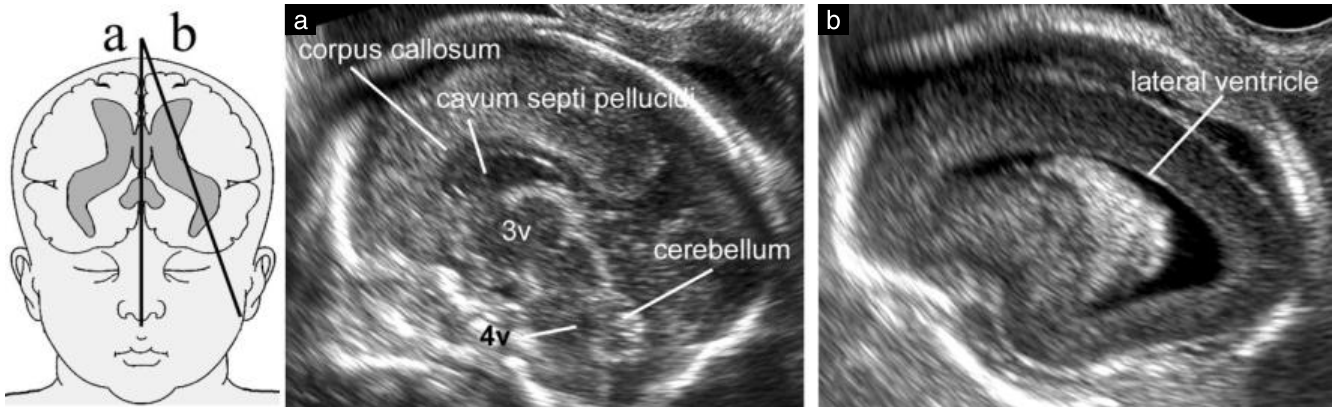


Figure 4 Sagittal planes of the fetal head. (a) Midsagittal plane; (b) parasagittal plane. 3v, *third ventricle*; 4v, *fourth ventricle*.

The *transthalamic plane* or *Mid-coronal-2 plane*¹². Both thalami are found in close apposition but in some cases the third ventricle may be observed in the midline with the interventricular foramina and the atrium of the lateral ventricles with the choroid plexus slightly cranial on each side (*Mid-coronal-3 plane*). Close to the cranial base and in the midline the basal cistern contains the vessels of the circle of Willis and the optic chiasma.

The *transcerebellar plane* or *Occipital-1 and 2 plane*. This plane is obtained through the posterior fontanelles and enables visualization of the occipital horns of the lateral ventricles and the interhemispheric fissure. Both cerebellar hemispheres and the vermis are also seen in this plane.

Sagittal planes (Figure 4)

Three sagittal planes are usually studied: the midsagittal; and the parasagittal of each side of the brain.

The *midsagittal* or *median plane*¹² shows the corpus callosum with all its components; the *cavum septi pellucidi*, and in some cases also the *cavum vergae* and *cavum veli interpositi*, the brain stem, pons, vermis and posterior fossa. Using color Doppler the anterior cerebral artery, pericallosal artery with their branches and the vein of Galen may be seen.

The *parasagittal* or *Oblique plane-1*¹² depicts the entire lateral ventricle, the choroid plexus, the periventricular tissue and the cortex.

Fetal spine

Three types of scanning planes can be used to evaluate the integrity of the spine. The choice depends upon the fetal position. Usually, only two of these scanning planes are possible in a given case.

In *transverse planes* or *axial planes*, the examination of the spine is a dynamic process performed by sweeping the transducer along the entire length of the spine and at the same time keeping in the axial plane of the level being examined (Figure 5). The vertebrae have different anatomic configurations at different levels. Fetal thoracic and lumbar vertebrae have a triangular shape, with the ossification centers surrounding the neural canal. The first cervical vertebrae are quadrangular in shape, and sacral vertebrae are flat.

In *sagittal planes* the ossification centers of the vertebral body and posterior arches form two parallel lines that converge in the sacrum. When the fetus is prone, a true sagittal section can also be obtained, directing the ultrasound beam across the unossified spinous process. This allows imaging of the spinal canal, and of the spinal cord within it (Figure 6). In the second and third trimesters of gestation the conus medullaris is usually found at the level of L2-L3³⁹.

In *coronal planes*, one, two or three parallel lines are seen, depending upon the orientation of the sound beam (Figure 7).

Integrity of the neural canal is inferred by the regular disposition of the ossification centers of the spine and the presence of soft tissue covering the spine. If a true sagittal

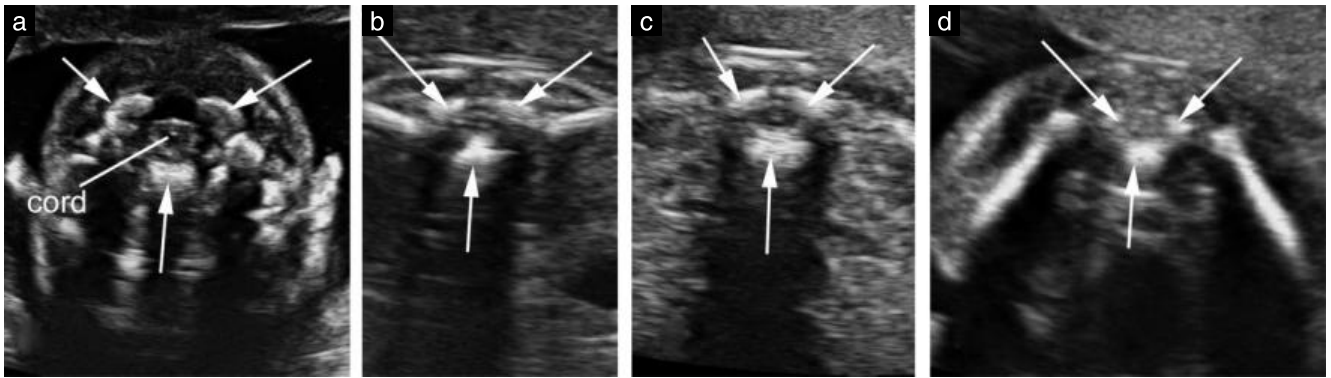


Figure 5 Axial views of the fetal spine at different levels. (a) Cervical; (b) thoracic; (c) lumbar; (d) sacral. The arrows point to the three ossification centers of the vertebrae. Note the intact skin overlying the spine. On images a–c the spinal cord is visible as a hypochoic ovoid with central white dot.

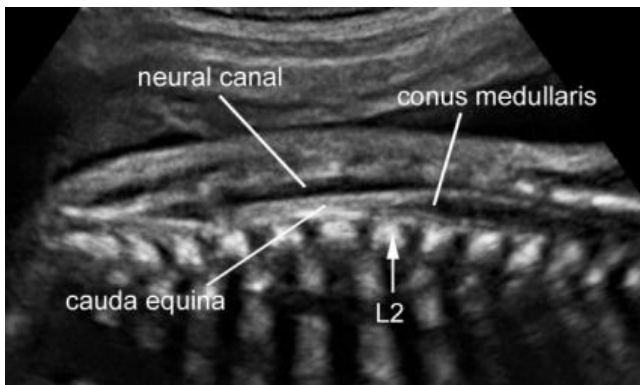


Figure 6 Sagittal view of the fetal spine at midgestation. Using the unossified spinous process of the vertebrae as an acoustic window, the contents of the neural canal are demonstrated. The conus medullaris is normally positioned at the level of the second lumbar vertebra (L2).

section can be obtained, visualizing the conus medullaris in its normal location further strengthens the diagnosis of normalcy.

EFFECTIVENESS OF ULTRASOUND EXAMINATION OF THE FETAL NEURAL AXIS

In a low risk pregnancy around midgestation, if the transventricular plane and the transcerebellar plane are satisfactorily obtained, the head measurements (head circumference in particular) are within normal limits for gestational age, the atrial width is less than 10.0 mm and the cisterna magna width is between 2–10 mm, many cerebral malformations are excluded, the risk of a CNS anomaly is exceedingly low and further examinations are not indicated¹⁷.

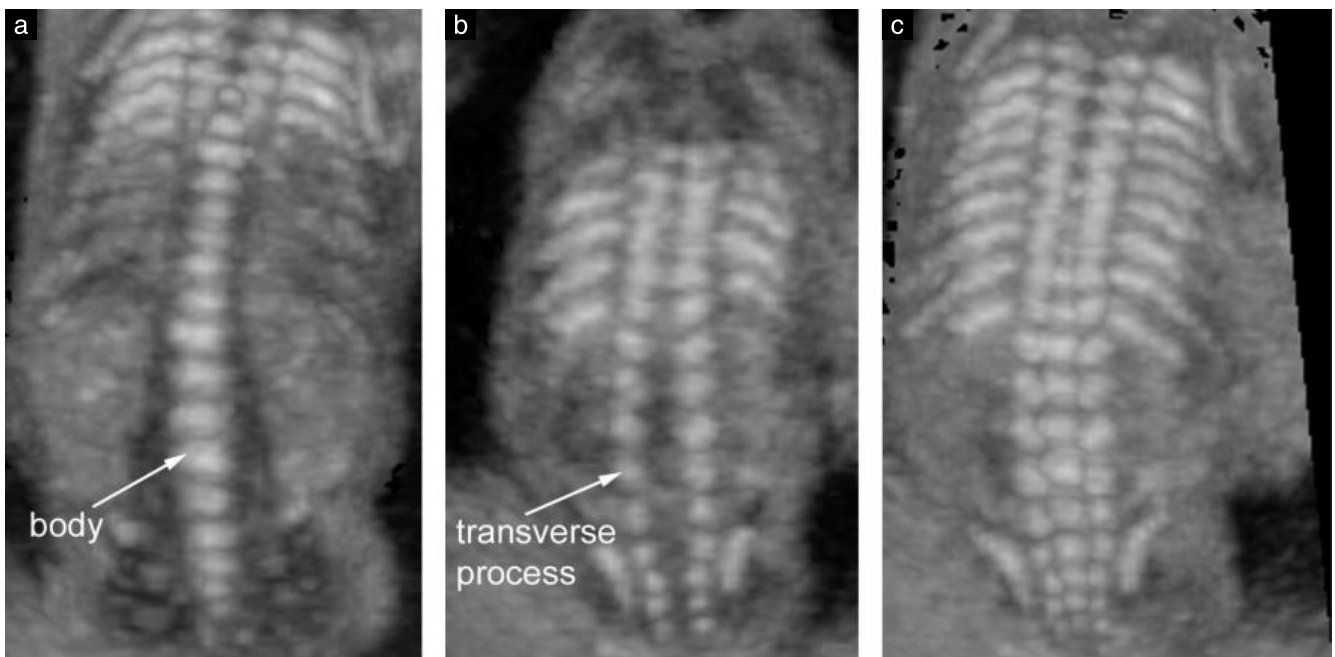


Figure 7 Coronal views of the fetal spine. These images were obtained with three-dimensional ultrasound from the same sonographic volume using different angulations and beam-thicknesses. (a) A thin ultrasound beam is oriented through the bodies of the vertebrae; (b) the same ultrasound beam is oriented more posteriorly to demonstrate the posterior arches of the vertebrae; (c) a thick ultrasound beam is used to demonstrate simultaneously the three ossification centers.

It is beyond the scope of these guidelines to review the available literature on the sensitivity of antenatal ultrasound in the prediction of neural anomalies. Some studies of low risk patients undergoing basic examinations have reported sensitivities in excess of 80%^{40,41}. However, these results probably greatly overestimate the diagnostic potential of the technique. These surveys had invariably very short follow-up and almost only included open neural tube defects, whose recognition was probably facilitated by systematic screening with maternal serum alphafetoprotein. Diagnostic limitations of prenatal ultrasound are well documented and occur for a number of reasons⁴². Some even severe anomalies may be associated with only subtle findings in early gestation⁴³. The brain continues to develop in the second half of gestation and into the neonatal period thus limiting the detection of anomalies of neuronal proliferation (such as microcephaly⁴⁴, tumors⁴⁵ and cortical malformations⁴²). Also, some cerebral lesions are not due to faulty embryological development but represent the consequence of acquired prenatal or perinatal insults^{46–48}. Even in expert hands some types of anomalies may be difficult or impossible to diagnose *in utero*, in a proportion that is yet impossible to determine with precision.

REFERENCES

- Myriantopoulos NC. Epidemiology of central nervous system malformations. In: Vinken PJ, Bruyn GW, editors. *Handbook of Clinical Neurology*. Elsevier: Amsterdam, 1977; 139–171.
- Levine D, Barnes PD, Robertson RR, Wong G, Mehta TS. Fast MR imaging of fetal central nervous system abnormalities. *Radiology* 2003; **229**: 51–61.
- Griffiths PD, Paley MN, Widjaja E, Taylor C, Whitby EH. In utero magnetic resonance imaging for brain and spinal abnormalities in fetuses. *BMJ* 2005; **331**: 562–565.
- Malinger G, Ben-Sira L, Lev D, Ben-Aroya Z, Kidron D, Lerman-Sagie T. Fetal brain imaging: a comparison between magnetic resonance imaging and dedicated neurosonography. *Ultrasound Obstet Gynecol* 2004; **23**: 333–340.
- Malinger G, Lev D, Lerman-Sagie T. Is fetal magnetic resonance imaging superior to neurosonography for detection of brain anomalies? *Ultrasound Obstet Gynecol* 2002; **20**: 317–321.
- Ghi T, Pilu G, Savelli L, Segata M, Bovicelli L. Sonographic diagnosis of congenital anomalies during the first trimester. *Placenta* 2003; **24** (Suppl B): S84–S87.
- Monteagudo A, Timor-Tritsch IE. First trimester anatomy scan: pushing the limits. What can we see now? *Curr Opin Obstet Gynecol* 2003; **15**: 131–141.
- Bronshtein M, Ornoy A. Acrania: anencephaly resulting from secondary degeneration of a closed neural tube: two cases in the same family. *J Clin Ultrasound* 1991; **19**: 230–234.
- Blaas HG, Eik-Nes SH, Vainio T, Isaksen CV. Alobar holoprosencephaly at 9 weeks gestational age visualized by two- and three-dimensional ultrasound. *Ultrasound Obstet Gynecol* 2000; **15**: 62–65.
- Blaas HG, Eik-Nes SH, Isaksen CV. The detection of spina bifida before 10 gestational weeks using two- and three-dimensional ultrasound. *Ultrasound Obstet Gynecol* 2000; **16**: 25–29.
- Johnson SP, Sebire NJ, Snijders RJ, Tunkel S, Nicolaides KH. Ultrasound screening for anencephaly at 10–14 weeks of gestation. *Ultrasound Obstet Gynecol* 1997; **9**: 14–16.
- Timor-Tritsch IE, Monteagudo A. Transvaginal fetal neurosonography: standardization of the planes and sections by anatomic landmarks. *Ultrasound Obstet Gynecol* 1996; **8**: 42–47.
- Malinger G, Katz A, Zakut H. Transvaginal fetal neurosonography. Supratentorial structures. *Isr J Obstet Gynecol* 1993; **4**: 1–5.
- Pilu G, Segata M, Ghi T, Carletti A, Perolo A, Santini D, Bonasoni P, Tani G, Rizzo N. Diagnosis of midline anomalies of the fetal brain with the three-dimensional median view. *Ultrasound Obstet Gynecol* 2006; **27**: 522–529.
- Monteagudo A, Timor-Tritsch IE, Mayberry P. Three-dimensional transvaginal neurosonography of the fetal brain: 'navigating' in the volume scan. *Ultrasound Obstet Gynecol* 2000; **16**: 307–313.
- van den Wijngaard JA, Groenenberg IA, Wladimiroff JW, Hop WC. Cerebral Doppler ultrasound of the human fetus. *Br J Obstet Gynaecol* 1989; **96**: 845–849.
- Filly RA, Cardoza JD, Goldstein RB, Barkovich AJ. Detection of fetal central nervous system anomalies: a practical level of effort for a routine sonogram. *Radiology* 1989; **172**: 403–408.
- Falco P, Gabrielli S, Visentin A, Perolo A, Pilu G, Bovicelli L. Transabdominal sonography of the cavum septum pellucidum in normal fetuses in the second and third trimesters of pregnancy. *Ultrasound Obstet Gynecol* 2000; **16**: 549–553.
- Malinger G, Lev D, Kidron D, Heredia F, Hershkovitz R, Lerman-Sagie T. Differential diagnosis in fetuses with absent septum pellucidum. *Ultrasound Obstet Gynecol* 2005; **25**: 42–49.
- Pilu G, Reece EA, Goldstein I, Hobbins JC, Bovicelli L. Sonographic evaluation of the normal developmental anatomy of the fetal cerebral ventricles: II. The atria. *Obstet Gynecol* 1989; **73**: 250–256.
- Cardoza JD, Filly RA, Podrasky AE. The dangling choroid plexus: a sonographic observation of value in excluding ventriculomegaly. *AJR Am J Roentgenol* 1988; **151**: 767–770.
- Cardoza JD, Goldstein RB, Filly RA. Exclusion of fetal ventriculomegaly with a single measurement: the width of the lateral ventricular atrium. *Radiology* 1988; **169**: 711–714.
- Mahony BS, Nyberg DA, Hirsch JH, Petty CN, Hendricks SK, Mack LA. Mild idiopathic lateral cerebral ventricular dilatation in utero: sonographic evaluation. *Radiology* 1988; **169**: 715–721.
- Bromley B, Nadel AS, Pauker S, Estroff JA, Benacerraf BR. Closure of the cerebellar vermis: evaluation with second trimester US. *Radiology* 1994; **193**: 761–763.
- Shepard M, Filly RA. A standardized plane for biparietal diameter measurement. *J Ultrasound Med* 1982; **1**: 145–150.
- Snijders RJ, Nicolaides KH. Fetal biometry at 14–40 weeks' gestation. *Ultrasound Obstet Gynecol* 1994; **4**: 34–48.
- Pilu G, Falco P, Gabrielli S, Perolo A, Sandri F, Bovicelli L. The clinical significance of fetal isolated cerebral borderline ventriculomegaly: report of 31 cases and review of the literature. *Ultrasound Obstet Gynecol* 1999; **14**: 320–326.
- Kelly EN, Allen VM, Seaward G, Windrim R, Ryan G. Mild ventriculomegaly in the fetus, natural history, associated findings and outcome of isolated mild ventriculomegaly: a literature review. *Prenat Diagn* 2001; **21**: 697–700.
- Wax JR, Bookman L, Cartin A, Pinette MG, Blackstone J. Mild fetal cerebral ventriculomegaly: diagnosis, clinical associations, and outcomes. *Obstet Gynecol Surv* 2003; **58**: 407–414.
- Laskin MD, Kingdom J, Toi A, Chitayat D, Ohlsson A. Perinatal and neurodevelopmental outcome with isolated fetal ventriculomegaly: a systematic review. *J Matern Fetal Neonatal Med* 2005; **18**: 289–298.
- Achiron R, Schimmel M, Achiron A, Mashiah S. Fetal mild idiopathic lateral ventriculomegaly: is there a correlation with fetal trisomy? *Ultrasound Obstet Gynecol* 1993; **3**: 89–92.
- Gaglioti P, Danelon D, Bontempo S, Mombro M, Cardaropoli S, Todros T. Fetal cerebral ventriculomegaly: outcome in 176 cases. *Ultrasound Obstet Gynecol* 2005; **25**: 372–377.

33. Heiserman J, Filly RA, Goldstein RB. Effect of measurement errors on sonographic evaluation of ventriculomegaly. *J Ultrasound Med* 1991; **10**: 121–124.
34. Mahony BS, Callen PW, Filly RA, Hoddick WK. The fetal cisterna magna. *Radiology* 1984; **153**: 773–776.
35. Monteagudo A, Timor-Tritsch IE. Development of fetal gyri, sulci and fissures: a transvaginal sonographic study. *Ultrasound Obstet Gynecol* 1997; **9**: 222–228.
36. Toi A, Lister WS, Fong KW. How early are fetal cerebral sulci visible at prenatal ultrasound and what is the normal pattern of early fetal sulcal development? *Ultrasound Obstet Gynecol* 2004; **24**: 706–715.
37. Droulle P, Gaillet J, Schweitzer M. [Maturation of the fetal brain. Echoanatomy: normal development, limits and value of pathology]. *J Gynecol Obstet Biol Reprod (Paris)* 1984; **13**: 228–236.
38. Cohen-Sacher B, Lerman-Sagie T, Lev D, Malinger G. Sonographic developmental milestones of the fetal cerebral cortex: a longitudinal study. *Ultrasound Obstet Gynecol* 2006; **27**: 494–502.
39. Robbin ML, Filly RA, Goldstein RB. The normal location of the fetal conus medullaris. *J Ultrasound Med* 1994; **13**: 541–546.
40. Crane JP, LeFevre ML, Winborn RC, Evans JK, Ewigman BG, Bain RP, Frigoletto FD, McNellis D. A randomized trial of prenatal ultrasonographic screening: impact on the detection, management, and outcome of anomalous fetuses. The RADIUS Study Group. *Am J Obstet Gynecol* 1994; **171**: 392–399.
41. Ewigman BG, Crane JP, Frigoletto FD, LeFevre ML, Bain RP, McNellis D. Effect of prenatal ultrasound screening on perinatal outcome. RADIUS Study Group. *N Engl J Med* 1993; **329**: 821–827.
42. Malinger G, Lerman-Sagie T, Watemberg N, Rotmensch S, Lev D, Glezerman M. A normal second-trimester ultrasound does not exclude intracranial structural pathology. *Ultrasound Obstet Gynecol* 2002; **20**: 51–56.
43. Bennett GL, Bromley B, Benacerraf BR. Agenesis of the corpus callosum: prenatal detection usually is not possible before 22 weeks of gestation. *Radiology* 1996; **199**: 447–450.
44. Bromley B, Benacerraf BR. Difficulties in the prenatal diagnosis of microcephaly. *J Ultrasound Med* 1995; **14**: 303–306.
45. Schlembach D, Bornemann A, Rupprecht T, Beinder E. Fetal intracranial tumors detected by ultrasound: a report of two cases and review of the literature. *Ultrasound Obstet Gynecol* 1999; **14**: 407–418.
46. Simonazzi G, Segata M, Ghi T, Sandri F, Ancora G, Bernardi B, Tani G, Rizzo N, Santini D, Bonasoni P, Pilu G. Accurate neurosonographic prediction of brain injury in the surviving fetus after the death of a monochorionic cotwin. *Ultrasound Obstet Gynecol* 2006; **27**: 517–521.
47. Ghi T, Simonazzi G, Perolo A, Savelli L, Sandri F, Bernardi B, Santini D, Bovicelli L, Pilu G. Outcome of antenatally diagnosed intracranial hemorrhage: case series and review of the literature. *Ultrasound Obstet Gynecol* 2003; **22**: 121–130.
48. Ghi T, Brondelli L, Simonazzi G, Valeri B, Santini D, Sandri F, Ancora G, Pilu G. Sonographic demonstration of brain injury in fetuses with severe red blood cell alloimmunization undergoing intrauterine transfusions. *Ultrasound Obstet Gynecol* 2004; **23**: 428–431.

ACKNOWLEDGMENTS

These guidelines were developed under the auspices of the ISUOG Education Committee. Chair, Dario Paladini, University of Naples, Italy

Appreciation is particularly extended to specialty consultants who contributed to this project:

Gustavo Malinger, MD

Fetal Neurology Clinic, Department of Obstetrics and Gynecology, Wolfson Medical Center, Tel-Aviv University, Israel

Ana Monteagudo, MD

Department of Obstetrics and Gynecology, New York University School of Medicine, New York, USA

Gianluigi Pilu, MD

Department of Obstetrics and Gynecology, University of Bologna, Italy

Ilan Timor-Tritsch, MD

Department of Obstetrics and Gynecology, New York University School of Medicine, New York, USA

Ants Toi, MD

Department of Medical Imaging, Mount Sinai Hospital, University of Toronto, Canada

Copies of this document will be available at: <http://www.isuog.org>

ISUOG Secretariat
Unit 4, Blythe Mews
Blythe Road
London W14 0HW, UK
e-mail: info@isuog.org

Cavum septi pellucidi (CSP) ratio: a marker for partial agenesis of the fetal corpus callosum

K. KARL^{1,2}, T. ESSER¹, K. S. HELING³ and R. CHAOUI³

¹Center for Prenatal Diagnosis Munich, Munich, Germany; ²Department of Obstetrics and Gynecology, Ludwig-Maximilians-University, Munich, Germany; ³Center for Prenatal Diagnosis and Human Genetics, Berlin, Germany

KEYWORDS: agenesis; cavum septi pellucidi; cavum septi pellucidi size; corpus callosum; fetal neurosonography; partial agenesis

ABSTRACT

Objective While complete agenesis of the corpus callosum is often suspected on fetal ultrasound due to absence of the cavum septi pellucidi (CSP), suspicion of partial agenesis of the corpus callosum (pACC) is a challenge since the CSP is almost always present. The aim of this study was to measure the length and width of the CSP and calculate the length-to-width ratio (CSP ratio), and compare these between fetuses with pACC and normal fetuses.

Methods In this retrospective case–control study, the length and width of the CSP were measured in the axial plane of the fetal head, and the CSP length-to-width ratio calculated, in 323 normal fetuses and in 20 fetuses with pACC between 20 and 34 weeks' gestation. From the normal population we constructed reference ranges in relation to biparietal diameter (BPD). For all fetuses we calculated Z-scores for the CSP ratio.

Results In the normal population, the length and width of the CSP increased with increasing BPD, while the CSP ratio decreased. The CSP was short (< 5th centile) in 85% (17/20) of fetuses with pACC and wide (> 95th centile) in 65% (13/20). The CSP ratio was small (< 5th centile) in 95% (19/20) of pACC fetuses, with 16/20 (80%) having a ratio below an empirical cut-off of 1.5. Analysis of Z-scores showed that fetuses with pACC had a significantly smaller CSP ratio ($P < 0.0001$) compared with the normal population.

Conclusions Fetuses with a normal-sized corpus callosum have a rectangular-shaped CSP, with a CSP ratio > 1.5 in the second half of gestation. Most fetuses with pACC have an abnormally shaped, wide and short CSP, with a decreased CSP ratio. This simple ratio has the potential to identify fetuses at high risk for pACC. Copyright © 2017 ISUOG. Published by John Wiley & Sons Ltd.

INTRODUCTION

Complete agenesis of the corpus callosum (cACC) is the most common commissural anomaly diagnosed prenatally^{1,2}. In expert hands it is often suspected on imaging of the axial planes, when the cavum septi pellucidi (CSP) is absent and additional signs, such as teardrop-shaped lateral ventricles, are found^{1–3}. However, in partial agenesis of the corpus callosum (pACC), often the CSP is present, which makes it difficult to suspect anomalies of the corpus callosum prenatally^{4,5}. In recent years, there has been increasing interest in the assessment of changes in the size and shape of the CSP as a clue to the presence of several fetal anomalies, including numerical aneuploidies⁴, 22q11 deletion⁵ and pACC^{6,7}. The aim of the present study, therefore, was to compare the length and width of the CSP in normal fetuses with those in fetuses with pACC, and to propose a new, simple ratio, the CSP ratio (ratio of CSP length to width), for the identification of fetuses suspected of having pACC.

PATIENTS AND METHODS

This was a retrospective case–control study performed on stored images from fetuses between 20 and 34 weeks' gestation. At our centers, the routine comprehensive scan after 20 weeks attempts to include documentation of the CSP in the axial plane of the fetal head, as recommended⁸, and in addition visualization and measurement of the length of the corpus callosum. The corpus callosum is visualized either directly, in the midsagittal plane on two-dimensional (2D) ultrasound with color Doppler demonstration of the pericallosal artery, or indirectly, by acquiring a three-dimensional (3D) volume with multiplanar reconstruction. All examinations are performed using high-resolution ultrasound equipment (Voluson E8 or Voluson E10 machine, GE Medical

Correspondence to: Dr K. Karl, Center for Prenatal Diagnosis Munich, Tegernseer Landstraße 64, D-81541 Munich, Germany (e-mail: k.karl@praenatalschall.de)

Accepted: 8 January 2017

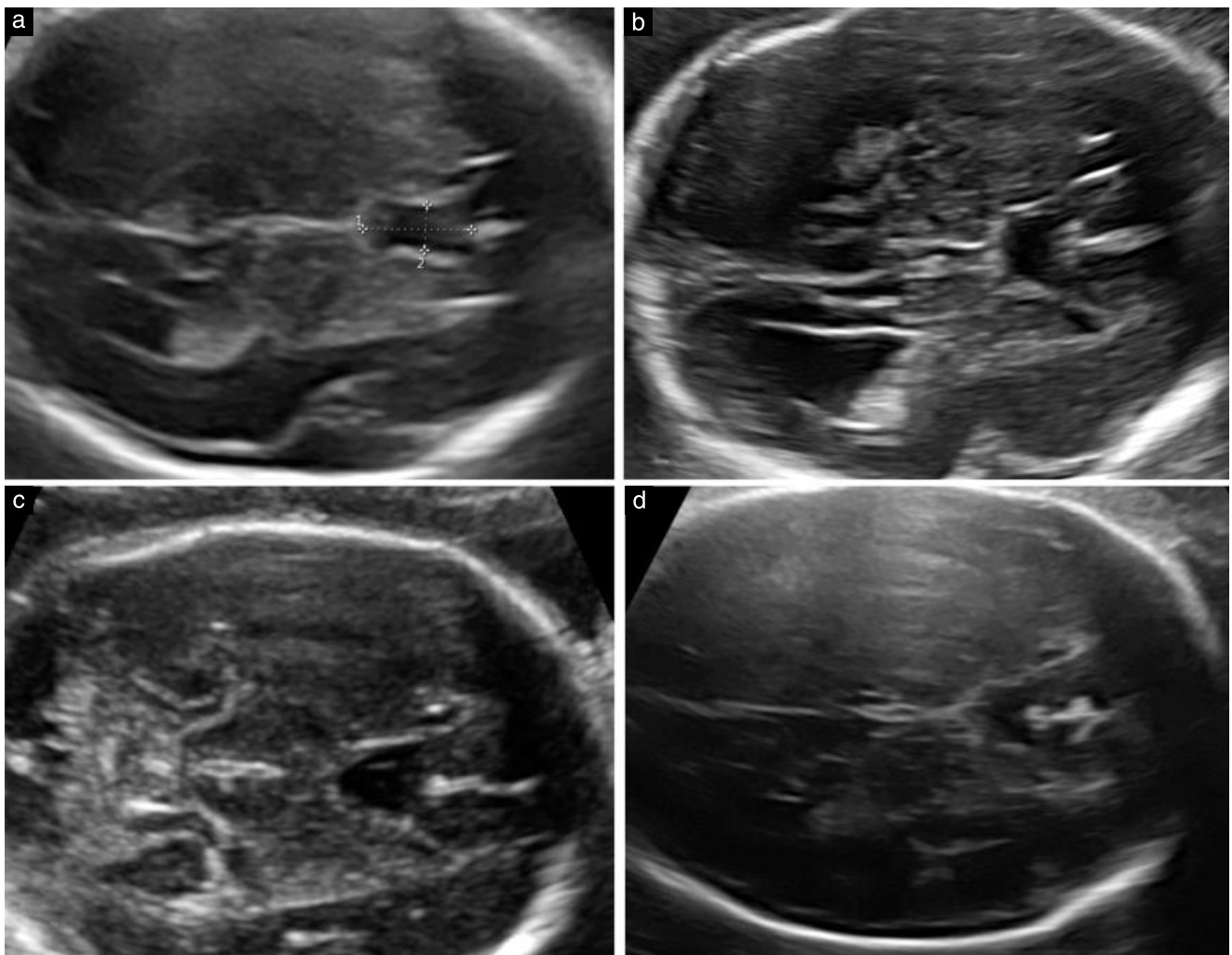


Figure 1 Axial planes of fetal head showing: (a) measurement of width and length of normal cavum septi pellucidi (CSP) at 23 weeks; and (b,c,d) cases of partial agenesis of corpus callosum between 23 and 29 weeks of gestation, with typical abnormal shape of CSP, which is shorter, wider and more square or circular in shape.

Systems, Zipf, Austria) and convex transabdominal probes (RAB 4–8, RM-6C or RAB6C transducer). All ultrasound images are stored in an image archiving system (Viewpoint®, GE Medical Systems), which allows offline measurements. As a standard requirement of our institutions, all patients provided signed informed consent for the fetal examination and agreed to storage of digital images for quality control and later data evaluation. The study included healthy fetuses and fetuses diagnosed with pACC.

For the normal population, we searched the databases of both centers over the 2-year period of 2014 and 2015 for cases in which a 2D image of the corpus callosum with a length measurement was available. Fetuses with only a reconstructed corpus callosum from a 3D volume were excluded. For evaluation of the CSP, the fetal head had to be insonated in the transventricular plane. In this plane, the complete CSP had to be clearly visible (Figure 1). Additional criteria for inclusion were singleton pregnancy and gestational age 20 + 0 to 34 + 0 weeks of gestation, according to last menstrual period and confirmed by an early crown–rump length

measurement. The following conditions were criteria for exclusion: twin pregnancy, fetal growth restriction, diabetic pregnancy and presence of any intracranial or extracranial abnormality or chromosomal aberration.

For the pACC population, the databases were searched for cases with an anomaly of the corpus callosum. Those with cACC and absent CSP, were excluded. Included were all cases with pACC and a CSP present (Figure 1). pACC was defined as interrupted or short corpus callosum, with anteroposterior length < 5th centile^{9,10}. Fetuses with microcephaly, holoprosencephaly or a thickened but not shortened corpus callosum were excluded. Only images from the first examination in which the diagnosis was suspected were considered. When an anomaly of the corpus callosum is suspected, the patient is offered transvaginal fetal neurosonography, fetal magnetic resonance imaging (MRI), a diagnostic invasive procedure, a second opinion and counseling by a neuropediatrician. Postnatal records were analyzed in cases with continuing pregnancy and autopsy reports, if available, were evaluated in cases in which the patient opted for termination of pregnancy.

Data collection and statistical analysis

In both control and study groups, the following data were collected: gestational age at examination, biparietal diameter (BPD, in mm), length of corpus callosum (in mm), associated intracranial signs, such as colpocephaly, ventriculomegaly or anomalies, associated extracerebral anomalies or syndromic conditions, karyotype, if available, and outcome. Length and width of the CSP (in mm) were measured on the images stored in the patient archiving system and the ratio of length to width was then calculated to obtain the CSP ratio. The width of the CSP was measured at the level of the middle of the CSP (Figure 1), as described by Abele *et al.*⁴, and not at its largest point^{11,12}, since some fetuses may have a triangular-shaped CSP¹³. For CSP length, the calipers were placed on the echogenic borders: the callosal sulcus anteriorly and the fornix posteriorly (Figure 1). In order to minimize bias, the final diagnosis was available only at data evaluation. The examiners measuring the CSP were, therefore, unaware of the origin of the images, i.e. whether they were cases or controls. CSP length, width and ratio were then correlated to BPD and regression analysis was performed to assess a possible relationship between length, width, CSP ratio and BPD.

Intraobserver variability was calculated for both operators by having each operator perform two measurements in the same image from 30 normal cases, without seeing the results. Intraobserver agreement was quantified by calculation of the mean difference between measurement 1 and measurement 2 for both operators and using Bland and Altman's 95% limits of agreement (LOA). Interobserver variability was assessed by comparing for the same cases the means of the two measurements of Operators 1 and 2 and calculating the mean difference with 95% LOA. For fetuses with pACC, Z-scores were calculated using the CSP ratio equation and analyzed by *t*-test, comparing the mean values of Z-scores. Analysis was performed using the statistical packages GraphPad Prism and GraphPad InStat for Windows (GraphPad Software, San Diego, CA, USA).

RESULTS

The study population included a total of 343 pregnancies: 323 normal fetuses with a normal corpus callosum length and 20 fetuses with pACC. Detection of pACC was achieved mainly by routine visualization of the corpus callosum in the midsagittal plane at a median age of 22 + 2 weeks with a median BPD of 57 (range, 51–75) mm. Corpus callosum length was, by definition, shorter in cases of pACC than in normal fetuses, using published reference ranges⁹; this was also confirmed after data evaluation, using our own chart, generated from the assessment of normal fetuses (Figure 2).

In the normal population, the length of the CSP increased linearly with increasing head size: CSP length (in mm) = 0.1258 × BPD (in mm) + 2.557 ± 1.211 (Figure 3). The width of the CSP also increased linearly with increasing head size: CSP width (in mm) = 0.006738 × BPD

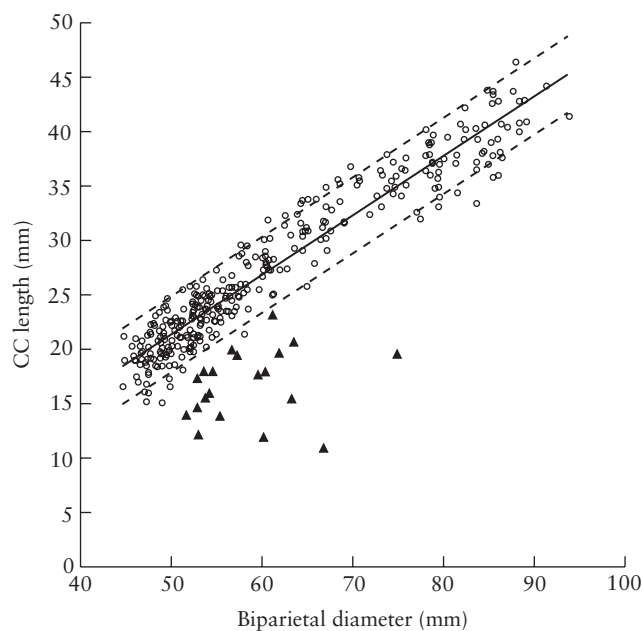


Figure 2 Individual measurements of corpus callosum (CC) length in normal fetuses (O), with reference range (median and 5th and 95th centiles), and in 20 fetuses with partial agenesis of the corpus callosum (▲), in relation to biparietal diameter.

(in mm) + 0.2597 ± 0.6269 (Figure 4). The CSP ratio for the normal population decreased linearly in comparison to head size: CSP ratio = 2.819 – 0.006969 × BPD (in mm) ± 0.3668 (Figure 5).

Of the 20 fetuses with pACC, 17 (85%) had a CSP length < 5th centile (Figure 3) and 13 (65%) had a CSP width > 95th centile (Figure 4) compared with our normal population. The CSP ratio showed the best predictive performance, with 19/20 (95%) fetuses < 5th centile and, considering an empirical cut-off of 1.5, 16/20 (80%) of the fetuses had a ratio below this cut-off (Figure 5). Only 8/20 fetuses with pACC had a CSP ratio < 1, i.e. a CSP width larger than its length, the cut-off proposed by Shen *et al.*⁶ as being diagnostic of pACC. We did not observe false-positive cases with a normal, long corpus callosum and a low CSP ratio. Figure 6 shows the box-and-whisker plot comparing the CSP ratio Z-scores of pACC and normal cases; those with pACC had a significantly smaller CSP ratio ($P < 0.0001$) compared with the normal population.

The Bland–Altman plot with 95% LOA confirmed reliable reproducibility and an absence of systematic error for measurement of CSP width and length and the CSP ratio. The interobserver reliability was found to be high, with intraclass correlation coefficients ranging from 0.904 to 0.978.

Evaluation of the 20 individual cases of pACC showed 11 fetuses with an apparently normal brain, although with a suspected abnormal CSP and anterior complex, as described by the groups of Guibaud and Vinals^{13,14}. In the remaining nine cases, there were associated central nervous system (CNS) findings, some in combination, which included colpocephaly ($n = 5$), lissencephaly ($n = 2$), ventriculomegaly ≥ 10 mm ($n = 2$) and an interhemispheric

cyst ($n = 1$). In eight cases, there were associated non-CNS anomalies, including three chromosomal aberrations, one fetus with Zellweger syndrome diagnosed postnatally, three unknown syndromes and one fetus with ventricular septal defect. There were 13 terminations of pregnancy and seven live births, with one infant death (the case with Zellweger syndrome). The remaining six children were alive and well clinically after 6 months and diagnosis

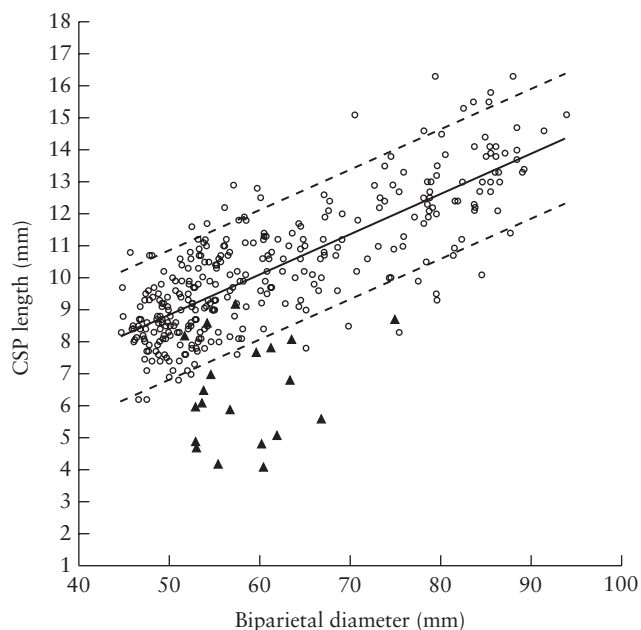


Figure 3 Individual measurements of cavum septi pellucidi (CSP) length in normal fetuses (○), with reference range (median and 5th and 95th centiles), and in 20 fetuses with partial agenesis of the corpus callosum (▲), in relation to biparietal diameter.

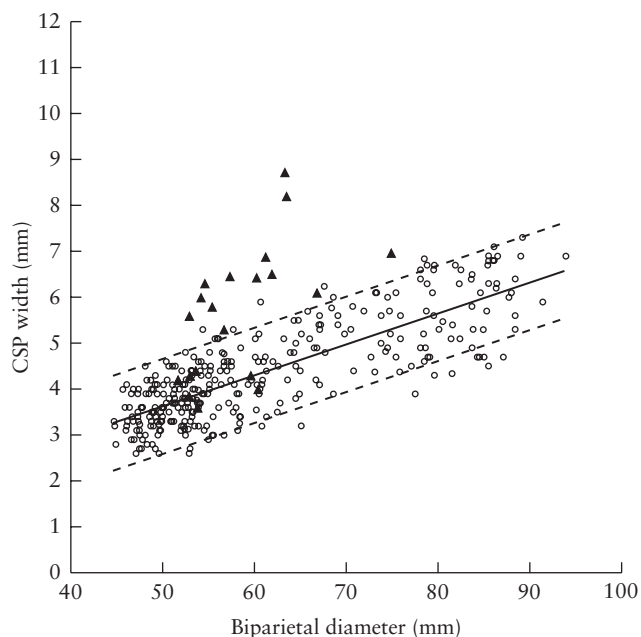


Figure 4 Individual measurements of cavum septi pellucidi (CSP) width in normal fetuses (○), with reference range (median and 5th and 95th centiles), and in 20 fetuses with partial agenesis of the corpus callosum (▲), in relation to biparietal diameter.

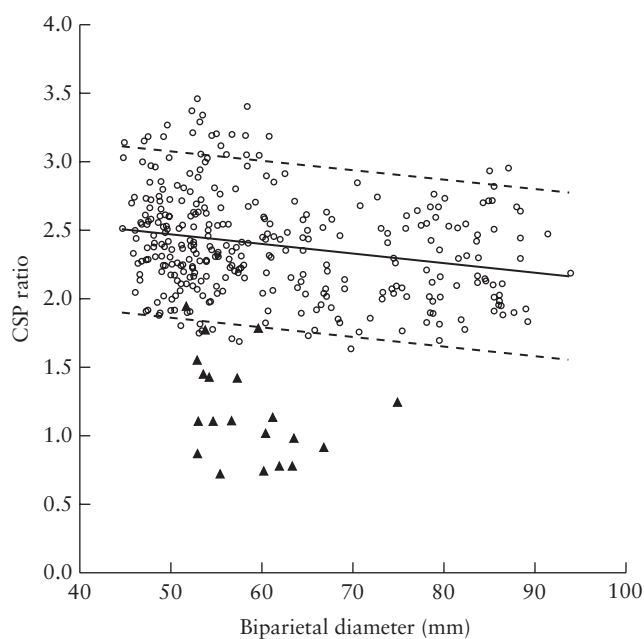


Figure 5 Individual measurements of length-to-width ratio of cavum septi pellucidi (CSP) in normal fetuses (○), with reference range (median and 5th and 95th centiles), and in 20 fetuses with partial agenesis of the corpus callosum (▲), in relation to biparietal diameter.

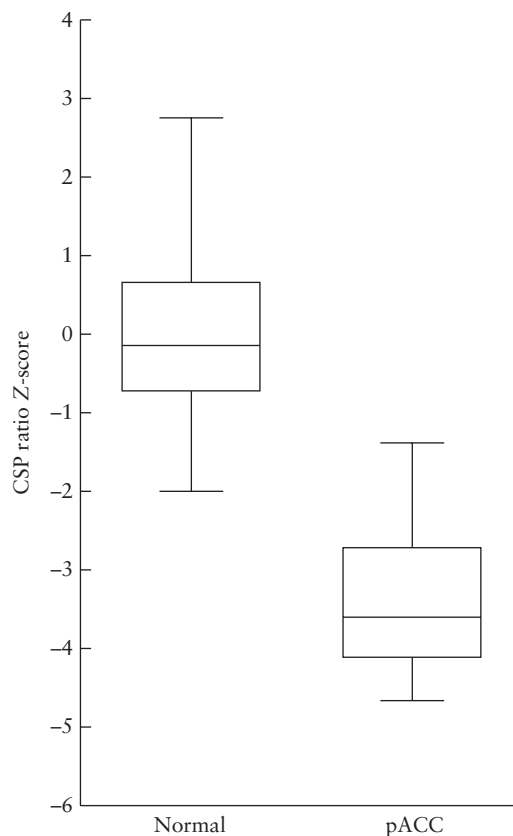


Figure 6 Box-and-whisker plot of cavum septi pellucidi (CSP) ratio (length to width) expressed as Z-score in normal fetuses and in study group of 20 fetuses with partial agenesis of the corpus callosum (pACC). Boxes and internal lines show median and interquartile range and whiskers represent range. Fetuses with pACC had a highly significantly smaller CSP ratio ($P < 0.0001$) compared with normal population.

was confirmed at neonatal neurosonography. Fetal MRI was performed in 13 cases and confirmed the ultrasound diagnosis of pACC. The CSP ratio did not differ between fetuses with and those without CNS anomalies.

DISCUSSION

Visualization of the CSP is part of the International Society of Ultrasound in Obstetrics and Gynecology guidelines for the basic evaluation of the CNS (Figure 1a) and is used as a landmark for identification of the correct axial plane when measuring the BPD^{8,15}. Absence of the CSP is now accepted as the main clue for suspicion of cACC, together with other signs in the axial plane of the fetal head, such as a teardrop configuration of the lateral ventricles, wide interhemispheric fissure and, occasionally, borderline ventriculomegaly and a dilated third ventricle¹⁶. The diagnosis is then confirmed in the midsagittal and coronal views in the context of a fetal neurosonogram^{15–17}. While, in most cases, the signs suggesting cACC are well known and the detection rate in experienced hands is high¹⁶, detection of pACC is, according to Ghi *et al.*, ‘extremely difficult because the corpus callosum is detectable and the axial view of the fetal head is often unremarkable’¹⁸. Our data show, however, that the measurements of CSP length (Figure 3) and width (Figure 4), and the length-to-width ratio (i.e. CSP ratio) (Figure 5), are important hints with the potential to improve the antenatal detection of pACC.

Herrera *et al.*⁷ reported on the increased width of the CSP in 26 fetuses, in 19 (73%) of which there was dysgenesis of the corpus callosum. In a study published recently in this Journal, on fetuses with pACC, Shen *et al.* found that a new hint for pACC was an abnormal, wide CSP, with ‘its width larger than its length’⁶. Our study on 20 fetuses with pACC support these observations, showing, in the majority of cases, an abnormal size and shape of the CSP, visualized in the axial view of the fetal head (Figure 1b–d). We found that the CSP was wide in 13 (65%) and short in 17 (85%) of the 20 cases, and the CSP length-to-width ratio was below the reference range in all except one case (19/20, 95%). We believe that the shape and size of the CSP in the axial plane of the fetal head are simple hints for suspicion of an abnormal corpus callosum, which can be confirmed or excluded on visualization and measurement of the corpus callosum itself in the midsagittal view. We found the sign reported by Shen *et al.*⁶, of a CSP wider than it is longer, corresponding to a ratio ≤ 1 , in only eight (40%) of our 20 cases. Interestingly, this rate of 40% with a CSP ratio < 1 is similar to the 34% rate of abnormal CSP reported by Shen *et al.*⁶, while the remaining 66% of their 56 pACC cases were described as being ‘normal’. We hope that an improved detection rate of pACC can be achieved by observation of the associated abnormal shape of the CSP and its objective quantification using the CSP ratio. In all suspicious cases, the examiner should obtain a midsagittal view of the corpus callosum to confirm or exclude its abnormal size and appearance. pACC with absence of a CSP has been reported with various different frequencies, including 10%¹⁸, 16%¹⁹ and 21%⁶. In our

study, we excluded *a priori* fetuses with pACC in which the CSP was not visualized, as the study focused on the dimensions of the CSP.

It is important to discuss the technique and the level at which CSP is measured, since incorrect measurement may lead to false positives or false negatives with regard to suspicion of pACC. We measured the width of the CSP at the middle, similar to the reported measurements of Abele *et al.*⁴, so our charts are comparable to theirs. In two other studies reporting on normal values, the measurements were obtained at the largest part^{11,12}, which increases the confidence interval. It should be borne in mind that the shape of the CSP is variable between fetuses; a recent evaluation showed that in the transventricular plane, the CSP had a square form in 73% of the normal cases and a triangular form, with anterior base, in 27%¹³. We think that measuring the CSP at the largest part may increase the rate of false-positive diagnosis in normal cases. Interestingly, we found that all except one case in our study had a CSP that was more circular than triangular in shape, so we believe the best level at which to measure its width is the middle.

pACC is diagnosed more frequently in postnatal life than prenatally due to its high association with neurodevelopmental delay^{2,20}. However, these studies may have been affected by selection bias, since they included mainly patients with neurological findings. Several prenatal studies have reported similar neurodevelopmental outcome in fetuses with pACC and those with cACC, with delay in about 25–30% of cases; however, there was a lack of long-term follow-up of the surviving children^{18,19,21,22}. The high rate of termination reflects the strong association of both forms of callosal anomaly with other structural defects and chromosomal or genetic anomalies²¹.

A strength of our study is that we have proposed reference ranges for the CSP width, length and length-to-width ratio, in fetuses with a confirmed normal length and shape of the corpus callosum, and we showed that the majority of fetuses with pACC had abnormal values, particularly of the CSP ratio.

Our study has, however, limitations, especially its retrospective nature and the lack of complete long-term follow-up of the survivors. Another limitation is that it is unknown whether normal fetuses, with a normal-sized corpus callosum, can have a low CSP ratio, a question regarding false positives which can only be assessed in a longitudinal prospective study.

In conclusion, we have shown that evaluation of the CSP in a basic screening examination should include determination not only of its presence or absence but also its shape. An abnormal length-to-width ratio of the CSP, which can be quantified easily, is a simple hint for the possible presence of pACC and should lead to direct insonation of the corpus callosum in the midsagittal view. However, prospective studies are needed in order to show the feasibility of applying this ratio in clinical practice, for the detection of pACC as well as other callosal anomalies.

REFERENCES

- Pilu G, Sandri F, Perolo A, Pittalis MC, Grisolia G, Cocchi G, Foschini MP, Salvioli GP, Bovicelli L. Sonography of fetal agenesis of the corpus callosum: a survey of 35 cases. *Ultrasound Obstet Gynecol* 1993; 3: 318–329.
- Santo S, D'Antonio F, Homfray T, Rich P, Pilu G, Bhide A, Thilaganathan B, Papageorghiou AT. Counseling in fetal medicine: agenesis of the corpus callosum. *Ultrasound Obstet Gynecol* 2012; 40: 513–521.
- Pilu G, Segata M, Ghi T, Carletti A, Perolo A, Santini D, Bonasoni P, Tani G, Rizzo N. Diagnosis of midline anomalies of the fetal brain with the three-dimensional median view. *Ultrasound Obstet Gynecol* 2006; 27: 522–529.
- Abe H, Babiy-Pachomow O, Sonek J, Hoopmann M, Schaelike M, Kagan KO. The cavum septi pellucidi in euploid and aneuploid fetuses. *Ultrasound Obstet Gynecol* 2013; 42: 156–160.
- Chaoui R, Heling K-S, Zhao Y, Sinkovskaya E, Abuhamad A, Karl K. Dilated cavum septi pellucidi in fetuses with microdeletion 22q11. *Prenat Diagn* 2016; 36: 911–915.
- Shen O, Gelot AB, Moutard ML, Jouannic JM, Sela HY, Garel C. Abnormal shape of the cavum septi pellucidi: an indirect sign of partial agenesis of the corpus callosum. *Ultrasound Obstet Gynecol* 2015; 46: 595–599.
- Herrera M, Rebolledo M, Arenas J. Increasing size of the cavum septi pellucidi: sign of midline anomalies of the fetal brain. *Ultrasound Obstet Gynecol* 2015; 46: 12. (Abstract)
- International Society of Ultrasound in Obstetrics & Gynecology Education Committee. Sonographic examination of the fetal central nervous system: guidelines for performing the 'basic examination' and the 'fetal neurosonogram'. *Ultrasound Obstet Gynecol* 2007; 29: 109–116.
- Rizzo G, Pietrolucci ME, Capponi A, Arduini D. Assessment of corpus callosum biometric measurements at 18 to 32 weeks' gestation by 3-dimensional sonography. *J Ultrasound Med* 2011; 30: 47–53.
- Pashaj S, Merz E, Wellek S. Biometry of the fetal corpus callosum by three-dimensional ultrasound. *Ultrasound Obstet Gynecol* 2013; 42: 691–698.
- Jou HJ, Shyu MK, Wu SC, Chen SM, Su CH, Hsieh FJ. Ultrasound measurement of the fetal cavum septi pellucidi. *Ultrasound Obstet Gynecol* 1998; 12: 419–421.
- Falco P, Gabrielli S, Visentin A, Perolo A, Pilu G, Bovicelli L. Transabdominal sonography of the cavum septum pellucidum in normal fetuses in the second and third trimesters of pregnancy. *Ultrasound Obstet Gynecol* 2000; 16: 549–553.
- Vinals F, Correa F, Gonçalves-Pereira PM. Anterior and posterior complexes: a step towards improving neurosonographic screening of midline and cortical anomalies. *Ultrasound Obstet Gynecol* 2015; 46: 585–594.
- Cagneaux M, Guibaud L. From cavum septi pellucidi to anterior complex: how to improve detection of midline cerebral abnormalities. *Ultrasound Obstet Gynecol* 2013; 42: 485–486.
- Karl K, Kainer F, Heling KS, Chaoui R. Fetal neurosonography: extended examination of the CNS in the fetus. *Ultraschall Med* 2011; 32: 342–361.
- Paladini D, Pastore G, Cavallaro A, Massaro M, Nappi C. Agenesis of the fetal corpus callosum: sonographic signs change with advancing gestational age. *Ultrasound Obstet Gynecol* 2013; 42: 687–690.
- Malinger G, Lev D, Oren M, Lerman-Sagie T. Non-visualization of the cavum septi pellucidi is not synonymous with agenesis of the corpus callosum. *Ultrasound Obstet Gynecol* 2012; 40: 165–170.
- Ghi T, Carletti A, Contro E, Cera E, Falco P, Tagliavini G, Michelacci L, Tani G, Youssef A, Bonasoni P, Rizzo N, Pelusi G, Pilu G. Prenatal diagnosis and outcome of partial agenesis and hypoplasia of the corpus callosum. *Ultrasound Obstet Gynecol* 2010; 35: 35–41.
- Volpe P, Paladini D, Resta M, Stanziano A, Salvatore M, Quarantelli M, De Robertis V, Buonadonna AL, Caruso G, Gentile M. Characteristics, associations and outcome of partial agenesis of the corpus callosum in the fetus. *Ultrasound Obstet Gynecol* 2006; 27: 509–516.
- Goodyear PW, Bannister CM, Russell S, Rimmer S. Outcome in prenatally diagnosed fetal agenesis of the corpus callosum. *Fetal Diagn Ther* 2001; 16: 139–145.
- D'Antonio F, Pagani G, Familiari A, Khalil A, Sagies T-L, Malinger G, Leibovitz Z, Garel C, Moutard M-L, Pilu G, Bhide A, Acharya G, Leombroni M, Manzoli L, Papageorghiou A, Prefumo F. Outcomes associated with isolated agenesis of the corpus callosum: a meta-analysis. *Pediatrics* 2016; 138: e20160445–e20160445.
- Moutard M-L, Kieffer V, Feingold J, Lewin F, Baron J-M, Adamsbaum C, Gelot A, Isapof A, Kieffer F, de Villemeur TB. Isolated corpus callosum agenesis: a ten-year follow-up after prenatal diagnosis (how are the children without corpus callosum at 10 years of age?). *Prenat Diagn* 2012; 32: 277–283.



ISUOG Practice Guidelines: performance of fetal magnetic resonance imaging

Clinical Standards Committee

The International Society of Ultrasound in Obstetrics and Gynecology (ISUOG) is a scientific organization that encourages sound clinical practice, and high-quality teaching and research related to diagnostic imaging in women's healthcare. The ISUOG Clinical Standards Committee (CSC) has a remit to develop Practice Guidelines and Consensus Statements as educational recommendations that provide healthcare practitioners with a consensus-based approach, from experts, for diagnostic imaging. They are intended to reflect what is considered by ISUOG to be the best practice at the time at which they are issued. Although ISUOG has made every effort to ensure that Guidelines are accurate when issued, neither the Society nor any of its employees or members accepts any liability for the consequences of any inaccurate or misleading data, opinions or statements issued by the CSC. The ISUOG CSC documents are not intended to establish a legal standard of care because interpretation of the evidence that underpins the Guidelines may be influenced by individual circumstances, local protocol and available resources. Approved Guidelines can be distributed freely with the permission of ISUOG (info@isuog.org).

These guidelines are based on consensus reached between participants following a survey of current practices, conducted by ISUOG in 2014 (Appendix S1).

INTRODUCTION

Fetal magnetic resonance imaging (MRI) is an important diagnostic imaging adjunct to ultrasonography¹, particularly for the assessment of fetal brain development². A survey conducted by ISUOG in 2014 (Appendix S1), in which 60 international perinatal centers participated, showed that fetal MRI is being performed in one or more centers in at least 27 countries worldwide. However, the quality of imaging, sequences used and operator experience appear to differ widely between centers³.

The impact of such differences should be reduced by development of guidelines to define better the role of fetal MRI in relation to prenatal diagnostic ultrasound. The aim of this document is to provide information on state-of-the-art fetal MRI for those performing the examination, as well as for clinicians interpreting the results.

What is the purpose of fetal MRI?

The purpose of fetal MRI is to complement an expert ultrasound examination^{4,5}, either by confirmation of the ultrasound findings or through the acquisition of additional information⁶. MRI is not currently used as a primary screening tool in prenatal care, although standardized and complete assessment of the fetal anatomy is probably feasible. Figure 1 presents the survey participants' opinions regarding indications for which MRI can provide useful information.

Is fetal MRI a safe procedure?

MRI is not associated with known adverse fetal effects at any point in pregnancy, when performed without administration of contrast media⁷. There are no reported adverse effects of MRI performed at 1.5 Tesla (1.5 T)⁸. However, there have been no human studies of possible adverse effects at higher field strength, such as 3.0 T^{7,9,10}, although recent data show that it may be safe in a porcine model¹¹.

Under which circumstances should fetal MRI be performed?

There is general consensus that fetal MRI is indicated following an expert ultrasound examination in which the diagnostic information about an abnormality is incomplete. Under these circumstances, MRI may provide important information that may confirm or complement the ultrasound findings and alter or modify patient management.

Presently, factors influencing the decision to perform fetal MRI include, but are not limited to: experience/equipment of the ultrasound and MRI facilities, accessibility to MRI, maternal conditions, gestational age, safety concerns, legal consideration regarding termination of pregnancy (TOP) and parental wishes after appropriate counseling^{3,10,12,13}.

The ISUOG survey addressed the necessity of MRI for selected indications and used a 7-point rating scale to weight the responses from 0 (not at all indicated) to 7 (definitely indicated) (Figure 1). The variety of responses is likely to reflect the divergence seen between various specialties and the spectrum of pathologies seen at each

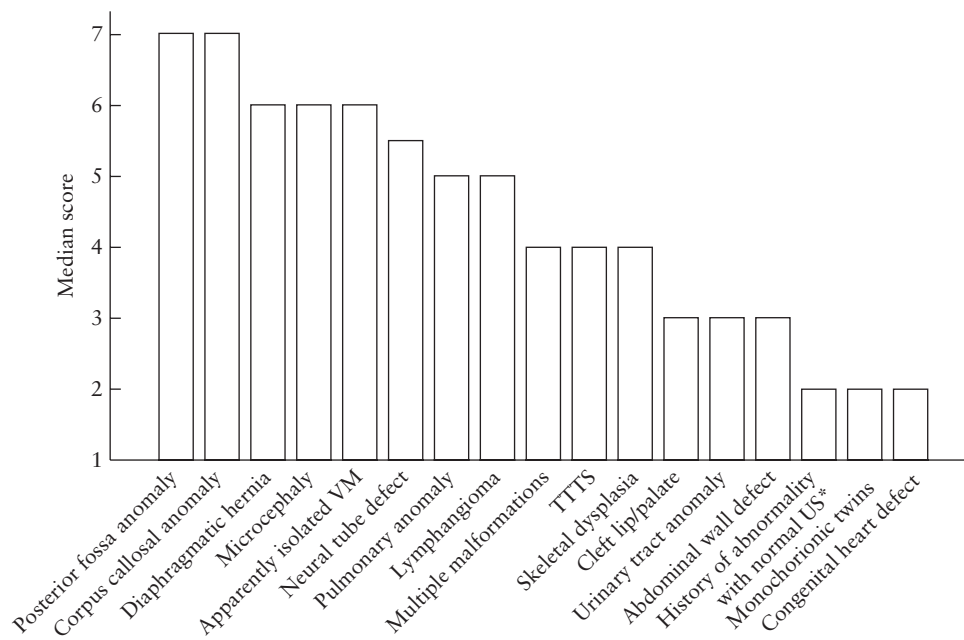


Figure 1 Results of ISUOG survey on indications for fetal magnetic resonance imaging (MRI), rated on a scale from 0 (fetal MRI not at all indicated) to 7 (definitely an indication for fetal MRI). *History of abnormality in previous pregnancy or in family member, with normal ultrasound (US) findings in current pregnancy. TTTS, twin–twin transfusion syndrome; VM, ventriculomegaly.

Table 1 The multidisciplinary team: proposed participants and their role in performing fetal magnetic resonance imaging (MRI)

Participant	Role
Obstetrician, radiologist	Performs sonographic/neurosonographic examination; provides information to parent(s) regarding findings and possible diagnoses; provides counseling; indicates need for fetal MRI
Radiologist, obstetrician	Available during MRI examination for acquisition of appropriate planes and changes of protocol as needed; interpretation and reporting of findings; provides counseling
Multidisciplinary team when available/necessary: obstetrician, pediatric radiologist or neuroradiologist, pediatric neurologist, geneticist, other pediatric subspecialist, social worker, psychologist	Provides counseling and recommendations based on neurosonography, MRI, genetic findings, laboratory findings and/or family history

center. The opinions may also reflect different levels of experience when performing fetal ultrasound and MRI.

In general, performance of an ultrasound examination following only the minimum recommendations for second-trimester ultrasound/basic brain examination, as proposed by ISUOG⁵, is insufficient prior to requesting MRI. Additional views, such as orthogonal views, higher frequency probes and/or transvaginal imaging are required to detail the specific abnormality^{14,15}.

The practice of TOP and associated medicolegal implications may influence the use of fetal MRI at local institutions. In countries in which the decision about TOP has to be made before 24 weeks, the performance of MRI prior to this time may help an individual couple decide on the future of their pregnancy; however, in general, MRI is better reserved for later in the second or third trimester¹³. Although available data are still inconclusive, MRI for parental reassurance regarding the absence of associated pathologies in fetuses with apparently isolated conditions may be recommended

in fetuses with isolated ventriculomegaly¹⁶, agenesis of the corpus callosum¹⁷, absent septum pellucidum and cerebellar or vermian anomalies¹⁸. In addition, fetal MRI has been found to be helpful in mono chorionic twin pregnancies after iatrogenic or natural demise of a cotwin to find pathological changes in the surviving twin^{19,20}.

At what gestational age should fetal MRI be performed?

Fetal MRI performed before 18 weeks does not usually provide information additional to that obtained on ultrasound examination. In some cases, additional information can be obtained before 22 weeks¹³ but MRI becomes increasingly helpful thereafter. Specific examples of pathologies that can be evaluated in the third trimester include, but are not limited to, those of cortical development and neck masses that may cause airway compromise²¹. Most organs can be visualized in detail between 26 and 32 weeks of pregnancy, when pathologies related to abnormal development are more

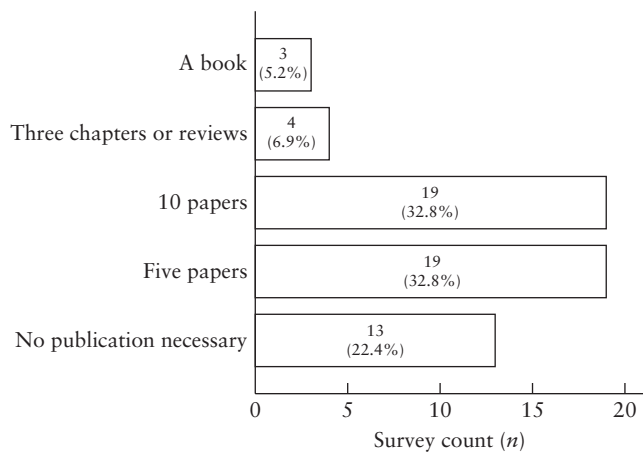


Figure 2 Results of ISUOG survey regarding how much an institution should have published in the field of fetal magnetic resonance imaging in order to qualify as a teaching center.

fully evolved, but each pregnancy and each fetus will differ. It may become more difficult for the woman to stay comfortable in the scanner with advancing gestation and consideration of left-lateral offset is recommended.

Who should perform fetal MRI?

When indicated, performed properly and interpreted correctly, MRI not only contributes to diagnosis but may be an important component of treatment choice, delivery planning and counseling. Practitioners who interpret fetal MRI should be familiar with fetal diagnosis, as it differs from diagnosis in other patient populations. Choice of appropriate protocols and techniques requires extensive training; thus, the performance of fetal MRI should be limited to individuals with specific training and expertise. The same applies to interpretation of the examination. In many centers this will require a multispecialty collaborative approach, including experts in the field of prenatal diagnosis, perinatology, neonatology, pediatric neurology and neuroradiology, genetics and other related specialties (Table 1), in order to integrate the clinical and family histories and the ultrasound and MRI findings, to optimize patient care. Consultation with a geneticist and other pediatric subspecialists may be required in order to provide the patient with the best counseling and management options.

Table 2 Steps in performance of fetal magnetic resonance imaging (MRI)

Indication	Dependent on quality of previous ultrasound examinations, clinical question and gestational age
Counseling of pregnant woman	Explanation of indication, performance, expected outcome and consequences of the procedure, information about the possibility of an accompanying person, discussion with respect to contraindications and claustrophobia and sedative drug prescription if necessary
Prerequisites for MRI unit	Written referral with clear indication of clinical question(s), ultrasound report and images (if possible), gestational age confirmed/determined by first-trimester ultrasound
At the MRI unit	Clarification of possible contraindications, comfortable positioning of woman (either supine or lateral decubitus position), adequate coil positioning, performance of examination according to pertinent protocol
After examination	Inform patient about when the report will be ready; in the case of immediate consequences resulting from MRI examination, information regarding results should be provided promptly to the referring physician
Storage of images, report	Electronic storage of images, analysis of images, structured reporting (Table 3)

Where should a practitioner train for fetal MRI?

Although at present we are unaware of the existence of a recognized fetal MRI specialization, individuals who perform fetal MRI should have undergone specialized training in collaboration with a teaching center, enabling them to perform a state-of-the-art fetal MRI examination after a sufficient amount of cases (GOOD PRACTICE POINT; i.e. recommended best practice based on the clinical experience of the guideline development group).

A teaching center is defined as an institution that is able to teach students, physicians and radiographers/technologists skillful performance of fetal MRI. In order to qualify as a teaching center certain requirements should be fulfilled, which include:

1. multidisciplinary specialists working in the field, including, but not limited to, fetomaternal specialists, radiologists and obstetricians;
2. institutional experience, with at least 500 fetal MRIs and at least two examinations performed per week;
3. publication of scientific papers or reference material in this field (Figure 2).

RECOMMENDATIONS

Performance of fetal MRI according to standardized criteria (Table 2) will improve the management of pregnancies complicated by a fetal malformation or acquired condition (GOOD PRACTICE POINT).

How should fetal MRI be performed?

Field strength

At present, 1.5 T is the most commonly used field strength, providing acceptable resolution even as early as 18 weeks²². 3 T has the potential to provide images with higher resolution and better signal-to-noise ratio than does 1.5 T, while maintaining a comparable or lower energy deposition²². Nonetheless, higher field strength is currently not recommended for *in-vivo* fetal imaging¹⁰.

Course of examination

1. Exclude contraindications for MRI²².

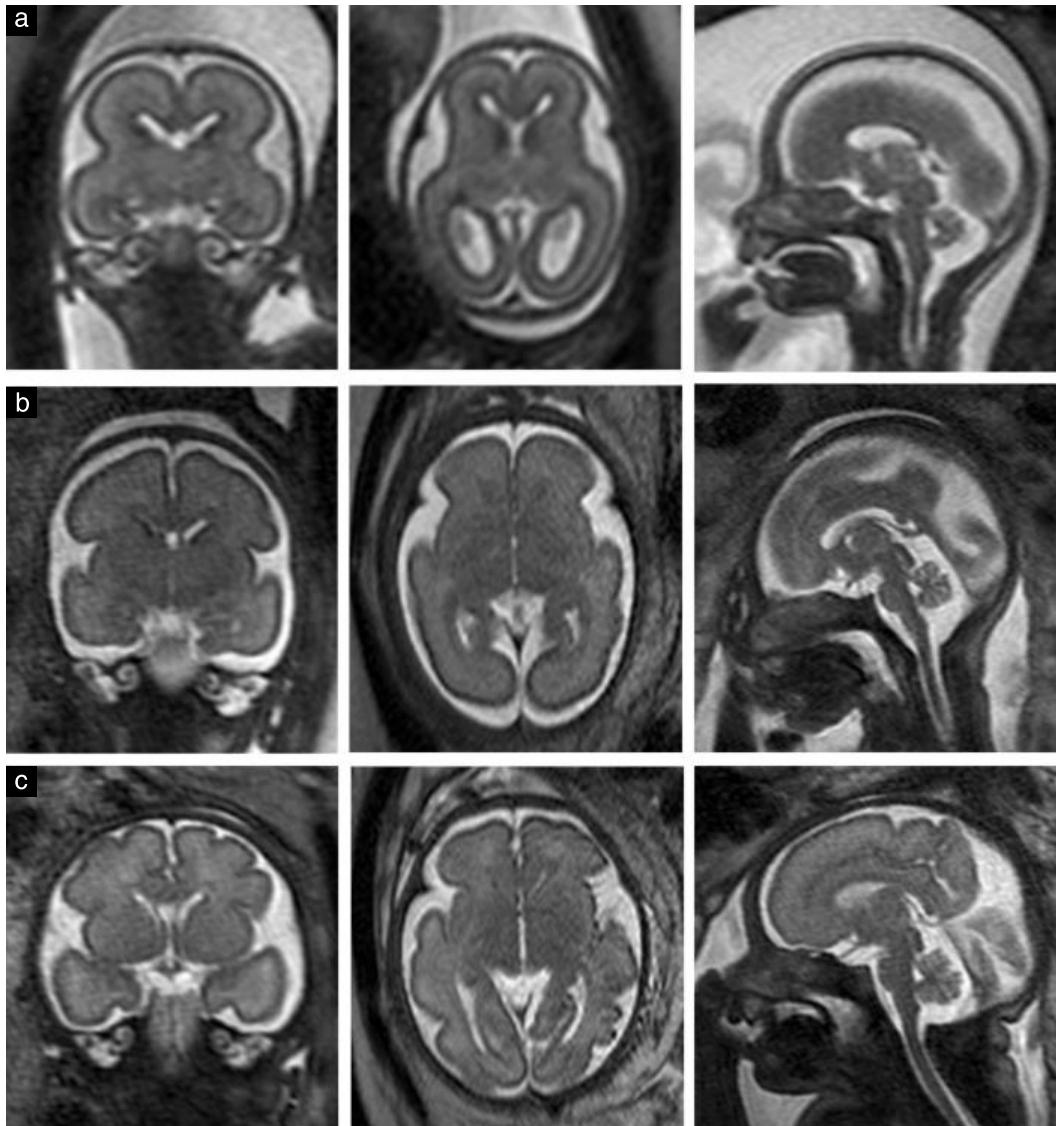


Figure 3 Coronal, axial and sagittal (left to right) T2-weighted fast (turbo) spin-echo sequences (with long echo time) of normal fetal brain at 21+0 (a), 28+1 (b) and 31+1 (c) weeks.

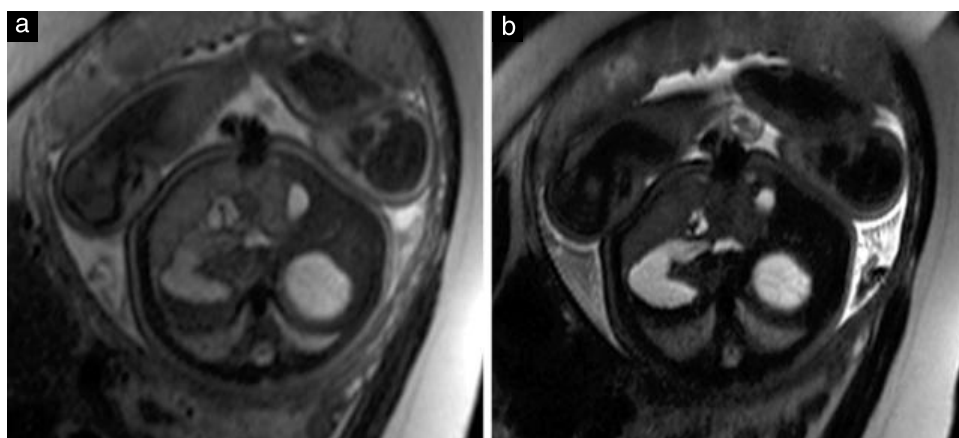


Figure 4 Axial T2-weighted fast (turbo) spin-echo sequences in a normal 39+4-week fetus showing how a shorter echo time (TE) gives greater detail of the fetal body: (a) TE = 80 ms; (b) TE = 140 ms.

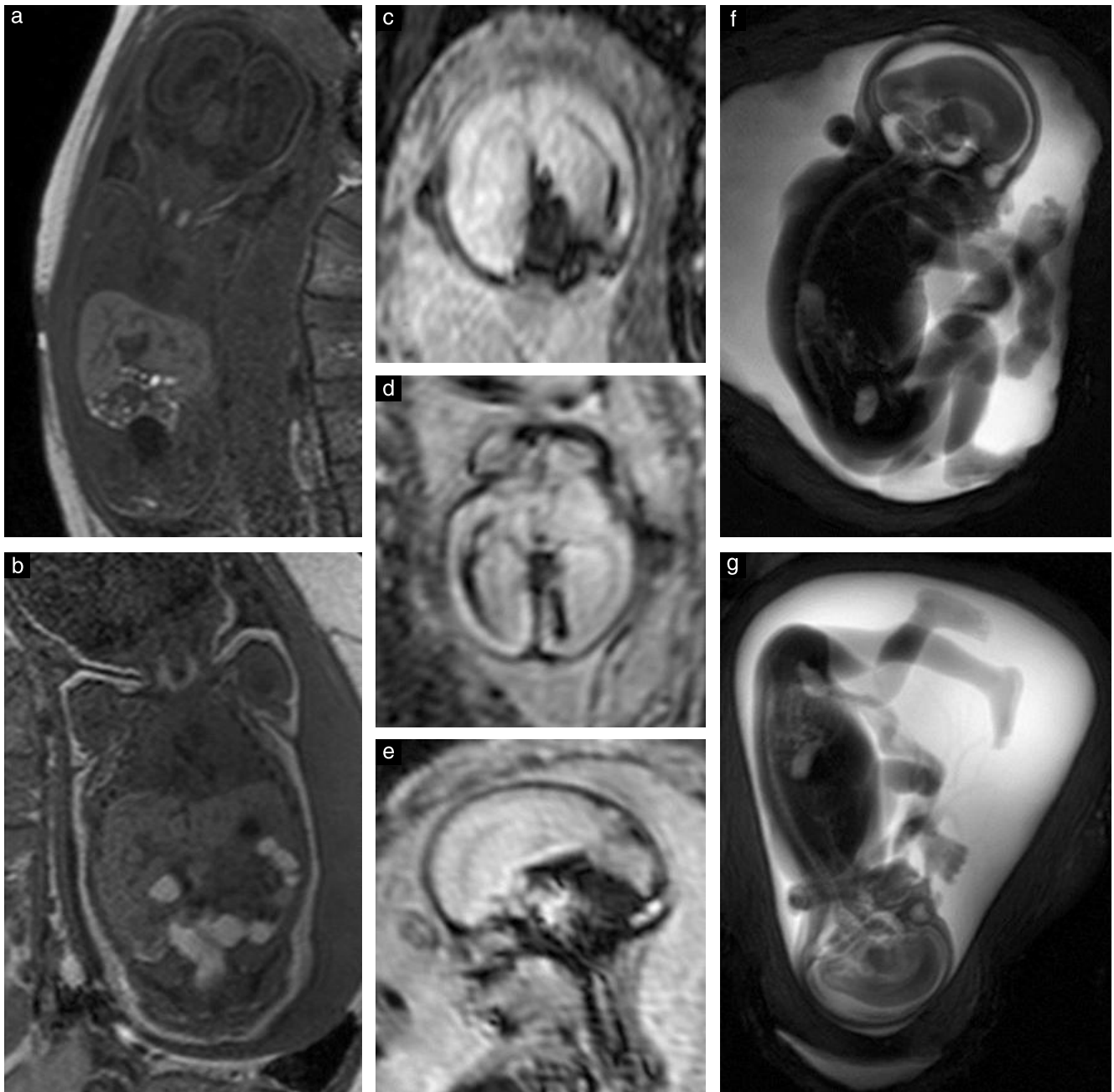


Figure 5 T2-weighted contrast is the mainstay of fetal magnetic resonance imaging (MRI). Other sequences include: T1-weighted MRI (a,b), used here in normal fetuses at 27 + 1 (a) and 38 + 3 (b) weeks of gestation, showing hyperintensity of the thyroid gland and meconium-filled bowel loops; single-shot high-resolution gradient echo echoplanar sequences, seen here in coronal (c), axial (d) and sagittal (e) planes in a 22 + 6-week fetus with an intracranial hemorrhage, showing hypointense blood-breakdown products; and magnetic resonance cholangiopancreatography sequence (40 mm thick), used here in a 24 + 4-week fetus with a cardiac malformation (not shown) (f) and a 20 + 1-week fetus with genu recurvatum (g), which allows detection of proportions and positions of hands and feet.

2. Obtain informed consent from the pregnant woman.
3. Note gestational age, ideally as assessed by first-trimester ultrasound²³, and pertinent prior clinical assessment and ultrasound findings.
4. Consider using sedation to reduce fetal movements and/or artifacts, and in anxious or claustrophobic patients.
5. Place the patient on the table in a comfortable position²⁴.
6. In some cases, and according to the safety regulations at the particular institution, consider accommodation of an accompanying person in the examination room²⁵.
7. Acquire localizer sequences.
8. Ensure correct coil placement, with first organ of interest in the center of the coil; plan for next sequences.
9. Assess the primary organ of interest.
10. When indicated, proceed to perform a complete examination of the whole fetus and the extrafetal structures (including umbilical cord, placenta and maternal cervix).



Figure 6 Sagittal T2-weighted magnetic resonance image of a normal 21 + 5-week fetus, showing the profile with intact palate.

11. Inform referring physician expeditiously if a condition becomes apparent that needs rapid intervention, such as suspected placental abruption or hypoxic ischemic fetal brain injury.

Choice of sequences

1. T2-weighted contrast is the mainstay of fetal MRI and is usually achieved using T2-weighted fast (turbo) spin-echo (SE) or steady-state free-precession (SSFP) sequences. Fast (turbo) SE sequences with long echo time (TE) should be used in imaging of the fetal brain (Figure 3). A shorter TE gives more contrast in the fetal body (Figure 4). SSFP sequences provide T2 information in moving fetuses and allow, for instance, the differentiation of vessels from solid tissue²⁶.
2. T1-weighted contrast is acquired by the use of two-dimensional gradient echo (GRE) sequences at 1.5 T. An average duration of 15 s permits perfor-

mance during a maternal breath-hold, which facilitates the acquisition of images that are free from movement artifacts²⁷. T1-weighted contrast identifies methemoglobin in subacute hemorrhage, calcification, glands and meconium²⁷ (Figure 5a,b).

3. Single-shot high-resolution (SSH) GRE echoplanar (EP) sequences are used to visualize bony structures, calcification and the breakdown products of blood, such as deoxyhemoglobin, which suggests a recent bleed, or hemosiderin, which represents an older hemorrhage²⁸ (Figure 5c–e).
4. Optional sequences include: diffusion-weighted imaging, diffusion tensor imaging, dynamic SSFP sequences and SSH magnetic resonance cholangiopancreatography sequences, which supply three-dimensional-like images (Figure 5f,g).

In all cases, the field-of-view should be adjusted to the region of interest. A slice thickness of 3–5 mm with a 10–15% intersection gap will be appropriate in most cases. The examination should include at least T2 information in three orthogonal planes of the fetal brain and body, and T1- and GRE-EP sequences in one or two planes, preferably frontal and sagittal.

This ‘minimum’ protocol should be executable in less than 30 min, even allowing for fetal movement and sequence repetition. Only examinations that are performed following this protocol should be regarded as ‘state of the art’ (GOOD PRACTICE POINT).

Standardized planes for fetal brain examination

1. Sagittal sections through the head, including a mid-sagittal plane depicting the corpus callosum, aqueduct and pituitary.
2. Coronal sections parallel to the brainstem with symmetrical visualization of the inner ear structures.
3. Axial sections, perpendicular to the sagittal sections, parallel to the course of the corpus callosum (or skull base in the case of absence of the corpus callosum), with lateral symmetry adjusted according to the coronal sections.

Table 3 Structured report for detailed fetal magnetic resonance imaging examination

Method	Imaging conditions (e.g. degradation by fetal movement, maternal obesity, premature termination of examination), field strength, coil, sequences, planes
Head	Profile, hard and soft palate (Figure 6), skull, ocular measurements
Brain	Age-related sulcation and gyration, lamination of brain parenchyma (after 30 weeks: myelination and premyelination), ventricular system, cerebellum, midline structures and width of cerebrospinal fluid spaces (Figure 3)
Chest	Configuration of thorax, lung signals, gross regularity of heart (not examined in detail) (Figure 7a,b)
Abdomen	Fetal situs, stomach and gallbladder (fluid filling), fluid and meconium signals of bowels (Figure 7c,d), kidneys, urinary bladder (fluid filling); on request: female/male external genitals (in case of latter: descent of testes) (Figure 8)
Extrafetal structures	Umbilical cord (number of vessels), amount of amniotic fluid, position and characteristics of placenta, cervical length (Figure 9) only if substantially shortened
Skeleton (when examined)	Course and completeness of spine, shape, length and position of bones, fingers and toes (not always possible to assess, especially in presence of minimal amniotic fluid, i.e. after 32–35 weeks)

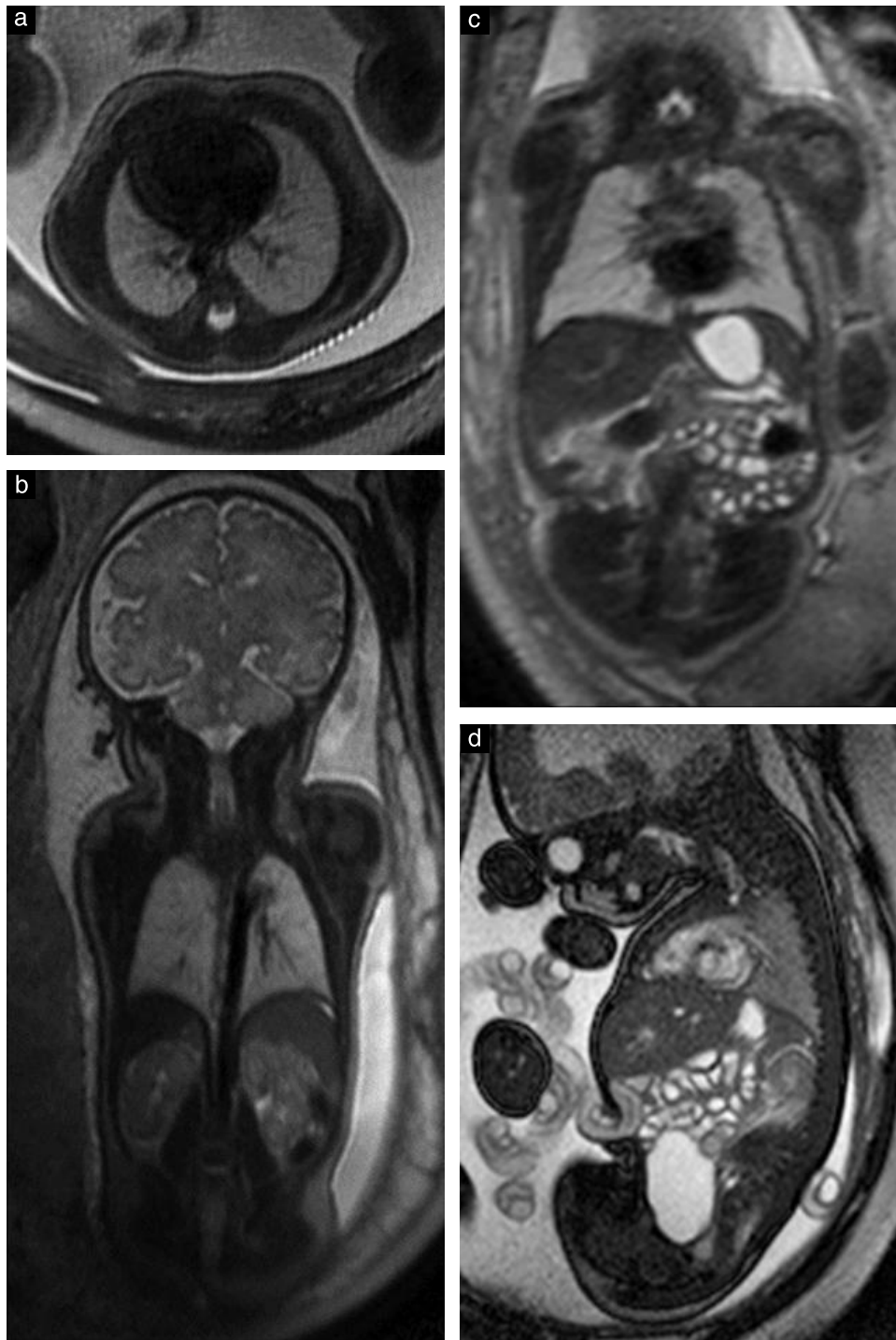


Figure 7 Magnetic resonance imaging (MRI) of normal fetal chest (a,b) and abdomen (c,d). (a) Axial T2-weighted MRI in a 34 + 2-week fetus, showing normally shaped thorax and lungs with age-matched regular signals; (b) coronal image at 35 + 3 weeks, showing additionally parts of liver, kidneys and adrenal gland on right side. (c) Coronal T2-weighted MRI in a 32 + 2-week fetus, displaying fluid-filled stomach and bowel loops; (d) sagittal steady-state free-precession image in a 35 + 6-week fetus, showing in addition the fluid-filled urinary bladder. Note hyperintensity of the heart in (d), in contrast to T2-weighted image (c).

Standardized planes for fetal body examination

These are more difficult to achieve, as the fetus is usually in a position that will not allow strictly orthogonal placement of slices.

1. Sagittal sections can be achieved by placing the middle slice through the thoracic spine and the umbilical cord insertion.
2. Coronal sections have to be adjusted to the course of the spine (parallel to the thoracic spine and the frontal body wall at the level of the abdomen).
3. Axial slices should be perpendicular to the long axis of the spine at the level of the region of interest. To perform lung volumetry, for instance, the axial sections should be perpendicular to the thoracic spine.

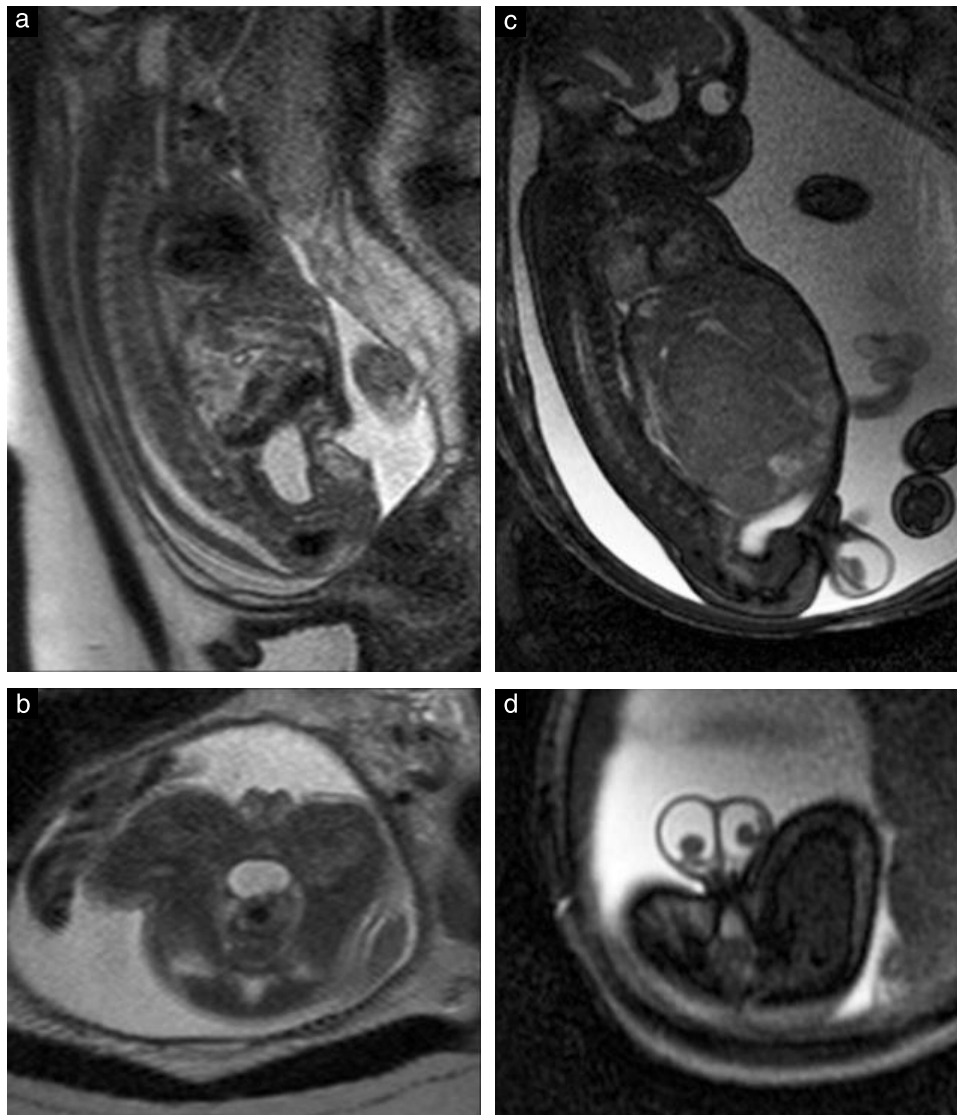


Figure 8 T2-weighted sagittal (a) and axial (b) magnetic resonance images in a normal 31 + 1-week female fetus, showing external genitalia. Steady-state free-precession sagittal (c) and axial (d) images in a 35 + 1-week male fetus with descended testes and hydrocele, in this case as a consequence of a liver tumor.

Although usually measurements will already have been made with ultrasound, measuring certain structures at the MRI examination may be of benefit in particular cases¹². When measuring fluid-containing structures, it is important to remember that MRI measurements are usually around 10% greater than the corresponding ultrasound measurements. In lung volumetry, normal gestational-age related MRI measurements correlate with fetal body volume²⁹ and are considered predictive of outcome in cases of lung pathology³⁰.

Storage of magnetic resonance images

The whole examination should be stored according to local practice, preferably in electronic format. CDs of the examinations can be produced for the patient to enable second-opinion assessment (GOOD PRACTICE POINT).

Reporting

Two types of examination should be distinguished clearly and identified in the report:

1. A targeted examination, which looks only for a certain category of fetal anomaly. The aim is to target a specific organ or address a particular question and not to evaluate the entire fetus.
2. A detailed examination, which includes a standardized evaluation of the whole fetal anatomy in a similar way to that described by the ISUOG guidelines⁵ for second-trimester ultrasound (or other locally used guidelines) (Table 3). This examination may include structures less amenable to MRI than to ultrasound examination, for example cardiac structures. Extrafetal structures, such as the umbilical cord, placenta and cervix, and the amniotic fluid (amount and signal intensity), should be described when indicated clinically. Structures not sought routinely in these examinations need to be indicated clearly in the report.

Standardized reports should follow the suggested structure outlined in Table 3 (GOOD PRACTICE POINT).

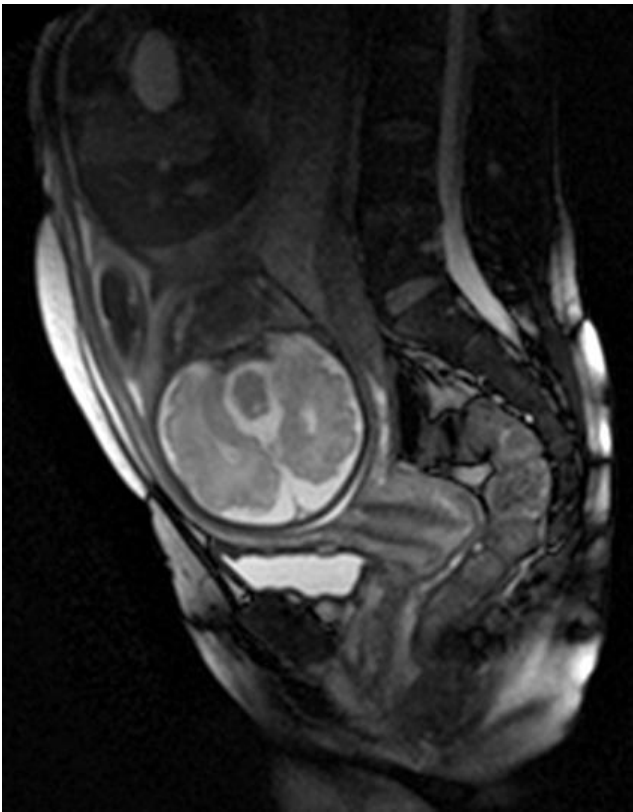


Figure 9 T2-weighted sagittal magnetic resonance image through maternal abdomen, showing normal cervix at 33 weeks' gestation.

As MRI is usually not a first-line examination, but a complementary examination following an ultrasound examination performed in the second trimester³¹, the emphasis of the examination and report should be on structures that are more difficult to assess with ultrasound. A detailed anatomical assessment may be performed on demand.

GUIDELINE AUTHORS

D. Prayer*, Division of Neuroradiology and Musculoskeletal Radiology, Department of Radiology, Medical University of Vienna, Vienna, Austria
G. Malinger*, Division of Ultrasound in Obstetrics & Gynecology, Lis Maternity Hospital, Sourasky Medical Center and Sackler Faculty of Medicine, Tel Aviv University, Tel Aviv, Israel
P. C. Brugger, Division of Anatomy, Center for Anatomy and Cell Biology, Medical University of Vienna, Vienna, Austria
C. Cassidy, Texas Children's Hospital and Fetal Center, Houston, TX, USA
L. De Catte, Department of Obstetrics & Gynecology, University Hospitals Leuven, Leuven, Belgium
B. De Keersmaecker, Department of Obstetrics & Gynecology, University Hospitals Leuven, Leuven, Belgium
G. L. Fernandes, Fetal Medicine Unit, Department of Obstetrics, ABC Medicine University, Santo Andre, Brazil

P. Glanc, Departments of Radiology and Obstetrics & Gynecology, University of Toronto and Sunnybrook Research Institute, Obstetrical Ultrasound Center, Department of Medical Imaging, Body Division, Sunnybrook Health Sciences Centre, Toronto, Canada

L. F. Gonçalves, Fetal Imaging, William Beaumont Hospital, Royal Oak and Oakland University William Beaumont School of Medicine, Rochester, MI, USA

G. M. Gruber, Division of Anatomy, Center for Anatomy and Cell Biology, Medical University of Vienna, Vienna, Austria

S. Laifer-Narin, Division of Ultrasound and Fetal MRI, Columbia University Medical Center - New York Presbyterian Hospital, New York, NY, USA

W. Lee, Department of Obstetrics and Gynecology, Baylor College of Medicine and Texas Children's Pavilion for Women, Houston, TX, USA

A.-E. Millischer, Radiodiagnostics Department, Hôpital Necker-Enfants Malades, Assistance Publique-Hôpitaux de Paris, Université Paris Descartes, Paris, France

M. Molho, Diagnostique Ante Natal, Service de Neuroradiologie, CHU Sud Réunion, St Pierre, La Réunion, France

J. Neelavalli, Department of Radiology, Wayne State University School of Medicine, Detroit, MI, USA

L. Platt, Department of Obstetrics and Gynecology, David Geffen School of Medicine, Los Angeles, CA, USA

D. Pugash, Department of Radiology, University of British Columbia and Department of Obstetrics and Gynecology, BC Women's Hospital, Vancouver, Canada

P. Ramaekers, Prenatal Diagnosis, Department of Obstetrics and Gynecology, Ghent University Hospital, Ghent, Belgium

L. J. Salomon, Department of Obstetrics, Hôpital Necker-Enfants Malades, Assistance Publique-Hôpitaux de Paris, Université Paris Descartes, Paris, France

M. Sanz, Department of Obstetrics and Gynecology, Baylor College of Medicine and Texas Children's Pavilion for Women, Houston, TX, USA

I. E. Timor-Tritsch, Division of Obstetrical & Gynecological Ultrasound, NYU School of Medicine, New York, NY, USA

B. Tutschek, Department of Obstetrics & Gynecology, Medical Faculty, Heinrich Heine University, Düsseldorf, Germany and Prenatal Zurich, Zürich, Switzerland

D. Twickler, University of Texas Southwestern Medical Center, Dallas, TX, USA

M. Weber, Division of Neuroradiology and Musculoskeletal Radiology, Department of Radiology, Medical University of Vienna, Vienna, Austria

R. Ximenes, Fetal Medicine Foundation Latin America, Centrus, Campinas, Brazil

N. Raine-Fenning, Department of Child Health, Obstetrics & Gynaecology, School of Medicine, University of Nottingham and Nurture Fertility, The Fertility Partnership, Nottingham, UK

*D. P. and G. M. contributed equally to this article.

CITATION

These Guidelines should be cited as: 'Prayer D, Malinge G, Brugger PC, Cassady C, De Catta L, De Keersmaecker B, Fernandes GL, Glanc P, Gonçalves LF, Gruber GM, Laifer-Narin S, Lee W, Millischer A-E, Molho M, Neelavalli J, Platt L, Pugash D, Ramaekers P, Salomon LJ, Sanz M, Timor-Tritsch IE, Tutschek B, Twickler D, Weber M, Ximenes R, Raine-Fenning N. ISUOG Practice Guidelines: performance of fetal magnetic resonance imaging. *Ultrasound Obstet Gynecol* 2017; **49**: 671–680.'

REFERENCES

- Hedrick HL, Flake AW, Crombleholme TM, Howell LJ, Johnson MP, Wilson RD, Adzick NS. History of fetal diagnosis and therapy: Children's Hospital of Philadelphia experience. *Fetal Diagn Ther* 2003; **18**: 65–82.
- Jokhi RP, Whitby EH. Magnetic resonance imaging of the fetus. *Dev Med Child Neurol* 2011; **53**: 18–28.
- Malinge G, Lev D, Lerman-Sagie T. Is fetal magnetic resonance imaging superior to neurosonography for detection of brain anomalies? *Ultrasound Obstet Gynecol* 2002; **20**: 317–321.
- Sonographic examination of the fetal central nervous system: guidelines for performing the 'basic examination' and the 'fetal neurosonogram'. *Ultrasound Obstet Gynecol* 2007; **29**: 109–116.
- Salomon LJ, Alfirevic Z, Berghella V, Bilardo C, Hernandez-Andrade E, Johnsen SL, Kalache K, Leung KY, Malinge G, Munoz H, Prefumo F, Toi A, Lee W. Practice guidelines for performance of the routine mid-trimester fetal ultrasound scan. *Ultrasound Obstet Gynecol* 2011; **37**: 116–126.
- Jakab A, Pogledic I, Schwartz E, Gruber G, Mitter C, Brugger PC, Langs G, Schopf V, Kasprian G, Prayer D. Fetal cerebral magnetic resonance imaging beyond morphology. *Semin Ultrasound CT MR* 2015; **36**: 465–475.
- Ray JG, Vermeulen MJ, Bharatha A, Montanera WJ, Park AL. Association between MRI exposure during pregnancy and fetal and childhood outcomes. *JAMA* 2016; **316**: 952–961.
- Bouyssi-Kobar M, du Plessis AJ, Robertson RL, Limperopoulos C. Fetal magnetic resonance imaging: exposure times and functional outcomes at preschool age. *Pediatr Radiol* 2015; **45**: 1823–1830.
- Victoria T, Jaramillo D, Roberts TP, Zarnow D, Johnson AM, Delgado J, Rubesova E, Vossough A. Fetal magnetic resonance imaging: jumping from 1.5 to 3 tesla (preliminary experience). *Pediatr Radiol* 2014; **44**: 376–386; quiz 373–375.
- Patenaude Y, Pugash D, Lim K, Morin L, Bly S, Butt K, Cargill Y, Davies G, Denis N, Hazlitt G, Naud K, Ouellet A, Salem S. The use of magnetic resonance imaging in the obstetric patient. *J Obstet Gynaecol Can* 2014; **36**: 349–363.
- Cannie MM, Keyzer FD, Laere SV, Leus A, de Mey J, Fourneau C, Ridder FD, Cauteren TV, Willekens I, Jani JC. Potential heating effect in the gravid uterus by using 3-T MR imaging protocols: Experimental study in miniature pigs. *Radiology* 2016; **279**: 754–761.
- Garel C. *MRI of the Fetal Brain: Normal Development and Cerebral Pathologies*. Springer: Berlin, Heidelberg, 2004.
- Reddy UM, Abuhamad AZ, Levine D, Saade GR. Fetal imaging: Executive summary of a Joint Eunice Kennedy Shriver National Institute of Child Health and Human Development, Society for Maternal-Fetal Medicine, American Institute of Ultrasound in Medicine, American College of Obstetricians and Gynecologists, American College of Radiology, Society for Pediatric Radiology, and Society of Radiologists in Ultrasound Fetal Imaging Workshop. *Am J Obstet Gynecol* 2014; **210**: 387–397.
- Malinge G, Ben-Sira L, Lev D, Ben-Aroya Z, Kidron D, Lerman-Sagie T. Fetal brain imaging: a comparison between magnetic resonance imaging and dedicated neurosonography. *Ultrasound Obstet Gynecol* 2004; **23**: 333–340.
- Malinge G, Kidron D, Schreiber L, Ben-Sira L, Hoffmann C, Lev D, Lerman-Sagie T. Prenatal diagnosis of malformations of cortical development by dedicated neurosonography. *Ultrasound Obstet Gynecol* 2007; **29**: 178–191.
- Melchiorre K, Bhide A, Gika AD, Pilu G, Papageorghiou AT. Counseling in isolated mild fetal ventriculomegaly. *Ultrasound Obstet Gynecol* 2009; **34**: 212–224.
- Moutard ML, Kieffer V, Feingold J, Lewin F, Baron JM, Adamsbaum C, Gelot A, Isapof A, Kieffer F, de Villemeur TB. Isolated corpus callosum agenesis: a ten-year follow-up after prenatal diagnosis (how are the children without corpus callosum at 10 years of age?). *Prenat Diagn* 2012; **32**: 277–283.
- Guibaud L, Larroque A, Ville D, Sanlaville D, Till M, Gaucherand P, Pracros JP, des Portes V. Prenatal diagnosis of 'isolated' Dandy-Walker malformation: imaging findings and prenatal counselling. *Prenat Diagn* 2012; **32**: 185–193.
- Griffiths PD, Sharrack S, Chan KL, Bamfo J, Williams F, Kilby MD. Fetal brain injury in survivors of twin pregnancies complicated by demise of one twin as assessed by in utero MR imaging. *Prenat Diagn* 2015; **35**: 583–591.
- Jatzko B, Rittenschöber-Bohm J, Mailath-Pokorny M, Worda C, Prayer D, Kasprian G, Worda K. Cerebral lesions at fetal magnetic resonance imaging and neurologic outcome after single fetal death in monochorionic twins. *Twin Res Hum Genet* 2015; **18**: 606–612.
- Twickler DM, Magee KP, Caire J, Zaretsky M, Fleckenstein JL, Ramus RM. Second-opinion magnetic resonance imaging for suspected fetal central nervous system abnormalities. *Am J Obstet Gynecol* 2003; **188**: 492–496.
- Shellock FG, Crues JV. MR procedures: biologic effects, safety, and patient care. *Radiology* 2004; **232**: 635–652.
- Salomon LJ, Alfirevic Z, Bilardo CM, Chalouhi GE, Ghi T, Kagan KO, Lau TK, Papageorghiou AT, Raine-Fenning NJ, Stirnemann J, Suresh S, Tabor A, Timor-Tritsch IE, Toi A, Yeo G. ISUOG practice guidelines: performance of first-trimester fetal ultrasound scan. *Ultrasound Obstet Gynecol* 2013; **41**: 102–113.
- Kienzl D, Berger-Kulemann V, Kasprian G, Brugger PC, Weber M, Bettelheim D, Pusch F, Prayer D. Risk of inferior vena cava compression syndrome during fetal MRI in the supine position - a retrospective analysis. *J Perinat Med* 2014; **42**: 301–306.
- Leithner K, Prayer D, Porstner E, Kapusta ND, Stammer-Safar M, Krampfl-Bettelheim E, Hilger E. Psychological reactions related to fetal magnetic resonance imaging: a follow-up study. *J Perinat Med* 2013; **41**: 273–276.
- Brugger PC, Stühr F, Lindner C, Prayer D. Methods of fetal MR: beyond T2-weighted imaging. *Eur J Radiol* 2006; **57**: 172–181.
- Asenbaum U, Brugger PC, Woitek R, Furtner J, Prayer D. [Indications and technique of fetal magnetic resonance imaging]. *Radiologe* 2013; **53**: 109–115.
- Prayer D, Brugger PC, Kasprian G, Witzani L, Helmer H, Dietrich W, Eppel W, Langer M. MRI of fetal acquired brain lesions. *Eur J Radiol* 2006; **57**: 233–249.
- Weidner M, Hagelstein C, Debus A, Walleyo A, Weiss C, Schoenberg SO, Schaible T, Busing KA, Kehl S, Neff KW. MRI-based ratio of fetal lung volume to fetal body volume as a new prognostic marker in congenital diaphragmatic hernia. *AJR Am J Roentgenol* 2014; **202**: 1330–1336.
- Zamora IJ, Sheikh F, Cassady CI, Olutoye OO, Mehollin-Ray AR, Ruano R, Lee TC, Welty SE, Belfort MA, Ethun CG, Kim ME, Cass DL. Fetal MRI lung volumes are predictive of perinatal outcomes in fetuses with congenital lung masses. *J Pediatr Surg* 2014; **49**: 853–858; discussion 858.
- Yagel S, Cohen SM, Porat S, Daum H, Lipschuetz M, Amsalem H, Messing B, Valsky DV. Detailed transabdominal fetal anatomic scanning in the late first trimester versus the early second trimester of pregnancy. *J Ultrasound Med* 2015; **34**: 143–149.

SUPPORTING INFORMATION ON THE INTERNET

The following supporting information may be found in the online version of this article:



Appendix S1 Survey conducted by the Fetal MRI Special Interest Group of the International Society of Ultrasound in Obstetrics and Gynecology in 2014



Editorial

Inferior vermian hypoplasia – preconception, misconception

ASHLEY J. ROBINSON

Department of Radiology, Children's Hospital of British
Columbia, 4480 Oak Street, Vancouver V6H 3V4, Canada
(e-mail: ash@radiologist.net)

Introduction

There is considerable confusion in the literature regarding the terminology used when describing abnormalities of the cerebellum and of the vermis in particular. Terminology such as 'closure of the fourth ventricle', 'craniocaudal growth of the vermis' and 'inferior vermian hypoplasia', as well as the numbering (using Roman numerals) of the cerebellar lobules from anterior to posterior, has left us with the preconception and misconception that the vermis grows from superior to inferior, and that partial agenesis or hypoplasia always involves the inferior lobules. In light of recent advances in our understanding of the embryology of the cerebellum and cisterna magna, certain terminology and concepts can be demonstrated to be incorrect and should be abandoned.

This Editorial reviews the normal development of the cerebellum, describing and dispelling several misconceptions regarding both normal and abnormal cerebellar development, with specific reference to the cerebellar vermis. Examples of cerebellar and vermian anatomy at pathology, *in-vitro* and *in-vivo* fetal magnetic resonance imaging (MRI) and pre- and postnatal imaging are reviewed and correlated with cerebellar embryology, phylogeny, somatotopic mapping and functional MRI. The evidence indicates that the cerebellar vermis develops more in a ventral to dorsal direction than in a superior to inferior one and, therefore, that the concept of 'inferior vermian hypoplasia' is incorrect. Three possible categories of vermian anomaly are seen: it may not necessarily be the inferior vermis that is hypoplastic; it may not only be the inferior vermis that is hypoplastic; or it may not be vermian hypoplasia at all. The term 'inferior vermian hypoplasia' should only be used if it can be proved that only the inferior vermis is abnormal. There is no generic term which encompasses all the various etiologies that can cause a small vermis; thus, more appropriate terminology may be 'vermian hypoplasia' or 'vermian dysplasia', with 'neovermian hypoplasia' in cases in which the central lobules are proved to be abnormal.

Embryology of the posterior fossa

The neural tube

The neural tube develops, during the 3rd and 4th weeks of embryogenesis, as a longitudinal groove along the dorsal layer of the trilaminar germ cell disc¹. This groove deepens until its edges meet and fuse over the top, forming a hollow tube, which closes off at the cranial and caudal ends on days 25 and 28, respectively. The cranial end of the neural tube differentiates into three distinct regions: the prosencephalon, caudal to this the mesencephalon, and even more caudally the rhombencephalon, each enclosing a brain vesicle containing amniotic fluid initially. The rhombencephalon segments into eight rhombomeres. The future cerebellum originates in the alar plate of the most rostral adjacent pair of these rhombomeres; namely, rhombomeres 1 and 2². Several genes (*Otx*, *Gbx*, *FGF*, *Hox*)³ play a role in the formation and function of the isthmic organizer at the junction of the mesencephalon and rhombomere 1, which in turn regulates cerebellar development through release of hormonal factors^{4–6}. The more caudal rhombomere 2 gives rise to the germinal matrix of the ventricular zone, which forms the deep cerebellar nuclei (fastigial, globose, emboliform and dentate from medial to lateral) and the Purkinje cell layer. The more rostral rhombomere 1 gives rise to the germinal matrix of the rhombic lips. Initially, this forms the external granular layer of the cerebellum, which subsequently migrates deeper to form the internal granular layer, a process which is completed by approximately 2 years postnatally.

The cerebellar vermis *per se* is not formed through fusion of the adjacent developing cerebellar hemispheres but develops as a direct proliferation of the mesial primordium, starting in the 5th week of gestation^{7,8}. Experimental evidence shows us that granule cells arising from the lateral upper rhombic lip migrate medially into the posterior cerebellum, whereas granule cells arising in the medial upper rhombic lip are confined to an anterior cerebellar distribution (Figure S1)⁸. Therefore, as the primordia are separate, the development of the posterior vermis is not dependent on that of the anterior vermis. This is evident in the case of rhombencephalosynapsis, in which the posterior vermis and most inferior lobule (nodulus (X)) can be preserved in the absence of the anterior lobe of the vermis^{9,10}. Thus, vermian hypoplasia can be segmental, and normal development of the inferior vermis is not dependent on normal development of the superior vermis.

Key point: The vermis does not form through fusion of the cerebellar hemispheres, it develops from its own mesial primordium. Additionally, different parts of the vermis develop from different parts of the mesial primordium. Segmental vermian abnormalities can therefore exist.

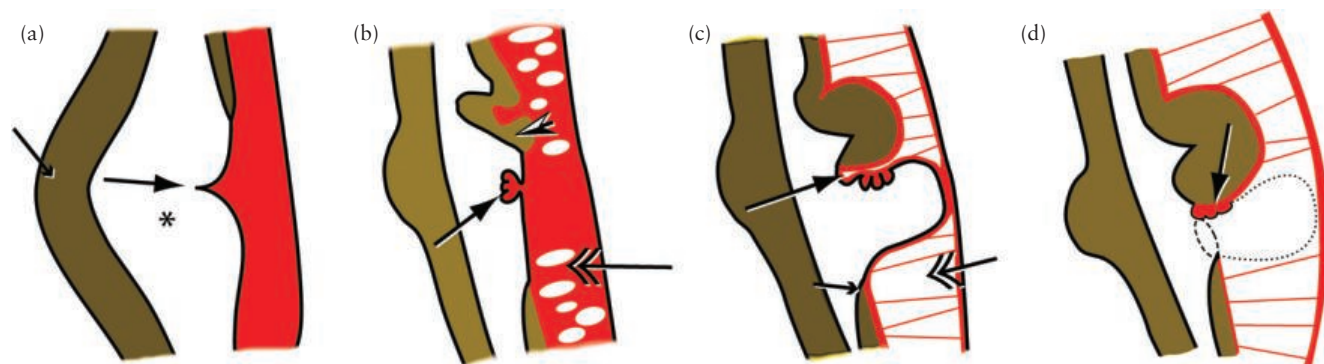


Figure 1 (a) During formation of the dorsal pontine flexure (small arrow) a transverse crease (large arrow) forms in the roof of the rhombencephalic vesicle (*), dividing it into anterior (cranial) and posterior (caudal) membranous areas. (b) The vermis (arrowhead) develops from the rhombic lip at the superior margin of the anterior membranous area. Choroid plexus develops in the crease (arrow). Cavitation starts in the overlying meninx primitiva (double arrow) to form the subarachnoid space. (c) As the cerebellum grows inferiorly the posterior membranous area bulges out between the vermis (large arrow) and the nucleus gracilis (small arrow), forming Blake's pouch. The subarachnoid space remains trabeculated by pia-arachnoid septations (double arrow). (d) Blake's pouch fenestrates (dotted line) and the neck of Blake's pouch becomes the foramen of Magendie (dashed line). The choroid plexus (arrow) now appears to be in the cisterna magna. (All images reproduced, with permission of the American Institute of Ultrasound in Medicine, from Robinson and Goldstein¹⁵.)

The roof of the rhombencephalon

At around 8–10 weeks' gestation, a focal dilatation of the neural tube is seen in the dorsal aspect of the developing hindbrain; this is the rhombencephalic vesicle, the predecessor to the fourth ventricle. At this level in the brainstem, which is known as the open medulla, the two alar laminae do not touch in the midline dorsally, and the gap is bridged by a layer of tela choroidea¹¹ known as the area membranacea, which forms the roof of the rhombencephalic vesicle.

The hindbrain develops a kink, known as the dorsal pontine flexure, which causes a transverse crease to form in the area membranacea, dividing it into a more rostral anterior membranous area and a more caudal posterior membranous area (Figure 1). The cerebellum develops from the rhombic lips at the cranial end of the area membranacea and the vermis and cerebellum grow exophytically, inferiorly and laterally, to cover it. Due to its thinness, this layer of tela choroidea has not, until recently, been resolvable by *in-vivo* imaging, thus giving the false impression that the fourth ventricle is open to the developing subarachnoid space initially and then closes due to caudal growth of the overlying vermis¹². This apparent developmental process is therefore often referred to in older literature as 'closure' of the fourth ventricle. This is typically complete by around 18 weeks' gestation, although physiological variation may give the appearance that the vermis is incomplete at the time of the initial mid-trimester assessment¹³.

As the vermis grows caudally it invaginates into the rhombencephalic vesicle, and the posterior membranous area protrudes beneath the vermis into the overlying meninx primitiva^{14,15}. This evagination, first described in 1900, is known as Blake's pouch¹¹, and where Blake's pouch constricts to pass through the cerebellar vallicula (the normal space inferior to the vermis, superior to the nucleus gracilis and medial to the cerebellar hemispheres)

it is known as Blake's metapore (Figure 1d). Even though Blake's pouch itself lies within the subarachnoid space of the developing cisterna magna, it is a direct extension of the fourth ventricle and therefore the fluid contained in Blake's pouch is intraventricular.

Normal linear echoes (the cisterna magna septa), which are typically seen in the fetal and neonatal cisterna magna and are most often described as bridging arachnoid septations¹⁶, have recently been shown to represent the walls of Blake's pouch and the cisterna magna septa are a potential marker for normal development¹⁵ (Figure 2a).

The cisterna magna

The future cisterna magna therefore forms in two compartments: a mesial compartment between the cisterna magna septa, which is derived from the rhombencephalic vesicle (Blake's pouch), and compartments lateral to the cisterna magna septa which develop through cavitation of the meninx primitiva overlying the surface of the brain, forming the subarachnoid space proper (Figures 2b and c).

Blake's pouch usually, but not always, fenestrates to a variable degree^{11,17} down to the obex (the inferior recess of the fourth ventricle), which leads to communication between the mesial ventricular-derived compartment and the true subarachnoid space of the cisterna magna. Fenestration and disappearance of Blake's pouch thus leaves an opening at Blake's metapore^{15,17,18}, which is known as the foramen of Magendie, allowing communication between the fourth ventricle and cisterna magna. Thus, the foramen of Magendie does not demarcate the true junction between the ventricular system and subarachnoid space of the cisterna magna.

A small communication beneath the vermis, between the fourth ventricle and the 'cisterna magna', often described in the literature on ultrasound^{12,15,19–21}

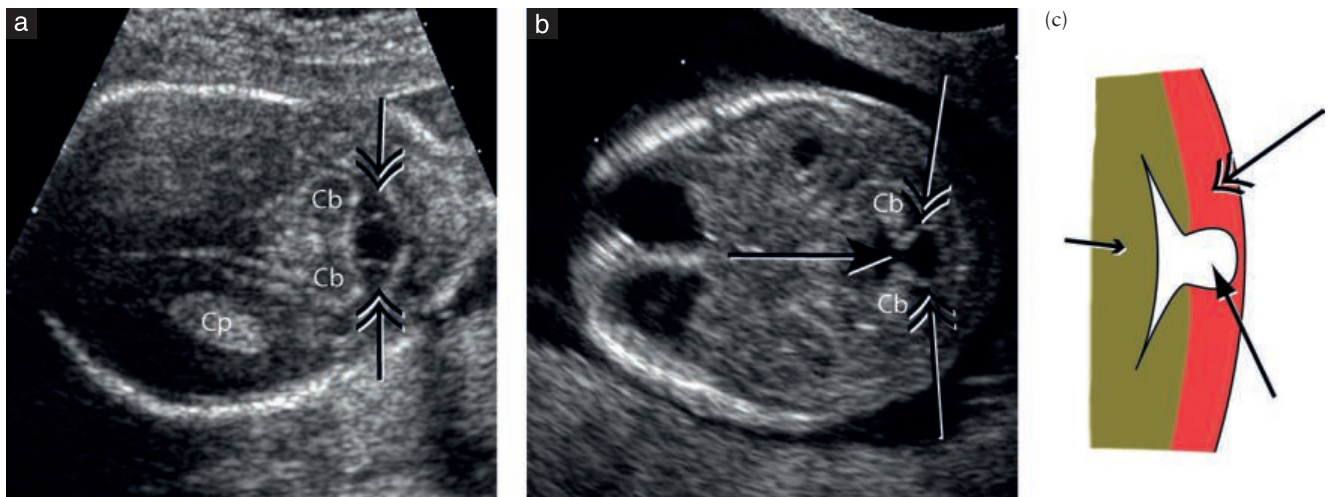


Figure 2 (a) The cisterna magna septa (double arrows) are a normal structure thought to represent the walls of Blake's pouch. Cb, cerebellar hemispheres; Cp, choroid plexus in lateral ventricle. (Reproduced, with permission of the American Institute of Ultrasound in Medicine, from Robinson and Goldstein¹⁵.) (b) On axial sonography, Blake's pouch can be seen within the developing subarachnoid space of the cisterna magna (double arrows). Blake's metapore (arrow) is visible between the developing cerebellar hemispheres. The walls of Blake's pouch are continuous with the walls of the fourth ventricle. The mesial portion of the future cisterna magna is derived from the ventricular system owing to fenestration of Blake's pouch. (Reproduced, with permission, from Robinson and Goldstein¹⁵.) (c) Diagrammatic representation showing the brainstem (small arrow) and Blake's pouch (large arrow), within the meninx primitiva (double arrow) that will cavitate and form the true subarachnoid space of the cisterna magna.

and sometimes seen on mid-sagittal images, therefore represents the normal Blake's metapore. Imaging the posterior fossa in the semicoronal plane will show this normal opening^{12,15,21} (Figure 3), but can give a false appearance of a vermian defect²² and, unfortunately, is often described wrongly as 'Dandy-Walker variant' (*vide infra*). This error can be avoided by making sure that the cavum septi pellucidi is included in the image, thus ensuring that the scan plane is truly axial or modified-axial.

Key point: A small gap between the vermis and the brainstem is normal and is known as Blake's metapore as it contains the neck of Blake's pouch. Once Blake's pouch fenestrates, the metapore is known as the foramen of Magendie.

Phylogeny of the cerebellum

'Ontogeny recapitulates phylogeny', or embryology repeats evolution. This important principle states that the development observed during embryology is like a 'time-lapse photography' rendition of the various steps taken during evolution; thus, structures that evolved first also develop first in the embryo, although the separate steps become somewhat merged.

The oldest part of the cerebellum, the archicerebellum, comprises the bilateral flocculi and the mesial nodulus (X), and is known as the flocculonodular lobe (Figure 4a and S2)²³. Functionally, this lobe plus some of the adjacent uvula (IX) comprise the vestibulocerebellum, which has connections with the vestibular nuclei (which, although situated within the brainstem, are considered surrogate deep cerebellar nuclei) and semicircular canals, receives visual information from the superior colliculi, and is involved in balance, position and tone. These

functions appear early in evolution, are shared among all vertebrates and phylogenetically are first seen in fish and amphibians; consequently they are the earliest to appear embryologically.

The next part of the cerebellum to appear is the paleocerebellum, which comprises the lobules of the anterior lobe of the vermis (lingula (I), centralis (II, III), culmen (IV, V)) and, importantly although often forgotten, but in fact supported by the literature^{23,24}, the more caudal lobules of the posterior lobe of the vermis (pyramis (VIII)) and some of the adjacent uvula (IX)). The paleocerebellum plus adjacent paravermian tissue in the cerebellar hemispheres is known functionally as the spinocerebellum and, due to its connections with the spinocerebellar tracts and efferent connections via the deep cerebellar nuclei to the cerebral cortex, it is involved in proprioception and synergy of movement and locomotion. Phylogenetically this is first seen in higher amphibians and, in relative terms, is largest in reptiles and birds.

The final part of the cerebellum to appear is the neocerebellum (also known as the cerebrocerebellum or pontocerebellum), which comprises the most rostral lobules of the posterior vermis (between the primary and pre-pyramidal fissures) (i.e. declive (VI), folium (VIIa), tuber (VIIb)) plus the majority of the contiguous cerebellar hemispheres. Functionally, it is involved with motion intent, planning, precision, force and extent, and increasingly it is recognized to regulate cognitive and language functions²⁵. Phylogenetically, this is seen in mammals only and it is largest in humans; it is therefore the latest to appear both in evolution and embryologically. It contributes the most to the transcerebellar diameter, and thus is one of the most widely used markers for normal cerebellar development in the fetus.

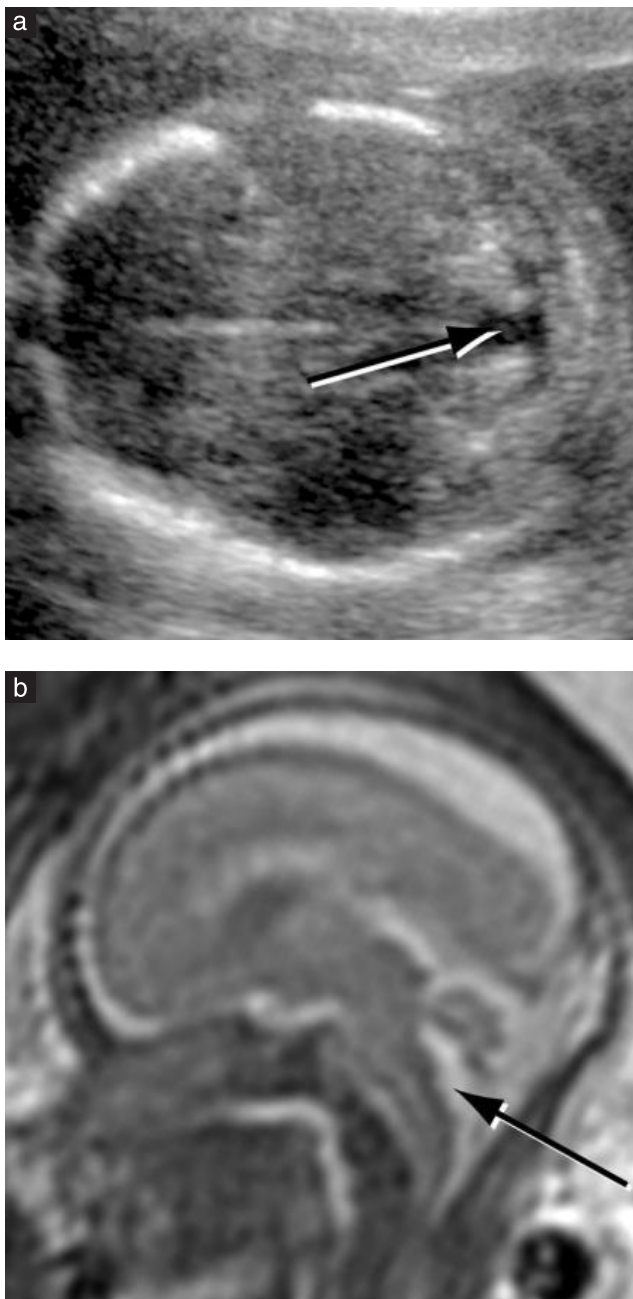


Figure 3 (a) Modified axial sonogram at 19 gestational weeks demonstrates a small gap inferior to the vermis and between the cerebellar hemispheres (arrow) which represents the foramen of Magendie. (b) Sagittal magnetic resonance image in same fetus at 21 weeks, after referral for 'inferior vermian hypoplasia', demonstrating small gap inferior to the vermis (arrow) in keeping with the foramen of Magendie. Follow-up imaging and outcome were normal. (Reproduced, with permission of Wolters Kluwer Health, from Robinson *et al.*¹⁹.)

A similar pattern of development is seen in the deep cerebellar nuclei, among which the phylogenetically older nuclei, the fastigial nuclei, are the most medial within the white matter and connect primarily with the archicerebellum, followed by the globose and emboliform nuclei, which are more lateral and connect primarily with the paleocerebellum, and finally the dentate, the most

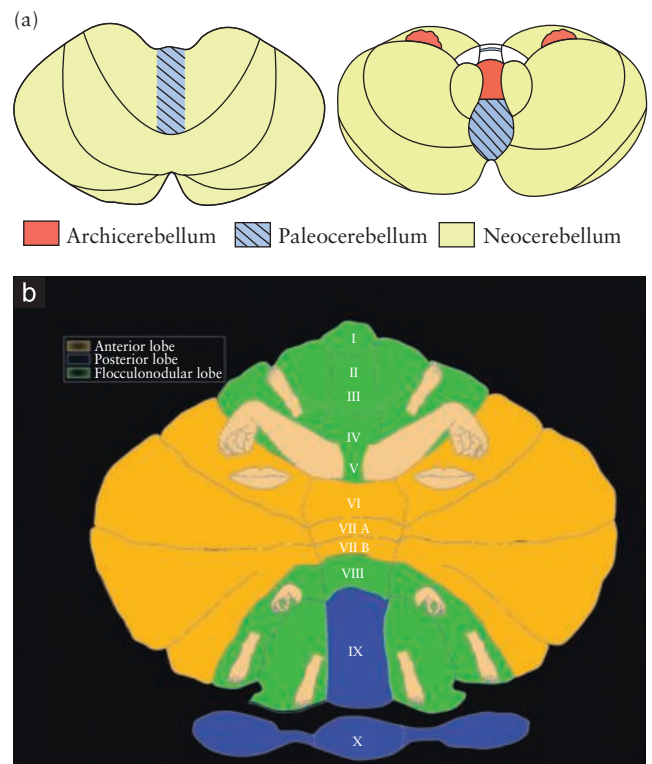


Figure 4 (a) Phylogenetic origins of the cerebellum. Phylogenetically, the archicerebellum is oldest and is only seen in fish and lower amphibians. The paleocerebellum is newer, is seen in higher amphibians and is larger in reptiles and birds. The neocerebellum is the most recent phylogenetically, is only found in mammals and is largest in humans. Note that the central lobules of the vermis are of neocerebellar origin. Superior (left) and inferior (right) views are shown. (Reproduced, with permission of Lippincott Williams & Wilkins, from Barr²³.) (b) Phylogenetically older functions which are common to more species map further away from the 'equator' than do newer functions which are seen in fewer species. A general correlation with evolutionary steps is seen, i.e. bipedality before manual dexterity before oromotor skills and associated cognitive and language skills, which developed last. cf Figure S2. (Reproduced, with permission of Macmillan Publishers Ltd, from Manni and Petrosini²⁶.)

lateral nuclei, which are connected primarily with the neocerebellum.

It therefore appears that, from an evolutionary and embryological perspective, rather than the anterior lobe developing first followed by the posterior lobe, the cerebellum actually develops with the most rostral and most caudal parts appearing together, initially adjacent to each other, with the more phylogenetically recent structures subsequently developing between these older structures, akin to the opening of a flower in which the outer petals are the first to appear and the inner ones appear later. Thus, the more anterior and posterior lobules and the associated medial deep cerebellar nuclei appear first, and the more central lobules, hemispheres and associated most lateral deep cerebellar nuclei appear last.

Key point: Phylogeny supports development of the vermis more in a ventrodorsal direction than in a craniocaudal direction.

Somatotopic mapping of the cerebellum

Further evidence in support of this pattern of development is seen when we look at the most recently proposed somatotopic map of the cerebellum (Figures 4b and S3)²⁶. This reveals an initially confusing pattern in which, moving from superior to inferior, the posterior lobe appears inverted compared with the anterior lobe. However, when we look at the overall pattern of the anterior and posterior lobes as being a reflection on either side of the cerebellar 'equator', not only does it start to make sense, it also matches phylogeny.

It follows that controls for the more basic or phylogenetically older functions of the lower limbs and trunk appear first and are represented in the areas closer to the brainstem and also closer to the midline, i.e. centralis (II, III), culmen (IV, V) and uvula (IX), whereas higher and phylogenetically newer functions, such as the fine motor control of the hands, mouth and lips and the associated cognitive functions of language, appear last and are represented more laterally and in the more central lobules of the vermis, i.e. declive (VI), folium (VIIa) and tuber (VIIb), and adjoining simplex, crus I and crus II of the ansiform lobes of the cerebellar hemispheres, respectively.

Key point: Somatotopic mapping supports development of the vermis more in a ventrodorsal direction than in a craniocaudal direction.

Functional magnetic resonance imaging of the cerebellum

The previously proposed cerebellar somatotopic map has in fact been confirmed by functional studies of the cerebellum by MRI (Figure S4)^{27–31}, i.e. the posterior lobe and anterior lobe appear as reflections of each other on either side of the cerebellar 'equator.'

Key point: Functional MRI supports development of the vermis more in a ventrodorsal direction than in a craniocaudal direction.

Observation of the cerebellum *in vitro* and *in vivo*

There is direct observational evidence that this pattern of development is exactly what we see in the developing fetus *in vivo*. The flocculonodular lobe (X) is divided from the main part of the cerebellum by the posterolateral fissure, which, along with the primary fissure that divides the main anterior and posterior lobes, is the first to appear^{32,33}. The next fissures to appear are the secondary (or 'post-pyramidal'), pre-pyramidal, pre-culmenate and pre-central fissures (Figure 5)^{5,19,34,35}. There is, however, a delay of approximately 6 weeks between what is resolvable histologically compared with *in-vitro* imaging³⁶, and also of approximately 2–3 weeks between *in-vitro* compared with *in-vivo* imaging. At best, by fetal MRI a single low-signal area is seen representing the white-matter core of each lobule; thus, at mid-trimester, typically only seven lobules can be seen because the lobules that mature later (declive (VI), folium

(VIIa), tuber (VIIb)) are indistinguishable¹⁹ and so only one structure representing these three lobules can be resolved between the primary and pre-pyramidal fissures (Figure 5a). Reimaging the same fetus later in gestation can demonstrate that this one structure develops into three separate lobules, bringing the total up to nine, which is the normal complement (Figure 5b). This may lead to misdiagnosis of vermian hypoplasia at earlier gestations³⁷ because the pyramis (VIII) and uvula (IX) can be misinterpreted as being the folium and tuber (lobules VIIa and VIIb) with the inferior-most lobules being considered erroneously to have not yet developed.

Key point: Direct observation, both *in vitro* and *in vivo*, supports development of the vermis more in a ventrodorsal direction than in a craniocaudal direction.

In many cases of 'inferior vermian hypoplasia' we have no evidence that it is actually the inferior lobules that are deficient, because often we cannot distinguish the inferior vermian lobules from the other lobules of the vermis by antenatal imaging. Some of the vermian lobules do have distinguishing features based on the sub-lobules and folia; for example, the lingula (I), centralis (II, III), culmen (IV, V), folium (VIIa), tuber (VIIb), uvula (IX) and nodulus (X) each have one primary division, the culmen (IV, V) has two anterior and three posterior secondary divisions, the declive (VI) has one primary and several secondary divisions, and the pyramis (VIII) has one primary and one secondary division. Therefore, most of the lobules are essentially identical⁴. A unique feature of the declive (VI), folium (VIIa) and tuber (VIIb), which makes them difficult to distinguish on early imaging, is that all three are united to the arbor vitae by a single white-matter core, whereas all the other named lobules have their own individual white-matter cores (Figure 5d). One reason for making such a distinction from the other lobules by giving them separate names is likely the fact that the folium (VIIa) and tuber (VIIb) are in direct contiguity laterally with crus I and crus II of the ansiform lobes, which form the majority of the cerebellar hemispheres (Figure S5).

Key point: Features that distinguish the different vermian lobules either do not exist or are simply non-resolvable at the time of imaging; therefore, in 'inferior vermian hypoplasia' it may not be possible to prove that it is the inferior lobules that are deficient; in fact, it may not be 'inferior' vermian hypoplasia at all.

Biometric measurement of the cerebellum

Biometric measurement of the cerebellum also supports the aforementioned model for cerebellar development. Growth of the vermian craniocaudal diameter has been confirmed both ultrasonographically and by MRI^{38–45}, but, importantly, so has relative growth of both the superior and the inferior lobes which grow symmetrically on either side of the primary fissure without any significant change in ratio with gestational age¹⁹. If the inferior vermian grew later, linear growth of both lobes would not be seen and there would be a change in the ratio of the anterior and posterior lobes throughout gestation.

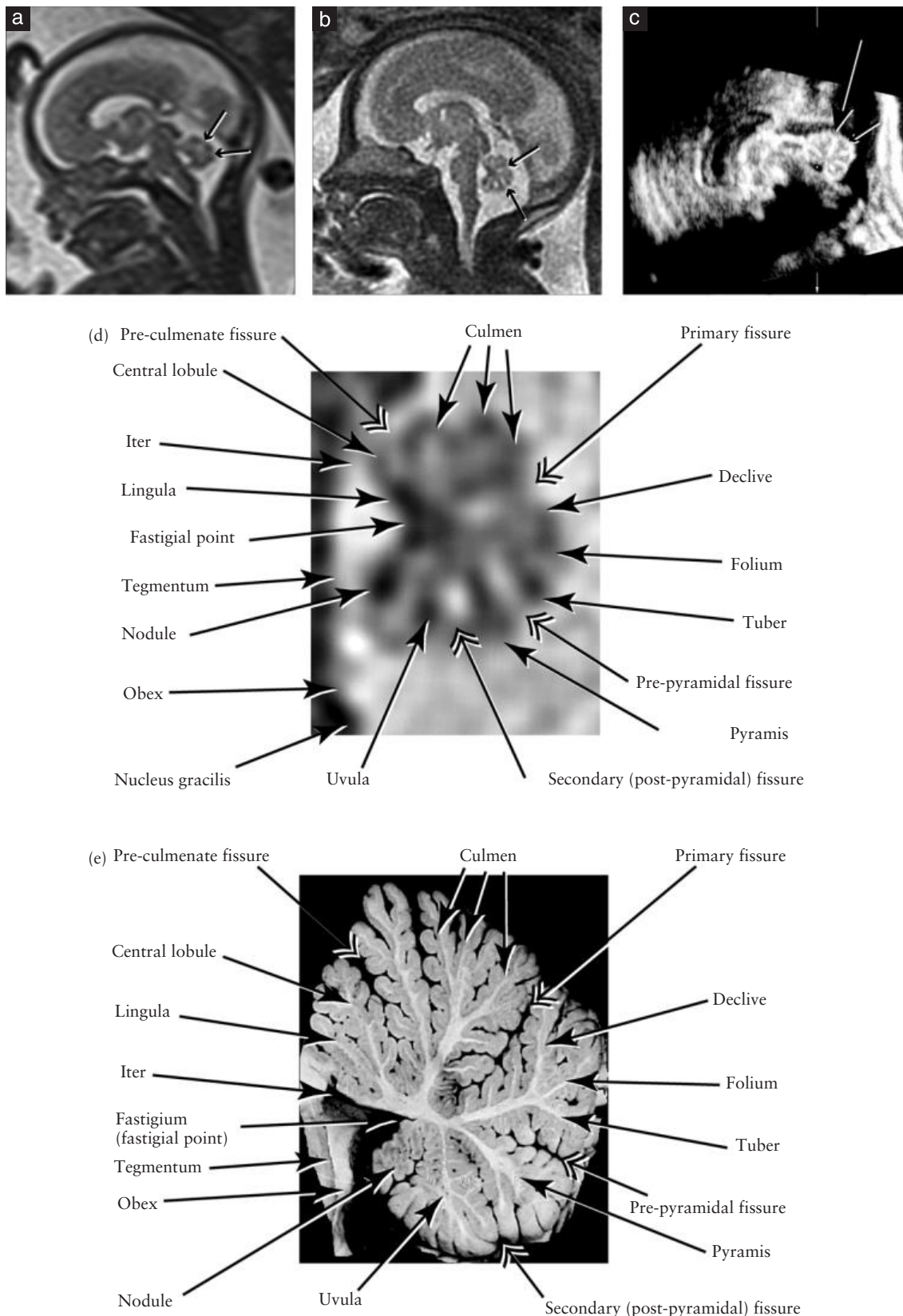


Figure 5 (a) In mid-gestation only one lobule (declive) is seen between the primary and pre-pyramidal fissures. (b) In the same fetus later in gestation, the same single lobule can be resolved into three lobules (declive (VI), folium (VIIa), tuber (VIIb)). (Reproduced, with permission of Wolters Kluwer Health, from Robinson *et al.*¹⁹.) (c) Sagittal three-dimensional ultrasound reconstruction just able to resolve three lobules (small arrow) below the primary fissure (large arrow). (d) Magnified inset of (b) with all fissures and lobules labeled. (Reproduced, with permission, from Robinson *et al.*¹⁹.) (e) Gross adult specimen with all fissures and lobules labeled. (Adapted from Duvernoy¹⁰⁵.)

Key point: Biometric measurement supports development of the vermis more in a ventrodorsal direction than in a craniocaudal direction.

Pathology of the posterior fossa

The Dandy–Walker continuum

Classic Dandy–Walker malformation was described initially in infants with hydrocephalus and was thought to be the sequela of atresia of the foramina of Luschka and Magendie^{46–48}; however, current theories suggest that it is a more global developmental defect affecting the roof of the rhombencephalon^{7,15} and leading to variable degrees of vermian hypoplasia and variable fenestration of the fourth ventricular outlet foramina, with variable associated anomalies (Figure 6)⁴⁹. The term ‘Dandy–Walker variant’ was introduced to describe those patients with vermian hypoplasia but without the other features of the classic triad (namely, elevation of the torcula and enlarged posterior fossa) (Table 1).

Current theories suggest that the spectrum of findings with respect to the posterior fossa ‘cyst’ in the Dandy–Walker continuum might result from two potential processes: either arrest of vermian development so it does not cover the fourth ventricle, or failure of adequate fenestration of the fourth ventricular outflow foramina, leading to an enlarged Blake’s pouch with secondary elevation and compression of the vermis. In classic Dandy–Walker malformation these two processes are thought to occur together.

Several interesting facts have been described in histopathological studies of Dandy–Walker fetuses^{50,51}. Rather than the inferior vermian lobules being absent, typically all of the lobules were actually present and the overall features resembled those of an arrested 12-week fetus. Reduced arborization of the lobules and weak neurofilament protein expression was seen throughout the vermis, including both the inferior lobe and the superior lobe, although the inferior lobules were more severely affected. Also, the nodulus (X) appeared elongated, overriding the uvula (IX) and in one case the pyramis (VIII), with abnormal caudal displacement of the germinal matrix, as if it were drawn out by the distention of the fourth ventricle (superior margin of Blake’s pouch) (Figure S6). These effects appeared to be mechanical. It was also noted that the Purkinje cells and deep cerebellar nuclei (which arise from the periventricular germinal matrix) were normal: the abnormality affected the germinal matrix of the rhombic lips only, i.e. the abnormality was confined to derivatives of rhombomere 1. Compared to normal there is also an apparent gradient of increasing severity of abnormality in a superior to inferior direction, possibly due to genetic and concentration gradients within the molecular milieu of the developing vermis due to increasing distance from the isthmic organizer.

Key point: It may be that it is not only the inferior vermis that is abnormal since in the Dandy–Walker continuum

there appears to be a rostrocaudal gradient of severity of abnormality and the superior vermis is also abnormal. Genetic gradients may account for this.

Inferior vermian hypoplasia

The term ‘inferior vermian hypoplasia’ is growing in usage, apparently as an alternative to the nomenclature ‘Dandy–Walker variant’^{52–56}, and has evolved as a result of terminology such as ‘closure of the 4th ventricle’, ‘craniocaudal growth of the vermis’, ‘craniocaudal diameter’ and ‘fusion’ of the cerebellar hemispheres as well as the numbering of the cerebellar lobules from superior to inferior. We are currently saddled with the preconception that the vermis grows in a superior-to-inferior direction and that, due to craniocaudal development of the vermis, partial agenesis involves its inferior part⁵⁷. Consequently, when development appears incomplete, as indeed it always appears before 18 weeks, we have a misconception that it must be the inferior vermis that is deficient. However, even in a normal vermis there is always an inferior gap early in gestation, and yet the inferior lobules (flocculonodular (X), uvula (IX), pyramis (VIII)) are the ones that we expect to develop first. This has been shown on *in-vitro* imaging, when the posterolateral, pre- and post-pyramidal fissures (and therefore the lobules either side of them, i.e. flocculonodular (X), uvula (IX), pyramis (VIII)) can be seen as early as 16 weeks’ gestation, whereas the declive (VI), folium (VIIa) and tuber (VIIb) are not distinguishable from each other (Figure S7)³³. Thus, the inferior gap seen in every fetus this early in gestation cannot be due to deficiency of the inferior lobules; it must be due to the overall smaller size of the vermis, in particular the relative lack of development of the declive (VI), folium (VIIa) and tuber (VIIb). Therefore when truly deficient it may be due to a deficiency generally or focally in any part of the vermis, because the vermis will not extend as far inferiorly as it should.

Conceptually, when the budding flower is not fully open, is it that the outside petals are missing, or is it that the inner petals have failed to grow and push the outer petals into their normal position? In view of the ontological appearance of the cerebellar structures, it is more likely that, in cases of arrested development, the flocculonodular lobe (X) and lobules closer to the brainstem (lingula, centralis (II, III), culmen (IV, V), nodulus (X), uvula (IX), pyramis (VIII)) would be present, and the ‘neo’-vermian lobules (declive (VI), folium (VIIa), tuber (VIIb)) and contiguous cerebellar hemispheres (lobus simplex and ansiform) would fail to develop. Hence, in this situation the term ‘neovermian hypoplasia’ may be more appropriate. A clinical example of this may be seen in idiopathic autism, in which selective volume loss in the neovermian lobules can be observed^{58,59}, but the archicerebellar lobules are normal (Figure S8).

The opposite may also occur if a destructive episode damages the lobules which are developing at that time, allowing the lobules that appear later to develop normally, i.e. the ‘archi’-vermian lobules and adjacent cerebellum

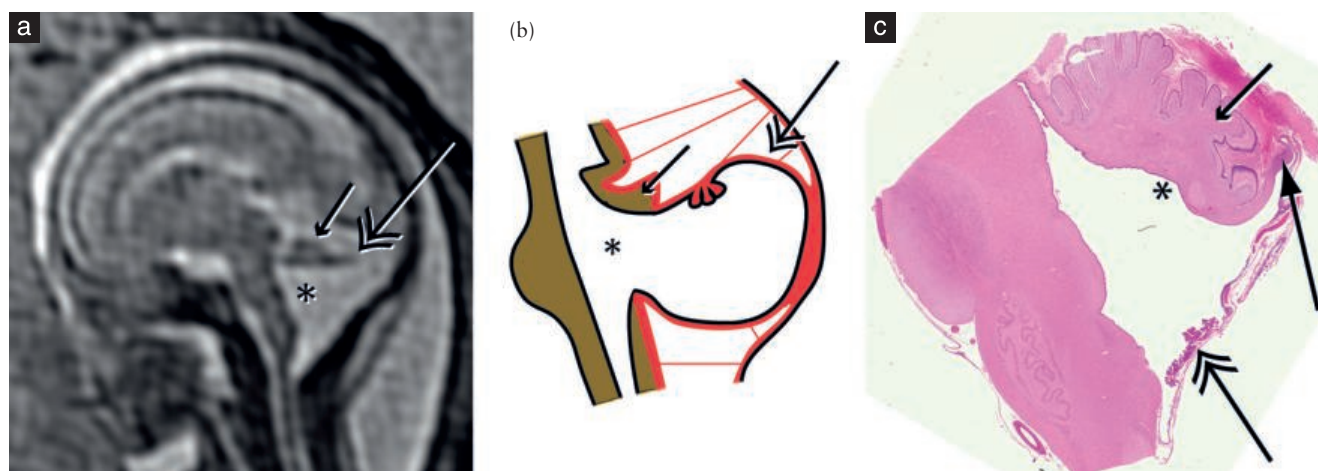


Figure 6 (a) In Dandy–Walker continuum, the vermian is elevated and abnormally lobulated (small arrow), with enlargement of the fourth ventricle (*) and Blake's pouch. The elongated nodulus (X) and displaced germinal matrix can be seen in the superior margin of Blake's pouch (double arrow). (b) Diagrammatic representation showing the small vermian (small arrow), enlarged Blake's pouch (double arrow) and fourth ventricle (*). (Reproduced, with permission of the American Institute of Ultrasound in Medicine, from Robinson and Goldstein¹⁵.) (c) Histological specimen showing abnormal vermian (small arrow) and choroid plexus (double arrow) displaced into the inferior wall of Blake's pouch, which remains intact. The fastigial recess is abnormally formed (*) and the germinal matrix (large arrow) is displaced from its normal position just below the fastigial recess into the superior margin of Blake's pouch.

Table 1 Categorization of 'cystic' posterior fossa malformations

Findings	Vermis		Cisterna magna septa	Choroid plexus position	Diagnosis
	Rotation/elevation	Hypoplasia			
Enlarged Blake's pouch, enlarged posterior fossa, elevated torcula, (often hydrocephalus)	Yes: > 40–45°	Yes: variable, may be severe	Invisible: apposed to side walls of cisterna magna	Inferior margin of Blake's pouch	Vermian hypoplasia, a.k.a. Dandy–Walker malformation
Enlarged Blake's pouch, normal-sized posterior fossa, normal torcula	Yes: usually 30–45°	Yes: variable to intermediate	Invisible: apposed to side walls of cisterna magna	Inferior margin of Blake's pouch	Vermian hypoplasia, a.k.a. Dandy–Walker variant or 'inferior vermian hypoplasia'
Enlarged Blake's pouch, normal-sized posterior fossa, normal torcula	Yes: mild to moderate (usually < 30°)	No: may be misdiagnosed as 'inferior vermian hypoplasia'	Visible: bowed laterally	Superior margin of Blake's pouch	Blake's pouch cyst, a.k.a. persistent Blake's pouch
Enlarged Blake's pouch, enlarged posterior fossa	No	No	Visible: bowed laterally	Superior margin of Blake's pouch	Mega cisterna magna (may represent mega Blake's pouch)
True cyst that does not communicate with the fourth ventricle (not Blake's pouch)	No	No: may have extrinsic compression	Normal, but may be distorted by mass effect	Superior margin of Blake's pouch	Posterior fossa arachnoid cyst

Compiled and adapted from Robinson *et al.*¹⁹, Garel³⁷, Guibaud and des Portes⁵⁷, Bonnevie and Brodal⁷⁸ and Volpe *et al.*⁹⁷. a.k.a., also known as.

would be deficient, but the 'neo'-vermis and hemispheres would be normal. A clinical example of this may be seen in fetal alcohol syndrome, when the archicerebellar lobules may be affected due to depletion of the Purkinje cells which exist at the time of the toxic alcohol level^{60–62}, but without affecting subsequent development; therefore, the archicerebellar lobules are selectively damaged, but the neocerebellar lobules are normal (Figure S9).

Thus, depending on the nature and timing of the insult, a completely different clinical picture would

be expected, tending towards either ataxia, hypotonia, balance and visual disturbance (vestibulocerebellum, spinocerebellum), or alternatively a disturbance of executive functions, memory, language and cognition (neocerebellum) which have been shown to localize to the tuber (VIIb) and contiguous ansiform lobes^{28,63–67}.

Key point: 'Inferior vermian hypoplasia' may actually be due to hypoplasia of other vermian lobules, for example the neovermian lobules, leading to overall reduction in craniocaudal growth. This may explain why

in certain cases of 'inferior vermian hypoplasia' we may see only cognitive defects.

Isolated 'inferior vermian hypoplasia' vs Blake's pouch cyst

The term 'isolated inferior vermian hypoplasia' has been used to describe that subset within 'inferior vermian hypoplasia' in which there are no known underlying or associated abnormalities^{68–70} and this group generally has a better outcome^{71–76}.

Unfortunately, it is likely that, until very recently, due to the subtleties of distinguishing between 'inferior vermian hypoplasia' and Blake's pouch cyst (*vide infra*), in the literature these two groups of patients, with differing outcomes, have been included together. The problem lies in our poor ability even by modern antenatal imaging techniques, except perhaps in expert hands, to distinguish an isolated persistent Blake's pouch from true vermian hypoplasia, because both have an enlarged Blake's pouch and both have a rotated vermis, and the difference in definition is based purely on the appearance of the vermis⁷⁷. Thus, the essential task is to ensure that the vermis is normal. However, to achieve this we need to be sure that we evaluate *all* of the vermis, and not just the inferior part.

One suggested useful landmark for differentiating between Blake's pouch cyst and vermian hypoplasia is the position of the choroid plexus: if it is in its normal position on the inferior surface of the vermis (superior margin of the cyst), this is compatible with Blake's pouch cyst, because it indicates that the anterior membranous area formed normally; if it is on the inferior margin of the cyst, this indicates that the anterior membranous area formed abnormally (Figure 6c)^{18,78,79}, warranting further evaluation of the vermis. This landmark is, however, extremely difficult to see.

It is often impossible to tell prenatally whether vermian hypoplasia is isolated since associated abnormalities, for example genetic or chromosomal ones, may be undetectable⁸⁰. In one study, 50% of Dandy–Walker and 'inferior vermian hypoplasia' patients had abnormal outcome even if the abnormality appeared to be isolated⁸¹. In another study, postnatal imaging and follow-up findings were normal in six out of 19 cases of 'isolated inferior vermian hypoplasia', and the 13 with postnatal confirmation of hypoplasia had good overall outcome, with only mild developmental delays in a subset of infants⁶⁸.

Key point: The position of the choroid plexus may be useful to distinguish true vermian hypoplasia from Blake's pouch cyst, which have different outcomes.

Blake's pouch cyst (or 'persistent Blake's pouch')

In Blake's pouch cyst (Figure 7) there is thought to be inadequate fenestration of both Blake's pouch and the foramina of Luschka, leading to imbalance of cerebrospinal fluid (CSF) egress into the subarachnoid space of the cisterna magna, with consequent dilatation of the fourth ventricle¹⁸. Although the pouch communicates freely with the fourth ventricle, there is a failure of communication between the pouch and the perimedullary subarachnoid spaces^{17,82}.

In most of the lower species, including dogs, Blake's pouch is a normal persistent structure, yet in these species the vermis grows even more caudally than it does in humans, thereby obliterating the mesial portion of Blake's metapore and dividing it into two lateral metapores¹¹. However, other than in humans, the foramina of Luschka are also larger and therefore the normal non-fenestration of Blake's pouch does not impede CSF egress. In contrast, in humans, with smaller foramina of Luschka, non-fenestration of Blake's pouch causes it to enlarge and elevate/rotate the vermis away from the brainstem,

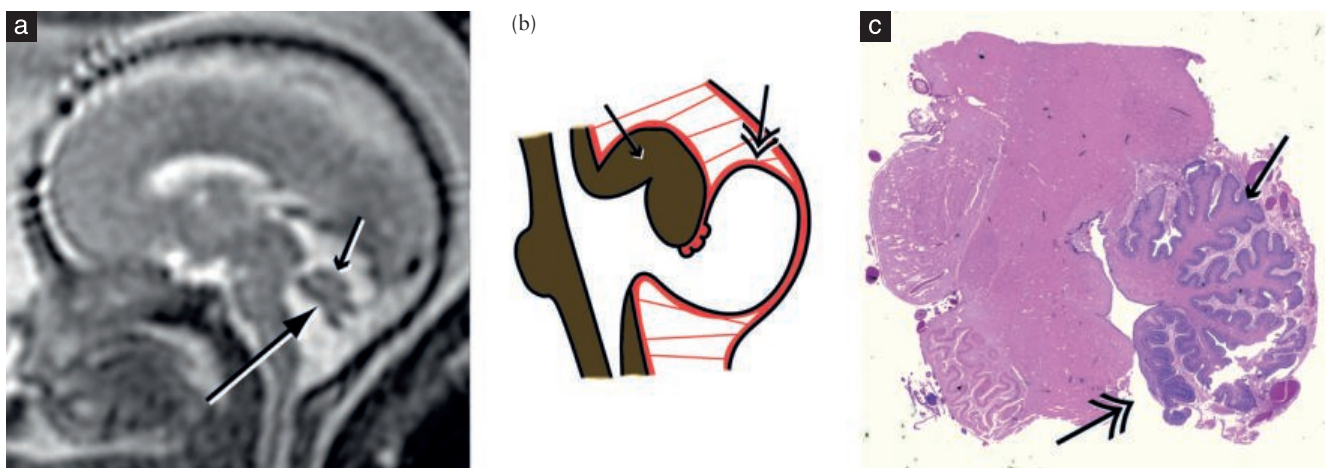


Figure 7 (a) In persistent Blake's pouch, the vermis is elevated away from the brainstem but the major landmarks of the primary fissure (small arrow) and fastigial recess (large arrow) appear normal and the lobulation appears normal. (Reproduced, with permission from Taylor and Francis Group LLC Books, from Robinson and Blaser¹⁰⁶.) Diagrammatic representation showing Blake's pouch (double arrow) elevating a normal vermis (small arrow). (Reproduced, with permission of the American Institute of Ultrasound in Medicine, from Robinson and Goldstein¹⁵.) (c) Pathological specimen of the same fetus with Blake's pouch collapsed (double arrow) and vermian lobulation apparently normal (arrow). (Reproduced, with permission, from Robinson and Blaser¹⁰⁶.)

but, because this causes a gap between the inferior vermis and the brainstem, this can lead to the false-positive diagnosis of 'inferior vermian hypoplasia'. This theory of Blake's pouch cyst explains why historically there has been poor correlation of ultrasound and autopsy findings in apparent cystic malformations of the posterior fossa⁸³, because postmortem the cyst deflates and the vermis derotates back into a normal position. This same scenario is seen in children and adults with Blake's pouch cyst, in whom there is no intrinsic vermian hypoplasia. CSF shunting or third ventriculostomy to decompress the ventricular system results in a return to normal appearance and clinical normality of these patients once the hydrocephalus has resolved^{84,85}.

Isolated elevation/rotation of the vermis due to a persistent Blake's pouch does not necessarily indicate an adverse outcome^{12,15,68,79,86–89}. In one study, one third of cases of Blake's pouch cyst or mega cisterna magna underwent spontaneous resolution *in utero* and 90% of survivors with no associated anomalies had normal developmental outcome at 1–5 years once the initial referral misdiagnosis of vermian hypoplasia had been excluded⁸¹. In another large retrospective study of 19 cases of Blake's pouch cyst, associated anomalies were seen in eight. There were two neonatal deaths and eight terminations. Of nine survivors, one had trisomy 21, and the other eight were neurodevelopmentally normal, although obstructive hydrocephalus was seen in one⁷⁷.

It has also been suggested in several cases in the literature that persistent Blake's pouch phenotype can be 'acquired' if the balance of CSF egress is upset by the presence of fetal intraventricular hemorrhage^{81,89} or fetal infection^{90,91}, which result in tetraventricular dilatation and enlargement of the 'cisterna magna' (i.e. enlargement of Blake's pouch contained within the cisterna magna), presumably through resultant debris within the ventricular system causing obstruction of the fenestrations in both the foramina of Luschka and Blake's pouch, in much the same way as can be demonstrated postnatally^{92,93} (Figure S10). However, it is important to recognize that, depending on the nature and timing of the insult, injury to the developing brain itself can also result from endotoxins, free radicals and inflammatory cytokines^{94–96}.

Mega cisterna magna may in fact represent mega Blake's pouch but with better CSF egress such that the vermis is not elevated.

Key point: Blake's pouch cyst can give the appearance of 'inferior vermian hypoplasia' when there is no intrinsic abnormality of the vermis at all. Evidence suggests that *in-utero* infection or intraventricular hemorrhage may cause this appearance.

Conclusions

The vermis *appears* to grow in a craniocaudal direction, thus giving rise to the preconception that when it is incomplete the deficiency must affect the inferior vermis; however, evidence indicates that the vermis and cerebellum develop more in a ventral-to-dorsal

direction, with the more phylogenetically recent structures developing in-between the older structures, akin to the opening of a flower. Deficiency generally or focally in any part of the vermis, or enlargement of Blake's pouch leading to elevation of an intrinsically normal vermis, can both give the appearance of 'inferior vermian hypoplasia' and can be difficult to differentiate. The term 'inferior vermian hypoplasia' is incorrect because it is not *necessarily* the inferior vermis that is abnormal, it may not *only* be the inferior vermis that is abnormal, or the vermis may not be abnormal *at all*. The term should be abandoned in favor of simply vermian hypoplasia or vermian dysplasia unless it can be proved that it is the inferior vermis that is deficient, and recognizing the fact that the etiology may be due to hypoplasia, atrophy, destruction or disruption (Table S1). The part of the vermis affected depends on the nature and the timing of the insult, which can selectively damage structures existing at the time of the insult, or selectively damage those which develop after the insult; this concept thus governs the resulting constellation of clinical findings. In certain cases it may even be more appropriate to use the term 'neovermian hypoplasia' in recognition of the fact that the declive (VI), folium (VIIa) and tuber (VIIb) may be the only lobules affected.

Acknowledgments

I would like to thank the following: Dr Ants Toi, Department of Medical Imaging, Mt. Sinai Hospital, Toronto, for the images in Figures 3a and 5c; Dr Susan Blaser, Department of Radiology, Hospital for Sick Children, Toronto, for the images in Figures 3b, 5a, 5b, 6a and 7a; Dr Ruth Goldstein, Department of Radiology, University of California, San Francisco, for the images in Figures 2a and 2b; and Dr William Halliday, Department of Pathology, Hospital for Sick Children, Toronto, for the images in Figures 6c and 7c.

REFERENCES

1. Sadler TW. *Langman's Essential Medical Embryology*. Lippincott Williams & Wilkins, Baltimore, 2005; 16–26.
2. Sarnat HB, Flores-Sarnat L. Normal Development of the nervous system. In *Pediatric Neuropsychiatry*. Lippincott Williams & Wilkins, Ed. Coffey CE, Brumback RA. 2006; 9.
3. Sato T, Joyner AL, Nakamura H. How does Fgf signaling from the isthmic organizer induce midbrain and cerebellum development? *Growth Differ* 2004; **46**, 487–494.
4. Demareel P. Abnormalities of cerebellar foliation and fissuration: classification, neurogenetics and clinicoradiological correlations. *Neuroradiology* 2002; **44**: 639–646.
5. Adamsbaum C, Moutard ML, André C, Merzoug V, Ferey S, Quéré MP, Lewin F, Fallet-Bianco C. MR of the fetal posterior fossa. *Pediatr Radiol* 2005; **35**: 124–140.
6. Aruga J, Ogura H, Shutoh F, Ogawa M, Franke B, Nagao S, Mikoshiba K. Locomotor and oculomotor impairment associated with cerebellar dysgenesis in Zic3-deficient (Bent tail) mutant mice. *Eur J Neurosci* 2004; **20**: 2159–2167.
7. Barkovich. *Pediatric Neuroimaging*. 3rd Ed. Lippincott Williams & Wilkins, Philadelphia. 2000; 337–341.
8. Sgaier SK, Millet S, Villanueva MP, Berenshteyn F, Song C, Joyner AL. Morphogenetic and cellular movements that shape

- the mouse cerebellum; insights from genetic fate mapping. *Neuron* 2005; 45: 27–40.
9. Utsunomiya H, Takano K, Ogasawara T, Hashimoto T, Fukushima T, Okazaki M. Rhombencephalosynapsis: Cerebellar. Embryogenesis. *Am J Neuroradiol* 1998; 19: 547–549.
 10. Pasquier L, Marcorelles P, Loget P, Pelluard F, Carles D, Perez MJ, Bendavid C, de La Rochebrochard C, Ferry M, David V, Odent S, Laquerrière A. Rhombencephalosynapsis and related anomalies: a neuropathological study of 40 fetal cases. *Acta Neuropathol* 2009; 117: 185–200.
 11. Blake JA. The roof and lateral recesses of the fourth ventricle considered morphologically and embryologically. *J Comp Neurol* 1900; 10: 79–108.
 12. Ben-Ami M, Perlitz Y, Peleg D. Transvaginal sonographic appearance of the cerebellar vermis at 14–16 weeks' gestation. *Ultrasound Obstet Gynecol* 2002; 19: 208–209.
 13. Bromley B, Nadel AS, Pauker S, Estroff JA, Benacerraf BR. Closure of the cerebellar vermis: evaluation with second trimester US. *Radiology* 1994; 193: 761–763.
 14. Strand RD, Barnes PD, Poussaint TY, Estroff JA, Burrows PE. Cystic retrocerebellar malformations: unification of the Dandy-Walker complex and the Blake's pouch. *Pediatr Radiol* 1993; 23: 258–260.
 15. Robinson AJ, Goldstein R. The cisterna magna septa: vestigial remnants of Blake's pouch and a potential new marker for normal development of the rhombencephalon. *J Ultrasound Med* 2007; 26: 83–95.
 16. Knutzon RK, McGahan JP, Salamat MS, Brant WE. Fetal cisterna magna septa: a normal anatomic finding. *Radiology* 1991; 180: 799–801.
 17. Raybaud C. Cystic malformations of the posterior fossa. Abnormalities associated with the development of the roof of the fourth ventricle and adjacent meningeal structures. *J Neuroradiol* 1982; 9: 103–133.
 18. Tortori-Donati P, Fondelli MP, Rossi A, Carini S. Cystic malformations of the posterior cranial fossa originating from a defect of the posterior membranous area. Mega cisterna magna and persisting Blake's pouch: two separate entities. *Childs Nerv Syst* 1996; 12: 303–308.
 19. Robinson AJ, Blaser S, Toi A, Chitayat D, Halliday W, Pantazi S, Gundogan M, Laughlin S, Ryan G. The Fetal Cerebellar Vermis: Assessment for Abnormal Development by Ultrasonography and Magnetic Resonance Imaging. *Ultrasound Q* 2007; 23: 211–223.
 20. Oh KY, Rassner UA, Frias AE Jr, Kennedy AM. The fetal posterior fossa: clinical correlation of findings on prenatal ultrasound and fetal magnetic resonance imaging. *Ultrasound Q* 2007; 23: 203–10.
 21. Phillips JJ, Mahony BS, Siebert JR, Lalani T, Fligner CL, Kapur RP. Dandy-Walker malformation complex: correlation between ultrasonographic diagnosis and postmortem neuropathology. *Obstet Gynecol* 2006; 107: 685–93.
 22. Laing FC, Frates MC, Brown DL, Benson CB, Di Salvo DN, Doubilet PM. Sonography of the fetal posterior fossa: false appearance of mega-cisterna magna and Dandy-Walker variant. *Radiology* 1994; 192: 247–251.
 23. *Barr's The Human Nervous System: An anatomical viewpoint* (9th revised edn). Kiernan JA (ed). Lippincott Williams and Wilkins; Sept 2008.
 24. The Cerebellum. University of Western Ontario Instructional Web Server. <http://instruct.uwo.ca/anatomy/530/cblm.htm> [Accessed 6 May 2013].
 25. Tavano A, Grasso R, Gagliardi C, Triulzi F, Bresolin N, Fabbro F, Borgatti R. Disorders of cognitive and affective development in cerebellar malformations. *Brain* 2007; 130: 2646–60.
 26. Manni E, Petrosini L. A century of cerebellar somatotopy: a debated representation. *Nature Reviews Neuroscience* 2004; 5: 241–249.
 27. Grodd W, Hülsmann E, Ackermann H. Functional MRI localizing in the cerebellum. *Neurosurg Clin N Am* 2005; 16: 77–99.
 28. Stoodley CJ, Schmahmann JD. Functional topography in the human cerebellum: a meta-analysis of neuroimaging studies. *Neuroimage* 2009; 44: 489–501.
 29. Bushara KO, Wheat JM, Khan A, Mock BJ, Turski PA, Sorenson J, Brooks BR. Multiple tactile maps in the human cerebellum. *Neuroreport* 2001; 12: 2483–6.
 30. Grodd W, Hülsmann E, Lotze M, Wildgruber D, Erb M. Sensorimotor mapping of the human cerebellum: fMRI evidence of somatotopic organization. *Hum Brain Mapp* 2001; 13: 55–73.
 31. Rijntjes M, Buechel C, Kiebel S, Weiller C. Multiple somatotopic representations in the human cerebellum. *Neuroreport* 1999; 10: 3653–3658.
 32. Nakayama T, Yamada R. MR imaging of the posterior fossa structures of human embryos and fetuses. *Radiat Med* 1999; 17: 105–14.
 33. Chong BW, Babcock CJ, Pang D, Ellis WG. A magnetic resonance template for normal cerebellar development in the human fetus. *Neurosurgery* 1997; 41: 924–928.
 34. Stazzone MM, Hubbard AM, Bilaniuk LT, Harty MP, Meyer JS, Zimmerman RA, Mahboubi S. Ultrafast MR imaging of the normal posterior fossa in fetuses. *AJR Am J Roentgenol* 2000; 175: 835–839.
 35. Guibaud L. Practical approach to prenatal posterior fossa abnormalities using MR. *Pediatr Radiol* 2004; 34: 700–711.
 36. Larsell O, Jansen J. Human cerebellum. In *The Comparative Anatomy and Histology of the Cerebellum: The Human Cerebellum, Cerebellar Connections, and Cerebellar Cortex*. The University of Minnesota Press: Minneapolis, 1972, pp 3–64.
 37. Garel C. Posterior fossa malformations: main features and limits in prenatal diagnosis. *Pediatr Radiol* 2010; 40: 1038–1045.
 38. Achiron R, Kivilevitch Z, Lipitz S, Gamzu R, Almog B, Zalel Y. Development of the human fetal pons: in utero ultrasonographic study. *Ultrasound Obstet Gynecol* 2004; 24: 506–510.
 39. Malinger G, Ginath S, Lerman-Sagie T, Watemberg N, Lev D, Glezerman M. The fetal cerebellar vermis: normal development as shown by transvaginal ultrasound. *Prenat Diagn* 2001; 21: 687–692.
 40. Smith PA, Johansson D, Tzannatos C, Campbell S. Prenatal measurement of the fetal cerebellum and cisterna cerebellomedullaris by ultrasound. *Prenat Diagn* 1986; 6: 133–141.
 41. Chang CH, Chang FM, Yu CH, Ko HC, Chen HY. Three-dimensional ultrasound in the assessment of fetal cerebellar transverse and antero-posterior diameters. *Ultrasound Med Biol* 2000; 26: 175–182.
 42. Garel C. *MR of the fetal brain. Normal development and Cerebral Pathologies*. 2nd ed. Berlin Heidelberg: Springer-Verlag. 2004; 95.
 43. Triulzi F, Parazzini C, Righini A. MR of fetal and neonatal cerebellar development. *Semin Fetal Neonatal Med* 2005; 10: 411–420.
 44. Bertucci E, Gindes L, Mazza V, Re C, Lerner-Geva L, Achiron R. Vermian biometric parameters in the normal and abnormal fetal posterior fossa: three-dimensional sonographic study. *J Ultrasound Med* 2011; 30: 1403–1410.
 45. Tilea B, Alberti C, Adamsbaum C, Armoogum P, Oury JF, Cabrol D, Sebag G, Kalifa G, Garel C. Cerebral biometry in fetal magnetic resonance imaging: new reference data. *Ultrasound Obstet Gynecol* 2009; 33: 173–181.
 46. Dandy WE, Blackfan KD. Internal hydrocephalus. An experimental, clinical, and pathological study. *Am J Dis Child* 1914; 8: 406–482.
 47. Dandy WE. The diagnosis and treatment of hydrocephalus due to occlusion of the foramina of Magendie and Luschka. *Surg Gynecol Obstet* 1921; 32: 112–124.

48. Taggart JK, Walker AE. Congenital atresias of the foramina of Luschka and Magendie. *Arch Neurol Psychiatr* 1942; 48: 583–612.
49. Hirsch JF, Pierre-Kahn A, Renier D, Sainte-Rose C, Hoppe-Hirsch E. The Dandy-Walker malformation. A review of 40 cases. *J Neurosurg* 1984; 61: 515–522.
50. Kapur RP, Mahony BS, Finch L, Siebert JR. Normal and abnormal anatomy of the cerebellar vermis in midgestational human fetuses. *Birth Defects Res A Clin Mol Teratol* 2009; 85: 700–709.
51. Russo R, Fallet-Bianco C. Isolated posterior cerebellar vermal defect: a morphological study of midsagittal cerebellar vermis in 4 fetuses—early stage of Dandy-Walker continuum or new vermal dysgenesis? *J Child Neurol* 2007; 22: 492–500.
52. Limperopoulos C, du Plessis AJ. Disorders of cerebellar growth and development. *Curr Opin Pediatr* 2006; 18: 621–627.
53. Chang MC, Russell SA, Callen PW, Filly RA, Goldstein RB. Sonographic detection of inferior vermian agenesis in Dandy-Walker malformations: prognostic implications. *Radiology* 1994; 193: 765–770.
54. Ko SF, Wang HS, Lui TN, Ng SH, Ho YS, Tsai CC. Neurocutaneous melanosis associated with inferior vermian hypoplasia: MR findings. *J Comput Assist Tomogr* 1993; 17: 691–695.
55. Aynaci FM, Mocan H, Bahadir S, Sari A, Aksoy A. A case of Menkes' syndrome associated with deafness and inferior cerebellar vermian hypoplasia. *Acta Paediatr* 1997; 86: 121–123.
56. Bornstein E, Goncalves Rodríguez JL, Álvarez Pavón EC, Quiroga H, Or D, Divon MY. First-trimester sonographic findings associated with a dandy-walker malformation and inferior vermian hypoplasia. *J Ultrasound Med* 2013; 32: 1863–1868.
57. Guibaud L, des Portes V. Plea for an anatomical approach to abnormalities of the posterior fossa in prenatal diagnosis. *Ultrasound Obstet Gynecol* 2006; 27: 477–481.
58. Courchesne E, Saitoh O, Yeung-Courchesne R, Press GA, Lincoln AJ, Haas RH, Schreibman L. Abnormality of cerebellar vermian lobules VI and VII in patients with infantile autism: identification of hypoplastic and hyperplastic subgroups with MR imaging. *AJR Am J Roentgenol* 1994; 162: 123–130.
59. Kaufmann WE, Cooper KL, Mostofsky SH, Capone GT, Kates WR, Newschaffer CJ, Bukelis I, Stump MH, Jann AE, Lanham DC. Specificity of cerebellar vermian abnormalities in autism: a quantitative magnetic resonance imaging study. *J Child Neurol* 2003; 18: 463–470.
60. Sowell ER, Jernigan TL, Mattson SN, Riley EP, Sobel DF, Jones KL. Abnormal development of the cerebellar vermis in children prenatally exposed to alcohol: size reduction in lobules I–V. *Alcohol Clin Exp Res* 1996; 20: 31–34.
61. Goodlett CR, Marcussen BL, West JR. A single day of alcohol exposure during the brain growth spurt induces brain weight restriction and cerebellar Purkinje cell loss. *Alcohol* 1990; 7: 107–114.
62. O'Hare ED, Kan E, Yoshii J, Mattson SN, Riley EP, Thompson PM, Toga AW, Sowell ER. Mapping cerebellar vermal morphology and cognitive correlates in prenatal alcohol exposure. *Neuroreport* 2005; 16: 1285–1290.
63. Kim JS, Park SH, Lee KW. Spasmus nutans and congenital ocular motor apraxia with cerebellar vermian hypoplasia. *Arch Neurol* 2003; 60: 1621–1624.
64. Stoodley CJ, Valera EM, Schmahmann JD. Functional topography of the cerebellum for motor and cognitive tasks: an fMRI study. *Neuroimage* 2012; 59: 1560–1570.
65. Stoodley CJ, Valera EM, Schmahmann JD. An fMRI study of intra-individual functional topography in the human cerebellum. *Behav Neurol* 2010; 23: 65–79.
66. Bernard JA, Seidler RD. Relationships Between Regional Cerebellar Volume and Sensorimotor and Cognitive Function in Young and Older Adults. *Cerebellum* 2013; 12: 721–737.
67. Bolduc ME, du Plessis AJ, Sullivan N, Guizard N, Zhang X, Robertson RL, Limperopoulos C. Regional cerebellar volumes predict functional outcome in children with cerebellar malformations. *Cerebellum* 2012; 11: 531–542.
68. Limperopoulos C, Robertson RL, Estroff JA, Barnewolt C, Levine D, Bassan H, du Plessis AJ. Diagnosis of inferior vermian hypoplasia by fetal magnetic resonance imaging: potential pitfalls and neurodevelopmental outcome. *Am J Obstet Gynecol* 2006; 194: 1070–1076.
69. Alkan O, Kizilkilic O, Yildirim T. Malformations of the midbrain and hindbrain: a retrospective study and review of the literature. *Cerebellum* 2009; 8: 355–365.
70. Keogan MT, DeAtkine AB, Hertzberg BS. Cerebellar vermian defects: antenatal sonographic appearance and clinical significance. *J Ultrasound Med* 1994; 13: 607–611.
71. Fenichel GM, Phillips JA. Familial aplasia of the cerebellar vermis. Possible X-linked dominant inheritance. *Arch Neurol* 1989; 46: 582–583.
72. Imamura S, Tachi N, Oya K. Dominantly inherited early-onset non-progressive cerebellar ataxia syndrome. *Brain Dev* 1993; 15: 372–376.
73. Sasaki-Adams D, Elbabaa SK, Jewells V, Carter L, Campbell JW, Ritter AM. The Dandy-Walker variant: a case series of 24 pediatric patients and evaluation of associated anomalies, incidence of hydrocephalus, and developmental outcomes. *J Neurosurg Pediatr* 2008; 2: 194–199.
74. Long A, Moran P, Robson S. Outcome of fetal cerebral posterior fossa anomalies. *Prenat Diagn* 2006; 26: 707–710.
75. Bolduc ME, Limperopoulos C. Neurodevelopmental outcomes in children with cerebellar malformations: a systematic review. *Dev Med Child Neurol* 2009; 51: 256–267.
76. Patek KJ, Kline-Fath BM, Hopkin RJ, Pilipenko VV, Crombleholme TM, Spaeth CG. Posterior fossa anomalies diagnosed with fetal MRI: associated anomalies and neurodevelopmental outcomes. *Prenat Diagn* 2012; 32: 75–82.
77. Paladini D, Quarantelli M, Pastore G, Sorrentino M, Sglavo G, Nappi C. Abnormal or delayed development of the posterior membranous area of the brain: anatomy, ultrasound diagnosis, natural history and outcome of Blake's pouch cyst in the fetus. *Ultrasound Obstet Gynecol* 2012; 39: 279–287.
78. Bonnevie K, Brodal A. Hereditary hydrocephalus in the house mouse: IV. The development of cerebellar anomalies during fetal life with notes on the normal development of the mouse cerebellum. *Lkr Norske Vidensk Akad Oslo 1 Matj-nat KI* 1946; 4: 4–60.
79. Nelson MD Jr, Maher K, Gilles FH. A different approach to cysts of the posterior fossa. *Pediatr Radiol* 2004; 34: 720–732.
80. Guibaud L, Larroque A, Ville D, Sanlaville D, Till M, Gaucherand P, Pracros JP, des Portes V. Prenatal diagnosis of 'isolated' Dandy-Walker malformation: imaging findings and prenatal counselling. *Prenat Diagn* 2012; 32: 185–193.
81. Gandolfi Colleoni G, Contro E, Carletti A, Ghi T, Campobasso G, Rembouskos G, Volpe G, Pilu G, Volpe P. Prenatal diagnosis and outcome of fetal posterior fossa fluid collections. *Ultrasound Obstet Gynecol* 2012; 39: 625–631.
82. Arai H, Sato K. Posterior fossa cysts: clinical, neuroradiological and surgical features. *Childs Nerv Syst* 1991; 7: 156–164.
83. Carroll SG, Porter H, Abdel-Fattah S, Kyle PM, Soothill PW. Correlation of prenatal ultrasound diagnosis and pathologic findings in fetal brain abnormalities. *Ultrasound Obstet Gynecol* 2000; 16: 149–153.
84. Calabro F, Arcuri T, Jinkins JR. Blake's pouch: an entity within the Dandy-Walker continuum. *Neuroradiology* 2000; 42: 290–295.
85. Cornips EM, Overvliet GM, Weber JW, Postma AA, Hoebeirigs CM, Baldewijns MM, Vles JS. The clinical spectrum of Blake's pouch cyst: report of six illustrative cases. *Childs Nerv Syst* 2010; 26: 1057–1064.
86. Klein O, Pierre-Kahn A, Boddaert N, Parisot D, Brunelle F. Dandy-Walker malformation: prenatal diagnosis and prognosis. *Childs Nerv Syst* 2003; 19: 484–489.

87. Zalel Y, Gilboa Y, Gabis L, Ben-Sira L, Hoffman C, Wiener Y, Achiron R. Rotation of the vermis as a cause of enlarged cisterna magna on prenatal imaging. *Ultrasound Obstet Gynecol* 2006; 27: 490–493.
88. Triulzi F, Parazzini C, Righini A. Magnetic resonance imaging of fetal cerebellar development. *Cerebellum* 2006; 5: 199–205.
89. Barkovich AJ, Kjos BO, Norman D, Edwards MS. Revised classification of posterior fossa cysts and cystlike malformations based on the results of multiplanar MR imaging. *AJR Am J Roentgenol* 1989; 153: 1289–1300.
90. Malinger G, Lev D, Zahalka N, Ben Aroia Z, Watemberg N, Kidron D, Sira LB, Lerman-Sagier T. Fetal cytomegalovirus infection of the brain: the spectrum of sonographic findings. *Am J Neuroradiol* 2003; 24: 28–32.
91. Dogan Y, Yuksel A, Kalelioglu IH, Has R, Tatli B, Yildirim A. Intracranial ultrasound abnormalities and fetal cytomegalovirus infection: report of 8 cases and review of the literature. *Fetal Diagn Ther* 2011; 30: 141–149.
92. Cramer BC, Walsh EA. Cisterna magna clot and subsequent post-hemorrhagic hydrocephalus. *Pediatr Radiol* 2001; 31: 153–159.
93. Dinçer A, Kohan S, Ozek MM. Is all “communicating” hydrocephalus really communicating? Prospective study on the value of 3D-constructive interference in steady state sequence at 3T. *AJNR Am J Neuroradiol* 2009; 30: 1898–1906.
94. Tam EW, Ferriero DM, Xu D, Berman JI, Vigneron DB, Barkovich AJ, Miller SP. Cerebellar development in the preterm neonate: effect of supratentorial brain injury. *Pediatr Res* 2009; 66: 102–106.
95. Volpe JJ. Neurobiology of periventricular leukomalacia in the premature infant. *Pediatr Res* 2001; 50: 553–562.
96. Duncan JR, Cock ML, Scheerlinck JP, Westcott KT, McLean C, Harding R, Rees SM. White matter injury after repeated endotoxin exposure in the preterm ovine fetus. *Pediatr Res* 2002; 52: 941–949.
97. Volpe P, Contro E, De Musso F, Ghi T, Farina A, Tempesta A, Volpe G, Rizzo N, Pilu G. Brainstem-vermis and brainstem-tentorium angles allow accurate categorization of fetal upward rotation of cerebellar vermis. *Ultrasound Obstet Gynecol* 2012; 39: 632–635.
98. Murray JC, Johnson JA, Bird TD. Dandy-Walker malformation - etiologic heterogeneity and empiric recurrence risks. *Clinical Genetics* 1985; 28: 272–283.
99. Osenbach RK, Menezes AH. Diagnosis and management of the Dandy-Walker malformation: 30 years of experience. *Pediatr Neurosurg* 1992; 18: 179–189.
100. Boddaert N, Desguerre I, Bahi-Buisson N, Romano S, Valayannopoulos V, Saillour Y, Seidenwurm D, Grevent D, Berteloot L, Lebre AS, Zilbovicius M, Puget S, Salomon R, Attie-Bitach T, Munnich A, Brunelle F, de Lonlay P. Posterior fossa imaging in 158 children with ataxia. *J Neuroradiol* 2010; 37: 220–230.
101. Winter TC, Ostrovsky AA, Komarniski CA, Uhrich SB. Cerebellar and frontal lobe hypoplasia in fetuses with trisomy 21: usefulness as combined US markers. *Radiology* 2000; 214: 533–538.
102. Poretti A, Limperopoulos C, Roulet-Perez E, Wolf NI, Rauscher C, Prayer D, Müller A, Weissert M, Kotzaeridou U, Du Plessis AJ, Huisman TA, Boltshauser E. Outcome of severe unilateral cerebellar hypoplasia. *Dev Med Child Neurol* 2010; 52: 718–724.
103. Limperopoulos C, Folkherth R, Barnewolt CE, Connolly S, Du Plessis AJ. Posthemorrhagic cerebellar disruption mimicking Dandy-Walker malformation: fetal imaging and neuropathology findings. *Semin Pediatr Neurol* 2010; 17: 75–81.
104. Lehman AM, Eydoux P, Doherty D, Glass IA, Chitayat D, Chung BY, Langlois S, Yong SL, Lowry RB, Hildebrandt F, Trnka P. Co-occurrence of Joubert syndrome and Jeune asphyxiating thoracic dystrophy. *Am J Med Genet* 2010; 152A: 1411–1419.
105. Duvernoy H. *The Human Brainstem and Cerebellum*. Springer Verlag. 1995.
106. Robinson AJ, Blaser S. In-utero MR imaging of developmental abnormalities of the fetal cerebellar vermis. In *Imaging the central nervous system of the fetus and neonate*. Griffiths, Paley, Whitby (Eds.) Taylor & Francis, April 2006.

SUPPORTING INFORMATION ON THE INTERNET

The following supporting information may be found in the online version of this article:



Table S1 Associations with cerebellar hypoplasia (updated and adapted from Alkan *et al.*⁶⁹, Guibaud *et al.*⁸⁰, Murray *et al.*⁹⁸, Osenbach and Menezes⁹⁹, Boddaert *et al.*¹⁰⁰, Winter *et al.*¹⁰¹, Poretti *et al.*¹⁰², Limperopoulos *et al.*¹⁰³, Lehman *et al.*¹⁰⁴)

Figure S1 The more inferior parts of the cerebellum and vermis derive their granule cells from the more lateral upper rhombic lip germinal matrix, whereas cells originating in the mesial germinal matrix are confined to an anterior cerebellar distribution. (Reproduced with permission from Elsevier, from Sgaier *et al.*⁸.)

Figure S2 Functional origins of the cerebellum. The vestibulocerebellum (blue) includes the flocculonodular lobe (X) and adjacent uvula (IX), the spinocerebellum (green) includes the anterior lobe and the pyramis (VIII) and contiguous medial hemispheres and the neocerebellum (yellow) includes the declive (VI), folium (VIIa) and tuber (VIIb) and the majority of the cerebellar hemispheres. (Adapted from Duvernoy¹⁰⁵.)

Figure S3 Somatotopic map of the cerebellum. This appears incompatible with a craniocaudal development pattern, but entirely compatible with a ventrodorsal one. The anterior lobe is a reflection of the posterior lobe on either side of the cerebellar ‘equator’. Feet are represented at the cranial and caudal extents, upper limbs inside that, and mouth inside that (centrally). (Reproduced, with permission from Macmillan Publishers Ltd, from Manni and Petrosini²⁶.)

Figure S4 Functional magnetic resonance imaging of the cerebellum demonstrates a pattern in which phylogenetically older functions map further away from the ‘equator’ than do newer functions. This pattern replicates the previously proposed somatotopic map. (Reproduced, with permission from Elsevier, from Grodd *et al.*²⁷.)

Figure S5 Diagram of the cerebellum demonstrating both the naming system and the corresponding numbering system for all of the vermian lobules, plus their corresponding cerebellar lobules and fissures. Lobule VI is also known as the declive (not labeled). (Reproduced, with permission from Macmillan Publishers Ltd, from Manni and Petrosini²⁶.)

Figure S6 (a) Dandy–Walker (DW) fetus demonstrating that all of the vermian lobules are present and abnormal and the nodulus (X) is elongated and distorted (arrow). (b) Normal fetus for comparison. (c) Histological specimen from DW fetus again showing distortion of the nodulus (X). (d) Normal fetus for comparison. (e) DW fetus: the germinal matrix (arrow) appears to have been pulled inferiorly by the superior margin of Blake’s pouch. (f) Normal position of the germinal matrix (arrow) below the fastigial recess. (g) Neurofilament protein expression in DW fetus shows marked reduction in the inferior vermis (arrow); however, there is also reduction in the superior vermis (double arrow) and a gradient of increasing severity of abnormality in a superior to inferior direction. (h) Normal neurofilament protein expression for comparison. (All images reproduced, with permission from Sage Publications, from Russo and Fallet-Bianco⁵¹.)

Figure S7 In this specimen at 16 weeks’ gestation the pre-pyramidal and post-pyramidal (secondary) fissures can be seen; thus, the pyramis (VIII) and uvula (IX) are present even though there is a gap separating the inferior vermis from the brainstem. (Reproduced, with permission from Lippincott Williams & Wilkins, from Chong *et al.*³³.)

Figure S8 In idiopathic autism, the affected lobules (numbered in red) are those that are phylogenetically newer (neocerebellum (yellow)) and appear later during embryogenesis. The vestibulocerebellum (blue) and spinocerebellum (green) are spared. (Adapted from Duvernoy¹⁰⁵.)

Figure S9 In fetal alcohol syndrome, the affected lobules (numbered in red) are those that are phylogenetically older (vestibulocerebellum (blue), spinocerebellum (green)) and appear earlier during embryogenesis, therefore suffering depleted Purkinje cells during exposure to toxic alcohol levels. The neovermian lobules (yellow) are spared. (Adapted from Duvernoy¹⁰⁵.)

Figure S10 (a) Sagittal half-Fourier acquisition single-shot turbo spin-echo (HASTE) magnetic resonance image (MRI) in a fetus with sonographically diagnosed intraventricular hemorrhage. The cerebellar vermis (arrow) is elevated but appears normal otherwise, with normal landmarks and biometry. There is no ‘inferior vermian hypoplasia’. (b) Axial HASTE image in the same fetus, demonstrating unilateral low signal in the caudothalamic groove (arrow). (c) Parasagittal oblique diffusion-weighted image in the same fetus, demonstrating restricted diffusion (arrow), which was also corroborated on the apparent diffusion coefficient map, in keeping with germinal matrix hemorrhage. (d) Coronal MRI in a different 30-week-gestation neonate, showing blood within Blake’s pouch (*) in continuity with the fourth ventricle, but the subarachnoid space of the cisterna magna has normal fluid signal (arrows). (e) Sagittal MRI in the same neonate, showing blood within Blake’s pouch (*) and an elevated and compressed vermis (arrow), giving a vermian hypoplasia phenotype.



Prenatal features of isolated subependymal pseudocysts associated with adverse pregnancy outcome

H. ESTEBAN*, E. BLONDIAUX*, E. AUDUREAU†, C. SILEO*, M. L. MOUTARD‡, A. GELOT§, J. M. JOUANNIC¶, H. DUCOU LE POINTE* and C. GAREL*

*Service de Radiologie, Hôpital Trousseau – Hôpitaux Universitaires de l'Est Parisien (APHP), Université Pierre et Marie Curie, Paris, France; †Unité de Biostatistique et Epidémiologie, Assistance Publique – Hôpitaux de Paris, Hôpital Henri Mondor, Université Paris Est Créteil, Créteil, France; ‡Service de Neuropédiatrie, Hôpital Trousseau – Hôpitaux Universitaires de l'Est Parisien (APHP), Université Pierre et Marie Curie, Paris, France; §Département de Neuropathologie, Service d'Anatomie et Cytologie Pathologiques, Hôpital Trousseau – Hôpitaux Universitaires de l'Est Parisien (APHP), Université Pierre et Marie Curie, Paris, France; ¶Pôle de Périnatalité, Centre Pluridisciplinaire de Diagnostic Prénatal de l'Est Parisien, Hôpital Trousseau – Hôpitaux Universitaires de l'Est Parisien (APHP), Université Pierre et Marie Curie, Paris, France

KEYWORDS: fetal brain; germinolysis cysts; magnetic resonance imaging; periventricular cysts; prenatal diagnosis; prenatal ultrasound; SEPC; subependymal pseudocysts

ABSTRACT

Objectives To identify at prenatal ultrasound (US) the features of apparently isolated subependymal pseudocysts (SEPC) that may indicate underlying pathology and should lead to further investigations.

Methods This was a retrospective study of cases with SEPC detected on prenatal US and/or magnetic resonance imaging (MRI). Those with apparently isolated SEPC at US were classified into two groups as follows: Group 1 (n = 29): normal prenatal US and MRI (except for SEPC) and normal outcome; Group 2 (n = 12): normal prenatal cerebral US (except for SEPC) and abnormal prenatal cerebral MRI with or without abnormal outcome. A third group (n = 9) included cases with abnormal prenatal US and MRI. The latter cases with obvious cerebral abnormalities at US were excluded from the statistical analysis as they do not represent a diagnostic dilemma for clinicians. Groups 1 and 2 were analyzed, comparing them with respect to their SEPC characteristics (size, number, location in relation to the caudothalamic notch and the ventricular horns and morphology) and extracerebral abnormalities.

Results The mean \pm SD SEPC great axis was longer in Group 2 (11.67 \pm 5.82 mm) than it was in Group 1 (8.00 \pm 5.64 mm) (P = 0.021), suggesting an optimal cut-off for size of SEPC of \geq 9 mm (sensitivity = 75%, specificity = 62%) to maximize sensitivity for predicting pathological outcome. SEPC adjacent to the temporal horns and SEPC located posterior to the caudothalamic notch were observed more frequently in

Group 2, indicating their association with poor outcome (P = 0.003 and P = 0.003, respectively). Atypical morphology and extracerebral abnormalities were observed more frequently in Group 2 (P = 0.013 and P = 0.044, respectively). There was no statistically significant difference between groups for either number or location of cysts along the inferior wall or adjacent to the lateral wall of the frontal horns (P = 0.591 and P = 0.156, respectively).

Conclusion When apparently isolated SEPC are observed at prenatal US, further investigations should be performed under the following circumstances: (1) SEPC great axis \geq 9 mm; (2) SEPC adjacent to the occipital and temporal horns; (3) SEPC located posterior to the caudothalamic notch; (4) SEPC with atypical morphology. Copyright © 2015 ISUOG. Published by John Wiley & Sons Ltd.

INTRODUCTION

Subependymal pseudocysts (SEPC) are located in the wall of the lateral ventricles. They result from the lysis of undifferentiated cells in the germinal matrix, which are particularly vulnerable because of their high mitotic activity¹.

SEPC are usually diagnosed on cranial ultrasound (US) examination during the postnatal period, being identified in an estimated 1–5% of newborns^{2–4}, with a higher incidence in premature babies⁵. Although isolated SEPC discovered after birth usually carry a good prognosis^{3,6} and most commonly regress spontaneously, they may be associated with a range of pathological

Correspondence to: Dr C. Garel, Department of Radiology, Hôpital d'Enfants Armand-Trousseau, 26 Avenue du Dr Arnold Netter, Paris, France (e-mail: catherine.garel@trs.aphp.fr)

Accepted: 23 January 2015

conditions of different severity. SEPC may result from hemorrhage within the germinal matrix (which is more vulnerable in premature babies) or be observed in the setting of focal hypoxic ischemic damage, sometimes resulting from toxins such as cocaine^{7,8}. They may also be associated with viral infections^{1,9–12}, metabolic diseases such as Zellweger syndrome¹³ and chromosomal abnormalities^{14,15}.

Due to improvements in US technology and skills, prenatal detection of SEPC has improved during the past few years and, increasingly, they are detected at routine prenatal US screening. However, prenatal studies focusing on SEPC are scarce; since Malinger's series¹⁶, only a few case reports have been published^{6,17–20}. When associated severe cerebral or extracerebral abnormalities are observed at prenatal US, the prognosis of SEPC in itself is not the main concern. Detecting apparently isolated SEPC at prenatal US is much more challenging. To address this, we conducted a retrospective study in fetuses with SEPC and compared the characteristics of SEPC at prenatal imaging in those with normal and those with abnormal imaging and/or clinical outcome. We hoped to identify SEPC features that might indicate an underlying abnormality and should lead to the performance of fetal brain magnetic resonance imaging (MRI) and additional investigations, such as genetic studies, maternal serology and amniocentesis.

METHODS

Patients and setting

This observational retrospective study included consecutive fetuses with SEPC detected at prenatal US and/or MRI in our institution between September 2008 and September 2012. All women were referred and the majority underwent both US and MRI. Cases with insufficient information about obstetric history, postnatal follow-up or fetopathological results were excluded. Institutional review board approval was granted for this study.

Imaging

Prenatal US examinations were performed on a Toshiba (Aplio, Toshiba, Tokyo, Japan) US system equipped with transabdominal probes (3.5–6 MHz) or, in cases of cephalic presentation and poor quality of transabdominal scanning, a transvaginal probe (6 MHz). Examinations were conducted according to the ISUOG guidelines regarding prenatal neurosonography²¹. Fetal MRI was performed with a 1.5-Tesla MR system (Achieva Philips Medical Systems, Best, The Netherlands), using a phased-array abdominal coil. Imaging sequences included at least T2-weighted single-shot turbo spin-echo sequences (repetition time/echo time, 15 000/120 ms; field of view depending on gestational age; section thickness, 4 mm; spacing, 2 mm; matrix, 256 × 256) performed in planes that were strictly axial, sagittal and coronal. Postnatal imaging was performed using either cranial US

or brain MRI or both. All examinations were performed and re-analyzed retrospectively by trained radiologists.

Data collection and classification

We obtained the following prenatal data from medical records: obstetric history, reason for referral to our department, maternal serology results, amniocentesis results, family history of congenital diseases, consanguinity, gestational age at diagnosis and SEPC imaging features at initial scan. Moreover, cerebral and extracerebral abnormalities detected by prenatal US and/or MRI were recorded.

Postnatal data included: gestational age at birth, imaging studies after birth (US or MRI) and evolution of imaging features (stability, progression, regression), clinical follow-up data regarding neurodevelopmental status obtained from medical records, and age at last follow-up exam. The neurodevelopmental status was assessed by neuropediatricians using the Bayley's scales of infant development (BSID-III)²² and head circumference and onset of seizures were also recorded. The clinical outcome was evaluated and considered abnormal in the presence of a low level according to Bayley's scales and/or an adverse finding such as microcephaly or onset of seizures.

Following parental counseling, termination of pregnancy (TOP) was discussed in some pathological cases, according to French legislation. Pathological confirmation was available for all terminated fetuses. Gestational age at TOP and the fetopathological data were recorded.

In order to analyze SEPC features with regard to clinical and imaging outcomes, we classified the study population into three groups: Group 1 included cases with normal prenatal US and MRI findings (except for SEPC) and normal clinical outcome; Group 2 included cases with normal cerebral prenatal US (except for SEPC) and abnormal cerebral prenatal MRI with or without abnormal outcome; Group 3 included cases with abnormal prenatal US and MRI findings. These latter cases with obvious cerebral abnormalities at US were excluded from the statistical analysis as they do not represent a diagnostic issue. Nevertheless, clinical and imaging characteristics of this third subgroup are reported because they highlight SEPC features that could be encountered in apparently isolated SEPC.

Cases were considered pathological if the clinical outcome was abnormal or if the pregnancy was terminated.

Imaging features of subependymal pseudocysts

SEPC were defined as cystic lesions located along the inferior wall or adjacent to the lateral wall of the frontal horns (Figure 1) or adjacent to the temporal or occipital horns (Figure 2). Cystic lesions located above the external angle of the lateral ventricle were not considered SEPC and were probably ischemic lesions, including periventricular leukomalacia, as described by Malinger *et al.*¹⁶ (Figure 3).

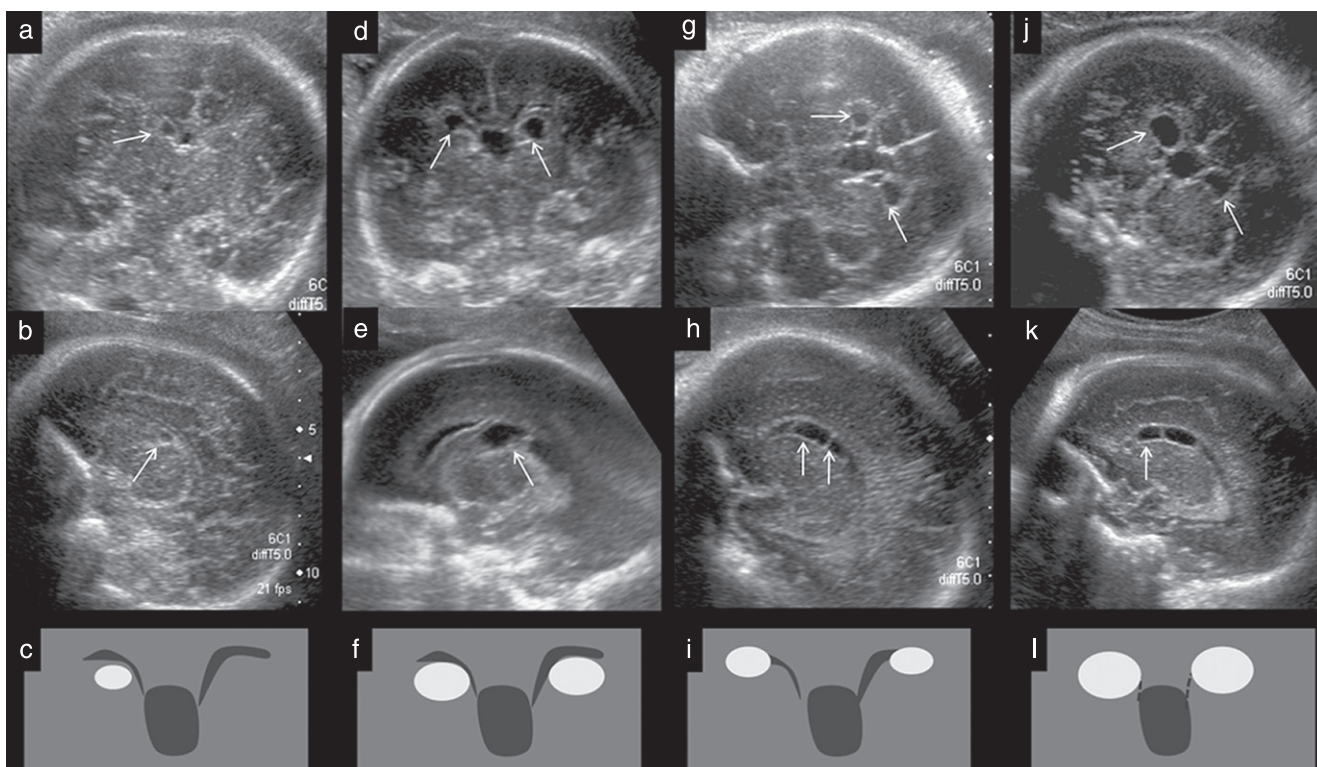


Figure 1 Typical sonographic patterns of subependymal pseudocysts (SEPC) (arrows) in coronal (a,d,g,i) and parasagittal (b,e,h,k) views. (a,b,c) SEPC located below the frontal horns: germinolysis cysts (images from a 34-week fetus). (d,e,f) Larger germinolysis SEPC located below the frontal horns (30 weeks). (g,h,i) SEPC lateral to the frontal horns (34 weeks). (j,k,l) Larger SEPC lateral to the virtual frontal horns should not be mistaken for enlarged frontal horns (33 weeks). Note that, in all cases, SEPC are located below or lateral to the frontal horns.

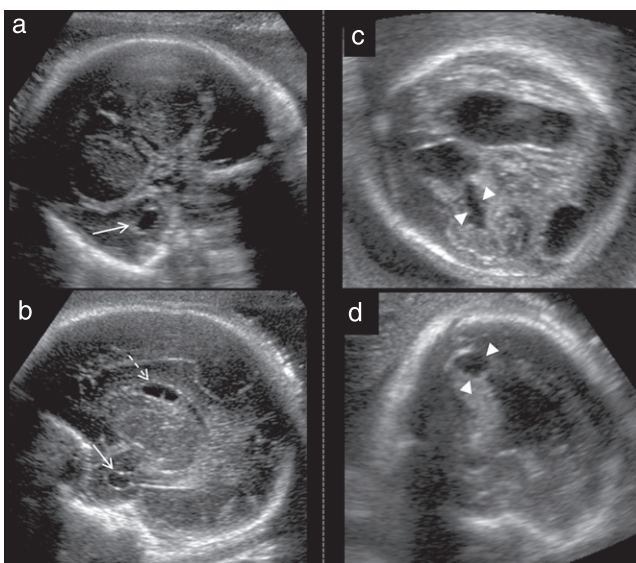


Figure 2 Ultrasound images of temporal and occipital subependymal pseudocysts (SEPC) in coronal (a,c) and parasagittal (b,d) views. (a,b) Temporal SEPC (solid arrows) in context of pseudo-TORCH syndrome associated with SEPC lateral to the frontal horns (dotted arrow). (c,d) Occipital SEPC (arrowheads) in context of cytomegalovirus fetal infection associated with ventricular dilatation.

We described SEPC on both prenatal US and prenatal MRI in terms of size, number, uni/bilaterality and anatomical location in relation to the frontal (along the

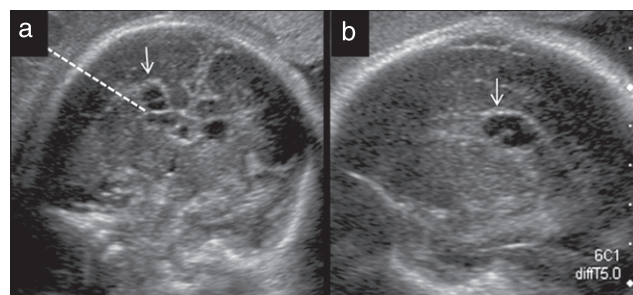


Figure 3 Ultrasound images of periventricular leukomalacia in coronal (a) and parasagittal (b) views: cystic lesions (solid arrows) are located above the external angle of the lateral ventricle (dotted line).

inferior wall or adjacent to the lateral wall of the frontal horns), temporal or occipital horns. We also evaluated the location of the SEPC in relation to the caudothalamic notch, differentiating between SEPC extending anterior to, those extended up to and those extending posterior to the caudothalamic notch (Figure 4).

Regarding SEPC morphology, the ratio between their anteroposterior diameter and height was evaluated on parasagittal slices. We also evaluated the shape of the SEPC (oval or square) and their margins (well- or ill-defined). When the SEPC were multiple, the septa separating them were also analyzed. SEPC were considered typical if they showed well-defined margins and an oval shape, with height smaller than

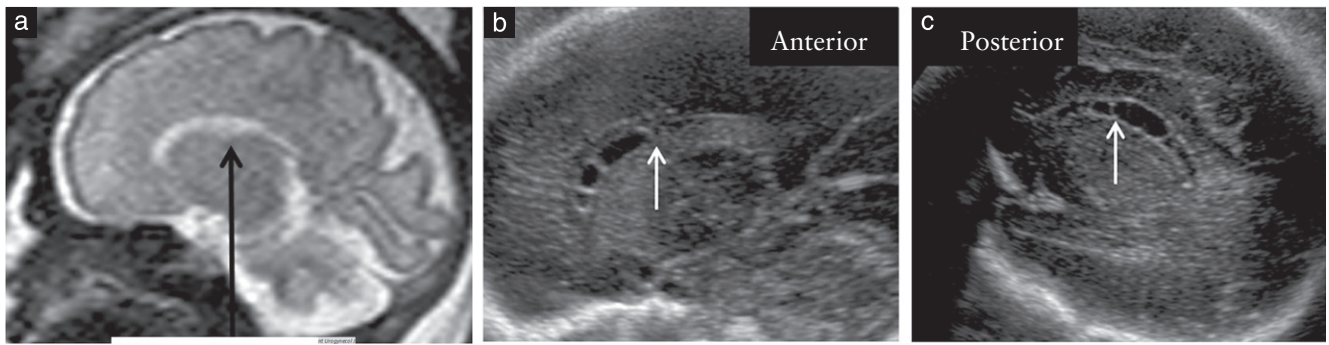


Figure 4 (a) Evaluation of subependymal pseudocyst (SEPC) location in relation to the caudothalamic notch on a T2-weighted parasagittal magnetic resonance slice (black arrow). On sonographic parasagittal views (b,c), SEPC were differentiated according to their extension anterior to, up to or posterior to the caudothalamic notch (white arrows).

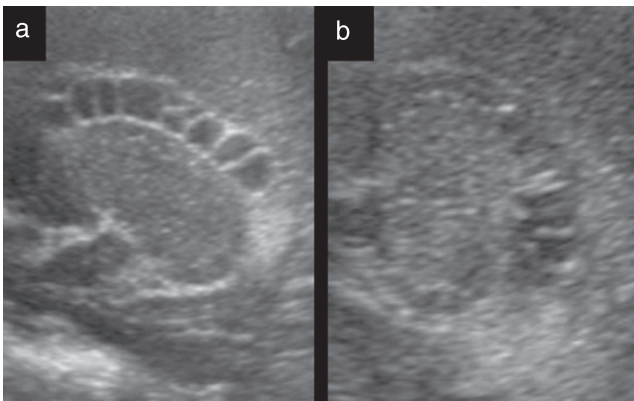


Figure 5 Atypical sonographic morphology of subependymal pseudocysts (SEPC) in parasagittal views. (a) SEPC height is greater than the anteroposterior diameter in a case of suspected metabolic disorder with associated white-matter abnormalities. (b) SEPC present with ill-defined margins in a case of a chromosomal disorder (del 2p 3.1) associated with renal multicystic dysplasia. In both cases, SEPC extend posterior to the caudothalamic notch.

the anteroposterior diameter. Multiple SEPC showed a typical ‘string-of-beads’ pattern (oval cystic lesions with well-defined borders, well separated from one another). SEPC were considered atypical if they showed ill-defined margins or a square shape or if their height was greater than their anteroposterior diameter (Figure 5).

Statistical analysis

Results are presented as mean \pm SD or median (range) for continuous data and n (%) for categorical data. Comparisons between Groups 1 and 2 were made using the chi-square or Fisher’s exact test, for categorical variables, and unpaired t -test or Mann–Whitney U -test, for continuous variables, after normality of the distribution had been assessed by means of the Shapiro–Wilk test. Receiver–operating characteristics (ROC) curve analysis was performed, computing the Youden’s index (defined as sensitivity + specificity – 1) and the distance between the ROC curve and the upper left corner (defined as (specificity – 1)² + (1 – sensitivity)²), to identify the optimal

cut-off for size of SEPC to maximize sensitivity (> 70%) for predicting a pathological outcome.

Multivariate logistic regression models were performed to identify independent predictors of pathological outcome, using Firth’s bias correction to account for the limited sample size and following a stepwise backwards procedure by removing non-significant variables at each step.

Agreement between US and MRI findings with respect to SEPC features was investigated using agreement proportions and kappa coefficients for categorical data, and Wilcoxon’s signed ranks test for paired data, comparing mean number and size of SEPC as assessed by the two techniques.

A two-tailed P -value < 0.05 was considered statistically significant. All statistical analyses were performed using STATA statistical software (Version 12.1, Stata Corp., College Station, TX, USA).

RESULTS

Inclusion criteria and study population

We retrieved from our Paediatric Radiology Department database 61 cases with SEPC detected at prenatal US and/or MRI during the 4-year study period. Of these, 11 were excluded due to insufficient information about obstetric history, postnatal follow-up or fetopathological data. No statistically significant difference was found between included and excluded cases with regard to available data (gestational age, imaging findings). In the 50 cases meeting the inclusion criteria, we performed the following imaging examinations: both MRI and US ($n=48$) and targeted US only ($n=2$).

The following findings were observed at US screening before referral: SEPC ($n=35$), ventricular dilatation ($n=6$), intrauterine growth restriction ($n=2$) and other cerebral and extracerebral abnormalities ($n=5$). In our department, additional SEPC were found at targeted neurosonography ($n=12$) and MRI ($n=3$). Moreover, a few women were referred to our department following maternal cytomegalovirus (CMV) seroconversion ($n=5$)

or because of a history of cerebral abnormalities in a previous pregnancy ($n = 1$).

Group 1 included 29 cases (28 cases with both US and MRI and one case with US only). In all cases, the clinical outcome was normal.

Group 2 included 12 cases (11 cases with both US and MRI and one case with US only). Seven pregnancies were terminated. Five children were liveborn: one child had an abnormal clinical outcome, one neonate died at 2 days and three children had an abnormal outcome but were lost to follow-up (at 1, 12 and 18 months) (Table 1).

Group 3 included nine cases (Table S1). Seven were terminated and two had abnormal clinical outcome (Table 2).

At prenatal US, the following extracerebral abnormalities were observed: multicystic renal dysplasia ($n = 1$), cleft palate ($n = 1$), hepatomegaly and intestinal tract abnormalities ($n = 5$) and bone dysplasia ($n = 1$); such abnormalities were sometimes multiple in the same patient. Extracerebral abnormalities were significantly associated with an abnormal outcome ($P = 0.044$).

In Group 2, MRI detected white-matter abnormalities ($n = 9$) (Figure 6) and abnormal gyration ($n = 1$) that were not visible at prenatal US. MRI was not performed in a case of del 2p3.1 (which underwent TOP) and MRI was normal in a case of cloacal malformation (perinatal death).

In Group 3, all cerebral abnormalities detected at prenatal US were confirmed by fetal brain MRI and included: microcephaly, gyration disorders, posterior fossa, corpus callosum and parenchymal abnormalities. Fetal MRI detected four additional white-matter abnormalities.

In all 14 (66.7%) cases in which the parents elected to terminate the pregnancy following prenatal counseling, the fetopathological data confirmed the prenatal data: metabolic disorder ($n = 9$, six cases in Group 2 and three in Group 3), congenital infection ($n = 3$, Group 3), chromosomal abnormality ($n = 2$, one case in Group 2 and one in Group 3) and bone dysplasia ($n = 1$, Group 3). The nine cases of metabolic disorders included pyruvate dehydrogenase deficiency ($n = 1$), Zellweger syndrome ($n = 1$), lysosomal storage disorder ($n = 1$) and six cases suggestive of aminoacidopathy with white-matter spongiosis and marked astrocytic gliosis at neuropathological examination. The types of chromosomal abnormalities were del 2p3.1 ($n = 1$) and del 5p15.3pter ($n = 1$).

Prenatal parameters associated with a pathological outcome

The prenatal parameters and their relationship with clinical and imaging outcomes are summarized in Table 3. None of these parameters was significantly associated with adverse outcome. The mean gestational age at SEPC diagnosis did not differ significantly between Groups 1 and 2 ($P = 0.694$).

Comparative analysis of SEPC features at MRI and US

The agreement between US and MRI was excellent, ranging globally from 91.1% (SEPC being uni- or bilateral, SEPC morphology) to 100% (SEPC location relative to caudothalamic notch) and yielding kappa values from 0.77 to 1 (all significant at the $P < 0.0001$ level). There was no statistically significant difference between the mean number of SEPC measured with US and with MRI ($P = 0.076$). The measured size of the SEPC was larger with MRI (12.4 ± 7.20 mm) than with US (9.17 ± 5.93 mm) ($P < 0.0001$).

Characteristics of SEPC associated with a pathological outcome

Characteristics of SEPC for Groups 1 and 2 are summarized in Table 4. SEPC great-axis dimension was significantly associated with a pathological outcome, with Group 2 having a longer mean great axis compared with Group 1 ($P = 0.021$). ROC curve analysis suggested an optimal cut-off of ≥ 9.00 mm that maximized sensitivity (sensitivity, 75%; specificity, 62%; area under the ROC curve, 0.73), with maximized Youden's index (0.37) and minimal distance between the ROC curve and the upper left corner (0.45). Moreover, SEPC adjacent to the temporal horns and SEPC posterior to the caudothalamic notch were observed more frequently in Group 2, indicating their association with poor outcome ($P = 0.003$ and $P = 0.003$, Table 4). While Group 3 was not included in the statistical analysis, note that occipital SEPC were observed only in Group 3 (Table S2). Also noteworthy is that there was no statistical difference between Groups 1 and 2 regarding the outcome between cases with frontal SEPC along the inferior wall and those in which they were adjacent to the lateral wall of the frontal horns ($P = 0.156$).

In 47 cases, SEPC were well-depicted at US, with their morphology considered to be typical in 45 cases and atypical in two cases (in Group 2). Atypical morphology was significantly associated with pathological outcome ($P = 0.013$).

Neither the number of SEPC at prenatal US nor their laterality was significantly associated with pathological outcome.

In multivariate analysis, three predictors were independently associated with a pathological outcome, i.e. SEPC adjacent to the temporal horns ($P = 0.009$), atypical SEPC morphology ($P = 0.023$) and SEPC great-axis ≥ 9 mm ($P = 0.061$).

Postnatal evolution of SEPC and clinical follow-up

The postnatal follow-up by US or MRI was shorter (mean, 1.5 months) than was the clinical follow-up (mean, 9.9 (SD, 12.2; range, 1–42) months). At postnatal US and/or MRI, SEPC had disappeared in 41% of cases, decreased in size in 6% and remained unchanged in 53%.

In Group 1, postnatal imaging was performed in 27/29 infants (cranial US ($n = 18$) and/or MRI ($n = 11$)); SEPC

Table 1 Summary of family history, prenatal imaging and clinical outcome in fetuses with apparently isolated subependymal pseudocysts (SEPC) at ultrasound (US), and either additional abnormalities detected at prenatal magnetic resonance imaging (MRI), adverse clinical outcome, or both (Group 2)

Case	Family history	CMV seroconversion	GA at US screening (wks)	Reason for referral	GA at referral US (wks)	CNS US findings (except for SEPC)	Other US abnormalities	GA at MRI (wks)	MRI findings (except for SEPC)	Outcome	Final diagnosis
1	None	Yes	32	SEPC	34	None	Hepatomegaly	34	White-matter abnormalities	Delivery: 39 wks	Lost to follow-up at 18 months
2	None	None	26	SEPC	27	None	Renal multicystic dysplasia	NP	NP	TOP: 32 wks	Del 2p3.1
3	None	None	31	SEPC	33	None	None	33	White-matter abnormalities	TOP: 34 wks	Aminoacidopathy
4	None	None	26	SEPC	31	None	None	31	White-matter abnormalities	TOP: 39 wks	Aminoacidopathy
5	TOP (previous pregnancy)	None	24	SEPC	35	None	None	35	White-matter abnormalities	TOP: 37 wks	Aminoacidopathy
6	Consanguinity, microcephaly in sibling	None	32	Cloacal malformation	32	None	Cloacal malformation	32	None	Delivery: 40 wks, perinatal death	Cloacal malformation
7	None	Yes	35	SEPC	37	None	Hepatomegaly	37	Abnormal gyration	Delivery: 39 wks	Unexplained gigantism, lost to follow-up at 12 months
8	None	None	33	SEPC	35	None	None	35	White-matter abnormalities	TOP: 36 wks	Aminoacidopathy
9	None	None	34	IUGR	35	None	None	35	White-matter abnormalities	Delivery: 37 wks	Pseudo-TORCH syndrome
10	None	None	33	SEPC	34	None	None	35	White-matter abnormalities	TOP: 36 wks	Aminoacidopathy
11	None	None	34	SEPC	36	None	None	36	White-matter abnormalities	Delivery: 37 wks	White-matter abnormalities at postnatal MRI, lost to follow-up at 1 month
12	Consanguinity, neurodevelopmental disability in sibling	None	23	IUGR	31	None	None	31	White-matter abnormalities	TOP: 32 wks	Aminoacidopathy

CMV, cytomegalovirus; CNS, central nervous system; GA, gestational age; IUGR, intrauterine growth restriction; NP, not performed; TOP, termination of pregnancy; wks, weeks.

Table 2 Summary of family history, prenatal imaging and clinical outcome in fetuses with subependymal pseudocysts (SEPC) identified at ultrasound (US) in association with other abnormalities at prenatal US and magnetic resonance imaging (MRI) (Group 3)

Case	Family history	CMV seroconversion	GA at US screening (wks)	Reason for referral	GA at referral US (wks)	CNS US findings (except for SEPC)	Other US abnormalities	GA at MRI (wks)	MRI findings (except for SEPC)	Outcome	Final diagnosis
1	Maternal alcoholism	None	28	Maternal alcoholism	33	Thin CC, small cerebellum	Typical facial dysmorphism	33	Thin CC, small cerebellum	Delivery: 35 wks	Fetal alcohol syndrome
2	None	None	26	SEPC	31	Cerebellar hypoplasia	None	31	Pontocerebellar hypoplasia	TOP: 34 wks	Del 5p
3	CMV	Yes	24	Intestinal tract abnormalities	25	Abnormal gyration, microcephaly, intracranial calcifications	Hepatosplenomegaly, bowel loops hyperechogenicity	25	Abnormal gyration, microcephaly, intracranial calcifications	TOP: 26 wks	CMV
4	None	None	36	SEPC	37	Microcephaly	None	37	Microcephaly	TOP: 38 wks	Aminoacidopathy
5	None	None	24	SEPC, ventriculomegaly	31	Opercular dysplasia	None	32	Diffuse polymicrogyria, opercular dysplasia, white-matter abnormalities	TOP: 34 wks	Zellweger syndrome
6	CMV, HIV+	Yes	32	Ventriculomegaly	33	Ventriculomegaly	None	33	White-matter abnormalities	Delivery: 38 wks	CMV
7	CMV	Yes	26	Suspicion of cerebral hemorrhage	28	Polymicrogyria, opercular dysplasia, microcephaly	Hepatosplenomegaly	28	Polymicrogyria, opercular dysplasia, microcephaly, laminar necrosis	TOP: 28 wks	CMV
8	Consanguinity, TOP for CC abnormalities and multiple malformations	None	22	Ventriculomegaly, small cerebellum	26	Ventricular hemorrhage, microcephaly, abnormal gyration	None	26	Ventricular hemorrhage, microcephaly, abnormal gyration	TOP: 28 wks	Pyruvate dehydrogenase deficiency
9	None	None	34	SEPC	35	Small vermis	Bone dysplasia, polyhydramnios	35	Small vermis	TOP: 36 wks	Lysosomal storage disorder

CC, corpus callosum; CMV, cytomegalovirus; CNS, central nervous system; GA, gestational age; HIV+, positive for human immunodeficiency virus; TOP, termination of pregnancy; wks, weeks.

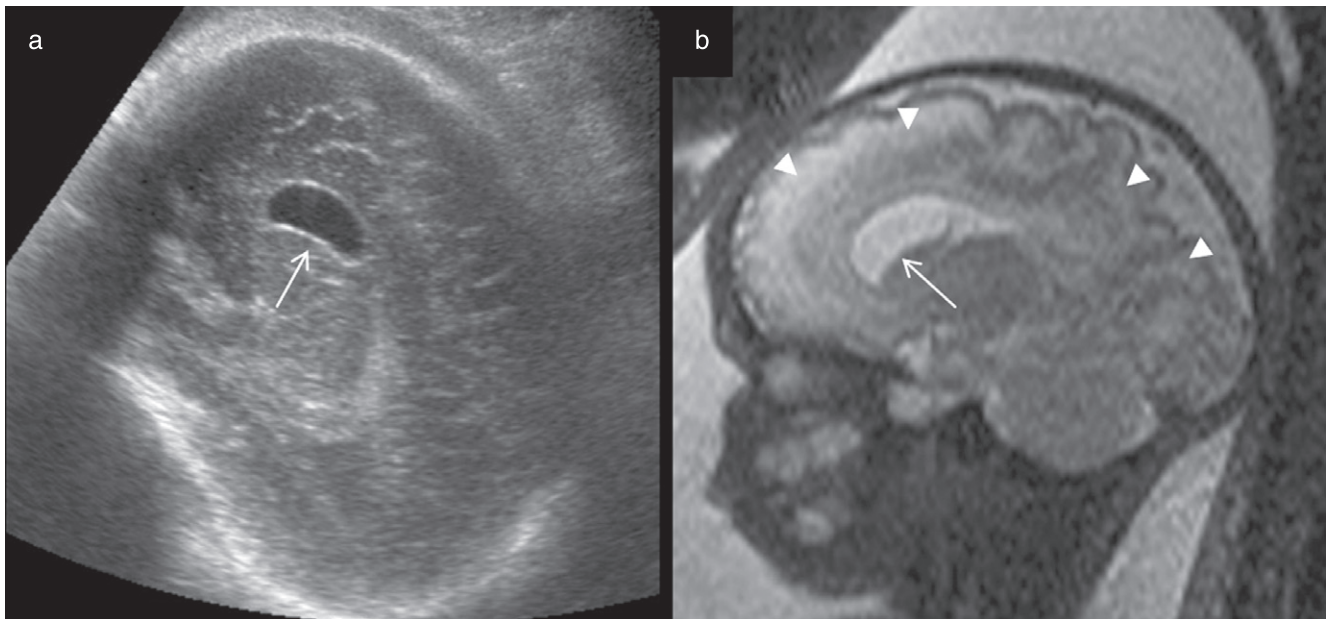


Figure 6 Imaging of subependymal pseudocysts (SEPC) in a fetus with suspicion of a metabolic disorder at 35 weeks of gestation: SEPC lateral to the frontal horn on sonographic parasagittal view (a) and T2-weighted parasagittal magnetic resonance (MR) slice (b) are well demonstrated with both techniques (arrow), whereas diffuse white-matter abnormalities (hyperintensities on T2-weighted sequences) (arrowheads) are depicted only on MR imaging. Pathological examination confirmed white-matter abnormalities with spongiform changes and fibrous astrocytosis associated with SEPC, in keeping with an aminoacidopathy.

remained unchanged in 14 cases, they had decreased in size in two and they had disappeared in 11.

In Group 2, imaging follow-up was available in three of five cases, in all of which the SEPC remained unchanged in size and morphology: a case of white-matter abnormality at fetal brain MRI (cranial US performed at 1 month); a case of suspected metabolic disorder with normal clinical evolution during the first months of age (postnatal MRI performed at 2 months); and a case of suspected cloacal malformation, confirmed at postnatal examination. This child died in the immediate postnatal period due to respiratory distress; SEPC were unchanged on cranial US at day 1 postnatally. In the other two cases, imaging follow-up was not available. These were a case of CMV seroconversion with white-matter abnormalities, with normal clinical follow-up at 18 months, and a case of SEPC associated with gyration abnormalities, which presented at 1 year with unexplained gigantism.

In Group 3, the SEPC had disappeared at postnatal imaging in both cases. One was a case of white-matter abnormalities in the context of congenital CMV infection which was confirmed at postnatal MRI. At clinical evaluation, the child presented with right vestibular anomaly and left moderate deafness. She could walk at 26 months but required psychomotor rehabilitation. The other was a case of fetal alcohol syndrome; this child presented with microcephaly and psychomotor impairment.

DISCUSSION

There is much confusion in the literature regarding SEPC. The term 'pseudocysts' is favoured due to the absence of epithelial lining^{4,23,24}. 'Congenital cysts' have been

Table 3 Maternal and pregnancy characteristics of the study population of fetuses with apparently isolated subependymal pseudocysts (SEPC) at ultrasound (US), according to study group

Characteristic	Group 1 (n = 29)	Group 2 (n = 12)	P
Reason for referral			0.89
SEPC at US screening	22 (71.0)	9 (29.0)	
Other	7 (70.0)	3 (30.0)	
Maternal seroconversion			0.139
Cytomegalovirus	1 (33.3)	2 (66.7)	
None	28 (73.7)	10 (26.3)	
Karyotype			0.116
Normal	29 (72.5)	11 (27.5)	
Chromosomal abnormality	0 (0.0)	1 (100.0)	
Maternal pathology			0.574
No	26 (72.2)	10 (27.8)	
Yes	3 (60.0)	2 (40.0)	
Family history			0.282
Not relevant	27 (75.0)	9 (25.0)	
Neurodevelopmental disability	1 (33.3)	2 (66.7)	
Metabolic disorder	0 (0.0)	1 (100.0)	
Polycystic kidneys	1 (100.0)	0 (0.0)	
Consanguinity			0.139
No	28 (73.7)	10 (26.3)	
Yes	1 (33.3)	2 (66.7)	
GA at SEPC diagnosis (weeks)	30.88 ± 3.88	30.34 ± 4.22	0.694

Data are given as *n* (%) or mean ± SD. Group 1 had no further findings; Group 2 had either additional abnormalities detected at prenatal cerebral magnetic resonance imaging, adverse clinical outcome, or both. GA, gestational age.

described in the literature as coarctation of the frontal horn cysts and are considered normal variants^{25–27}. This imaging description has not been confirmed by

Table 4 Characteristics of subependymal pseudocysts (SEPC) and extracerebral abnormalities detected at ultrasound (US) in fetuses with apparently isolated SEPC at ultrasound (US), according to study group

Characteristic/abnormality	Group 1 (n = 29)	Group 2 (n = 12)*	P
SEPC location relative to ventricles			0.003
Frontal horns	28 (82.4)	6 (17.6)	
Temporal horn	1 (20.0)	4 (80.0)	
Occipital horn	0 (0.0)	0 (0.0)	
SEPC location relative to CTN			0.003
Anterior or up to CTN	28 (82.4)	6 (17.6)	
Posterior to CTN	1 (20.0)	4 (80.0)	
Uni/bilaterality			0.189
Unilateral	9 (90.0)	1 (10.0)	
Bilateral	20 (69.0)	9 (31.0)	
SEPC morphology			0.013
Typical	29 (78.4)	8 (21.6)	
Atypical	0 (0.0)	2 (100.0)	
Extracerebral abnormality			0.044
Renal dysplasia	0 (0.0)	1 (100.0)	
Hepatomegaly	0 (0.0)	2 (100.0)	
Intestinal bud abnormality	0 (0.0)	0 (0.0)	
Cleft palate	1 (100.0)	0 (0.0)	
Number of SEPC	2.45 ± 0.78	2.60 ± 0.70	0.591
SEPC great axis (mm)	8.00 ± 5.64	11.67 ± 5.82	0.021

Data are given as *n* (%) or mean ± SD. Group 1 had no further findings; Group 2 had either additional abnormalities detected at prenatal cerebral MRI, adverse clinical outcome, or both. *SEPC not well depicted in two cases. CTN, caudothalamic notch.

histopathological analysis. In retrospect, it is probable that connatal cysts have been mistaken for SEPC adjacent to the lateral wall of the frontal horns. The term 'germinolytic cysts' refers to their pathogenesis, SEPC developing in the remnants of the germinal matrix, which can be found around the lateral ventricles until about 15–16 gestational weeks. Thereafter, the germinal matrix regresses spontaneously and remains only below the frontal horns by 26–28 weeks²⁸. Typically, SEPC are located below the frontal horns, in the caudothalamic notch or lateral to the external angle of the frontal horns. They should be differentiated from cysts of periventricular leukomalacia that develop outside the germinal matrix, in the periventricular white matter, and usually extend above the external angle of the frontal horns¹⁶.

The large number of cases (*n* = 61) examined in our institution during the 4-year study period is probably due to our center being a tertiary referral center in fetal medicine. Interestingly, the great majority (47/50) of SEPC included in the study were diagnosed by US.

In accordance with data in the literature, we found that the majority of isolated SEPC were associated with a normal outcome^{10,16}. The rate of pathological outcome in our population was higher (21/50) than that of a screening population, as would be expected in a tertiary referral center. As reported previously, SEPC were observed in the setting of congenital infections, chromosomal anomalies and metabolic disorders^{23,29}.

We separated cases with apparently isolated SEPC, i.e. cases with normal US findings other than SEPC, into two groups: those with no further findings (Group 1), and those with either additional abnormalities detected at prenatal MRI, adverse clinical outcome, or both (Group 2). Comparison of these groups allowed us to identify sonographic features of SEPC that might indicate underlying pathology.

We found a statistically significant difference between the temporal and frontal (either below or adjacent to the frontal horns) locations of SEPC with respect to outcome: a temporal location was strongly associated with adverse outcome. Occipital SEPC were observed in two cases of CMV infection (Group 3), with many other cerebral abnormalities being identified at US. Posterior location of SEPC in relation to the caudothalamic notch and an SEPC great-axis length ≥ 9 mm were also significantly more common in cases with adverse outcome. Tropism of CMV for the germinal matrix is well documented and SEPC are related to germinal matrix necrosis³⁰. If damage of the germinal matrix occurs early, SEPC may be observed in locations at which germinal matrix is still present, e.g. posterior to the caudothalamic notch or at the level of the temporal and occipital horns, and their size might be larger than in physiological conditions. Our findings are in agreement with those of other studies reporting the overall excellent prognosis of SEPC, but these studies considered only SEPC located adjacent to the frontal horns, with no focus on the caudothalamic notch^{31–33}.

Atypical morphology of the SEPC is also a good marker for underlying disease, suggesting that necrosis of the germinal matrix resulting from an acute ischemic event may generate SEPC presenting with ill-defined borders or an unusual morphology.

The agreement between MRI and US was excellent regarding SEPC location and morphological evaluation. The assessment of SEPC size was more accurate with US than it was with MRI as it was possible to delineate properly the limits of each SEPC and to assess the presence of septa between them. At MRI, multiple adjacent small SEPC could be considered incorrectly as a single large cystic lesion.

In bilateral multiple SEPC, a positive likelihood ratio of 9 for a chromosomal abnormality or a congenital infection has been reported in newborns³⁴. We did not find this in fetuses.

At imaging follow-up, approximately 40% of SEPC had disappeared, just over half remained unchanged in size and very few SEPC had decreased in size. No SEPC increased in size after birth. Postnatal evolution of SEPC is poorly documented in the literature. It has been reported that the majority of SEPC have resolved by the age of 12 months, at US follow-up^{3,4,31}. SEPC are thus expected to regress after birth if isolated and observed in an unremarkable context. When considering the four infants with prenatal brain MR abnormalities, the postnatal evolution of SEPC in our study was variable as they disappeared in three cases and remained unchanged in one.

In our series, all children with normal prenatal US and MRI findings (except for SEPC) had a favorable clinical outcome, as described in previous studies^{4,24,31}. Mild neurological deficiencies have been described during the first year³⁵ but a normal neurodevelopmental status was observed after a 3-year follow-up³⁶. The risk for neurodevelopmental disability was significantly higher when SEPC were associated with fetal infection, intrauterine growth restriction, malformations and chromosomal aberrations or persistence of the cysts during follow-up³. The three children lost to follow-up in Group 2 showed marked white-matter abnormalities at prenatal MRI. In one case, postnatal MRI was performed and confirmed these findings. Our results also showed that detection of extracerebral abnormalities (e.g. hepatomegaly) associated with SEPC should raise suspicion for an underlying pathology.

The two main limitations of our study are the relatively small number of cases and the short period of postnatal follow-up, which did not allow us to draw definitive conclusions about the children's neurodevelopmental status.

In conclusion, this observational study suggests that the following criteria should raise suspicion of an underlying pathology when apparently isolated SEPC are discovered on prenatal cerebral US: SEPC great axis ≥ 9 mm; SEPC located adjacent to occipital and temporal horns; SEPC extending posterior to the caudothalamic notch; SEPC presenting with atypical morphology. Under these four conditions, further investigations, such as targeted neurosonography and fetal brain MRI, should be offered in order to rule out additional brain abnormalities. Moreover, the detection of extracerebral abnormalities associated with SEPC at prenatal US should lead to further investigations.

REFERENCES

- Shaw CM, Alvord EC, Jr. Subependymal germinolysis. *Arch Neurol* 1974; 31: 374–381.
- Levene MI. Diagnosis of subependymal pseudocyst with cerebral ultrasound. *Lancet* 1980; 2: 210–211.
- Makhoul IR, Zmora O, Tamir A, Shahar E, Sujov P. Congenital subependymal pseudocysts: own data and meta-analysis of the literature. *Isr Med Assoc J* 2001; 3: 178–183.
- Rademaker KJ, De Vries LS, Barth PG. Subependymal pseudocysts: ultrasound diagnosis and findings at follow-up. *Acta Paediatr* 1993; 82: 394–399.
- Larcos G, Gruenewald SM, Lui K. Neonatal subependymal cysts detected by sonography: prevalence, sonographic findings, and clinical significance. *AJR Am J Roentgenol* 1994; 162: 953–956.
- Correa F, Lara C, Carreras E, Vazquez E, Serra V. Evolution of fetal subependymal cysts throughout gestation. *Fetal Diagn Ther* 2013; 34: 127–130.
- Cohen HL, Sloves JH, Laungani S, Glass L, DeMarinis P. Neurosonographic findings in full-term infants born to maternal cocaine abusers: visualization of subependymal and periventricular cysts. *J Clin Ultrasound* 1994; 22: 327–333.
- Smith LM, Qureshi N, Renfro R, Sinow RM. Prenatal cocaine exposure and cranial sonographic findings in preterm infants. *J Clin Ultrasound* 2001; 29: 72–77.
- Lu JH, Emons D, Kowalewski S. Connatal periventricular pseudocysts in the neonate. *Pediatr Radiol* 1992; 22: 55–58.
- Ramenghi LA, Domizio S, Quartulli L, Sabatino G. Prenatal pseudocysts of the germinal matrix in preterm infants. *J Clin Ultrasound* 1997; 25: 169–173.
- Shackelford GD, Fulling KH, Glasier CM. Cysts of the subependymal germinal matrix: sonographic demonstration with pathologic correlation. *Radiology* 1983; 149: 117–121.
- Yamashita Y, Outani Y, Kawano Y, Horikawa M, Matsuishi T, Hashimoto T. Clinical analyses and short-term prognoses of neonates with subependymal cysts. *Pediatr Neurol* 1990; 6: 375–378.
- Russel IM, van Sonderen L, van Straaten HL, Barth PG. Subependymal germinolytic cysts in Zellweger syndrome. *Pediatr Radiol* 1995; 25: 254–255.
- De Keersmaecker B, Albert M, Hillion Y, Ville Y. Prenatal diagnosis of brain abnormalities in Wolf-Hirschhorn (4p-) syndrome. *Prenat Diagn* 2002; 22: 366–370.
- Wakahama Y, Nakayama M, Fujimura M. Autopsy findings in interstitial deletion 6q. *Pediatr Pathol* 1991; 11: 97–103.
- Malinger G, Lev D, Ben Sira L, Kidron D, Tamarkin M, Lerman-Sagie T. Congenital periventricular pseudocysts: prenatal sonographic appearance and clinical implications. *Ultrasound Obstet Gynecol* 2002; 20: 447–451.
- Bats AS, Molho M, Senat MV, Paupe A, Bernard JP, Ville Y. Subependymal pseudocysts in the fetal brain: prenatal diagnosis of two cases and review of the literature. *Ultrasound Obstet Gynecol* 2002; 20: 502–505.
- Rohrbach M, Chitayat D, Maegawa G, Shanske S, Davidzon G, Chong K, Clarke JT, Toi A, Tarnopolsky M, Robinson B, Blaser S. Intracerebral periventricular pseudocysts in a fetus with mitochondrial depletion syndrome: an association or coincidence. *Fetal Diagn Ther* 2009; 25: 177–182.
- Mochel F, Grebille AG, Benachi A, Martinovic J, Razavi F, Rabier D, Simon I, Boddaert N, Brunelle F, Sonigo P. Contribution of fetal MRI imaging in the prenatal diagnosis of Zellweger syndrome. *AJNR Am J Neuroradiol* 2006; 27: 333–336.
- Beltinger C, Saule H. Sonography of subependymal cysts in congenital rubella syndrome. *Eur J Pediatr* 1988; 148: 206–207.
- ISUOG Education Committee. Sonographic examination of the fetal central nervous system: guidelines for performing the 'basic examination' and the 'fetal neurosonogram'. *Ultrasound Obstet Gynecol* 2007; 29: 109–116.
- Bayley N. *Bayley scales of infant and toddler development*, third edn. Administration Manual. PsychCorps: San Antonio, TX 2006.
- Mito T, Ando Y, Takeshita K, Takada K, Takashima S. Ultrasonographical and morphological examination of subependymal cystic lesions in maturely born infants. *Neuropediatrics* 1989; 20: 211–214.
- Zorzi C, Angonese I. Subependymal pseudocysts in the neonate. *Eur J Pediatr* 1989; 148: 462–464.
- Enriquez G, Correa F, Lucaya J, Piqueras J, Aso C, Ortega A. Potential pitfalls in cranial sonography. *Pediatr Radiol* 2003; 33: 110–117.
- Epelman M, Daneman A, Blaser SI, Ortiz-Neira C, Konen O, Jarrin J, Navarro OM. Differential diagnosis of intracranial cystic lesions at head US: correlation with CT and MR imaging. *Radiographics* 2006; 26: 173–196.
- Tan ZY, Naidoo P, Kenning N. Case of the month. Ultrasound and MRI features of connatal cysts: clinicoradiological differentiation from other supratentorial periventricular cystic lesions. *Br J Radiol* 2010; 83: 180–183.
- Brisse H, Fallet C, Sebag G, Nessmann C, Blot P, Hassan M. Supratentorial parenchyma in the developing fetal brain: in vitro MR study with histologic comparison. *AJNR Am J Neuroradiol* 1997; 18: 1491–1497.
- Larroche JC. Sub-ependymal pseudo-cysts in the newborn. *Biol Neonate* 1972; 21: 170–183.
- Guibaud L, Attia-Sobol J, Buenerd A, Foray P, Jacquet C, Champion F, Arnould P, Pracros JP, Golfier F. Focal sonographic periventricular pattern associated with mild ventriculomegaly in foetal cytomegalic infection revealing cytomegalic encephalitis in the third trimester of pregnancy. *Prenat Diagn* 2004; 24: 727–732.
- Pal BR, Preston PR, Morgan ME, Rushton DI, Durbin GM. Frontal horn thin walled cysts in preterm neonates are benign. *Arch Dis Child Fetal Neonatal Ed* 2001; 85: F187–193.
- Trawber R, Rao S, Srinivasjois R, Thonell S, Nagarajan L, French N, Jacoby P, McMichael J. Outcomes of preterm neonates with frontal horn cysts: a retrospective study. *J Child Neurol* 2010; 25: 1377–1381.
- Wong F, Fraser S, Kelly E, Acton C. Clinical significance of isolated paraventricular cysts on cranial ultrasonography. *J Paediatr Child Health* 2004; 40: 552–555.
- Fernandez Alvarez JR, Amess PN, Gandhi RS, Rabe H. Diagnostic value of subependymal pseudocysts and choroid plexus cysts on neonatal cerebral ultrasound: a meta-analysis. *Arch Dis Child Fetal Neonatal Ed* 2009; 94: F443–446.
- Sudakoff GS, Mitchell DG, Stanley C, Graziani LJ. Frontal periventricular cysts on the first day of life. A one-year clinical follow-up and its significance. *J Ultrasound Med* 1991; 10: 25–30.
- Cevy-Macherel M, Forcada Guex M, Bickle Graz M, Truttmann AC. Neurodevelopment outcome of newborns with cerebral subependymal pseudocysts at 18 and 46 months: a prospective study. *Arch Dis Child* 2013; 98: 497–502.

SUPPORTING INFORMATION ON THE INTERNET

The following supporting information may be found in the online version of this article:



Table S1 Maternal and pregnancy characteristics in Group 3

Table S2 Description of subependymal pseudocyst characteristics and extracerebral abnormalities detected at prenatal ultrasound in Group 3



Application of a novel prenatal vertical cranial biometric measurement can improve accuracy of microcephaly diagnosis *in utero*

Z. LEIBOVITZ*†, C. SHIRAN‡, K. HARATZ†, M. TAMARKIN†, L. GINDES†, L. SCHREIBER§, G. MALINGER¶, L. BEN-SIRA***, D. LEV††, I. SHAPIRO*, H. BAKRY*, B. WEIZMAN*, A. ZREIK*, D. KIDRON‡‡, S. EGENBURG§§, A. ARAD§§ and T. LERMAN-SAGIE¶¶

*Department of Obstetrics and Gynecology, Bnai Zion Medical Center, Haifa, Israel; †Unit of Fetal Neurology and Prenatal Diagnosis, Department of Obstetrics and Gynecology, Wolfson Medical Center, Holon, Israel; ‡Maccabi Healthcare Services, North District, Israel; §Department of Pathology, Wolfson Medical Center, Holon, Israel; ¶Tel Aviv Sourasky Medical Center, Lis Maternity Hospital, Division of Ob-Gyn Ultrasound, Tel Aviv, Israel; **Department of Radiology, Tel Aviv Medical Center, Tel Aviv, Israel; ††Genetics Institute, Wolfson Medical Center, Holon, Israel; ‡‡Department of Pathology, Meir Medical Center, Kfar Saba, Israel; §§Department of Pathology, Bnai Zion Medical Center, Haifa, Israel; ¶¶Pediatric Neurology, Wolfson Medical Center, Holon, Israel

KEYWORDS: craniosynostosis; fetal microcephaly; molding; prenatal reference chart; ultrasound; vertical cranial biometry

ABSTRACT

Objective To construct a reference range for a new vertical measurement of the fetal head and to assess whether its combination with fetal head circumference (HC) can prevent the misdiagnosis of microcephaly in fetuses with an acrocephalic-like head deformation.

Methods A new vertical cranial biometric measurement was defined: the foramen magnum-to-cranium distance (FCD), measured between the foramen magnum and the upper inner cranial border along the posterior wall of the brainstem. The measurement was performed in a precise mid-sagittal plane using a three-dimensional multiplanar display of a sagittally acquired sonographic volume of the fetal head. The normal reference range was developed by measuring 396 healthy fetuses of low-risk singleton pregnancies between 15 and 40 gestational weeks. This reference was applied to 25 fetuses with microcephaly diagnosed prenatally (Fmic) based on $HC \geq 3 SD$ below the mean for gestational age. We determined an optimal FCD cut-off for combination with HC to detect all cases found with microcephaly at birth (micB), while excluding the fetuses with normal head circumference at birth (NHCB), who were described postnatally as having an acrocephalic-like cranial deformation.

Results In the healthy singleton fetuses, FCD increased with gestational age, with a quadratic equation providing an optimal fit to the data (adjusted $R^2 = 0.934$). The measurement could be assessed in 95.2% of cases. Of the 25 cases diagnosed with Fmic prenatally, on the basis

of HC alone, 14 were micB and 11 were NHCB. We observed FCD below the mean $-2SD$ for gestational age in all 14 micB cases, but in only four of the 11 NHCB cases ($P < 0.003$). An acrocephalic-like cranial deformation was described at birth in five of the seven NHCB cases with normal FCD. The mean $\pm SD$ FCD Z-score of the micB cases was significantly lower ($P < 0.001$) than that of the false-positive ones: $-3.85 \pm 0.96 SD$ and $-1.59 \pm 1.45 SD$, respectively. Based on HC measurement alone, the positive predictive value (PPV) was 56%. Combination of the HC and FCD criteria raised the PPV to 78%, decreasing the number of false positives from 11 to four, without missing any of the 14 micB cases.

Conclusions Fetal vertical cranial biometric assessment in the mid-sagittal plane is feasible and correlates well with gestational age. In our series, a vertical cranial deformation was a frequent cause of a false Fmic diagnosis made on the basis of HC alone. Combination of the new vertical cranial biometric measurement with HC measurement can exclude these cases and thus improve diagnostic accuracy for Fmic. Copyright © 2016 ISUOG. Published by John Wiley & Sons Ltd.

INTRODUCTION

Diagnosis of fetal microcephaly (Fmic) relies on the measurement of an abnormally small fetal head circumference (HC). However, the yield of the commonly used HC reference charts for prediction of microcephaly at birth (micB) is considered low. In 1984, Chervenak *et al.*¹, using a ref-

Correspondence to: Dr Z. Leibovitz, Ob/Gyn Department, Bnai Zion Medical Center, PO Box 4940, Haifa 31048, Israel (e-mail: zvi_l@yahoo.com; zvi.leibovitz.dr@gmail.com)

Accepted: 18 February 2016

reference range derived by Jeanty *et al.*², reported that only 46% of fetuses whose HC was 3 or more SD below the mean for gestational age were diagnosed with micB. In our recent study³, we showed that the application of two modern prenatal HC standards^{4,5} did not significantly improve micB prediction compared with the application of Jeanty *et al.*'s reference². This low predictive accuracy may result in misdiagnosis of Fmic, leading to unjustified terminations of pregnancy in countries in which this is an option.

There are many possible methodological reasons for the discrepancy between intrauterine and postnatal HC measurements which prevents accurate micB prediction^{3,6,7}. An acrocephalic-like (vertical) cranial deformation (due to molding or craniosynostosis) may also lead to a false diagnosis of Fmic⁸. We anticipated that the establishment of a novel reference range for vertical cranial dimensions would enable the exclusion of fetuses with a small HC due to a vertical cranial deformity and would not miss those with actual micB, since both the axial and vertical dimensions should be significantly reduced in such cases.

The first goal of this study was to construct reference data for vertical fetal head biometry in the mid-sagittal plane. The second was to apply the new reference to fetuses diagnosed as having Fmic based on HC measurement, in order to exclude cases that are false positive due to a vertical head deformity.

SUBJECTS AND METHODS

The normal growth of the fetal cranium in the mid-sagittal plane was assessed in singleton pregnancies with low obstetric risk, which had been referred to Bnai Zion Medical Center, Haifa, Israel between 2009 and 2012 for a routine fetal sonographic examination in the second or third trimester. Each fetus was examined once during the study. Additional inclusion criteria were: documented gestational age confirmed by early first-trimester ultrasound examination, normal fetal anatomy and growth at the second-trimester scan, and fetal HC within the normal range according to Jeanty *et al.*'s reference².

Fetal sonographic examinations were performed with Voluson E8, Voluson 730 Expert or Voluson 730 Pro (GE Healthcare Ultrasound, Milwaukee, WI, USA) machines equipped with three-dimensional (3D) probes. A transvaginal approach was used in cases of cephalic presentation and a transabdominal approach was used for non-cephalic presentation. To achieve an exact mid-sagittal cranial plane, we applied 3D multiplanar reconstruction using 4D View software (GE Healthcare Ultrasound). The fetal head was oriented in three standard orthogonal planes: coronal, mid-sagittal and axial (Figure 1a–c). The vertex was positioned upwards in the mid-sagittal plane. To reduce the amount of post-processing, all sonographic volumes were obtained by sagittal acquisition above the fetal vertex.

A new cranial biometric measurement was defined in the mid-sagittal plane: the foramen magnum-to-cranium distance (FCD). The FCD was measured as the distance

between the level of the foramen magnum and the upper inner cranial border, along the posterior wall of the brainstem. The level of the foramen magnum was demarcated by a line connecting between the lower echogenic edges of the clivus and the occipital bone (Figure 1b). Visualization of the internal cranial borders was enhanced by activation of volume contrast imaging mode, using a thin slice 1–2 mm in thickness. A vertical-to-axial ratio of the fetal skull dimensions was defined (FCD/HC) and the reference range of this ratio established according to gestational age.

The FCD was measured three times during each fetal examination, and the mean of these three values was used for analysis. One sonographic volume was examined in each case and the mid-sagittal plane was obtained independently for each measurement. All study measurements were performed by a single observer (C.S.). Intraobserver variability for FCD was expressed by the estimated repeatability coefficient, defined as $1.96 \times \sqrt{2} \times \text{SD}$, where the SD was assessed by subtraction of the mean of each set of three observations from the individual measurements in each case, with SD being calculated for the resulting differences across all cases. Applying this analysis one would expect the absolute difference between two measurements in a subject to differ by no more than the repeatability coefficient on 95% of occasions.

A Bland–Altman plot was used for analysis of the interobserver agreement for FCD measurements in a subgroup of 50 fetuses selected randomly and assessed by second observer (K.H.). The same sonographic volumes were examined by both observers. This analysis reveals a scatterplot of difference between the paired measurements against the mean values of the pairs, providing a mean difference of the studied subjects and $1.96 \times \text{SD}$ limits of agreement.

The mean values and SDs of FCD and FCD/HC were modeled as a function of the gestational week by curve estimation analysis based on the highest adjusted R^2 coefficient.

The developed references were then applied retrospectively to cases with Fmic diagnosed at one of two medical centers (Bnai Zion Medical Center, Haifa, Israel and Wolfson Medical Center, Holon, Israel) between 2007 and 2014. Inclusion criteria for these cases were: fetus with $\text{HC} \leq \text{mean} - 3\text{SD}$ for gestational age according to Jeanty *et al.*²; singleton pregnancy with gestational age documented in the first or early second trimester; available medical and imaging records made at diagnosis of Fmic; electronically archived 3D sonographic volumes appropriate for FCD measurement; and availability of data on the occipitofrontal circumference (OFC) at birth or fetal autopsy results. Confirmation of micB was on the basis of either $\text{OFC} \leq \text{mean} - 2\text{SD}$ ⁹ or brain weight $\leq \text{mean} - 2\text{SD}$ at autopsy¹⁰.

The FCD and FCD/HC of the Fmic cases were assessed using the developed reference ranges and cases were divided into two groups: those confirmed as micB postnatally and false-positive Fmic cases which had a normal head circumference at birth (NHCB). The FCD

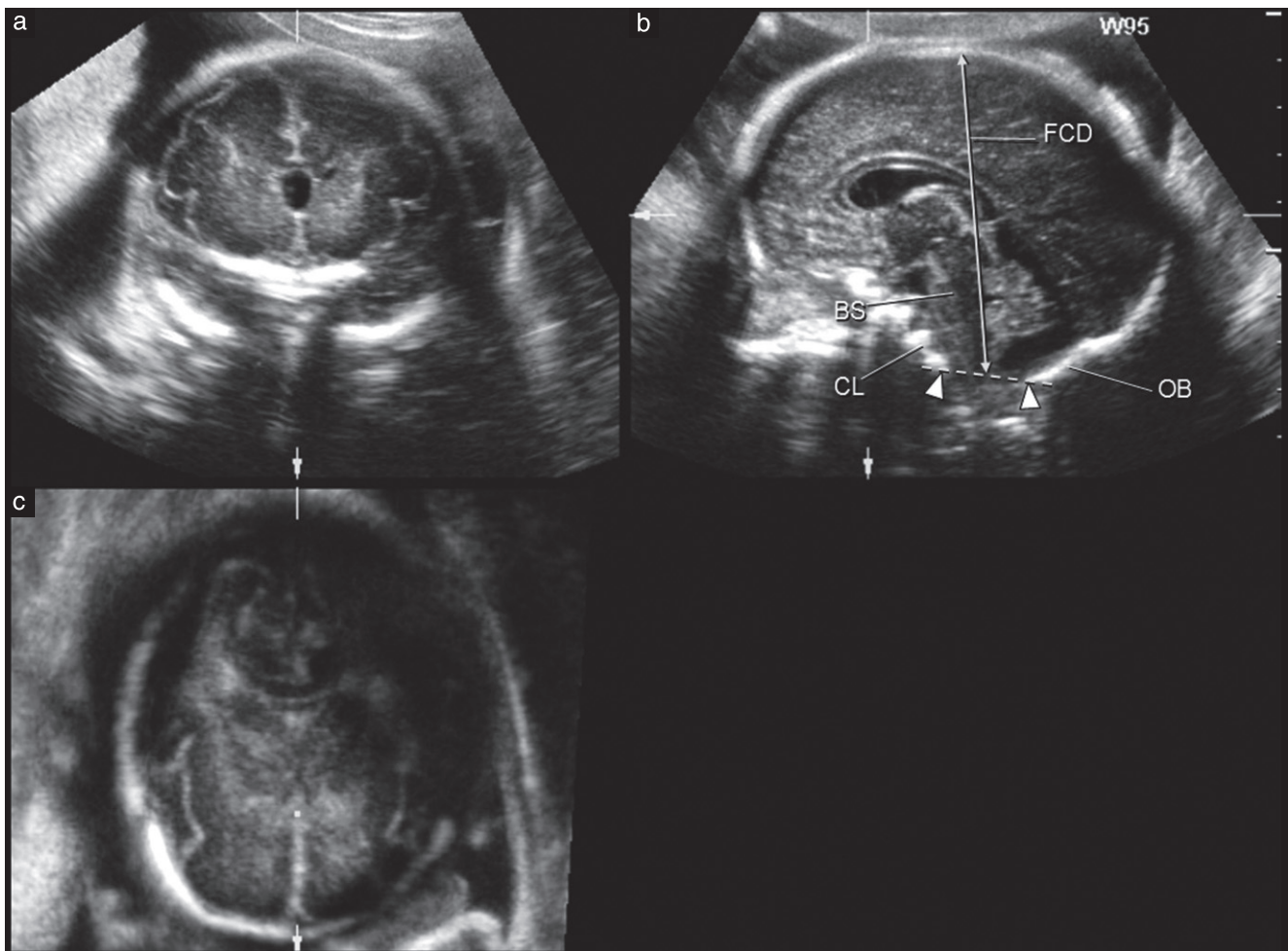


Figure 1 Measurement method for foramen magnum-to-cranium distance (FCD). Reconstructed three-dimensional (3D) multiplanar display of a 28-week fetus demonstrating three standard orthogonal sections: coronal (a), mid-sagittal (b) and axial (c). The 3D volume was obtained by sagittal acquisition above the fetal vertex, requiring only minimal post-processing to attain a precise mid-sagittal plane (b). FCD was measured in the mid-sagittal plane (b) as the distance from the level of the foramen magnum (---) to the inner upper border of the cranium, along the posterior margins of the brainstem (BS). Arrowheads indicate lower edges of the clivus (CL) and occipital bone (OB), defining the level of the foramen magnum.

and FCD/HC results were interpreted using Z-scores, thus indicating by how many SDs a particular result differed from the mean for gestational age.

We established optimal FCD and FCD/HC cut-offs aimed at detecting all micB cases while minimizing the number of false-positive Fmic cases by excluding NHCB fetuses which were described after birth as having an acrocephalic-like skull deformity. The positive predictive values (PPV) of FCD and FCD/HC for micB detection were assessed.

Data were analyzed using IBM SPSS statistics software (IBM Corporation Software Group, NY, USA). The study was approved by the Institutional Review Boards of the participating hospitals (Helsinki Committee Protocol) and informed consent for the sonographic examinations was acquired.

RESULTS

In total, 396 fetuses were assessed for establishment of normal vertical cranial biometry between 15 and 40

gestational weeks, and imaging quality was appropriate for performance of measurements in 377 (95.2%) of these fetuses.

The adjusted R^2 -based analysis of curve estimation for FCD and FCD/HC showed optimal fit using a second-degree polynomial equation (adjusted R^2 of 0.934 and 0.241, respectively). The modeled mean values and SDs of FCD and FCD/HC, according to gestational week, are provided in the graphs (also showing all normal cases) and tables in Appendix S1. The supplementary material also includes a Z-score calculator for FCD and FCD/HC assessment.

FCD increased with gestational age (Figure 2), while FCD/HC was relatively stable (Figure 3) and remained practically constant (range, 0.285–0.275) after 24 gestational weeks.

The FCD repeatability coefficient was 0.31 cm, i.e. the difference between paired measurements by a single observer in the same subject would not exceed this limit on 95% of occasions. Analysis of the interobserver agreement for FCD measurements made by two observers in the

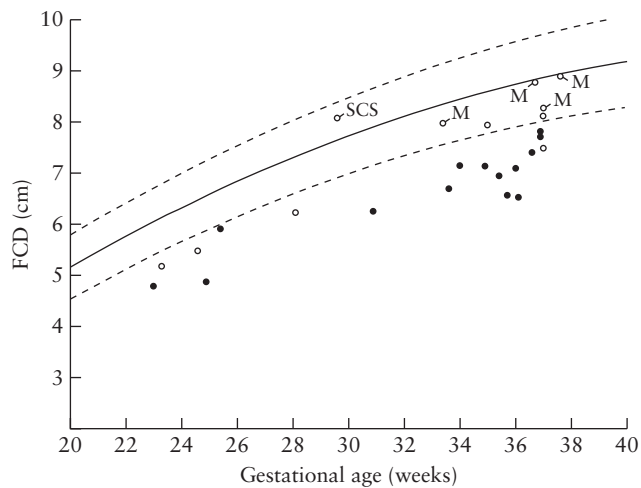


Figure 2 Foramen magnum-to-cranium distance (FCD) in 25 cases of fetal microcephaly (Fmic), plotted on FCD reference chart according to gestational age. The FCD reference was modeled according to second-order polynomial equations (Appendix S1). The FCD values of the 25 Fmic fetuses are subdivided into those diagnosed with microcephaly at birth (●) and those with normal head circumference at birth (○), among which a case of coronal craniosynostosis diagnosed with Saethre–Chotzen syndrome (SCS) and four cases with cranial molding (M) are indicated. Mean and $\pm 2SD$ are represented by solid and dashed curves, respectively.

same subjects (presented as Bland–Altman plot, Figure 4) resulted in a mean difference of 0.3 cm (95% limits of agreement, -0.57 to 1.17 cm). Intra- and interobserver analysis of FCD/HC was not assessed, because only a single HC evaluation was provided at each fetal examination.

Twenty-five cases of Fmic were identified on the basis of HC alone¹; 14 of these were diagnosed as having micB, and 11 as having NHCB. The mean gestational age at Fmic diagnosis was 32.8 ± 5.0 (range, 23–37.6) gestational weeks, and this did not differ significantly between micB and NHCB groups (32.9 ± 4.9 and 32.7 ± 5.3 , respectively).

The etiology could be determined in 13 of the 14 micB cases: primary microcephaly ($n=1$), malformation of cortical development ($n=2$), pontocerebellar hypoplasia ($n=2$), cytomegalovirus fetopathy ($n=2$), hypoxic/hemorrhagic brain damage ($n=1$), fetal alcohol syndrome ($n=1$), placental pathology ($n=2$), syndromic microcephaly ($n=1$) and Aicardi–Goutières syndrome ($n=1$).

An explanation for the discrepancy between the small fetal HC and normal OFC at birth was established in 10 of the 11 NHCB cases: five had a vertical cranial deformation diagnosed at birth (coronal craniosynostosis in one case and skull molding in four), three had Chiari-II malformation with an open spina bifida and in two there was placental pathology.

Termination of pregnancy was performed in 16 (64%) Fmic cases on parental request and according to the particular country's regulations (nine and seven fetuses from the micB and NHCB groups, respectively). Three of the seven terminated NHCB fetuses had a vertical

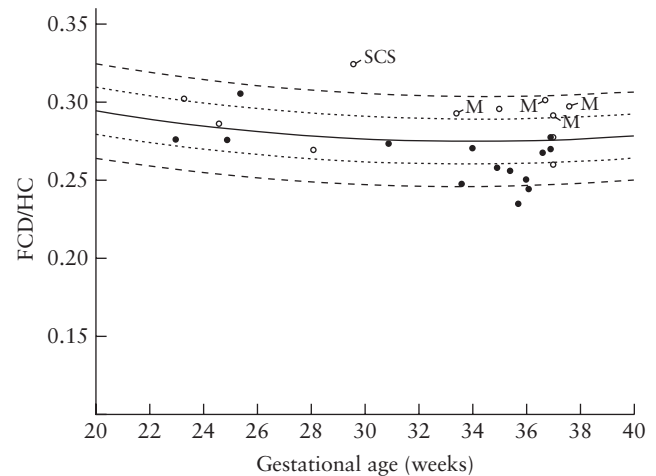


Figure 3 Foramen magnum-to-cranium distance/head circumference ratio (FCD/HC) in 25 cases of fetal microcephaly (Fmic), plotted on FCD/HC reference chart according to gestational age. The FCD/HC reference was modeled according to second-order polynomial equations (Appendix S1). The FCD/HC values of the 25 Fmic fetuses are subdivided into those diagnosed with microcephaly at birth (●) and those with normal head circumference at birth (○), among which a case of coronal craniosynostosis diagnosed with Saethre–Chotzen syndrome (SCS) and four cases with cranial molding (M) are indicated. Mean FCD, $\pm 1SD$ and $\pm 2SD$ are represented by solid, dotted and dashed curves, respectively.

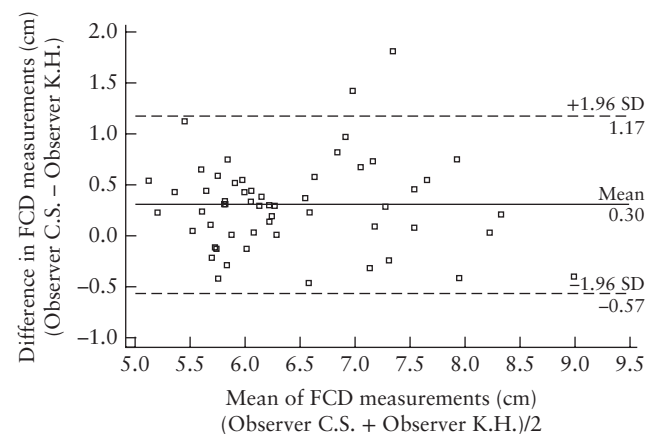


Figure 4 Bland–Altman plot showing interobserver agreement of foramen magnum-to-cranium distance (FCD) measurements in a subgroup of 50 fetuses selected randomly and assessed by two observers (C.S. and K.H.). For each fetus the difference between the paired measurements is plotted against the mean values of the pair (□). The mean difference (—) and 95% limits of agreement (---) are indicated.

cranial deformity (one with craniosynostosis and two with molding); the brain was anatomically normal on postmortem examination in all three. Three of the other four terminated NHCB fetuses had Chiari-II malformation and in one case the parents declined autopsy.

The Z-scores for HC, FCD and FCD/HC are presented according to group in Table 1. The micB fetuses had significantly lower FCD and FCD/HC Z-scores compared

Table 1 Z-scores of axial and vertical cranial biometry in 25 fetuses with a diagnosis of microcephaly (Fmic) and in the same fetuses, subdivided according to whether microcephaly was then confirmed at birth (micB) or there was a normal head circumference at birth (NHCB)

Reference	Fmic (n = 25)	micB (n = 14)	NHCB (n = 11)
HC z-score*	-3.36 (0.49)	-3.51 (0.55)†	-3.17 (0.33)†
FCD z-score	-2.86 (1.64)	-3.85 (0.96)‡	-1.59 (1.45)‡
FCD/HC z-score	0.49 (1.26)	-0.87 (0.83)§	0.90 (1.21)§

Data are presented as mean (SD). *According to Jeanty *et al.*². Results of micB and NHCB cases were compared by *t*-test for independent samples: † $P = 0.07$; ‡ $P = 0.0011$; § $P = 0.0011$. FCD, foramen magnum-to-cranium distance; Fmic, fetal microcephaly; HC, head circumference; micB, microcephaly at birth; NHCB, normal head circumference at birth.

with those with NHCB ($P = 0.0011$; *t*-test), while the HC Z-scores did not differ significantly between the groups.

A scatter chart of the FCD results for micB and NHCB cases relative to the normal FCD growth curves is provided in Figure 2. In all 14 micB cases, the FCD was more than 2 SD below the mean for gestational age, while only four of the 11 (36%) NHCB fetuses had FCD below this cut-off ($P < 0.003$, χ^2 test). This indicates that, in contrast to NHCB cases, the head size in micB cases is significantly smaller in both axial and vertical measurements.

Figure 3 illustrates FCD/HC for micB and NHCB fetuses plotted on the corresponding reference chart. Eighty-six percent (12/14) of the micB cases are located below the mean for gestational age, compared with only 18.2% (2/11) of those with NHCB ($P = 0.0037$, χ^2 test), suggesting that actual microcephaly is associated with fetal head flattening (a small vertical-to-axial ratio), whereas the false-positive cases (NHCB) tended to have a FCD/HC value higher than the mean. The corresponding proportions of micB and NHCB fetuses located below stricter FCD/HC cut-offs were: 92.9% *vs* 36.4% for cut-off of mean + 1 SD ($P = 0.031$, χ^2 test); and 100% *vs* 81.8% for mean + 1.5 SD ($P = 0.36$, χ^2 test).

All five cases in the NHCB group with an acrocephalic-like skull deformation noted at neonatal examination or autopsy had a normal FCD (Figure 2), a FCD/HC above the mean + 1SD (Figure 3) and estimated fetal weight below the 10th percentile¹¹. One of these five cases, with coronal craniosynostosis, was diagnosed as having Saethre–Chotzen syndrome (Figure 5a–c); four were anatomically normal fetuses with cranial molding (Figure 5d–f).

Using Jeanty *et al.*'s reference for Fmic diagnosis (HC 3SD below the mean)², micB was confirmed in only 14 of the 25 fetuses, resulting in a PPV of 56%. Combination of this HC reference with our optimal FCD cut-off (mean – 2SD) improved prediction of micB, identifying only 18 of the 25 fetuses as Fmic, giving an improved PPV of 78%, without missing any of the micB cases. Application of this FCD cut-off also excluded all the NHCB cases with a vertical cranial deformity.

In all except one of the 14 micB fetuses, FCD/HC was below the mean + 1SD. The exception (associated at 25 gestational weeks with severe early symmetrical intrauterine growth restriction, caused by multiple placental infarctions) had an FCD/HC Z-score of +1.5. Application of this cut-off (aimed at detection of all micB cases) resulted in a PPV of only 61% and to exclusion of only two of the five NHCB cases with acrocephalic-like skull deformation. However, with use of a less strict FCD/HC cut-off (mean + 1SD), detection of micB improved to 76.5% (missing only one micB case) and all five NHCB cases with acrocephalic-like skull deformation were excluded. We therefore suggest mean + 1SD as the preferred FCD/HC cut-off.

Improvement in PPV did not reach statistical significance for either FCD or FCD/HC, a finding which we attribute to the small size of the groups.

DISCUSSION

The accurate diagnosis of Fmic is important in order to differentiate fetuses that will be born with an abnormally small HC and with associated developmental abnormalities from those who will be normocephalic and develop normally¹².

Fmic, defined as HC 3SD below the mean, can be expected in 0.1% of pregnancies, if HC is distributed normally. However, the actual occurrence of such low HC measurements is probably higher. Based on reanalysis of the data of a recently published large Israeli population study on fetal head growth⁵ (courtesy of Dr Ety Daniel-Spiegel), 23 of 11 169 (0.2%) singleton pregnancies with certain dates and no fetal anatomical malformations or known syndromes were found to have $HC \leq \text{mean} - 3SD$, according to the established reference of Jeanty *et al.*². Only 56% (13/23) of these were diagnosed as being microcephalic postnatally, confirming that the accuracy of the established fetal HC-based prediction of micB is low.

A diagnosis of Fmic is challenging: we demonstrated recently³ that the established¹ and two modern^{4,5} HC references all resulted in significant overdiagnosis of Fmic (by ~40%), leading to erroneous terminations of apparently normal fetuses. We suggested that better prediction could be achieved by: using stricter HC cut-offs, and taking into account additional factors such as a family history of microcephaly, the presence of small-for-gestational age and the association of fetal anomalies. The application of these criteria led to an improvement in micB prediction, but it was still associated with a high false-negative rate, thus precluding detection of all micB cases³.

Issues regarding HC measurement methodology could explain some of the imprecision in Fmic diagnosis; however, our results indicated that an abnormal fetal cranial shape could also affect the diagnostic accuracy³. This led to our development of a novel reference for vertical cranial biometry. In this study, we applied the new reference to Fmic fetuses and proved that

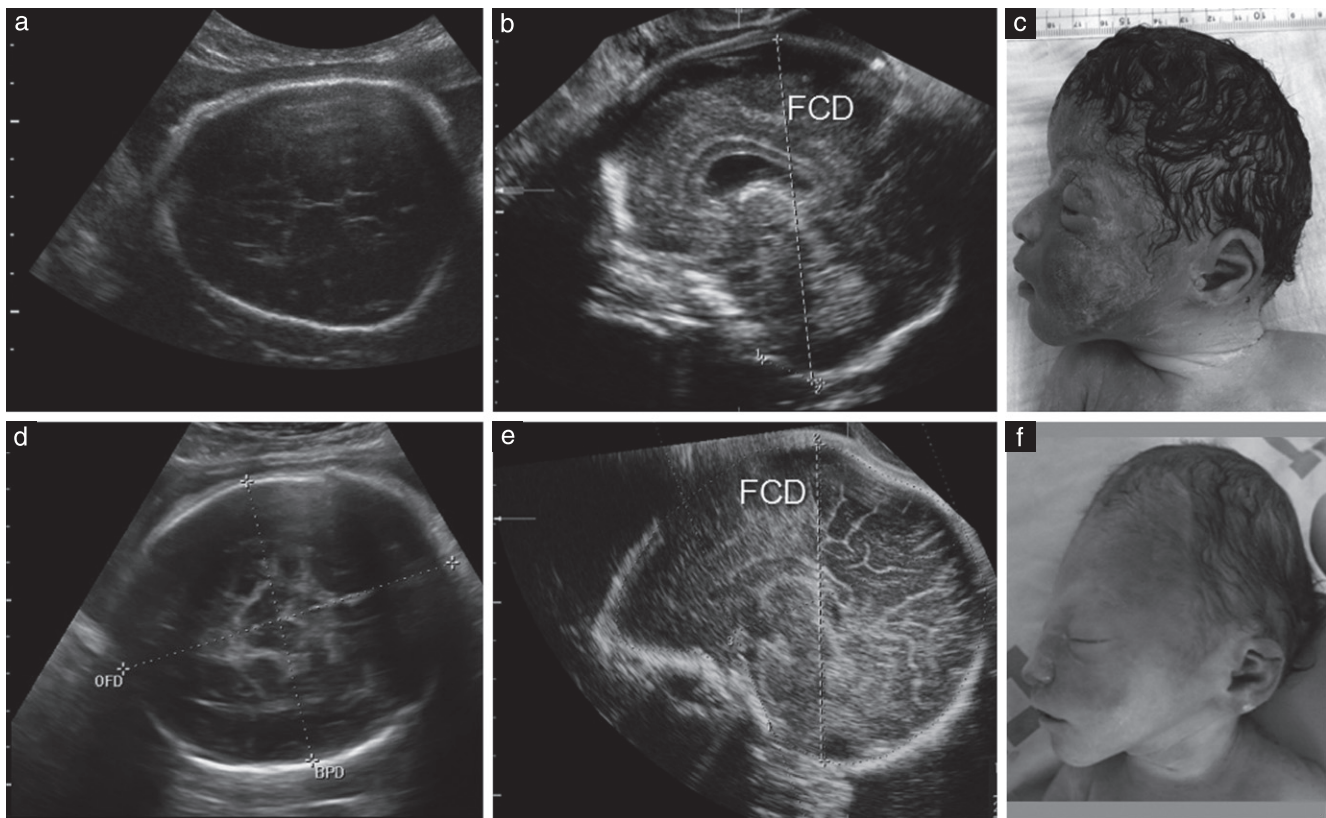


Figure 5 Vertical cranial deformations mimicking fetal microcephaly (Fmic). (a–c) Case with false-positive diagnosis of Fmic in 30th gestational week, caused by bilateral coronal craniosynostosis (Saethre–Chotzen syndrome). The fetus had normal cranial biometry and anatomy at the 22nd-week examination. At diagnosis of Fmic, the head circumference (HC) Z-score was -3 (a). The pregnancy was terminated on parental request 2 weeks later. The autopsy image (c) shows an acrocephalic cranial deformation. In retrospect, the foramen magnum-to-cranium distance (FCD) (b) and FCD/HC Z-scores were $+1.1$ and $+3.2$, respectively, both far above our newly developed cut-offs for microcephaly at birth (micB). (d–e) One of four false-positive cases of Fmic, characterized by acrocephalic-like cranial molding. Fetal biometry was normal at 23 weeks. At diagnosis of Fmic (37th week) the HC Z-score was -3.1 (d). The pregnancy was terminated on parental request. On retrospective evaluation, the FCD and FCD/HC Z-scores were -1.5 and $+1.1$, respectively, both not suggestive of micB. On autopsy (e) a vertical cranial deformation was noted. There was no premature closure of the cranial sutures and the brain weight was appropriate-for-gestational age.

we could differentiate efficiently between micB cases with $FCD \leq \text{mean} - 2 \text{SD}$ and $FCD/HC \leq \text{mean} + 1 \text{SD}$ and NHCB cases presenting normal FCD and relatively high FCD/HC values (above $\text{mean} + 1 \text{SD}$). Seventy-one percent (5/7) of the NHCB cases excluded by the FCD cut-off were described by the neonatologist/pathologist as having an acrocephalic-like skull deformity. We speculate that the two remaining cases with high FCD/HC probably also had a vertically deformed head, but this subjective observation was not described by the examining physician.

A sloping fetal forehead, depicted in the mid-sagittal plane of the fetal face, is indicative of Fmic^{13,14}. This interpreter-dependent sign is explained by a small cranial height (especially in the frontal region), which is typical of Fmic. In cases with difficult or impossible sonographic imaging of the facial profile, our reference ranges enable evaluation of the vertical cranial dimension.

The significantly different distribution of the micB and NHCB fetuses relative to our newly developed cut-offs (Figures 2 and 3) resulted in a higher PPV for micB diagnosis (78% for FCD with HC and 76.5% for FCD/HC

with HC) compared with 56% using HC alone. None of the 14 micB cases was missed using our optimal FCD cut-off. However, our Fmic series is relatively small due to the rarity of a measurement of $HC \leq \text{mean} - 3 \text{SD}$, and therefore the improvement in predictive performance of the FCD and FCD/HC cut-offs did not reach statistical significance. If the study had included 55 Fmic cases (assuming a similar distribution of the HC and FCD values), the improvement in PPV would have been significant.

Our series indicates that an acrocephalic-like skull deformity is frequent (5/11), and explains at least 45% of false Fmic diagnoses. The vertical deformation was expressed as FCD and FCD/HC values above our newly developed cut-offs. Of note, all five fetuses were small-for-gestational age, suggesting that, in these cases, the vertical cranial deformation of a small (but ultimately not microcephalic) HC, led to false suspicion of Fmic, which could be prevented by the application of these novel reference ranges. We assume that in fetuses with HC within the normal range, the effect of the vertical cranial deformation on the compensatory reduction of HC would

not result in suspicion of Fmic, although this assumption, as well as use of vertical cranial biometry in Fmic, craniosynostosis and molding needs to be investigated further.

The reason for there being a normal HC measurement at birth but a small HC measured *in utero* in cases with a vertical skull deformity stems from the difference in measurement techniques. Fetal HC is assessed according to anatomical brain landmarks in the axial transthalamic plane, which depicts the cavum septi pellucidi anteriorly, the thalamus and the third ventricle centrally, and the tentorial hiatus posteriorly¹⁵; the postnatal HC is measured as the maximum circumference of the head, from just above the glabella area to the area near the top of the occipital bone (opisthocranium)¹⁶. Since in most cases of vertical cranial elongation there is also a posterior skull inclination (Figure 5f), the postnatal measurement will be oblique, adjusted to the head shape, thus giving a larger result.

We found that FCD measurements were possible in almost all fetuses. However, inappropriate head position, parietal bone acoustic shadowing, maternal obesity and advanced gestational age prevented adequate imaging in 4.8% of the cases.

Although we used 3D multiplanar sonography, with only minimal post-processing, in order to achieve precise mid-sagittal fetal head imaging, this plane is attainable in experienced hands using two-dimensional ultrasound, allowing assessment of vertical cranial biometry according to the developed reference without the need for 3D imaging.

Our study had some limitations. It was designed to construct a reference for vertical cranial biometry and to evaluate its role in improvement of the diagnostic accuracy of Fmic. The Fmic study group was based on a relatively small cohort due to the rarity of these cases. Association of FCD and FCD/HC with additional signs of Fmic (such as sloping forehead) was beyond the scope of this study. The association between the vertical cranial measurements and the possible development of postnatal microcephaly in NHCB cases was not addressed. Furthermore, the effect of small FCD and FCD/HC on cognitive development was not studied.

In conclusion, assessment of FCD and FCD/HC as part of the Fmic work-up can improve the accuracy of prediction of micB by exclusion of NHCB cases with a vertical head deformation. According to our findings, this is a frequent cause of false-positive diagnosis of Fmic.

REFERENCES

- Chervenak FA, Jeanty P, Cantraine F, Chitkara U, Venus I, Berkowitz RL, Hobbins JC. The diagnosis of fetal microcephaly. *Am J Obstet Gynecol* 1984; 149: 512–517.
- Jeanty P, Cousaert E, Hobbins JC, Tack B, Bracken M, Cantraine F. A longitudinal study of fetal head biometry. *Am J Perinatol* 1984; 1: 118–128.
- Leibovitz Z, Daniel-Spiegel E, Malinger G, Haratz K, Tamarkin M, Gindes L, Schreiber L, Ben-Sira L, Lev D, Shapiro I, Bakry H, Weizman B, Zreik A, Egenburg S, Arad A, Tepper R, Kidron D, Lerman-Sagie T. Prediction of microcephaly at birth using three reference ranges for fetal head circumference: can we improve prenatal diagnosis? *Ultrasound Obstet Gynecol* 2016; 47: 586–592.
- Papageorghiou AT, Ohuma EO, Altman DG, Todros T, Cheikh Ismail L, Lambert A, Jaffer YA, Bertino E, Gravett MG, Purwar M, Noble JA, Pang R, Victora CG, Barros FC, Carvalho M, Salomon LJ, Bhutta ZA, Kennedy SH, Villar J; International Fetal and Newborn Growth Consortium for the 21st Century (INTERGROWTH-21st). International standards for fetal growth based on serial ultrasound measurements: the Fetal Growth Longitudinal Study of the INTERGROWTH-21st Project. *Lancet* 2014; 384: 869–879.
- Daniel-Spiegel E, Weiner E, Yarom I, Doveh E, Friedman P, Cohen A, Shalev E. Establishment of fetal biometric charts using quantile regression analysis. *J Ultrasound Med* 2013; 32: 23–33.
- Melamed N, Yogev Y, Danon D, Mashiach R, Meizner I, Ben-Haroush A. Sonographic estimation of fetal head circumference: how accurate are we? *Ultrasound Obstet Gynecol* 2011; 37: 65–71.
- Sarris I, Ioannou C, Chamberlain P, Ohuma E, Roseman F, Hoch L, Altman DG, Papageorghiou AT; International Fetal and Newborn Growth Consortium for the 21st Century (INTERGROWTH-21st). Intra- and interobserver variability in fetal ultrasound measurements. *Ultrasound Obstet Gynecol* 2012; 39: 266–273.
- Graham Jr JM, Sanchez-Lar PA. Vertex birth molding. In *Smith's Recognizable Patterns of Human Deformation* (4th edn), Graham Jr JM, Sanchez-Lar PA (eds). Elsevier: Philadelphia, 2016; 243–249.
- Fenton TR, Kim JH. A systematic review and meta-analysis to revise the Fenton growth chart for preterm infants. *BMC Pediatr* 2013; 13: 59.
- Maroun LL, Graem N. Autopsy standards of body parameters and fresh organ weights in nonmacerated and macerated human fetuses. *Pediatr Dev Pathol* 2005; 8: 204–217.
- Dollberg S, Haklai Z, Mimouni FB, Gorfein I, Gordon ES. Birth weight standards in the live-born population in Israel. *Isr Med Assoc J* 2005; 7: 311–314.
- Malinger G, Lev D, Lerman-Sagie T. Assessment of fetal intracranial pathologies first demonstrated late in pregnancy: cell proliferation disorders. *Reprod Biol Endocrinol* 2003; 1: 110.
- de Jong-Pleij EA, Ribbert LS, Pistorius LR, Tromp E, Bilardo CM. The fetal profile line: a proposal for a sonographic reference line to classify forehead and mandible anomalies in the second and third trimester. *Prenat Diagn* 2012; 32: 797–802.
- den Hollander NS, Wessels MW, Los FJ, Ursem NT, Niermeijer MF, Wladimiroff JW. Congenital microcephaly detected by prenatal ultrasound: genetic aspects and clinical significance. *Ultrasound Obstet Gynecol* 2000; 15: 282–288.
- Galan HL, Pandipati S, Filly RA. Ultrasound evaluation of fetal biometry and normal and abnormal fetal growth. In *Ultrasound in Obstetrics and Gynecology* (5th edn), Callen PW (ed). Saunders: Philadelphia, 2008; 225–265.
- Hall JG, Allanson JE, Gripp KW, Slavotinek AM. Head circumference (occipitofrontal circumference, OFC). In *Handbook of Physical Measurements* (2nd edn), Hall JG, Allanson JE, Gripp KW, Slavotinek AM (eds). Oxford University Press: New York, 2007; 72–83.

SUPPORTING INFORMATION ON THE INTERNET

The following supporting information may be found in the online version of this article:



Appendix S1 Vertical cranial biometry reference charts and calculator



Editorial

Diagnostic imaging tools to elucidate decreased cephalic biometry and fetal microcephaly: a systematic analysis of the central nervous system

L. GUIBAUD* and A. LACALM

Université Claude Bernard Lyon I, Imagerie Pédiatrique et Fœtale, Centre Pluridisciplinaire de Diagnostic Prénatal, Hôpital Femme Mère Enfant, Lyon-Bron, France

*Correspondence. (e-mail: laurent.guibaud@chu-lyon.fr)

Introduction

Although the most important feature warranting investigation of central nervous system (CNS) disorders during prenatal examination is ventriculomegaly, anomalies of cephalic biometry are also an important clue to the presence of fetal cerebral pathology. In routine practice, any decrease in cephalic biometry to < 5th percentile raises suspicion of underlying microcephaly. However, as discussed below, distinction must be made between suspicion of microcephaly and true microcephaly. True fetal microcephaly (as defined in Tool 2) is associated, in many prenatal cases, with morphological anomalies^{1–3}. It may be considered as part of a complex disorder, such as syndromes with or without chromosomal anomalies, or it may be associated exclusively with cerebral anomalies^{1,3}, being related either to primary cerebral organization disorders affecting all steps of CNS development, or to clastic events due to ischemohemorrhagic or infectious conditions; the latter is of particular interest currently, in light of the recent emergence of microcephaly related to Zika virus infection^{1–5}. Primary cerebral organization disorders include disorders of neural tube development (neural tube defect), prosencephalon cleavage (holoprosencephaly), precursor cell proliferation (microcephaly with simplified gyral pattern), neuroblast migration (lissencephaly) and corticogenesis (polymicrogyria). In all these cases, microcephaly is associated with structural CNS anomalies. However, in some cases, microcephaly can be truly isolated, i.e. with no associated structural anomalies, often being related to familial disorders and transmitted mostly as an autosomal recessive trait¹. In such cases, prenatal cephalic biometry is usually within the normal or subnormal limits and microcephaly develops after birth, with dramatic worsening of cephalic biometry during the first years of postnatal life^{6,7}. Such isolated familial microcephaly is rarely of concern when facing isolated microcephaly in the prenatal period.

As published previously for ventriculomegaly⁸, we outline here our systematic approach to the management of patients referred to our institution due to an unexplained decrease in cephalic biometry. Our approach is based on a set of diagnostic tools to diagnose and elucidate a decrease in fetal cephalic biometry, which may lead to suspicion of microcephaly with underlying CNS structural anomalies. It should be noted that its application should always be guided according to the clinical context. These tools are tailored for ultrasound examination, as recommended by Persutte⁹ and Kurtz *et al.*¹⁰, but can also be used for magnetic resonance imaging (MRI) investigation. Indeed, this etiological approach to the diagnosis of microcephaly is a perfect illustration of the potential contribution of MRI to the investigation of CNS anomalies, as ultrasound is often limited in more severe cases as a result of poor acoustic windows due to the narrowing of the sutures. In such cases, MRI undoubtedly offers more information than does ultrasound for cerebral anatomical analysis, especially regarding complete gyration and pericerebral space examination during the third trimester of pregnancy¹¹. Finally, we should emphasize that this article is intended not as an epidemiological study, but as a proposal to conduct a systematic analysis of the CNS when facing unexplained decreased cephalic biometry, based on a selection of pedagogical cases.

Tool 1: Context

As for unexplained ventriculomegaly, the clinical context should always be considered when facing an unexplained decrease in cephalic biometry. For the etiological work-up the context is crucial, as factors underlying microcephaly can be environmental, genetic or of unknown origin^{1,3}. Clinical data such as unexplained fever during pregnancy, drug use, alcohol consumption, risk factors for vascular clastic lesions (e.g. monochorionic twin pregnancy) and maternal phenylketonuria should be scrutinized and integrated into the work-up in order to diagnose environmental microcephaly. Consanguinity and cephalic biometry of both siblings and parents may also provide important clues in the diagnosis of microcephaly as well as of variants in cephalic biometry of genetic origin.

The context should also include a complete analysis of extracephalic biometry. This may help to differentiate between a predominant or exclusive decrease in cephalic biometry related to an encephaloclastic mechanism, such as that encountered in cytomegalovirus (CMV) infection or lissencephaly Type 3, and global reduction of fetal biometry, such as in severe global intrauterine growth restriction.

Tool 2: Determine severity of decreased cephalic biometry and follow up longitudinally

Unlike ventriculomegaly, for which there is consensus on its prenatal definition, there is no absolute threshold for the definition of prenatal microcephaly. However, as has been stated by Pilu *et al.*³ and Deloison *et al.*¹², the smaller the head dimension, the greater the probability of microcephaly with underlying pathology. For pediatricians, 'true' microcephaly refers to cephalic biometry > 3 SD below the mean for age and sex, as also reported in the prenatal period by Chervenak *et al.*². However, the issues regarding a positive diagnosis of microcephaly are completely different between the pre- and postnatal periods. In the postnatal period, the positive diagnosis based on 3 SD below the mean is a clinical threshold that leads to investigation of the underlying etiology by adequate work-up, this being otherwise indicated according to the clinical status and family history of the patient if the threshold is not reached. In the prenatal period, any decrease in cephalic biometry should be investigated in order to diagnose underlying CNS pathology as early as possible, even before reaching 3 SD below the mean, which is more likely to occur late in pregnancy at a time when termination of pregnancy is not permissible in many countries or the obstetric risks are greater.

The use of percentiles for routine prenatal sonography leads to suspicion of fetal microcephaly when cephalic biometry is below either the 5th or 3rd percentile, depending on the reference being used (the choice of appropriate reference is beyond the scope of this article). It should be noted that the 3rd percentile corresponds to approximately 2 SD, while 3 SD corresponds to 0.2 percentile. Thus, defining microcephaly as cephalic biometry $< 3^{\text{rd}}$ percentile leads to significant overdiagnosis of fetal microcephaly, including 3% of the general population, whereas only 0.2% of the general population are included using a limit of 3 SD^{12,13}. This accounts for the fact that prenatal head circumference (HC) between 2 SD and 3 SD below the gestational mean is not a particular risk factor for later abnormal neuropsychological development, as has been shown by Stoler-Poria *et al.*¹⁴. Thus, we propose that one should differentiate in the prenatal period between two different HC thresholds, i.e. a cut-off for 'diagnosis of microcephaly', defined as fetal HC ≥ 3 SD below the mean for gestational age, and a cut-off for 'prompting investigation', defined as fetal HC ≥ 2 SD below the mean, which should lead to prompt neurosonographic examination, as outlined in this article.

It should be emphasized also that the use of percentiles is not suitable for evaluation of the severity of decrease in cephalic biometry as it is based on the distance to the mean, thus, use of either SD or Z-scores is required¹². In routine practice, the distance to the mean can also be expressed using the growth delay (in number of gestational weeks) between the theoretical gestational age and the gestational age corresponding to the 50th percentile of the observed HC. For example, for a gestational age of X weeks, if the HC corresponds to the 50th percentile of

Table 1 Correlation between head circumference ± 2 SD from the mean and growth delay according to gestational age (from Hadlock *et al.*¹⁵)

Gestational age (weeks)	Growth delay (weeks)
12–18	± 1.3
18–24	± 1.6
24–30	± 2.3
30–36	± 2.7
36–42	± 3.4

X – 3 weeks, the growth delay is 3 weeks. The correlation between growth delay (in number of weeks) and SD of HC has been presented by Hadlock *et al.*¹⁵ (Table 1). Correct expression of the severity of the decrease in cephalic biometry is an important issue as, in some particularly severe cases, it can be a clue to etiology.

As mentioned above, it should be noted that decrease in cephalic biometry can be a progressive process. In some cases, microcephaly can be detected in the second trimester, especially in cases of spina bifida and in some syndromic entities, particularly chromosomal anomalies¹². However, microcephaly cannot be excluded by normal biometry during the second trimester, as shown by Bromley and Benacerraf¹⁶, and can be identified more easily or exclusively during the third trimester, in cases of underlying late developmental or clastic anomalies, respectively (Figure S1). Because of this potential for late manifestation of microcephaly, particular care should be taken when cephalic biometry is close to the 3rd percentile during the second trimester, especially if there is a discrepancy between small HC and extracerebral biometry. In such cases, close follow-up of the cephalic biometry and careful cerebral sonographic investigation using the following tools may help in diagnosing or excluding any underlying CNS anomalies, which may be more obvious during late pregnancy.

Tool 3: Investigate the pericerebral space

As we have previously maintained⁸, the pericerebral space, which is often overlooked, should in fact be included in a systematic approach to patients with an unexplained decrease in cephalic biometry, even though, to date, this remains subjective. Investigation of the pericerebral space is useful for accurate evaluation of the severity of any decrease in cephalic biometry and even, in some cases, for positive diagnosis of microcephaly, as well as for understanding the underlying mechanism. As diagnosis of microcephaly is based on sonographic measurement of the HC, by means of an ellipse drawn on or around the calvarium (depending on the reference being used), it follows that a decrease in this sonographic measurement should lead to a diagnosis of 'microcrania'. In fact, 'microcephaly' refers to reduction of the cerebral volume (or microencephaly), as defined by neuropathologists. In most cases, reduction of the sonographic cephalic measurement, or microcrania, based on the circumference of the calvarium, reflects underlying microencephaly. However, as

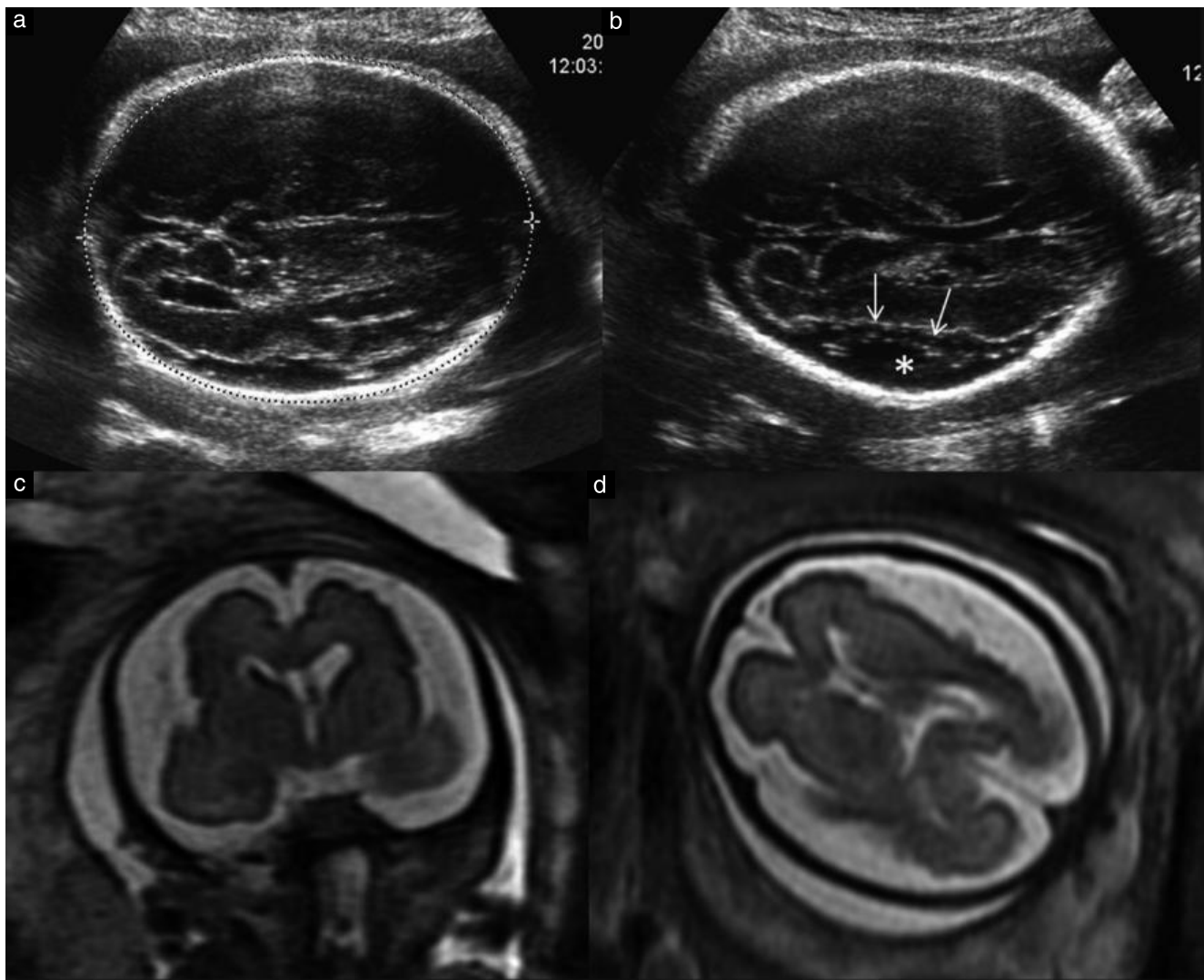


Figure 1 Fetal imaging in a patient referred at 27 gestational weeks due to unexplained enlargement of pericerebral space. Cephalic biometry was close to 50th percentile (head circumference, 270 mm). Axial sonographic images (a,b) confirming enlargement of the pericerebral space, which was more pronounced close to the corona radiata (*), associated with abnormal smooth cortical surface (arrows). Coronal (c) and axial (d) T2-weighted fetal magnetic resonance images (MRI) demonstrating both a major diffuse increase in pericerebral space and diffuse anomalies of the cortical ribbon, which show lack of gyration and an undulated cortical surface suggestive of diffuse polymicrogyria. Cephalic biometry at MRI gave biparietal and fronto-occipital diameters of -3 SD and -5 SD, respectively, according to the atlas of Garel³³. Pathological examination confirmed both microcephaly, as suggested by a cerebral weight of 140 g ($< 5^{\text{th}}$ percentile), and diffuse polymicrogyria, associated with neuronal and leptomeningeal cortical heterotopia, suggestive of a diffuse clastic mechanism (not shown).

stated clearly by Pilu *et al.*³, measurement of the calvarium represents, at best, a rough estimate of cerebral development. Depending on the size of the pericerebral space, the sonographic HC does not always reflect the underlying microcephaly, and, indeed, we have encountered cases in which a normal or subnormal sonographic HC is associated with severe underlying microcephaly due to markedly enlarged pericerebral space, as illustrated in Figure 1. In such cases, evaluation of the cerebral volume using MRI or, at least, use of MRI cerebral measurements (biparietal and fronto-occipital diameters) is more accurate than is sonographic cephalic measurement (Figure 1).

Investigation of the pericerebral space may also provide an etiological clue to diagnosis of the underlying cerebral pathology. In most severe encephaloclastic lesions, the pericerebral space is enlarged, as illustrated by the more

severe cases of CMV infection (Figure 2) or diffuse vascular ischemic lesions, as reported by Pilu *et al.*³. Such enlargement of the pericerebral space is also typical in lissencephaly Type 3, a developmental condition in which microcephaly is associated with akinesia, due to neuroapoptosis that leads to a marked neuronal depletion of the entire CNS with subsequent severe cerebral atrophy¹⁷ (see Figure S6). In some vascular clastic events, the enlargement of the pericerebral space can be more limited and localized, adjacent to the focal clastic lesion.

Tool 4: Look for the Sylvian fissure as the main marker of gyration

As the Sylvian fissure represents the main landmark for gyration, its analysis should be integrated into the imaging

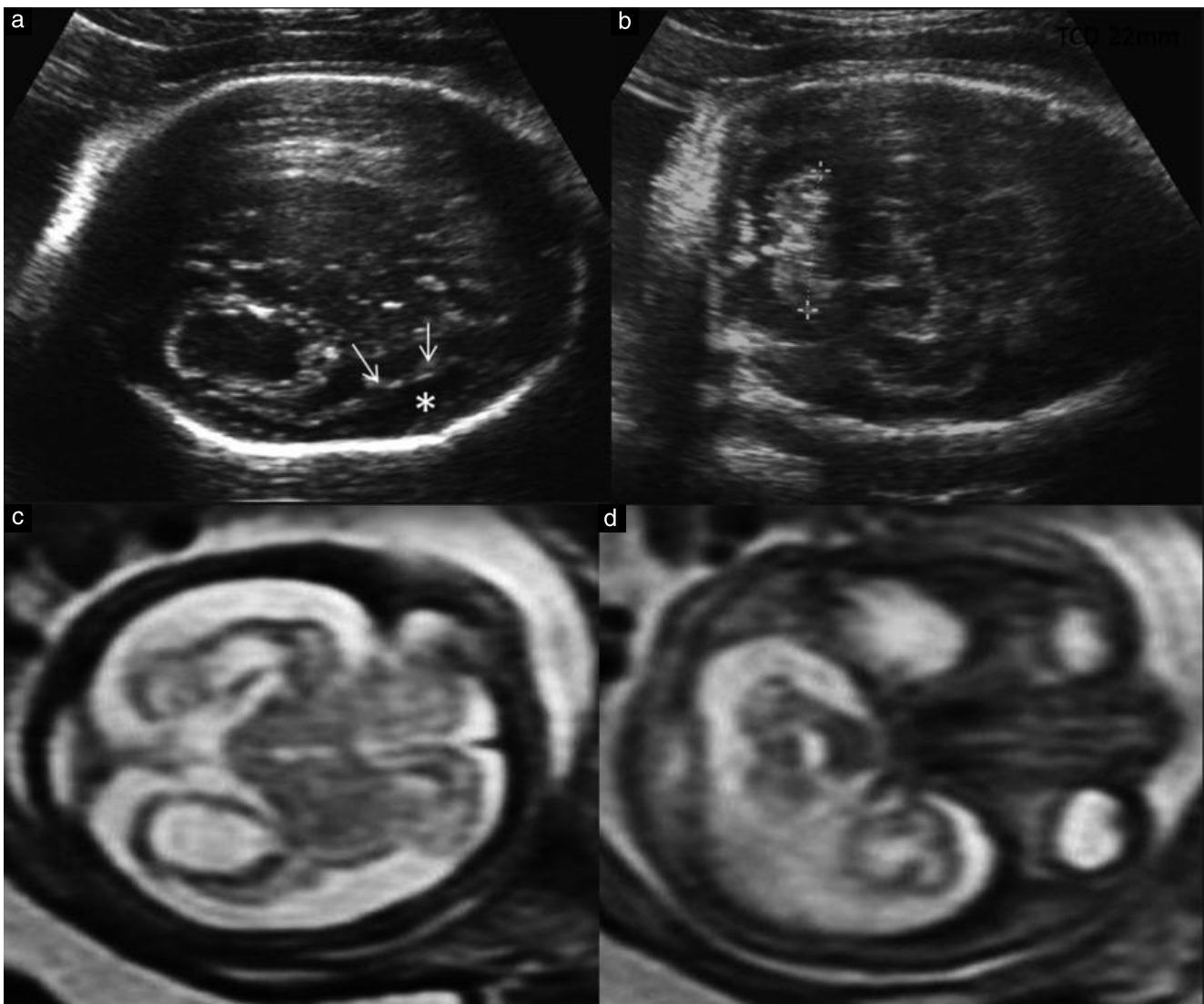


Figure 2 Fetal imaging in a patient referred at 29 gestational weeks due to unexplained ventriculomegaly, associated with significant reduction in cephalic biometry (head circumference corresponded to the 50th percentile at 25 weeks, equivalent to a decrease of between -3 SD and -4 SD). (a) Axial supratentorial sonographic image showing an echogenic periventricular band, echogenic foci suggestive of calcifications, an abnormal largely open Sylvian fissure (arrows) and increased pericerebral space (*). (c) Global increased pericerebral space was confirmed on T2-weighted magnetic resonance imaging in the axial plane, which also showed thinning of the parenchymal cerebral mantle more clearly. Axial sonographic (b) and T2-weighted magnetic resonance infratentorial (d) images demonstrating a major decrease in transverse cerebellar diameter (22 mm), suggestive of severe cerebellar hypoplasia. The combination of an ‘infectious clastic pattern’ with increased pericerebral space, diffuse cortical dysplasia (polymicrogyria) and cerebellar hypoplasia was highly suggestive of encephaloclastic cytomegalovirus fetopathy, which was confirmed by the biological work-up.

work-up of the fetal brain. Gyration should be scrutinized carefully when there is any decrease in cephalic biometry or true microcephaly, for both diagnostic and etiological purposes. This requires knowledge regarding the shape of the Sylvian fissure in the axial plane, according to gestational age. We published previously a reliable subjective method with which to assess the shape of the Sylvian fissure between 22 and 32 weeks of gestation using a simple score-based evaluation of operculization of the posterior part of the fissure in a standardized view on an axial cerebral plane^{18,19} (Figure S2). Using this method in routine prenatal imaging can help in the early diagnosis of anomalies of operculization. These anomalies can reflect underlying cortical developmental or clastic lesions, such as diffuse polymicrogyria (Figures 2 and

S1) or lissencephaly Type 1 (Figure 3)¹⁹, which are, in most cases, associated with microcephaly, but can also reflect extracortical developmental anomalies, especially abnormal cerebral volume. We have shown that lack of development of the anterior margin of the Sylvian fissure may be a clue to frontal hypoplasia and therefore be diagnostic of microcephaly, as also shown by Goldstein *et al.*²⁰ and Persutte *et al.*²¹ (Figure 4c and d).

Tool 5: Do not assume that a smooth cerebral surface indicates lissencephaly

It should be noted that a smooth cerebral surface with complete absence of folding or with reduced gyri and abnormal shallow sulci on sonographic examination does

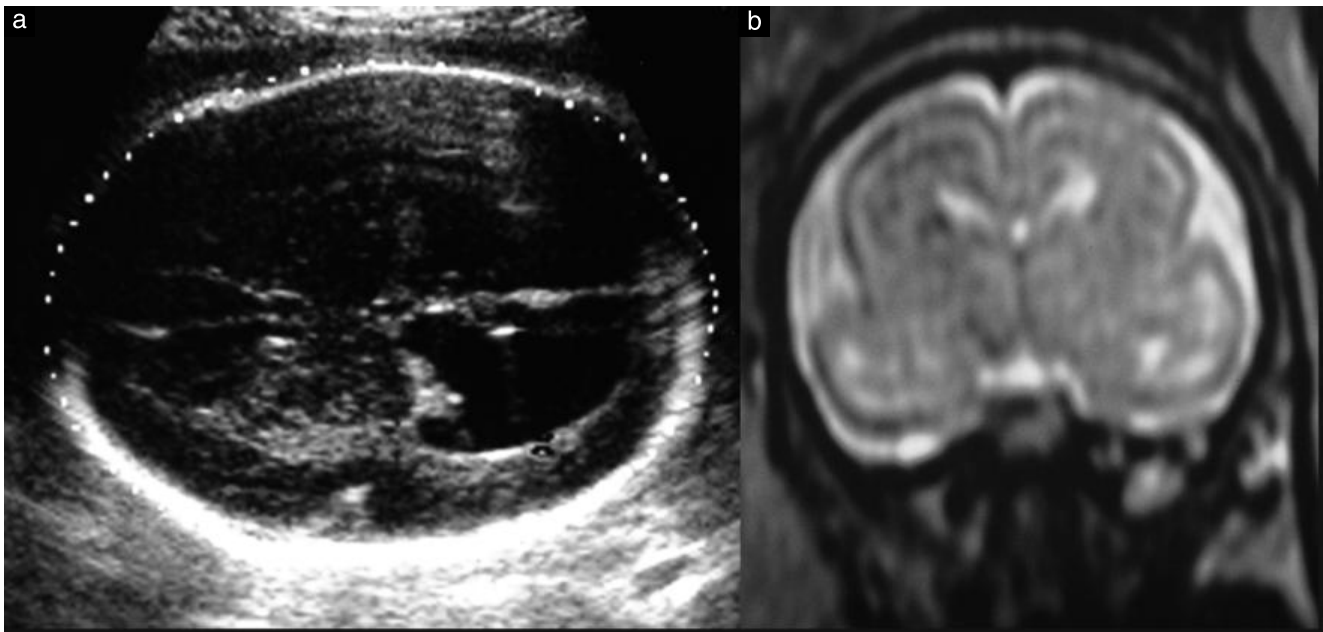


Figure 3 Fetal imaging in a patient referred at 28 gestational weeks due to ventriculomegaly and severe reduction in cephalic biometry. (a) Axial sonographic image showing an echogenic periventricular area and abnormal operculization of the Sylvian fissure, demonstrating rudimentary and moderate ventriculomegaly. Cephalic biometry corresponded to the 50th percentile at 24.5 weeks, equivalent to a decrease close to -3 SD. (b) Coronal T2-weighted magnetic resonance image (MRI) confirming suspicion of gyral anomalies, demonstrating a typical figure-of-eight-shaped appearance of the brain, with a thick cortex and smooth surface suggestive of lissencephaly Type 1, which was confirmed on postnatal MRI. Note that the echogenic periventricular area on sonographic examination was associated with abnormal waves of neuronal migration, as shown by MRI.

not necessarily indicate a diagnosis of lissencephaly. Although the term ‘lissencephaly’ means ‘smooth brain’ and refers to a paucity of gyral and sulcal development on the surface of the brain, it in fact has a particular etiology and histological characteristics²². Classic lissencephaly (or lissencephaly Type 1), the most common form, refers to a smooth brain associated with a thick or double cortex, with a specific histological layered structure; it is related, in two-thirds of cases, to either *LIS1* (Figure 3) or *DCX* gene mutation, or, in a few cases, to a mutation in one of the tubulin genes, mostly *TUBA1A*²³. However, the sonographic appearance of ‘smooth brain’ is also encountered in microcephaly with a simplified gyral pattern, which displays a normal or thin cortical ribbon (Figures 4 and S3), or with diffuse polymicrogyria (Figure 5)⁴. In these two entities, related to deficient precursor cell proliferation and cortical organization disorders, respectively, the putative genes involved differ completely from those involved in classic lissencephaly. Therefore, when faced with a smooth brain on sonographic examination, one should avoid using the term ‘lissencephaly’, because, in the absence of any confirmation by neuropathological examination, doing so may lead to inadequate genetic testing (for example, testing for *LIS1* or *DCX* gene mutation in a case of microcephaly with simplified gyral pattern, related in fact to one of the 12 currently known genes for this entity, such as *MCPH1* or *ASPM*). In such cases, fetal MRI can be of help, enabling differentiation between classic lissencephaly and microcephaly with simplified gyral pattern or diffuse polymicrogyria on the basis of an

analysis of cortical thickness (cortical ribbon) that cannot be achieved using ultrasound^{4,11}.

Tool 6: Look for clastic events

Diffuse cerebral clastic events, of either primitive vascular or infectious origin, result in cerebral atrophy and subsequently in both increased pericerebral space and ventriculomegaly. Therefore, as stated for the imaging work-up of unexplained ventriculomegaly⁸, one should look systematically for a clastic pattern when faced with an unexplained decrease in cephalic biometry. The clastic pattern associated with infection is similar to that described for ventriculomegaly. This ‘infectious clastic pattern’ can include a periventricular echogenic halo in the subependymal zone, which may be associated with germinolysis cysts, periventricular or parenchymal calcification, or pathognomonic cystic changes posterior to the occipital horn or anterior to the temporal horn⁸. This pattern can also be associated with an abnormal Sylvian fissure, suggestive of polymicrogyria, and, as mentioned previously, with enlarged pericerebral space adjacent to the abnormal cortical surface (Figure 2). Such a clastic pattern is typically encountered in severe CMV infection²⁴; it has also been described very recently, in Brazil, in Zika viral intrauterine infection, a mosquito-borne disease related closely to yellow fever, dengue fever and West Nile and Japanese encephalitis⁵. In the two cases reported by Oliveira Melo *et al.*⁵, the vertical intrauterine transmission of this viral infection led to

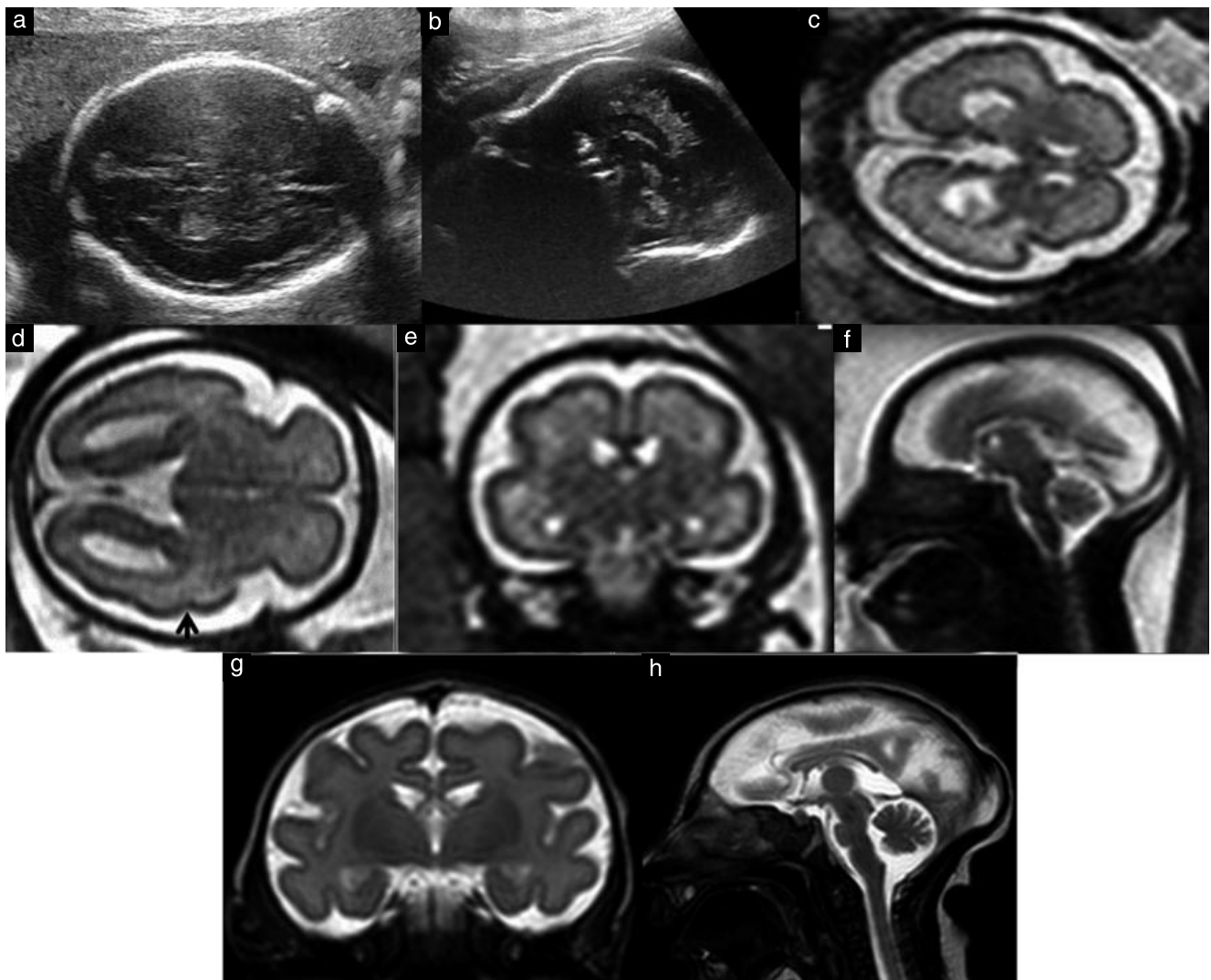


Figure 4 Fetal and postnatal imaging in a patient referred at 26 gestational weeks due to both a decrease in cephalic biometry and non-identification of the corpus callosum, with no context of consanguinity. At first sonographic examination, microcephaly was confirmed, with head circumference (HC) corresponding to the 50th percentile at 23 weeks, equivalent to a decrease of 2.5 SD, associated with normal extracranial biometry. Axial (a) and mid-sagittal (b) sonographic images showing both smooth cortical surface with a lack of gyral pattern (a) and presence of thin complete corpus callosum (b). Sonographic follow-up at 28.3 weeks demonstrated severe, non-progressive microcephaly (delayed by 3 weeks according to cephalic biometry) without any changes in gyral pattern (smooth cortical surface) on axial sonographic image (not shown). These findings were confirmed on axial (c) and coronal (e) T2-weighted fetal magnetic resonance imaging (MRI), which demonstrated smooth cortical surface, very few sulci and normal thickness of cortical ribbon. Note lack of operculization of Sylvian fissure and absence of superior temporal sulcus (c) compared with control at 28 weeks on axial T2-weighted fetal MRI (arrow) (d), in particular an absence of any anterior margin of the Sylvian fissure related to marked frontal hypoplasia, as stated in Guibaud *et al.*¹⁹. Sagittal T2-weighted fetal MRI (f) confirmed presence of a thin corpus callosum and revealed suspicion of a slight decrease in volume of the pons. Prenatal imaging data were suggestive of microcephaly with a highly simplified gyral pattern. After prenatal counseling, the parents elected to continue the pregnancy despite high probability of poor cognitive outcome. (g,h) Postnatal MRI at 8 days confirmed the diagnosis of microcephaly with a highly simplified gyral pattern (HC, 28.5 cm at term) as well as pontine hypoplasia.

fetal microcephaly and brain damage, including calcifications, suggestive of an underlying infectious condition, but also severe damage of the cerebellum, brainstem and thalami. In one case, bilateral cataracts, intraocular calcifications and unilateral microphthalmia were demonstrated.

The vascular clastic pattern differs slightly from that described for unexplained ventriculomegaly. For the latter, we underlined the hemorrhagic changes of both ventricular wall and lumen, which lead to the diagnosis of the underlying ischemohemorrhagic event⁸. In the

case of a decrease in cephalic biometry, the clastic vascular pattern includes mainly late anatomical changes related to diffuse ischemic events. Even if both hemispheres are involved, this includes asymmetrical parenchymal changes, such as abnormal parenchymal echogenicity, cavitations, parenchymal cleft, calcifications, asymmetrical ventriculomegaly and enlargement of the subarachnoid space (Figures 6 and S4), as well as diffuse and asymmetrical cortical anomalies²⁵. This pattern is typically encountered in severe brain damage following fetal death in monochorionic twin pregnancy.

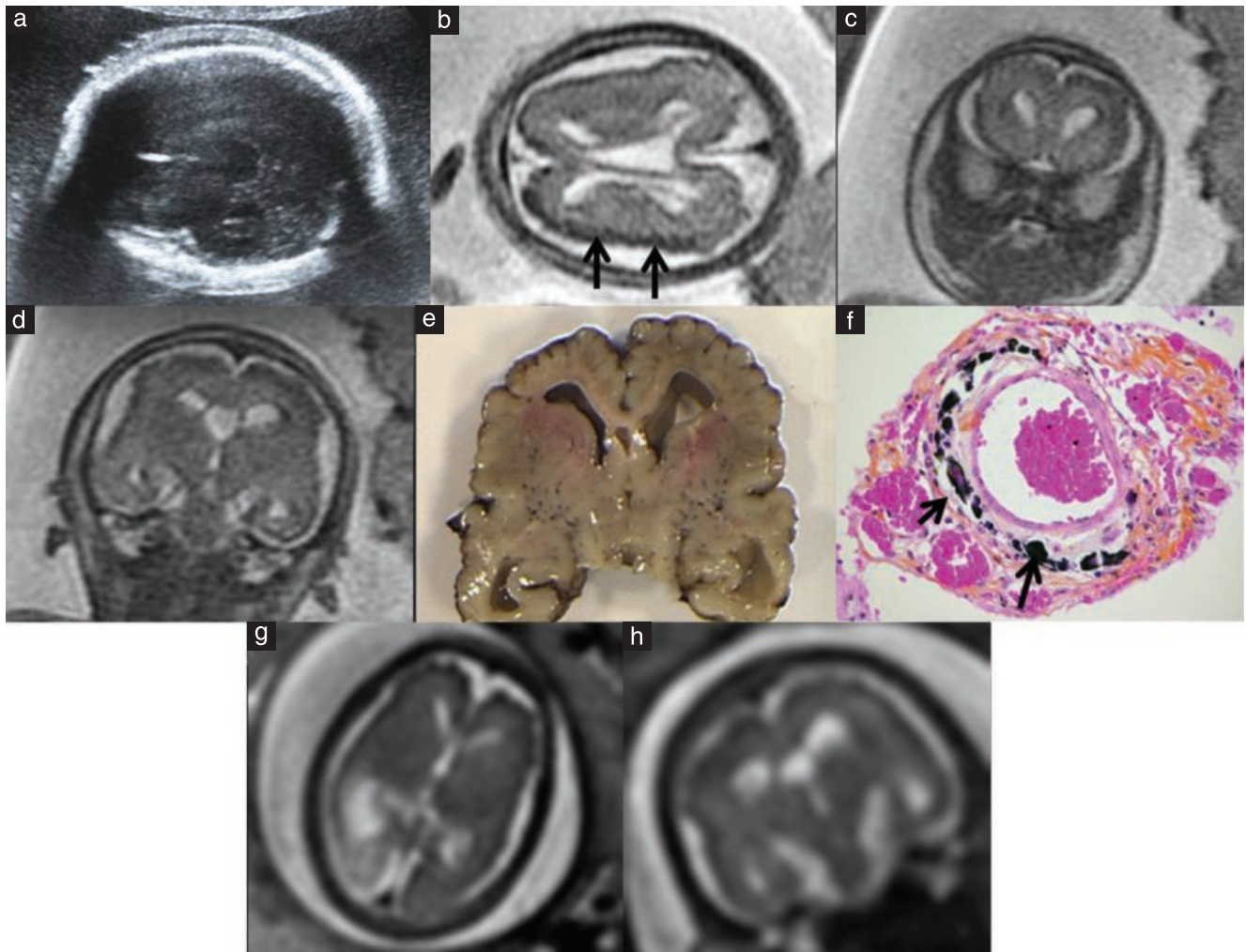


Figure 5 Fetal imaging in a patient referred at 29 gestational weeks due to a major decrease in cephalic biometry within the context of consanguinity, associated with medical history of neonatal death of the mother's first baby, with a prenatal imaging diagnosis of significant reduction in cephalic biometry related to 'lissencephaly'. This latter diagnosis was not confirmed by pathological examination because the parents declined autopsy. All genetic testing for classic lissencephaly was negative. Sonographic examination performed in our department confirmed major microcephaly with head circumference corresponding to the 50th percentile at 25 weeks, equivalent to a decrease to between -3 SD and -4 SD, associated with normal extracranial biometry. (a) Despite poor acoustic windows due to narrowing of sutures related to microcephaly, axial sonographic examination showed a smooth cortical surface as well as a very rudimentary Sylvian fissure. Axial (b) and coronal (c,d) T2-weighted fetal magnetic resonance (MR) images demonstrated abnormal gyration with undulated and mildly thickened cortical ribbon, suggestive of diffuse polymicrogyria. After prenatal counseling, the parents elected for termination of pregnancy due to high probability of severe postnatal outcome. Neuropathological examination confirmed diffuse polymicrogyria at macroscopy (e) and showed parietal arterial calcifications destroying the media (f, arrows), which was replaced by fibroblastic proliferation, leading to reduction of vascular lumen on microscopy. These findings were suggestive of diffuse polymicrogyria related to vascular insult, most likely due to underlying genetic vasculopathy, in keeping with the medical history. Interestingly, retrospective review of axial (g) and coronal (h) T2-weighted fetal MR images from previous pregnancy showed similar gyral anomalies, suggestive of diffuse polymicrogyria, which had been misinterpreted as lissencephaly.

Tool 7: Evaluate the midline

In the case of a decrease in cephalic biometry, the midline should be examined carefully to investigate etiology. It should be borne in mind that the appearance of the commissures, especially the corpus callosum, can be affected anatomically by severe microcephaly, regardless of underlying etiology.

One should assess the anterior complex on routine axial images²⁶. Holoprosencephaly, especially the most severe forms (alobar and semilobar), is usually associated with decreased cephalic biometry, so diagnosis relies on

the absence of a normal anterior complex, including non-identification of the cavum septi pellucidi, distortion of interhemispheric fissure and abnormal or absent frontal horns (Figure S5)²⁶. Analysis of the corpus callosum should be performed by an expert in fetal CNS imaging (neurosonogram or fetal MRI). It should be performed in the mid-sagittal plane. Absence of its anterior part can also be a clue to the diagnosis of semilobar holoprosencephaly, although microcephaly associated with corpus callosal agenesis/dysgenesis, including hypoplasia, has also been reported in some syndromes. However, it should be noted that, in severe microcephaly, corpus callosal hypoplasia

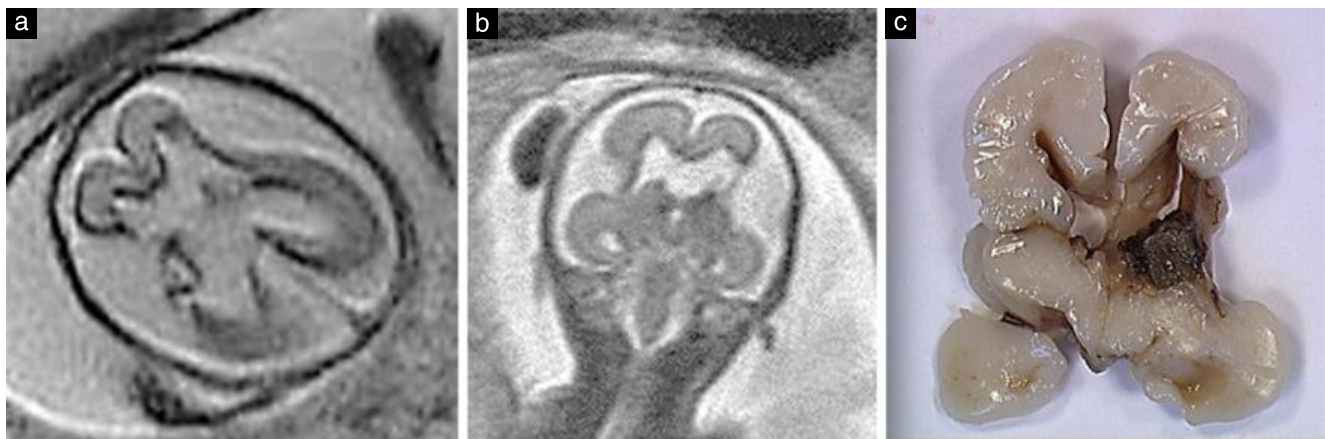


Figure 6 Fetal imaging in a patient referred at 22 gestational weeks due to enlarged pericerebral space with mild decrease in cephalic biometry (5th percentile). Axial (a) and coronal (b) T2-weighted fetal magnetic resonance images demonstrating major amputation of cerebral parenchyma adjacent to the insula, more pronounced on the left hemisphere, associated with no evidence of the septum pellucidum. Major increase of the pericerebral space adjacent to the clastic changes was also noted. (c) Macroscopic pathological examination confirmed clastic lesions adjacent to the insula with both porencephalic lesions and bilateral pseudoschizencephalies related to an ischemohemorrhagic phenomenon.

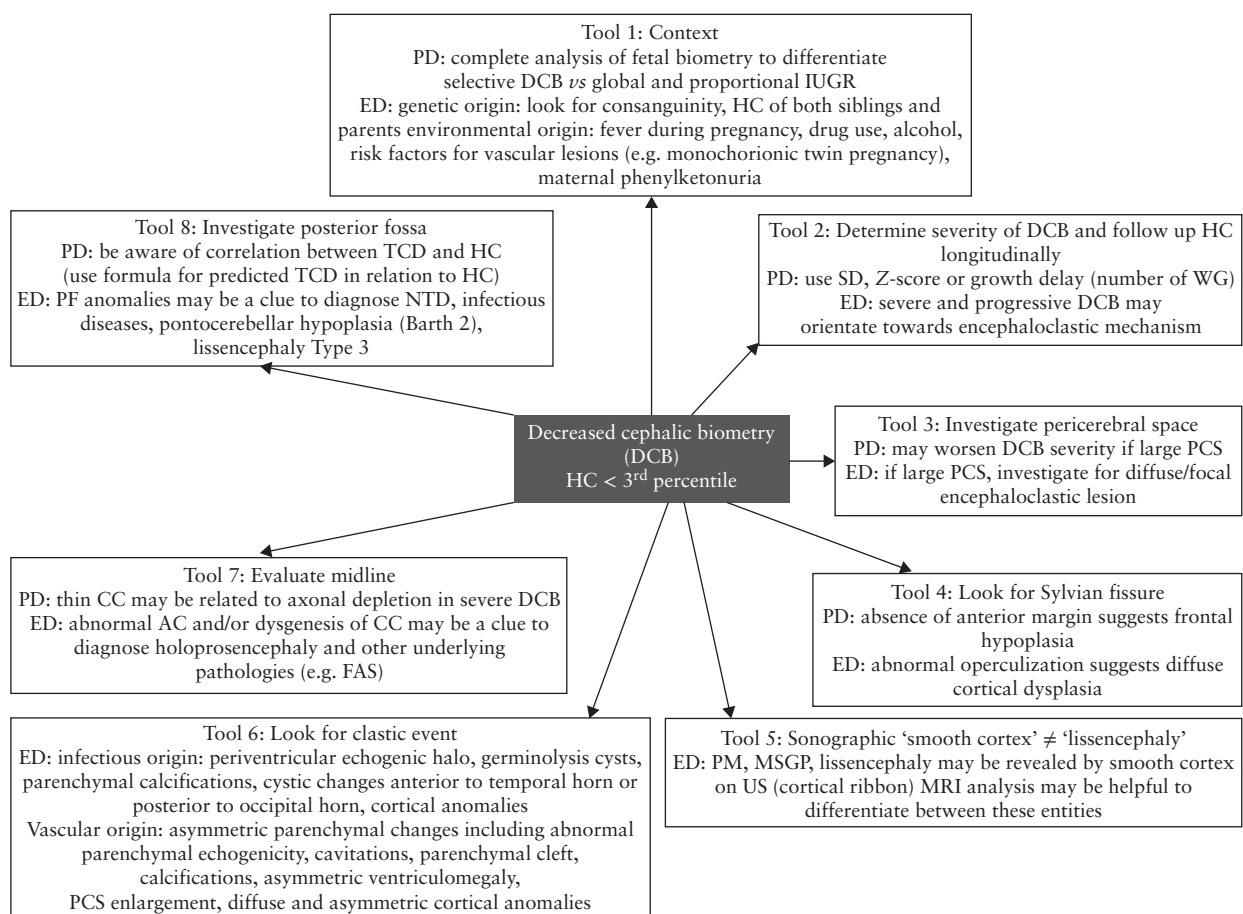


Figure 7 Diagnostic imaging tools to elucidate decreased cephalic biometry using a systematic analysis of the central nervous system. AC, anterior complex; CC, corpus callosum; ED, etiological diagnosis; FAS, fetal alcohol syndrome; HC, head circumference; IUGR, intrauterine growth restriction; MRI, magnetic resonance imaging; MSGP, microcephaly with simplified gyral pattern; NTD, neural tube defect; PCS, pericerebral space; PD, positive diagnosis; PF, posterior fossa; PM, polymicrogyria; TCD, transverse cerebellar diameter; US, ultrasound; WG, weeks' gestation.

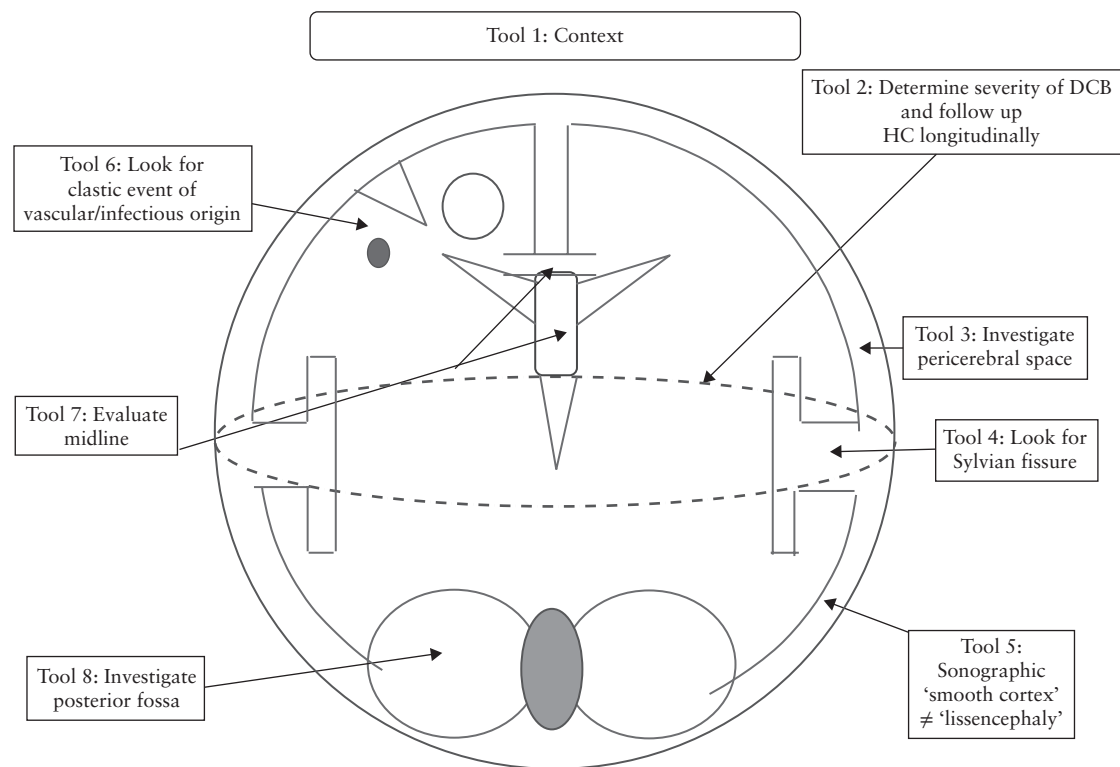


Figure 8 Summary of diagnostic imaging tools for use when investigating decreased cephalic biometry (DCB). HC, head circumference.

can be related exclusively to a major decrease in neurons and commissural axons, as illustrated in Figures 4 and S4. In such cases, corpus callosal hypoplasia should be considered as a consequence of the microcephaly and not as an etiological clue that may be helpful in investigating the underlying condition. In some cases, association between microcephaly and corpus callosal dysgenesis/agenesis can orientate the etiological diagnosis depending on either clinical or imaging patterns. For example, in a suggestive clinical context and even in the absence of apparent alcohol abuse, the association between microcephaly and hypoplastic corpus callosum, commonly associated with a characteristic abnormal profile (long upper lip), can be diagnostic of fetal alcohol syndrome²⁷.

Tool 8: Investigate the posterior fossa

As for the midline, investigation of the posterior fossa is important in the etiological work-up for any decrease in cephalic biometry, but one should be aware that reduction of supratentorial cephalic biometry can be associated with a decrease in the transverse cerebellar diameter (TCD). Indeed, these two parameters are correlated; we have shown recently that cerebellar growth occurs exponentially, relative to the increase in HC at a given gestational age²⁸.

As widely accepted, microcephaly can be a biometric clue in the diagnosis of neural tube defect, which can affect cephalic biometry as early as in the first trimester²⁹. In the series of Deloison *et al.*¹², spina bifida was diagnosed in five fetuses among 16 with small HC

on second-trimester ultrasound. Therefore, microcephaly should lead to the investigation of both the lumbosacral spine to detect myelomeningocele and the posterior fossa to detect Chiari-II malformation, which represent direct and indirect findings of spina bifida, respectively. Hypoplasia of the cerebellum and/or brainstem can also be an important clue for etiological diagnosis other than neural tube defect. Lissencephaly Type 3, a condition characterized by diffuse neuroapoptosis, results in cerebral atrophy leading to increased pericerebral space (see Tool 3), but also to severe pontocerebellar hypoplasia (Figure S6)¹⁷. Brainstem and cerebellar hypoplasia have also been reported in the so-called 'lethal microcephalies with simplified gyral pattern', such as in Amish lethal microcephaly related to *SLC2A19* gene mutation⁴, as well as in a novel entity described recently by Rajab *et al.*³⁰. Finally, cerebellar hypoplasia can be encountered in clastic events, such as CMV (Figure 2) and Zika virus infection, as mentioned previously.

One should be aware that a mild decrease in cephalic biometry can be associated with moderate reduction in infratentorial biometry, especially TCD. As previously suggested by Goldstein *et al.*³¹ and Guihard-Costa & Larroche³², we have shown recently a correlation between TCD and HC, based on a prospective cohort study of 65 250 pregnant women²⁸. Considering this correlation, we might consider using the predicted TCD in relation to the HC at a given gestational age (according to the following formula: expected TCD = $0.7355 * \exp(0.059 * HC)$) for biometric analysis of the posterior fossa when investigating decreased cephalic

biometry. This is of importance in cases of moderate reduction in cephalic biometry, close to -2 SD, associated with decreased TCD around the 3rd percentile. In such cases, the mild decrease in cephalic biometry may be considered to be associated with cerebellar hypoplasia. However, if TCD is corrected according to gestational age, the TCD may increase above the 5th percentile, leading to an assumption that the decrease in cephalic biometry is 'isolated'; this may affect prenatal counseling.

Conclusion

Systematic use of the tools described above should assist in elucidating cases of unexplained isolated decrease in cephalic biometry. Summarized in Figures 7 and 8, these tools can be divided into two groups. The first focuses on the positive diagnosis of a decrease in cephalic biometry or microcephaly, including direct and indirect imaging findings related to decreased biometry, and the second focuses on etiological diagnosis. Some tools can be used both for positive diagnosis and as a clue to orientate towards the underlying cause. For example, a major increase in pericerebral space associated with a decrease in cephalic biometry indicates and reinforces the severity of the microcephaly but will also orientate the etiological work-up towards an encephaloclastic mechanism, which can be either clastic (ischemic or infectious) or genetic (such as lissencephaly Type 3). In routine practice, these tools can be useful to ensure that a moderate decrease in cephalic biometry (to between -2 SD and -3 SD) is truly isolated, which is important for prenatal counseling. Indeed, a moderate, isolated and non-progressive decrease in cephalic biometry is, in most cases, associated with favorable outcome when the appropriate biological work-up (including cytogenetic and infectious testing) is also negative. This clinical message is of great importance for patients and medical teams facing a decrease in cephalic biometry, particularly in light of the recent exponential surge in Zika virus infection.

ACKNOWLEDGMENTS

We would like to thank the Department of Pathology and especially Dr Annie Buenerd for her major input regarding fetal CNS pathologies and her constant effort in correlating prenatal imaging findings with pathological data.

REFERENCES

- den Hollander NS, Wessels MW, Los FJ, Ursem NT, Niermeijer MF, Wladimiroff JW. Congenital microcephaly detected by prenatal ultrasound: genetic aspects and clinical significance. *Ultrasound Obstet Gynecol* 2000; 15: 282–287.
- Chervenak FA, Rosenberg J, Brightman RC, Chitkara U, Jeanty P. A prospective study of the accuracy of ultrasound in predicting fetal microcephaly. *Obstet Gynecol* 1987; 69: 908–910.
- Pilu G, Malinge G. Microcephaly. Visual Encyclopedia of Ultrasound in Obstetrics and Gynecology. www.isuog.org [Accessed 24 June 2013].
- Barkovich AJ, Raybaud CA. Congenital malformations of the brain and skull:

- microcephalies. In *Pediatric Neuroimaging* (5th edn). Lippincott Williams & Wilkins: Philadelphia, 2012; 399–403.
- Oliveira Melo AS, Malinge G, Ximenes R, Szejnfeld PO, Alves Sampaio S, Bispo de Filippis AM. Zika virus intrauterine infection causes fetal brain abnormality and microcephaly: tip of the iceberg? *Ultrasound Obstet Gynecol* 2016; 47: 6–7.
- Jaffe M, Tirosh E, Oren S. The dilemma in prenatal diagnosis of idiopathic microcephaly. *Dev Med Child Neurol* 1987; 29: 187–189.
- Schwärzler P, Homfray T, Bernard JP, Bland JM, Ville Y. Late onset microcephaly: failure of prenatal diagnosis. *Ultrasound Obstet Gynecol* 2003; 22: 640–642.
- Guibaud L, Lacalm A. Etiological diagnostic tools to elucidate 'isolated' ventriculomegaly. *Ultrasound Obstet Gynecol* 2015; 46: 1–11.
- Persutte WH. Microcephaly – no small deal. *Ultrasound Obstet Gynecol* 1998; 11: 317–318.
- Kurtz AB, Wapner RJ, Rubin CS, Cole-Beugler C, Ross RD, Goldberg BB. Ultrasound criteria for in utero diagnosis of microcephaly. *J Clin Ultrasound* 1980; 8: 11–16.
- Guibaud L. Contribution of fetal cerebral MRI for diagnosis of structural anomalies. *Prenat Diagn* 2009; 29: 420–433.
- Deloison B, Chalouhi GE, Bernard JP, Ville Y, Salomon LJ. Outcomes of fetuses with small head circumference on second-trimester ultrasonography. *Prenat Diagn* 2012; 32: 869–874.
- Leibovitz Z, Daniel-Spiegel E, Malinge G, Haratz K, Tamarkin M, Gindes L, Schreiber L, Ben-Sira L, Lev D, Shapiro I, Bakry H, Weizman B, Zreik A, Egenburg S, Arad A, Tepper R, Kidron D, Lerman-Sagie T. Prediction of microcephaly at birth using three reference ranges for fetal head circumference: can we improve prenatal diagnosis? *Ultrasound Obstet Gynecol* 2016; 47: 586–592.
- Stoler-Poria S, Lev D, Schweiger A, Lerman-Sagie T, Malinge G. Developmental outcome of isolated fetal microcephaly. *Ultrasound Obstet Gynecol* 2010; 36: 154–158.
- Hadlock FP, Deter RL, Harrist RB, Park SK. Fetal head circumference: relation to menstrual age. *Am J Roentgenol* 1982; 138: 649–653.
- Bromley B, Benacerraf BR. Difficulties in the prenatal diagnosis of microcephaly. *J Ultrasound Med* 1995; 14: 303–306.
- Allias F, Buenerd A, Bouvier R, Attia-Sobol J, Dijoud F, Clémenson A, Encha-Razavi. The spectrum of type III lissencephaly: a clinicopathological update. *Fetal Pediatr Pathol* 2004; 23: 305–317.
- Quarello E, Stirnemann J, Ville Y, Guibaud L. Assessment of fetal Sylvian fissure operculization between 22 and 32 weeks: a subjective approach. *Ultrasound Obstet Gynecol* 2008; 32: 44–49.
- Guibaud L, Salleret L, Larroche JC, Buenerd A, Alias F, Gaucherand P, Des Portes V, Pracros JP. Abnormal Sylvian fissure on prenatal cerebral imaging: significance and correlation with neuropathological and postnatal data. *Ultrasound Obstet Gynecol* 2008; 32: 50–60.
- Goldstein I, Reece EA, Pilu G, O'Connor TZ, Lockwood CJ, Hobbins JC. Sonographic assessment of the fetal frontal lobe: a potential tool for prenatal diagnosis of microcephaly. *Am J Obstet Gynecol* 1988; 158: 1057–1062.
- Persutte WH, Coury A, Hobbins JC. Correlation of fetal frontal lobe and transcerebellar diameter measurements: the utility of a new prenatal sonographic technique. *Ultrasound Obstet Gynecol* 1997; 10: 94–97.
- Barkovich AJ, Raybaud CA. Congenital malformations of the brain and skull: lissencephaly. In *Pediatric Neuroimaging* (5th edn). Lippincott Williams & Wilkins: Philadelphia, 2012; 419–428.
- Verloes A, Elmaleh M, Gonzales M, Laquerrière A, Gressens P. Genetic and clinical aspects of lissencephaly. *Rev Neurol (Paris)* 2007; 163: 533–547.
- Steinlin M, Nadal D, Eich GF, Martin E, Boltshauser EJ. Late intrauterine Cytomegalovirus infection: clinical and neuroimaging findings. *Pediatr Neurol* 1996; 15: 249–253.
- Garel C. Abnormalities of the fetal cerebral parenchyma: ischaemic and haemorrhagic lesions. In *MRI of the Fetal Brain*. Springer: Berlin, 2004; 247–261.
- Cagneaux M, Guibaud. From cavum septi pellucidi to anterior complex: how to improve detection of midline cerebral abnormalities. *Ultrasound Obstet Gynecol* 2013; 42: 485–486.
- Spohr HL, Wilms J, Steinhausen HC. Prenatal alcohol exposure and long-term developmental consequences. *Lancet* 1993; 341: 907–910.
- Massoud M, Lacalm A, Duyme M, College francais d'echographie foetale, Guibaud L. Allometric relationship between the transverse cerebellar diameter and the head circumference. Impact on prenatal counseling (Abstract). *Ultrasound Obstet Gynecol* (in press).
- Bernard JP, Cuckle HS, Stirnemann JJ, Salomon LJ, Ville Y. Screening for fetal spina bifida by ultrasound examination in the first trimester of pregnancy using fetal biparietal diameter. *Am J Obstet Gynecol* 2012; 207: 306.
- Rajab A, Manzini MC, Mochida GH, Walsh CA, Ross ME. A novel form of lethal microcephaly with simplified gyral pattern and brain stem hypoplasia. *Am J Med Genet A* 2007; 143A: 2761–2767.
- Goldstein I, Reece EA, Pilu G, Bovicelli L, Hobbins JC. Cerebellar measurements with ultrasonography in the evaluation of fetal growth and development. *Am J Obstet Gynecol* 1987; 156: 1065–1069.
- Guihard-Costa AM, Larroche JC. Differential growth between the fetal brain and its infratentorial part. *Early Hum Dev* 1990; 23: 27–40.
- Garel C. Cerebral biometry using MR: fronto-occipital diameter & cerebral biparietal diameter. In *MRI of the Fetal Brain*. Springer: Berlin, 2004; 87–88.

SUPPORTING INFORMATION ON THE INTERNET



Figures S1–S6 may be found in the online version of this article.



Systematic review and meta-analysis of isolated posterior fossa malformations on prenatal ultrasound imaging (part 1): nomenclature, diagnostic accuracy and associated anomalies

F. D'ANTONIO*, A. KHALIL*, C. GAREL†, G. PILU‡, G. RIZZO§, T. LERMAN-SAGIE¶, A. BHIDE*, B. THILAGANATHAN*, L. MANZOLI** and A. T. PAPAGEORGHIOU*

*Fetal Medicine Unit, Division of Developmental Sciences, St George's University of London, London, UK; †Hôpital d'Enfants Armand-Trousseau – Service de Radiologie, Cedex 12, Paris, France; ‡Department of Obstetrics and Gynecology, Sant'Orsola-Malpighi Hospital, University of Bologna, Bologna, Italy; §Department of Obstetrics and Gynecology, Università di Roma, Tor Vergata, Rome, Italy; ¶Fetal Neurology Clinic and Paediatric Neurology Unit, Wolfson Medical Center, Holon, Sackler School of Medicine, Tel Aviv University, Tel Aviv, Israel; **Department of Medicine and Aging Sciences, University of Chieti-Pescara, and EMISAC, CeSI Biotech, Chieti, Italy

KEYWORDS: Blake's pouch cyst; Dandy–Walker malformation; mega cisterna magna; posterior fossa; vermian hypoplasia

ABSTRACT

Objective To explore the outcome in fetuses with prenatal diagnosis of posterior fossa anomalies apparently isolated on ultrasound imaging.

Methods MEDLINE and EMBASE were searched electronically utilizing combinations of relevant medical subject headings for 'posterior fossa' and 'outcome'. The posterior fossa anomalies analyzed were Dandy–Walker malformation (DWM), mega cisterna magna (MCM), Blake's pouch cyst (BPC) and vermian hypoplasia (VH). The outcomes observed were rate of chromosomal abnormalities, additional anomalies detected at prenatal magnetic resonance imaging (MRI), additional anomalies detected at postnatal imaging and concordance between prenatal and postnatal diagnoses. Only isolated cases of posterior fossa anomalies – defined as having no cerebral or extracerebral additional anomalies detected on ultrasound examination – were included in the analysis. Quality assessment of the included studies was performed using the Newcastle–Ottawa Scale for cohort studies. We used meta-analyses of proportions to combine data and fixed- or random-effects models according to the heterogeneity of the results.

Results Twenty-two studies including 531 fetuses with posterior fossa anomalies were included in this systematic review. The prevalence of chromosomal abnormalities in fetuses with isolated DWM was 16.3% (95% CI, 8.7–25.7%). The prevalence of additional central nervous system (CNS) abnormalities that were missed

at ultrasound examination and detected only at prenatal MRI was 13.7% (95% CI, 0.2–42.6%), and the prevalence of additional CNS anomalies that were missed at prenatal imaging and detected only after birth was 18.2% (95% CI, 6.2–34.6%). Prenatal diagnosis was not confirmed after birth in 28.2% (95% CI, 8.5–53.9%) of cases. MCM was not significantly associated with additional anomalies detected at prenatal MRI or detected after birth. Prenatal diagnosis was not confirmed postnatally in 7.1% (95% CI, 2.3–14.5%) of cases. The rate of chromosomal anomalies in fetuses with isolated BPC was 5.2% (95% CI, 0.9–12.7%) and there was no associated CNS anomaly detected at prenatal MRI or only after birth. Prenatal diagnosis of BPC was not confirmed after birth in 9.8% (95% CI, 2.9–20.1%) of cases. The rate of chromosomal anomalies in fetuses with isolated VH was 6.5% (95% CI, 0.8–17.1%) and there were no additional anomalies detected at prenatal MRI (0% (95% CI, 0.0–45.9%)). The proportions of cerebral anomalies detected only after birth was 14.2% (95% CI, 2.9–31.9%). Prenatal diagnosis was not confirmed after birth in 32.4% (95% CI, 18.3–48.4%) of cases.

Conclusions DWM apparently isolated on ultrasound imaging is a condition with a high risk for chromosomal and associated structural anomalies. Isolated MCM and BPC have a low risk for aneuploidy or associated structural anomalies. The small number of cases with isolated VH prevents robust conclusions regarding their management from being drawn. Copyright © 2015 ISUOG. Published by John Wiley & Sons Ltd.

Correspondence to: Dr A. T. Papageorghiou, Fetal Medicine Unit, Division of Developmental Sciences, St George's University of London, London, SW17 0RE, UK (e-mail: apapageo@sgul.ac.uk)

Accepted: 17 April 2015

INTRODUCTION

The cerebellum and cerebellar vermis undergo protracted development during fetal and neonatal life such that the imaging appearance of the structures of the posterior fossa varies considerably with age at assessment¹. In pregnancy, routine ultrasound examination of the fetal head includes assessment of the shape and structure of the posterior fossa in the axial cerebellar plane².

Posterior fossa malformations encompass a heterogeneous spectrum of conditions characterized by progressive abnormal development of the posterior and anterior membranous areas³. A precise definition of each of the posterior fossa anomalies is necessary in order to counsel properly parents about the outcome of the pregnancy; this is particularly important because the outcome of these conditions varies considerably in relation to the type of anomaly. Therefore, the standard axial plane is insufficient for definitive diagnosis when dealing with posterior fossa malformations. In addition to detailed multiplanar sonography, magnetic resonance imaging (MRI) is usually performed prenatally to confirm the diagnosis and assess for the presence of associated anomalies, which are important determinants of neurodevelopmental outcome. Nevertheless, although accurate, fetal MRI may be affected by a significant risk of both false-positive and false-negative cases^{4,5}. Likewise, pathological confirmation of posterior fossa anomalies has been reported to have a low level of concordance with prenatal imaging^{5–7}.

The adoption of different nomenclature, diagnostic criteria and outcome measures has made parental counseling for posterior fossa anomalies extremely challenging. The presence of associated anomalies and the integrity of vermian structures are clearly important in determining the outcome of these conditions⁸. However, most of the published studies do not differentiate between cases with and without associated anomalies, and it is not certain whether these factors have an impact on outcome.

The aim of this systematic review and meta-analysis was to explore the outcome in fetuses with a prenatal ultrasound diagnosis of isolated posterior fossa anomalies. We discuss how accurate prenatal imaging is in reaching a correct diagnosis and establishing the presence of associated abnormalities.

METHODS

Protocol, eligibility criteria, information sources and search

This review was performed according to an *a-priori* designed protocol recommended for systematic reviews and meta-analyses^{9–11}. MEDLINE and EMBASE were searched electronically on 15 February 2014, utilizing combinations of the relevant medical subject heading (MeSH) terms, keywords and word variants for 'posterior fossa', 'Dandy–Walker', 'Blake's pouch cyst', 'vermian hypoplasia' and 'outcome' (Appendix S1). The search

was then updated on 14 July 2014. The search and selection criteria were restricted to the English language. Reference lists of relevant articles and reviews were hand-searched for additional reports. PRISMA guidelines were followed¹².

Study selection, data collection and data items

Studies were assessed according to the following criteria: population, outcome, gestational age at examination and type of imaging assessment of the posterior fossa.

Two authors (F.D., A.K.) reviewed all abstracts independently. Agreement regarding potential relevance was reached by consensus and full-text copies of relevant papers were obtained. The same two reviewers independently extracted relevant data regarding study characteristics and pregnancy outcome. Inconsistencies were discussed by the reviewers or with a third author and consensus reached. If more than one study was published for the same cohort with identical endpoints, the report containing the most comprehensive information on the population was included to avoid overlapping populations. For those articles in which information was not reported but the methodology was such that this information would have been recorded initially, the authors of the articles were contacted.

Quality assessment of the included studies was performed using the Newcastle–Ottawa Scale (NOS) for cohort studies. According to the NOS, each study is judged on three broad perspectives: selection of the study groups, comparability of the groups and ascertainment of outcome of interest¹³. Assessment of the selection of a study includes evaluation of the representativeness of the exposed cohort, selection of the non-exposed cohort, ascertainment of exposure and demonstration that the outcome of interest was not present at the start of the study. Assessment of the comparability of the study groups includes evaluation of the comparability of cohorts on the basis of the design or analysis. Finally, ascertainment of the outcome of interest includes evaluation of the type of assessment of the outcome of interest and length and adequacy of follow-up¹³. According to NOS, a study can be awarded a maximum of one star for each numbered item within the selection and outcome categories. A maximum of two stars can be given for comparability.

Risk of bias, summary measures and synthesis of results

The posterior fossa anomalies considered in this systematic review were defined on the basis of the morphological approach proposed by Tortori-Donati *et al.*¹⁴, and were: (1) Dandy–Walker malformation (DWM), defined by the classic triad of complete or partial agenesis of the cerebellar vermis, cystic dilatation of the fourth ventricle and enlarged posterior fossa with upward displacement of the tentorium, torcula and transverse sinuses; (2) mega cisterna magna (MCM), defined as a cisterna magna measuring > 10 mm and a normal vermis; (3) Blake's

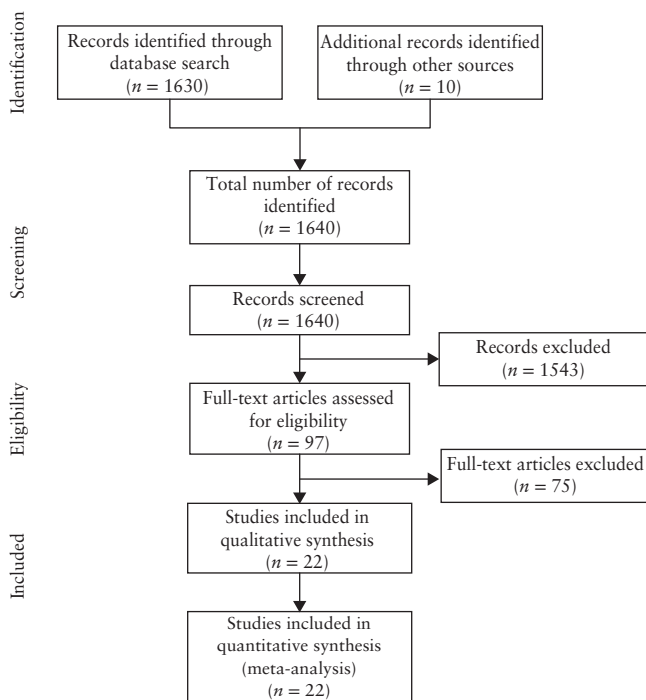


Figure 1 Flowchart summarizing selection of studies on isolated posterior fossa malformations diagnosed on prenatal ultrasound.

pouch cyst (BPC), defined as the presence of an upwardly displaced normal cerebellar vermis, normal appearance of the fastigium, tentorium and size of the cisterna magna; and (4) isolated vermian hypoplasia (VH), defined as a normally formed vermis but of smaller size, with an otherwise normal size and anatomy of the posterior fossa.

The rates of the following outcomes were analyzed: (1) chromosomal abnormalities; (2) additional major central nervous system (CNS) anomalies detected at prenatal MRI but missed at the initial ultrasound examination; (3) additional major CNS and extra-CNS anomalies detected at postnatal imaging or clinical evaluation but missed at prenatal imaging; and (4) concordance between prenatal and postnatal diagnoses.

For assessment of the incidence of abnormal karyotype, isolated posterior fossa anomalies were defined as having no additional CNS and extra-CNS anomalies detected at the ultrasound scan. Only cases that had their full karyotype tested pre- or postnatally were included. The presence of additional anomalies detected at pre- and postnatal MRI only and the rate of concordance between pre- and postnatal diagnoses were assessed only in fetuses with no additional anomalies and normal karyotype. In cases of DWM, ventriculomegaly was not included as an associated cerebral malformation because its development is related to dynamic changes in the cerebrospinal fluid, secondary to the mass effect of the cystic malformation.

Only studies reporting a prenatal diagnosis of posterior fossa anomalies were considered suitable for inclusion in the current systematic review; postnatal studies or studies from which cases diagnosed prenatally could not be extracted were excluded. Cases of Dandy–Walker variant

and those with a lack of a clear definition of the anomaly were not considered suitable for inclusion. Autopsy-based studies were excluded on the basis that fetuses undergoing termination of pregnancy are more likely to show associated major structural and chromosomal anomalies. Studies reporting the concordance between pre- and postnatal diagnosis of posterior fossa anomalies were excluded unless they provided information about whether the anomaly was isolated or not. Studies of non-isolated cases of posterior fossa anomalies were excluded, as were studies published before the year 2000, as we considered that advances in prenatal imaging techniques and improvements in the diagnosis and definition of CNS anomalies make these less relevant. Finally, studies not providing a clear classification of the posterior fossa anomalies analyzed were not considered suitable for inclusion in the current review¹⁵. The wide heterogeneity in nomenclature among published studies results in heterogeneity in risk stratification of these fetuses, therefore we included only studies providing a definition of the anomaly in accordance with that reported above.

Only full-text articles were considered eligible for inclusion; case reports, conference abstracts and case series with fewer than three cases of posterior fossa anomaly, irrespective of the fact that the anomalies were isolated or not, were excluded in order to avoid publication bias.

We used meta-analyses of proportions to combine data^{16,17}. Unfortunately, the low number of studies did not permit meaningful stratified meta-analysis to explore the test performance in subgroups of patients that may be less or more susceptible to bias. Assessment of potential publication bias was also problematic, both because of the outcome nature (rates with the left side limited to the value zero), which limits the reliability of funnel plots, and because of the low number of individual studies, which strongly limits the reliability of formal tests. Funnel plots displaying the outcome rate from individual studies *vs* their precision (1/standard error) were constructed with an exploratory aim. Tests for funnel plot asymmetry were not used when the total number of publications included for each outcome was < 10. In this case, the power of the tests was too low to distinguish chance from real asymmetry^{18,19}.

Between-study heterogeneity was explored using the I^2 statistic, which represents the percentage of between-study variation that is due to heterogeneity rather than chance. A value of 0% indicates no observed heterogeneity, whereas $I^2 \geq 50\%$ indicates a substantial level of heterogeneity. A fixed-effects model was used if substantial statistical heterogeneity was not present. On the other hand, if there was evidence of significant heterogeneity between included studies, a random-effects model was used.

All proportion meta-analyses were carried out using StatsDirect 2.7.9 (StatsDirect Ltd, Altrincham, UK) and MetaDisc (Meta-DiSc Statistical Methods, 2006, ftp://ftp.hrc.es/pub/programas/metadisc/MetaDisc_StatisticalMethods.pdf).

Table 1 General characteristics of 22 studies reporting on isolated posterior fossa malformations included in systematic review

Study	Country	Study design	Prenatal imaging	GA at US	Anomalies analyzed	US plane used for diagnosis
Tarui (2014) ²⁰	USA	Prospective	MRI	II–III trimester	VH	Multipplanar
Tonni (2014) ²¹	Italy/Chile	Prospective	US, MRI	II–III trimester	BPC, VH	Multipplanar
Ghali (2014) ²²	Australia	Retrospective	US, MRI	II–III trimester	DWM, MCM, BPC	Multipplanar
Zhao (2013) ²³	China	Prospective	US, MRI	II–III trimester	BPC	Multipplanar
Vatansever (2013) ²⁴	UK	Prospective	MRI	II–III trimester	MCM	Multipplanar
Guibaud (2012) ²⁵	France	Retrospective	US, MRI	II–III trimester	DWM	Multipplanar
Gandolfi Colleoni (2012) ²⁶	Italy	Retrospective	US, MRI	II–III trimester	DWM, BPC, MCM, VH	Multipplanar
Paladini (2012) ²⁷	Italy	Retrospective	US, MRI	II–III trimester	BPC	Multipplanar
Patek (2012) ²⁸	USA	Retrospective	US, MRI	II–III trimester	DWM, MCM, VH	Multipplanar
Bertucci (2011) ²⁹	Italy/Israel	Prospective	US, MRI	II–III trimester	DWM, BPC, MCM, VH	Multipplanar
Eggle (2011) ³⁰	Austria	Prospective	US	I–III trimester	BPC	Multipplanar
Ozkan (2011) ³¹	Turkey	Retrospective	US	II–III trimester	DWM	Multipplanar
Rizzo (2011) ³²	Multicenter	Prospective	US, MRI	II–III trimester	DWM, MCM, BPC	Multipplanar
Dror (2009) ³³	Israel	Prospective	US, MRI	II–III trimester	MCM	Multipplanar
Kontopoulos (2008) ³⁴	USA	Retrospective	US	II–III trimester	DWM	Not stated
Forzano (2007) ³⁵	UK	Retrospective	US, MRI	II trimester	MCM	Multipplanar
Long (2006) ³⁶	UK	Retrospective	US	II–III trimester	MCM	Multipplanar
Zalel (2006) ³⁷	Israel	Retrospective	US, MRI	II–III trimester	BPC	Multipplanar
Has (2004) ³⁸	Turkey	Retrospective	US, MRI	II–III trimester	DWM	Multipplanar
Leitner (2004) ³⁹	Israel	Retrospective	US	II–III Trimester	MCM	Axial plane
Ecker (2000) ⁴⁰	USA	Retrospective	US	II–III trimester	DWM	Axial plane
Kölble (2000) ⁴¹	Switzerland	Retrospective	US	I–III trimester	DWM	Axial plane

Only first author of each study is given. BPC, Blake's pouch cyst; DWM, Dandy–Walker malformation; GA, gestational age; MCM, mega cisterna magna, MRI, magnetic resonance imaging; US, ultrasound; VH, vermian hypoplasia.

RESULTS

Study selection and characteristics

A total of 1640 articles were identified, of which 97 full-text articles were assessed for their eligibility for inclusion (Appendix S2). A total of 22 studies were included in the systematic review (Figure 1)^{20–41}. These 22 studies included 531 fetuses with posterior fossa anomalies; of these, 226 (42.6%) did not show any additional structural anomaly at the scan and represent the population of this systematic review. The general characteristics of the included studies are reported in Table 1. For most of the included studies, the posterior fossa anatomy was assessed using a multiplanar approach. Fetal MRI was performed to confirm the diagnosis and to look for associated anomalies in the majority of the included studies. Postnatal confirmation of the anomaly was performed in most cases by ultrasound, computed tomography or MRI, however the majority of the studies lacked a standardized protocol for the postnatal assessment of these patients.

Quality assessment of the included studies was performed using NOS for cohort studies (Table 2). Almost all included studies showed an overall good rate with regard to selection and comparability of the study groups and for the ascertainment of the outcome of interest. The main weaknesses of these studies were represented by their retrospective design, small sample size comprising series from high-risk populations and a lack of standardized postnatal confirmation. Furthermore, the relatively short period of follow-up after birth did

not allow for a precise estimation of the overall rate of additional anomalies missed prenatally and detected only after birth.

Synthesis of results

Dandy–Walker malformation

There were 217 fetuses (in 11 studies) with DWM included in this review. Associated CNS and extra-CNS structural anomalies were present in 60.9% (95% CI, 45.3–75.3%) and 42.6% (95% CI, 22.7–64.0%) of cases, respectively. Ventriculomegaly was a common finding and was detected prenatally in 31.3% (95% CI, 14.0–51.8%) of cases with DWM.

The prevalence of chromosomal abnormalities in fetuses with DWM and no associated CNS or extra-CNS anomalies was 16.3% (95% CI, 8.7–25.7%; Table 3, Figure S1), with chromosomal deletions representing the most common anomaly (7.6% (95% CI, 2.6–14.8%)). The occurrence of hydrocephalus requiring ventriculoperitoneal shunt after birth is common in cases of DWM. Overall, ventriculomegaly occurred before or after birth in 68.0% (95% CI, 32.3–94.5%) of cases of DWM with no associated structural anomalies and normal karyotype. Ventriculomegaly requiring a ventriculoperitoneal shunt to reduce raised intracranial pressure occurred in 62.7% (95% CI, 27.9–91.3%) of cases.

The prevalence of additional CNS abnormalities missed at ultrasound and detected only on prenatal MRI was 13.7% (95% CI, 0.2–42.6%; Table 3), while the rates of additional CNS and extra-CNS anomalies

Table 2 Quality assessment of the 22 included studies according to Newcastle–Ottawa Scale

Study	Selection	Comparability	Outcome
Tarui (2014) ²⁰	★★★★	★★	★★★★
Tonni (2014) ²¹	★★★	★	★★
Ghali (2014) ²²	★★★	★	★★★★
Zhao (2013) ²³	★★	★	★★
Vatansever (2013) ²⁴	★★★	★	★★
Guibaud (2012) ²⁵	★★★	★	★★★★
Gandolfi Colleoni (2012) ²⁶	★★★	★	★★
Paladini (2012) ²⁷	★★★	★	★★★★
Patek (2012) ²⁸	★★★	★	★★★★
Bertucci (2011) ²⁹	★★★	★	★★
Egle (2011) ³⁰	★★	★	★★
Ozkan (2011) ³¹	★★	★	★
Rizzo (2011) ³²	★★★	★	★★
Dror (2009) ³³	★★★	★★	★★★★
Kontopoulos (2008) ³⁴	★★	★	★★
Forzano (2007) ³⁵	★★	★	★★
Long (2006) ³⁶	★★★	★	★★
Zalel (2006) ³⁷	★★★	★	★★★★
Has (2004) ³⁸	★★★	★	★★
Leitner (2004) ³⁹	★★	★	★★
Ecker (2000) ⁴⁰	★★★	★	★★
Kölblle (2000) ⁴¹	★★★	★	★★★★

A study can be awarded a maximum of one star for each numbered item within the selection and outcome categories. A maximum of two stars can be given for comparability.

missed at prenatal imaging by either ultrasound or MRI and detected only after birth were 18.2% (95% CI, 6.2–34.6%) and 18.9% (95% CI, 6.3–36.2%), respectively. The prenatal diagnosis of DWM was not confirmed after birth in 28.2% (95% CI, 8.5–53.9%) of cases (Table 3). Among the cases of isolated DWM that were not confirmed at birth ($n = 7$), two had a normal appearance of the posterior fossa on postnatal imaging, one a diagnosis of BPC, one of VH, one of Joubert syndrome and one of posterior fossa hemorrhage, while the last case showed an association of DWM and abnormality of the cortex.

Mega cisterna magna

There were 144 fetuses (in 10 studies) with a prenatal diagnosis of MCM included. The rates of additional CNS and extra-CNS anomalies were 12.6% (95% CI, 2.9–27.6%) and 16.6% (95% CI, 6.2–30.8%), respectively, with ventriculomegaly being the most common associated anomaly (11.7% (95% CI, 2.8–25.6%)). No fetus tested prenatally was found to have a chromosomal abnormality (0% (95% CI, 0.0–4.7%); Table 4, Figure S2). In addition, there were no significant associations with additional anomalies detected only at prenatal MRI, or with associated CNS and extra-CNS anomalies missed prenatally and detected after birth (Table 4). The prenatal diagnosis of MCM was not confirmed in 7.1% (95% CI, 2.3–14.5%) of cases. Among the cases not confirmed at birth, three were false-positive diagnoses with

a normal appearance of the posterior fossa described at postnatal imaging, and one was a posterior fossa arachnoid cyst.

Blake's pouch cyst

There were 86 fetuses (in nine studies) with a prenatal diagnosis of BPC included. The rates of associated CNS and extra-CNS structural anomalies were 11.5% (95% CI, 4.3–21.5%) and 25.3% (95% CI, 9.0–46.5%), respectively. There was only a single case of aneuploidy (trisomy 21) detected among 45 fetuses tested (Table 5, Figure S3). There was no case of associated CNS anomaly missed at the ultrasound scan and detected only at prenatal MRI in the cohort of fetuses included in this review (0% (95% CI, 0.0–6.4%)). Similarly, no associated CNS (0% (95% CI, 0.0–8.6%)) or extra-CNS (0% (95% CI, 0.0–16.1%)) anomalies were detected only after birth (Table 5). The prenatal diagnosis of BPC was not confirmed after birth in 9.8% (95% CI, 2.9–20.1%) of cases (Table 5), consisting of one case of posterior fossa arachnoid cyst, one of otherwise isolated MCM and one with normal postnatal imaging.

Vermian hypoplasia

There were 63 fetuses (in five studies) with a prenatal diagnosis of VH included. The rates of associated CNS and extra-CNS anomalies were 56.1% (95% CI, 25.0–84.7%) and 49.2% (95% CI, 31.5–67.1%), respectively. There was only one chromosomal anomaly detected (chromosomal deletion) among the 30 fetuses tested (Table 6, Figure S4). Although the number of fetuses with this outcome was very small, no additional anomalies were detected only at prenatal MRI (0% (95% CI, 0.0–45.9%)).

Finally, the proportions of cerebral and extra-CNS anomalies detected only after birth were 14.2% (95% CI, 2.9–31.9%) and 0% (95% CI, 0.0–18.5%), respectively (Table 6). The prenatal diagnosis was not confirmed in 32.4% (95% CI, 18.3–48.4%) of cases; all 10 cases consisted of false-positive diagnoses, with a normal appearance of the posterior fossa and cerebellar vermis at postnatal imaging in nine and one case of VH and associated cortical abnormalities.

DISCUSSION

Summary of evidence

This systematic review demonstrates that apparently isolated DWM carries a high risk of chromosomal abnormalities and associated malformations that can be misdiagnosed before birth. In contrast, isolated MCM and BPC are associated with a very low risk of aneuploidy and of associated structural anomalies discovered only at prenatal MRI or after birth. Isolated VH is associated with a low risk of aneuploidy and of additional anomalies detected only at prenatal MRI. A discrepancy between

Table 3 Pooled proportions (PP) for outcomes in fetuses with isolated Dandy–Walker malformation assessed prenatally for additional anomalies

Outcome	Studies (n)	Fetuses (n/N)	I ² (%)	Raw (95% CI) (%)	PP (95% CI) (%)
Chromosomal anomalies	11	9/60	0	15.00 (7.1–26.6)	16.32 (8.7–25.7)
Additional anomalies detected only at prenatal MRI	4	2/18	56.1	11.11 (1.4–34.7)	13.72 (0.2–42.6)
Additional anomalies detected only postnatally					
CNS anomalies	6	3/21	0	14.29 (3.1–36.3)	18.19 (6.2–34.6)
Extra-CNS anomalies	5	3/20	0	15.00 (3.2–37.9)	18.93 (6.3–36.2)
Discrepancy between pre- and postnatal diagnosis	6	7/33	54.9	21.21 (9.0–38.9)	28.18 (8.5–53.9)

CNS, central nervous system; MRI, magnetic resonance imaging.

Table 4 Pooled proportions (PP) for outcomes in fetuses with isolated mega cisterna magna assessed prenatally for additional anomalies

Outcome	Studies (n)	Fetuses (n/N)	I ² (%)	Raw (95% CI) (%)	PP (95% CI) (%)
Chromosomal anomalies	9	0/76	0	0.00 (0.0–4.7)	0.00 (0.0–4.7)*
Additional anomalies detected only at prenatal MRI	5	0/29	0	0.00 (0.0–11.9)	0.00 (0.0–11.9)*
Additional anomalies detected only postnatally					
CNS anomalies	6	1/60	0	1.67 (0.04–8.9)	3.65 (0.5–9.5)
Extra-CNS anomalies	5	1/40	0	2.50 (0.1–13.2)	4.66 (0.5–12.7)
Discrepancy between pre- and postnatal diagnosis	8	4/59	43.2	6.78 (1.9–16.5)	7.14 (2.3–14.5)

*Using Meta-Disc statistical analysis. CNS, central nervous system; MRI, magnetic resonance imaging.

pre- and postnatal diagnoses of posterior fossa anomalies is common in cases of DWM and VH, but less frequent in cases of MCM and BPC.

Strengths and limitations of the study

The strengths of this study are its robust methodology for identifying all possible studies for inclusion, assessing data quality and synthesizing all suitable data.

For several meta-analyses, the number of included studies was small, and some included small populations. Furthermore, many of the studies reviewed did not allow extraction of individual case data. Another limitation is the significant heterogeneity in the definitions used⁴².

Subtle chromosomal abnormalities such as microdeletions may be overlooked by routine chromosome analysis, highlighting the need for molecular cytogenetic techniques, which were not used in some of the included studies. It is therefore possible that this systematic review underestimates the prevalence of chromosomal abnormalities⁴³.

Advances in prenatal imaging techniques have led to more comprehensive assessment of the fetal brain; in this review, we considered only studies published between 2000 and 2014 in order to minimize the effect of changing imaging protocols. Despite these limitations, however, our review represents the best published estimate of outcomes for this group of conditions.

Implications for clinical practice

Objective standardized assessment of the posterior fossa is needed to differentiate precisely the possible

diagnoses. One such approach has been proposed^{3,25}: our review suggests that this approach is quite effective in the identification of MCM and BPC, but less effective for DWM, and inadequate for VH. Indeed variable criteria for the diagnosis of VH were used in different studies.

Isolated DWM was frequently associated with chromosomal aberrations and we therefore believe that karyotyping should be offered for fetuses with this prenatal diagnosis. Microarray analysis can also be considered where available. On the other hand, the risk of chromosomal anomalies is very low in cases of isolated MCM. With isolated BPC, the rate of chromosomal anomalies was in the order of 5%, but this should be considered with caution given the small number of cases.

Antenatal MRI is certainly indicated with isolated DWM, as associated intracranial anomalies escaping sonographic diagnosis were frequent, which was not the case for other anomalies. MCM was misdiagnosed in 7% of cases; in some a posterior fossa cyst was found after birth. Posterior fossa cysts may expand and cause obstructive hydrocephalus. MRI may be more effective than ultrasound, not only in differentiating isolated MCM from posterior fossa cysts, but also in identifying periventricular nodular heterotopia, a neuronal migration disorder with significant clinical implications⁴⁴. Isolated DWM is frequently found in association with anomalies that are only identified postnatally. However, parents of fetuses with isolated MCM or BPC can be reassured that this rarely occurs in such cases.

Our review highlights the need for an objective standard to confirm the diagnosis after birth. Recent studies have shown a low level of agreement between prenatal imaging

Table 5 Pooled proportions (PP) for outcomes in fetuses with isolated Blake's pouch cyst assessed prenatally for additional anomalies

Outcome	Studies (n)	Fetuses (n/N)	I ² (%)	Raw (95% CI) (%)	PP (95% CI) (%)
Chromosomal anomalies	8	1/45	0	2.22 (0.1–11.8)	5.16 (0.9–12.7)
Additional anomalies detected only at prenatal MRI	8	0/56	0	0.00 (0.0–6.4)	0.00 (0.0–6.4)*
Additional anomalies detected only postnatally					
CNS anomalies	6	0/41	0	0.00 (0.0–8.6)	0.00 (0.0–8.6)*
Extra-CNS anomalies	5	0/21	0	0.00 (0.0–16.1)	0.00 (0.0–16.1)*
Discrepancy between pre- and postnatal diagnosis	6	3/39	33.9	7.69 (1.6–20.9)	9.79 (2.9–20.1)

*Using Meta-Disc statistical analysis. CNS, central nervous system; MRI, magnetic resonance imaging.

Table 6 Pooled proportions (PP) for outcomes in fetuses with isolated vermian hypoplasia assessed prenatally for additional anomalies

Outcome	Studies (n)	Fetuses (n/N)	I ² (%)	Raw (95% CI) (%)	PP (95% CI) (%)
Chromosomal anomalies	4	1/30	0	3.33 (0.1–17.2)	6.54 (0.8–17.1)
Additional anomalies detected only at prenatal MRI	3	0/6	0	0.00 (0.0–45.9)	0.00 (0.0–45.9)*
Additional anomalies detected only postnatally					
CNS anomalies	3	2/18	0	11.11 (1.4–34.7)	14.20 (2.9–31.9)
Extra-CNS anomalies	3	0/18	0	0.00 (0.0–18.5)	0.00 (0.0–18.5)
Discrepancy between pre- and postnatal diagnosis	4	10/32	0	31.25 (16.1–50.0)	32.44 (18.3–48.4)

*Using Meta-Disc statistical analysis. CNS, central nervous system; MRI, magnetic resonance imaging.

and pathological examination in cases of termination of pregnancy^{5,6}. Challenges in the pathological assessment of posterior fossa structures, inconsistencies in diagnostic criteria and the lack of multiplanar assessment in older studies, may account for this heterogeneity.

Implications for research

The wide heterogeneity in classification and the definition of outcomes highlights the urgent need for prospective studies using a standardized classification of these anomalies, correlating them with pregnancy and postnatal outcomes.

Although posterior fossa anomalies are usually diagnosed in the second trimester, early detection has been reported^{30,44,45}. Large prospective studies on low-risk populations are needed to ascertain whether first-trimester assessment of the posterior fossa may lead to reliable early diagnosis.

Conclusions

DWM that is isolated on prenatal ultrasound imaging is frequently associated with chromosomal and structural anomalies. MCM and BPC are rarely associated with malformations that are undetected by ultrasound, and isolated MCM has a low risk for aneuploidy. The group of fetuses with an antenatal diagnosis of VH was heterogeneous, and the condition was often not confirmed at birth. We suggest that MRI is indicated in cases of DWM and MCM. Studies using a standardized classification are needed to define objectively the prognosis of these anomalies.

ACKNOWLEDGMENTS

We thank Prof. D. Paladini, Prof. T. Tarui, Prof. R. Palma-Dias, Prof. R. Has, Dr E. Bertucci, Dr K. Reidy, Dr R. Ghali, Dr J. Garcia-Flores, Dr A. Borrell, Dr Y. Leitner, Dr G. Tonni, Dr A. Long, Dr K. Patek, Dr C. Spaeth, Dr M. Scheier, Dr R. Lachmann, Dr N. Kölblle, Dr T. Harper, Dr P. H. Tang, Dr Z. Ozkan and Dr R. Russo for their contribution to this systematic review in terms of support and additional data supplied.

REFERENCES

- Robinson AJ, Blaser S, Toi A, Chitayat D, Halliday W, Pantazi S, Gundogan M, Laughlin S, Ryan G. The fetal cerebellar vermis: assessment for abnormal development by ultrasonography and magnetic resonance imaging. *Ultrasound Q* 2007; 23: 211–223.
- International Society of Ultrasound in Obstetrics & Gynecology Education Committee. Sonographic examination of the fetal central nervous system: guidelines for performing the 'basic examination' and the 'fetal neurosonogram'. *Ultrasound Obstet Gynecol* 2007; 29: 109–116.
- Garel C. Posterior fossa malformations: main features and limits in prenatal diagnosis. *Pediatr Radiol* 2010; 40: 1038–1045.
- Limperopoulos C, Robertson RL Jr, Khwaja OS, Robson CD, Estroff JA, Barnewolt C, Levine D, Morash D, Nemes L, Zaccagnini L, du Plessis AJ. How accurately does current fetal imaging identify posterior fossa anomalies? *AJR Am J Roentgenol* 2008; 190: 1637–1643.
- Tilea B, Delezoide AL, Khung-Savatovski S, Guimiot F, Vuillard E, Oury JF, Garel C. Comparison between magnetic resonance imaging and fetopathology in the evaluation of fetal posterior fossa non-cystic abnormalities. *Ultrasound Obstet Gynecol* 2007; 29: 651–659.
- Carroll SG, Porter H, Abdel-Fattah S, Kyle PM, Soothill PW. Correlation of prenatal ultrasound diagnosis and pathologic findings in fetal CNS abnormalities. *Ultrasound Obstet Gynecol* 2000; 16: 149–153.
- Phillips JJ, Mahony BS, Siebert JR, Lalani T, Fligner CL, Kapur RP. Dandy–Walker malformation complex: correlation between ultrasonographic diagnosis and postmortem neuropathology. *Obstet Gynecol* 2006; 107: 685–693.
- Klein O, Pierre-Kahn A, Boddaert N, Parisot D, Brunelle F. Dandy–Walker malformation: prenatal diagnosis and prognosis. *Childs Nerv Syst* 2003; 19: 484–489.
- Henderson LK, Craig JC, Willis NS, Tovey D, Webster AC. How to write a Cochrane systematic review. *Nephrology (Carlton)* 2010; 15: 617–624.
- NHS Centre for Reviews and Dissemination. *Systematic Reviews: CRD's Guidance for Undertaking Reviews in Healthcare*. University of York: York (UK), 2009.

11. Leeflang MM, Deeks JJ, Gatsonis C, Bossuyt PM; Cochrane Diagnostic Test Accuracy Working Group. Systematic reviews of diagnostic test accuracy. *Ann Intern Med* 2008; **149**: 889–897.
12. Prisma statement. <http://www.prisma-statement.org/>
13. Wells GA, Shea B, O'Connell D, Peterson J, Welch V, Losos M, Tugwell P. Newcastle–Ottawa Scale for assessing the quality of nonrandomised studies in meta-analyses. http://www.ohri.ca/programs/clinical_epidemiology/oxford.asp
14. Tortori-Donati P, Rossi A, Biancheri R. Brain Malformations. In *Pediatric Neuroradiology*, Tortori-Donati P, Rossi A, Raybaud C (eds). Springer: New York, 2005; 71–198.
15. Guibaud L, des Portes V. Plea for an anatomical approach to abnormalities of the posterior fossa in prenatal diagnosis. *Ultrasound Obstet Gynecol* 2006; **27**: 477–481.
16. Manzoli L, De Vito C, Salanti G, D'Addario M, Villari P, Ioannidis JP. Meta-analysis of the immunogenicity and tolerability of pandemic influenza A 2009 (H1N1) vaccines. *PLoS One* 2011; **6**: e24384.
17. Hunter JP, Saratzis A, Sutton AJ, Boucher RH, Sayers RD, Bown MJ. In meta-analyses of proportion studies, funnel plots were found to be an inaccurate method of assessing publication bias. *J Clin Epidemiol* 2014; **67**: 897–903.
18. Egger M, Davey Smith G, Schneider M, Minder C. Bias in meta-analysis detected by a simple, graphical test. *BMJ* 1997; **315**: 629–634.
19. Higgins JPT, Green S (eds). *Cochrane Handbook for Systematic Reviews of Interventions*, Version 5.0.2 [updated September 2009]. The Cochrane Collaboration, 2009. Available from www.cochrane-handbook.org.
20. Tarui T, Limperopoulos C, Sullivan NR, Robertson RL, du Plessis AJ. Long-term developmental outcome of children with a fetal diagnosis of isolated inferior vermian hypoplasia. *Arch Dis Child Fetal Neonatal Ed* 2014; **99**: F54–F58.
21. Tonni G, Grisolia G, Sepulveda W. Second trimester fetal neurosonography: reconstructing cerebral midline anatomy and anomalies using a novel three-dimensional ultrasound technique. *Prenat Diagn* 2014; **34**: 75–83.
22. Ghali R, Reidy K, Fink AM, Palma-Dias R. Perinatal and short-term neonatal outcomes of posterior fossa anomalies. *Fetal Diagn Ther* 2014; **35**: 108–111.
23. Zhao D, Liu W, Cai A, Li J, Chen L, Wang B. Quantitative evaluation of the fetal cerebellar vermis using the median view on three-dimensional ultrasound. *Prenat Diagn* 2013; **33**: 153–157.
24. Vatanserver D, Kyriakopoulou V, Allsop JM, Fox M, Chew A, Hajnal JV, Rutherford MA. Multidimensional analysis of fetal posterior fossa in health and disease. *Cerebellum* 2013; **12**: 632–644.
25. Guibaud L, Larroque A, Ville D, Sanlaville D, Till M, Gaucherand P, Pracros JP, des Portes V. Prenatal diagnosis of 'isolated' Dandy–Walker malformation: imaging findings and prenatal counselling. *Prenat Diagn* 2012; **32**: 185–193.
26. Gandolfi Colleoni G, Contro E, Carletti A, Ghi T, Campobasso G, Rembouskos G, Volpe G, Pilu G, Volpe P. Prenatal diagnosis and outcome of fetal posterior fossa fluid collections. *Ultrasound Obstet Gynecol* 2012; **39**: 625–631.
27. Paladini D, Quarantelli M, Pastore G, Sorrentino M, Sglavo G, Nappi C. Abnormal or delayed development of the posterior membranous area of the CNS: anatomy, ultrasound diagnosis, natural history and outcome of Blake's pouch cyst in the fetus. *Ultrasound Obstet Gynecol* 2012; **39**: 279–287.
28. Patek KJ, Kline-Fath BM, Hopkin RJ, Pilipenko VV, Crombleholme TM, Spaeth CG. Posterior fossa anomalies diagnosed with fetal MRI: associated anomalies and neurodevelopmental outcomes. *Prenat Diagn* 2012; **32**: 75–82.
29. Bertucci E, Gindes L, Mazza V, Re C, Lerner-Geva L, Achiron R. Vermian biometric parameters in the normal and abnormal fetal posterior fossa: three-dimensional sonographic study. *J Ultrasound Med* 2011; **30**: 1403–1410.
30. Egle D, Strobl I, Weiskopf-Schwendinger V, Grubinger E, Kraxner F, Mutz-Dehbalae IS, Strasak A, Scheier M. Appearance of the fetal posterior fossa at 11 + 3 to 13 + 6 gestational weeks on transabdominal ultrasound examination. *Ultrasound Obstet Gynecol* 2011; **38**: 620–624.
31. Ozkan ZS, Gilgin H, Aygün HB, Deveci D, Simsek M, Kumru S, Yüce H. Our clinical experience about prenatal diagnosis and neonatal outcomes of fetal central nervous system anomalies. *J Matern Fetal Neonatal Med* 2011; **24**: 502–505.
32. Rizzo G, Abuhamad AZ, Benacerraf BR, Chaoui R, Corral E, Addario VD, Espinoza J, Lee W, Mercè Alberto LT, Pooh R, Sepulveda W, Sinkovskaya E, Viñals F, Volpe P, Pietrolucci ME, Arduini D. Collaborative study on 3-dimensional sonography for the prenatal diagnosis of central nervous system defects. *J Ultrasound Med* 2011; **30**: 1003–1008.
33. Dror R, Malinger G, Ben-Sira L, Lev D, Pick CG, Lerman-Sagie T. Developmental outcome of children with enlargement of the cisterna magna identified in utero. *J Child Neurol* 2009; **24**: 1486–1492.
34. Kontopoulos EV, Quintero RA, Salihi HM, Bornick PW, Allen MH. Dandy–Walker syndrome and monozygotic twins: insight into a possible etiological mechanism. *J Matern Fetal Neonatal Med* 2008; **21**: 839–842.
35. Forzano F, Mansour S, Ierullo A, Homfray T, Thilaganathan B. Posterior fossa malformation in fetuses: a report of 56 further cases and a review of the literature. *Prenat Diagn* 2007; **27**: 495–501.
36. Long A, Moran P, Robson S. Outcome of fetal cerebral posterior fossa anomalies. *Prenat Diagn* 2006; **26**: 707–710.
37. Zalel Y, Gilboa Y, Gabis L, Ben-Sira L, Hoffman C, Wiener Y, Achiron R. Rotation of the vermis as a cause of enlarged cisterna magna on prenatal imaging. *Ultrasound Obstet Gynecol* 2006; **27**: 490–493.
38. Has R, Ermiş H, Yüksel A, Ibrahimoglu L, Yildirim A, Sezer HD, Başaran S. Dandy–Walker malformation: a review of 78 cases diagnosed by prenatal sonography. *Fetal Diagn Ther* 2004; **19**: 342–347.
39. Leitner Y, Goetz H, Gull I, Mesterman R, Weiner E, Jaffa A, Harel S. Antenatal diagnosis of central nervous system anomalies: can we predict prognosis? *J Child Neurol* 2004; **19**: 435–438.
40. Ecker JL, Shipp TD, Bromley B, Benacerraf B. The sonographic diagnosis of Dandy–Walker and Dandy–Walker variant: associated findings and outcomes. *Prenat Diagn* 2000; **20**: 328–332.
41. Kölblle N, Wissner J, Kurmanavicius J, Bolthausen E, Stallmach T, Huch A, Huch R. Dandy–Walker malformation: prenatal diagnosis and outcome. *Prenat Diagn* 2000; **20**: 318–327.
42. Robinson AJ. Inferior vermian hypoplasia – preconception, misconception. *Ultrasound Obstet Gynecol* 2014; **43**: 123–136.
43. Shaffer LG, Rosenfeld JA, Dabell MP, Coppinger J, Bandholz AM, Ellison JW, Ravnan JB, Torchia BS, Ballif BC, Fisher AJ. Detection rates of clinically significant genomic alterations by microarray analysis for specific anomalies detected by ultrasound. *Prenat Diagn* 2012; **32**: 986–995.
44. Lachmann R, Sinkovskaya E, Abuhamad A. Posterior brain in fetuses with Dandy–Walker malformation with complete agenesis of the cerebellar vermis at 11–13 weeks: a pilot study. *Prenat Diagn* 2012; **32**: 765–769.
45. Garcia-Posada R, Eixarch E, Sanz M, Puerto B, Figueras F, Borrrell A. Cisterna magna width at 11–13 weeks in the detection of posterior fossa anomalies. *Ultrasound Obstet Gynecol* 2013; **41**: 515–520.

SUPPORTING INFORMATION ON THE INTERNET

The following supporting information may be found in the online version of this article:



Appendix S1 Search strategy

Appendix S2 Excluded studies and reason for exclusion

Figures S1–S4 Pooled proportions of the incidence of chromosomal anomalies (a), additional anomalies detected only at prenatal magnetic resonance imaging (b), additional central nervous system (CNS) (c) and extra-CNS (d) anomalies detected only after birth, and discrepancy between pre- and postnatal findings (e) in fetuses with isolated Dandy–Walker malformation (Figure S1), mega cisterna magna (Figure S2), Blake's pouch cyst (Figure S3) and vermian hypoplasia (Figure S4).



Systematic review and meta-analysis of isolated posterior fossa malformations on prenatal imaging (part 2): neurodevelopmental outcome

F. D'ANTONIO*, A. KHALIL*, C. GAREL†, G. PILU‡, G. RIZZO§, T. LERMAN-SAGIE¶, A. BHIDE*, B. THILAGANATHAN*, L. MANZOLI** and A. T. PAPAGEORGHIOU*

*Fetal Medicine Unit, Division of Developmental Sciences, St George's University of London, London, UK; †Hôpital d'Enfants Armand-Trousseau – Service de Radiologie, Cedex 12, Paris, France; ‡Department of Obstetrics and Gynecology, Sant'Orsola-Malpighi Hospital, University of Bologna, Bologna, Italy; §Department of Obstetrics and Gynecology, Università di Roma, Tor Vergata, Rome, Italy; ¶Fetal Neurology Clinic and Paediatric Neurology Unit, Wolfson Medical Center, Holon, Sackler School of Medicine, Tel Aviv University, Tel Aviv, Israel; **Department of Medicine and Aging Sciences, University of Chieti-Pescara, and EMISAC, CeSI Biotech, Chieti, Italy

KEYWORDS: Blake's pouch cyst; Dandy–Walker malformation; mega cisterna magna; meta-analysis; neurodevelopmental outcome; posterior fossa anomaly; vermian hypoplasia

ABSTRACT

Objectives Diagnosis of isolated posterior fossa anomalies in children is biased by the fact that only those that are symptomatic are brought to the attention of the appropriate clinical personnel, and the reported rate is often affected by the adoption of different nomenclature, diagnostic criteria, outcome measures, duration of follow-up and neurodevelopmental tools. The aim of this systematic review was to explore the neurodevelopmental outcome of fetuses with a prenatal diagnosis of isolated posterior fossa anomalies.

Methods MEDLINE and EMBASE were searched electronically, utilizing combinations of the relevant medical subject heading terms for 'posterior fossa' and 'outcome'. Studies assessing the neurodevelopmental outcome in children with a prenatal diagnosis of isolated posterior fossa malformations were considered eligible. The posterior fossa anomalies analyzed included Dandy–Walker malformation (DWM), mega cisterna magna (MCM), Blake's pouch cyst (BPC) and vermian hypoplasia (VH). Two authors reviewed all abstracts independently. Quality assessment of the included studies was performed using the Newcastle–Ottawa Scale for cohort studies. Meta-analyses of proportions were used to combine data, and between-study heterogeneity was explored using the I^2 statistic.

Results A total of 1640 articles were identified; 95 were assessed for eligibility and a total of 16 studies were

included in the systematic review. The overall rate of abnormal neurodevelopmental outcome in children with a prenatal diagnosis of DWM was 58.2% (95% CI, 21.8–90.0%) and varied from 0–100%. In those with a prenatal diagnosis of MCM, the rate of abnormal neurodevelopmental outcome was 13.8% (95% CI, 7.3–21.9%), with a range of 0–50%. There was no significant association between BPC and the occurrence of abnormal neurodevelopmental delay, with a rate of 4.7% (95% CI, 0.7–12.1%) and range of 0–5%. Although affected by the very small number of studies, there was a non-significant occurrence of abnormal neurodevelopmental delay in children with a prenatal diagnosis of VH, with a rate of 30.7% (95% CI, 0.6–79.1%) and range of 0–100%.

Conclusions Fetuses diagnosed with isolated DWM are at high risk of abnormal neurodevelopmental outcome, while isolated MCM or BPC have a generally favorable outcome. The risk of abnormal developmental delay in cases with isolated VH needs to be further assessed. In view of the wide heterogeneity in study design, time of follow-up, neurodevelopmental tests used and the very small number of included cases, further future large prospective studies with standardized and objective protocols for diagnosis and follow-up are needed in order to ascertain the rate of abnormal neurodevelopmental outcome in children with isolated posterior fossa anomalies. Copyright © 2015 ISUOG. Published by John Wiley & Sons Ltd.

Correspondence to: Dr A. T. Papageorghiou, Fetal Medicine Unit, Division of Developmental Sciences, St George's University of London, London SW17 0RE, UK (e-mail: apapageo@sgul.ac.uk)

Accepted: 16 September 2015

INTRODUCTION

Advances in prenatal brain imaging have allowed detailed assessment of the anatomy of the posterior fossa; however, when an abnormality is found in this area of the fetal brain, parental counseling is particularly challenging because the terminology is often confusing and there are many small studies that make it difficult to reach firm conclusions regarding the long-term outcome of an individual fetus or infant. For instance, mega cisterna magna (MCM) and Blake's pouch cyst (BPC) have been reported to have a favorable outcome when isolated. Conversely, anomalies such as Dandy–Walker malformation (DWM) are commonly considered to have a poor prognosis^{1–4}.

The lack of an objective reference standard to confirm the diagnosis after birth represents another challenge. Magnetic resonance imaging (MRI) interpretation is hampered by high rates of both false-positive and false-negative diagnoses⁵. Likewise, pathological confirmation of posterior fossa anomalies has a low level of concordance with prenatal imaging⁶. In addition, many published studies do not differentiate between cases diagnosed before and after birth. Postnatal series might be biased by the fact that only symptomatic patients come to the attention of medical practitioners, meaning that they do not reflect the natural history of the disease.

Finally, how the neurodevelopmental outcome is assessed differs between studies. This is of particular relevance because the traditional role of the cerebellum as a mere center for motor control has been reconsidered in view of recent evidence, highlighting its influence on language, socialization and cognitive functions⁷. Therefore, the use of different targeted neurodevelopmental tests in order to assess accurately the neurocognitive status of these patients might be necessary. The adoption of different periods of follow-up among the studies means that the rate of abnormal neurocognitive outcome remains uncertain, because some developmental anomalies may be evident only later in life, while others, labeled as abnormal early in life, are mild and may have only a small effect on the overall quality of life⁸.

The adoption of different nomenclature, diagnostic criteria, outcome measures, duration of follow-up and neurodevelopmental tools means that there remains significant controversy regarding neurodevelopmental outcomes in children with posterior fossa abnormalities. The aim of this systematic review was to explore the neurodevelopmental outcomes in children diagnosed *in utero* with isolated posterior fossa anomalies.

METHODS

Protocol, eligibility criteria, information sources and search

This review was performed according to an *a-priori* designed protocol and based on recommended methods for systematic reviews and meta-analyses^{9–11}; PRISMA guidelines were followed during the conduct of this review¹².

MEDLINE and EMBASE were searched electronically on 15 February 2014, utilizing combinations of the relevant medical subject heading (MeSH) terms, keywords and word variants for 'posterior fossa', 'Dandy–Walker', 'Blake's pouch cyst', 'mega cisterna magna', 'vermian hypoplasia' or 'agenesis' and 'outcome' (Table S1). The search was then updated on 14 July 2014. The search and selection criteria were restricted to the English language. Reference lists of relevant articles and reviews were hand-searched for additional reports.

Study selection, data collection and data items

Studies were assessed according to the following criteria: population, outcome, gestational age at examination and type of imaging assessment of the posterior fossa.

Two authors (F.D., A.K.) reviewed all abstracts independently. Full-text copies of relevant papers were then obtained and relevant data regarding study characteristics and pregnancy outcome were extracted independently. Agreement regarding inclusion of studies and relevance of data was reached by consensus or by discussion with a third author (A.T.P.). If more than one study was published on the same patient cohort with identical endpoints, the report containing the most comprehensive information was included to avoid overlapping populations. For those articles in which information was not reported, but the methodology suggested that this information would have been recorded initially, the authors of the articles were contacted.

Quality assessment of the included studies was performed using the Newcastle–Ottawa Scale (NOS) for cohort studies. According to the NOS, each study was judged on three broad perspectives: selection of the study groups; comparability of the groups; and ascertainment of outcome of interest¹³. Assessment of the selection of a study includes evaluation of the representativeness of the exposed cohort, selection of the non-exposed cohort, ascertainment of exposure and demonstration that the outcome of interest was not present at the start of the study. Assessment of the comparability of the study includes evaluation of the comparability of cohorts on the basis of the design or analysis. Finally, ascertainment of the outcome of interest includes evaluation of the type of assessment of the outcome of interest, and the length and adequacy of follow-up. According to NOS, a study can be awarded a maximum of one star for each numbered item within the selection and outcome categories. A maximum of two stars can be given for comparability¹³.

Risk of bias, summary measures and synthesis of results

The posterior fossa anomalies considered in this systematic review were defined on the basis of the morphological approach proposed by Tortori-Donati *et al.*¹⁴ and were: (1) DWM was defined by the classic triad of complete or partial agenesis of the cerebellar vermis, cystic dilatation of the fourth ventricle and enlarged posterior fossa with upward displacement of the tentorium, torcula and

transverse sinuses; (2) MCM was defined as a cisterna magna measuring > 10 mm in the transverse cerebellar plane, and a normal cerebellar vermis; (3) BPC was defined by the presence of an upwardly displaced normal cerebellar vermis, normal-appearing fastigium, tentorium and size of the cisterna magna; (4) vermian hypoplasia (VH) was defined as a normally formed vermis but of smaller size, with the posterior fossa otherwise of normal size and anatomy.

Isolated abnormalities were defined as those posterior fossa abnormalities occurring with normal karyotype and no other associated major central nervous system (CNS) or extra-CNS anomalies detected either pre- or postnatally. In the case of DWM, ventriculomegaly was not included as an associated CNS anomaly because its development is related to dynamic changes in cerebrospinal fluid secondary to the mass effect of the cystic malformation¹⁴.

Abnormal neurodevelopmental outcome was defined as the overall presence of neurological, motor, cognitive, language or developmental deficits. A subanalysis considering the different types of neurodevelopmental abnormalities was performed whenever possible. Furthermore, the occurrence of ventriculomegaly, either before or after birth, and the need for any postnatal shunting procedure were assessed.

Only studies reporting a prenatal diagnosis of clearly defined isolated posterior fossa anomalies were considered suitable for inclusion in this systematic review. Only full-text articles were considered eligible for inclusion; case reports, conference abstracts and case series with fewer than three cases were excluded in order to avoid publication bias. In addition, we excluded from the analysis postnatal studies or studies from which cases diagnosed prenatally could not be extracted, cases of Dandy–Walker variant and those with a lack of a clear definition of the anomaly, and studies with non-isolated cases of posterior fossa anomalies. Studies published before the year 2000 were not included in the current systematic review for two related reasons: first, advances in prenatal imaging techniques are likely to have led to improvements in the diagnosis and characterization of CNS anomalies and therefore studies before this time are of little relevance to modern-day imaging; and second, older studies suffer from greater heterogeneity in definitions and nomenclature of the anomalies.

We used meta-analyses of proportions to combine data^{15,16}. Unfortunately, the low number of studies did not permit meaningful stratified meta-analyses to explore the test performance in subgroups of patients that may be less or more susceptible to bias. Furthermore, in view of the multitude of definitions, neurodevelopmental tests used and different ages at follow-up, we also decided to provide the rate of abnormal outcome for each study individually.

Assessment of the potential publication bias was also problematic, both because of the nature of the outcome (rates with the left side limited to the value zero), which limits the reliability of funnel plots, and because of the scarce number of individual studies, which strongly limits

the reliability of formal tests. Funnel plots displaying the outcome rate from individual studies *vs* their precision ($1/\text{standard error}$) were constructed with an exploratory aim. Tests for funnel-plot asymmetry were not used when the total number of publications included for each outcome was less than 10. In this case, the power of the tests is too low to distinguish chance from real asymmetry^{17,18}.

Between-study heterogeneity was explored using the I^2 statistic, which represents the percentage of between-study variation that is due to heterogeneity rather than chance. A value of 0% indicates no observed heterogeneity, whereas I^2 values of $\geq 50\%$ indicate a substantial level of heterogeneity. A fixed-effects model was used if substantial statistical heterogeneity was not present. In contrast, if there was evidence of significant heterogeneity between included studies, a random-effects model was used.

All proportion meta-analyses were carried out using StatsDirect 2.7.9 (StatsDirect Ltd, Altrincham, UK) and Meta-DiSc (Meta-DiSc Statistical Methods, 2006: [ftp://ftp.hrc.es/pub/programas/metadisc/Meta-DiSc StatisticalMethods.pdf](ftp://ftp.hrc.es/pub/programas/metadisc/Meta-DiSc%20StatisticalMethods.pdf)).

RESULTS

Study selection and characteristics

A total of 1640 articles were identified; 95 were assessed with respect to their eligibility for inclusion (Table S2) and a total of 16 studies were included in the systematic review (Figure 1 and Table 1). These 16 studies included 158 infants with isolated posterior fossa anomalies.

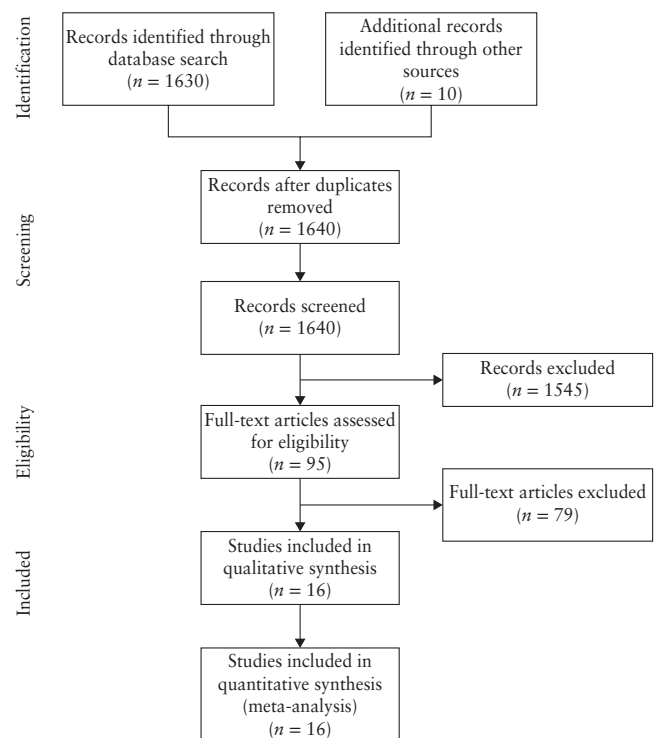


Figure 1 Flowchart summarizing selection of studies reporting on neurodevelopmental outcome of children with isolated posterior fossa anomalies diagnosed prenatally.

Table 1 General characteristics of 16 studies reporting on neurodevelopmental outcome of children with isolated posterior fossa malformations diagnosed prenatally

Study	Country	Study design	Prenatal imaging	Anomalies analyzed	Neurodevelopmental tool	Age at follow-up
Tarui (2014) ^{33*}	USA	Prosp.	MRI	VH	Wechsler Preschool and Primary Scale of Intelligence (3 rd or 4 th edn), Vineland Adaptive Behaviour Scale-II, Behavior Rating Inventory of Executive function, Child Behavior Checklist, Social Communication Questionnaire	Mean 6.1 years
Zhao (2013) ³¹	China	Prosp.	US, MRI	BPC	Basic neurological examination	1–3 years
Vatansever (2013) ²⁴	UK	Prosp.	MRI	MCM	Griffith Mental Developmental Scale (revised), Bayley Scales of Infant Development (3 rd edn)	1–2.1 years
Guibaud (2012) ^{19*}	France	Retro.	US, MRI	DWM	Clinical examination and early development scale	1.9–4 years
Gandolfi Colleoni (2012) ^{21*}	Italy	Retro.	US, MRI	DWM, BPC, MCM, VH	Basic neurological examination	1–5 years
Paladini (2012) ^{2*}	Italy	Retro.	US, MRI	BPC	Basic neurological examination	1 month to 3.5 years
Patek (2012) ^{28*}	USA	Retro.	US, MRI	MCM, VH	Parental assessment, healthcare assessment	2 months to 5.5 years
Bertucci (2011) ^{29*}	Italy/Israel	Prosp.	US, MRI	BPC, MCM, VH	Basic neurological examination	Mean 2 years
Ozkan (2011) ^{22*}	Turkey	Retro.	US	DWM	Basic neurological examination	NS
Dror (2009) ^{25*}	Israel	Prosp.	US, MRI	MCM	Gessell Developmental Schedules and Peabody Developmental Motor Scale	16–57 months
Forzano (2007) ^{30*}	UK	Retro.	US, MRI	MCM	Semi-structured questionnaire (psychomotor developmental milestones, seizures)	2 days to 3 months
Long (2006) ^{26*}	UK	Retro.	US	MCM	Basic neurological examination	4 years
Zalel (2006) ³²	Israel	Retro.	US, MRI	BPC	Basic neurological examination	1–7.5 years
Has (2004) ^{20*}	Turkey	Retro.	US, MRI	DWM	Basic neurological examination	3–5.5 years
Leitner (2004) ^{27*}	Israel	Retro.	US	MCM	Telephone interview, parental report	3 months to 3 years
Ecker (2000) ^{23*}	USA	Retro.	US	DWM	Basic neurological examination	6 weeks

Only first author of each study is given. *Additional information provided by the authors. BPC, Blake's pouch cyst; DWM, Dandy–Walker malformation; edn, edition; MCM, mega cisterna magna; MRI, magnetic resonance imaging; NS, not stated; Prosp., prospective; Retro., retrospective; US, ultrasound examination; VH, vermian hypoplasia.

Quality assessment of the included studies was performed using NOS for cohort studies (Table 2). All studies included a relatively small number of patients and had different periods of follow-up. Furthermore, most of the included studies did not use neurodevelopmental tests for the assessment of cognitive, affective and language anomalies and motor dysfunction. Finally, in view of the different imaging protocols used and types of postnatal confirmation of the anomaly, it is possible that infants with additional anomalies were included in the study population, thus affecting the overall values of abnormal neurodevelopmental outcome reported in this systematic review.

Synthesis of the results

Dandy–Walker malformation

Five studies including 13 infants with DWM, normal karyotype and no other associated CNS or extra-CNS anomalies were included in this systematic review. All studies except one¹⁹ used a basic neurological examination to assess the neurocognitive status of the patients. The overall rate of abnormal neurodevelopmental status

was 58.2% (95% CI, 21.8–90.0%) and varied from 0–100% (Table 3 and Figure 2a). A meta-analysis of the different neurodevelopmental abnormalities was possible only for the occurrence of abnormal motor outcome, which showed a 30.4% (95% CI, 8.1–59.3%) incidence of motor delay.

The study by Guibaud *et al.*¹⁹ included six fetuses with isolated DWM and normal standard karyotype. After excluding three fetuses with chromosomal microdeletions, detected using high-resolution cytogenetic analysis, and one further fetus with a false-positive diagnosis, the two remaining fetuses were included in the analysis. These two cases showed normal motor outcome but exhibited mild expressive language delay, although verbal reasoning was good, on postnatal assessment. Both infants developed hydrocephaly requiring a ventriculoperitoneal shunt to decompress the raised intracranial pressure¹⁹. Has *et al.*²⁰ included three cases with a prenatal diagnosis of isolated DWM, all of which showed severe delay in motor control, although specific tests to assess extensively the cerebellar function were not performed. Two of these three infants developed hydrocephaly after birth, requiring surgery²⁰. This finding highlights the common

Table 2 Quality assessment of the 16 included studies according to Newcastle–Ottawa Scale

Study	Selection	Comparability	Outcome
Tarui (2014) ³³	★★★★	★★	★★★★
Zhao (2013) ³¹	★★	★	★
Vatansever (2013) ²⁴	★★★	★	★★
Guibaud (2012) ¹⁹	★★★	★	★★★★
Gandolfi Colleoni (2012) ²¹	★★★	★	★★
Paladini (2012) ²	★★★	★	★★
Patek (2012) ²⁸	★★★	★	★★
Bertucci (2011) ²⁹	★★★	★	★
Ozkan (2011) ²²	★★	★	★
Dror (2009) ²⁵	★★★	★★	★★★★
Forzano (2007) ³⁰	★★	★	★★
Long (2006) ²⁶	★★★	★	★
Zalel (2006) ³²	★★★	★	★★
Has (2004) ²⁰	★★★	★	★★
Leitner (2003) ²⁷	★★	★	★
Ecker (2000) ²²	★★★	★	★

Only first author of each study is given. A study can be awarded a maximum of one star for each numbered item within the selection and outcome categories. A maximum of two stars can be given for comparability.

occurrence of hydrocephaly in cases of DWM. The development of hydrocephaly is probably related to dynamic changes in the cerebrospinal fluid, secondary to the mass effect of the cystic malformation¹⁹. In the study by Gandolfi Colleoni *et al.*²¹, two children were evaluated at 2 years of age, both showing severe motor impairment, while a third child had a postnatal diagnosis of Ritscher–Schinzel syndrome, presenting with mild language and psychomotor impairment. Finally, the studies by Ozkan *et al.*²² and Ecker *et al.*²³ had limited periods of follow-up and non-standardized assessment of the outcome measures (Table 4).

Overall, ventriculomegaly before or after birth occurred in 68.0% (95% CI, 32.3–94.5%) of fetuses with DWM despite no associated structural anomalies and normal karyotype. Ventriculomegaly requiring a ventriculoperitoneal shunt to reduce raised intracranial pressure occurred in 62.7% (95% CI, 27.9–91.3%) of the cases.

Mega cisterna magna

Eight studies including 81 infants with MCM were included in the systematic review. Only two studies

used specific tools to assess cerebellar function^{24,25}. The rate of abnormal neurodevelopmental outcome was 13.8% (95% CI, 7.3–21.9%) and ranged from 0–50% (Table 3 and Figure 2b). A meta-analysis of the different neurodevelopmental abnormalities was possible only for the occurrence of abnormal motor outcome, which showed an incidence of motor delay of 10.9% (95% CI, 4.6–19.5%).

In the largest of the studies, Dror *et al.*²⁵ included children with a prenatal diagnosis of isolated MCM with normal karyotype, evaluated by the Gesell Developmental Schedules and the Peabody Developmental Motor Scale. The age of postnatal follow-up ranged from 16 to 57 months. After excluding fetuses with additional anomalies, 17 patients were included in the analysis. Two children exhibited abnormal neurodevelopmental outcome, consisting of a generalized delay in all developmental aspects (Cases 1 and 2) and abnormal language and communication skills (Case 2) (Table 4). Children with a prenatal diagnosis of isolated MCM had significantly worse scores in their general developmental quotient, and in social interaction and visual–motor perception subtests; in contrast there was no difference in motor performance between children with a normal posterior fossa and those with MCM.

In the study by Vatansever *et al.*²⁴, the authors assessed the growth trajectories of the posterior fossa using semi-automatic segmentation of reconstructed fetal brain MRI. Six fetuses with isolated MCM were included in the study and the Griffith Mental Development Scale and Bailey Scales of Infant Development were used to ascertain the neurodevelopmental outcome of these children. Half of the included cases showed some degree of neurodevelopmental delay, including visuospatial perception and attention problems. Abnormal motor development was found in 1/13 infants in the study by Long *et al.*²⁶ and in 3/9 in that by Leitner *et al.*²⁷. Neither study used specific tests to assess cerebellar function, and in the study by Leitner *et al.*, the neurodevelopmental status was assessed by telephone interview conducted by pediatric neurologists²⁷. In the study by Gandolfi Colleoni *et al.*²¹, 16 cases with isolated MCM were analyzed and two children were found to have mild language disorder at around 3 years of age.

All other studies did not report any significant neurological anomaly in children with a prenatal diagnosis of isolated MCM, although no specific neurodevelopmental tool was used (Table 4)^{28–30}.

Overall, ventriculomegaly before or after birth occurred in 2.3% (95% CI, 0.1–12.3%) of cases of MCM

Table 3 Pooled proportions (PP) for occurrence of abnormal neurodevelopmental outcome in infants with prenatal diagnosis of posterior fossa anomaly

Anomaly	Studies (n)	Fetuses (n/N)	Raw (95% CI) (%)	I ² (%)	PP (95% CI) (%)
DWM	5	8/13	61.54 (31.6–86.1)	54.2	58.15 (21.8–90.0)
MCM	8	11/81	13.58 (7.0–23.0)	36.2	13.8 (7.3–21.9)
BPC	5	1/46	2.17 (0.1–11.5)	0.0	4.7 (0.7–12.1)
VH	4	3/18	16.67 (3.6–41.4)	77.7	30.7 (0.6–79.1)

BPC, Blake's pouch cyst; DWM, Dandy–Walker malformation; MCM, mega cisterna magna; VH, vermian hypoplasia.

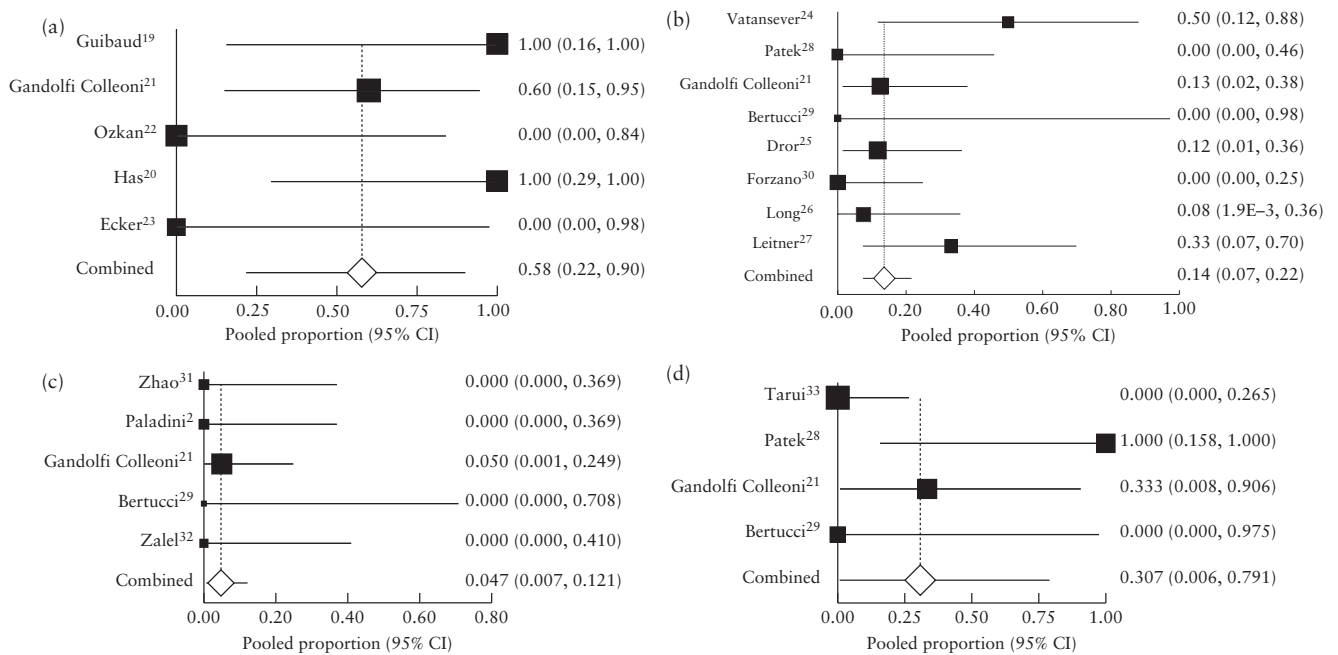


Figure 2 Pooled proportions of occurrence of abnormal overall neurodevelopmental outcome in infants with prenatal diagnosis of isolated posterior fossa malformations: (a) Dandy–Walker malformation; (b) mega cisterna magna; (c) Blake’s pouch cyst; (d) vermian hypoplasia. Only first author of each study is given.

with no associated structural anomalies and normal karyotype, but in no case included in this review was a ventriculoperitoneal shunt needed (pooled proportion (PP), 0% (95% CI, 0–8.2%)).

Blake’s pouch cyst

Five studies including 46 infants with a prenatal diagnosis of isolated BPC were included in this review. No study used a specific neurodevelopmental test to assess cerebellar function. The age of follow-up varied from 1 month to 10 years. There was no significant association between BPC and the occurrence of abnormal neurodevelopmental delay (PP, 4.7% (95% CI, 0.7–12.1%); range, 0–5%; Table 3 and Figure 2c). No fetus tested for motor control showed an abnormal outcome (PP, 0% (95% CI, 0–13.2%)).

In the study by Gandolfi Colleoni *et al.*²¹, the authors included 20 infants with a prenatal diagnosis of BPC, of which only one showed mild psychomotor disorder at 3 years. In the other included studies, no case of abnormal neurodevelopmental outcome was found^{2,29,31,32}, although no specific neurodevelopmental tool was used (Table 4).

The rate of ventriculomegaly occurring either before or after birth was 12.4% (95% CI, 2.9–27.1%) but it did not require shunting in any of the cases (PP, 0% (95% CI, 0–15.4%)).

Vermian hypoplasia

Four studies including 18 infants with a prenatal diagnosis of VH were included in this review. The duration of follow-up ranged from 6 months to 10 years.

There was high heterogeneity among the included studies, which reported a non-significant occurrence of abnormal neurodevelopmental delay among these children (PP, 30.7% (95% CI, 0.6–79.1%); range, 0–33%; Table 3 and Figure 2d). Of the included fetuses, none had abnormal motor outcome at assessment, performed at a variety of ages (PP, 0% (95% CI, 0–18.5%)).

In the largest series in this review, Tarui *et al.*³³ prospectively followed 20 children with a prenatal diagnosis of VH on MRI, with targeted neurodevelopmental tests including the assessment of cognitive, affective, language and behavioral measures at school age (Table 4). When considering only cases with isolated VH and a confirmed postnatal diagnosis, all 12 children had normal neurodevelopmental outcome.

No fetus with VH included in this review required a ventriculoperitoneal shunt (PP, 0% (95% CI, 0–24.7%)).

DISCUSSION

Summary of evidence

The findings of this systematic review show that children with a prenatal diagnosis of isolated DWM are at increased risk of abnormal neurodevelopmental outcome. Isolated MCM has a generally good outcome, although a small proportion of children may exhibit variable degrees of developmental delay. Isolated BPC is a benign condition and the rate of abnormal neurodevelopmental delay seems to be low. In view of the very small number of included studies, no clear evidence can be extracted for isolated VH.

Table 4 Summary of studies reporting on the rate of abnormal neurodevelopmental outcome in infants with prenatal diagnosis of isolated Dandy–Walker malformation ($n = 5$), mega cisterna magna ($n = 8$), Blake's pouch cyst ($n = 5$) or vermian hypoplasia ($n = 4$)

Study	Patients assessed (n)	Ab neurodev outcome (n (%))	Age at follow-up	Neurodevelopmental tool	Outcome in cases of abnormal development
<i>Dandy–Walker malformation</i>					
Guibaud (2012) ¹⁹	2	2 (100)	1.9–4 years	Clinical exam and early development scale	Case 1: Walking at 15 months; last visit at 32 months: two-word sentences, clumsy left-hand grip, upgaze impairment. Hydrocephaly at 1 month and ventriculoperitoneal shunting Case 2: Walking at 13 months; last visit at 4 years: good non-verbal reasoning (visuospatial IQ, 109; verbal IQ, 78), good receptive and weak expressive language (under speech therapy). Hydrocephaly at 4 months and ventriculoperitoneal shunting
Gandolfi Colleoni (2012) ^{21*}	5	3 (60)	2–10 years	Basic neurological exam	Case 1: Severe intellectual and motor impairment at 2 years (cerebral heterotopia diagnosed postnatally) Case 2: Severe neurological (mostly psychomotor) impairment at 2 years Case 3: Mild language and psychomotor impairment, postnatal diagnosis of Ritscher–Schinzel syndrome
Ozkan (2011) ^{22*}	2	—	NS	Basic neurological exam	Case 1: 3.5 years old with neuromotor impairment and abnormal electroencephalography findings, under anticonvulsive therapy Case 2: 3.0 years old with neuromotor impairment and cystoperitoneal shunt at 7 months, under anticonvulsive therapy Case 3: 5.5 years old with neuromotor impairment and cystoperitoneal shunt at 2 months
Has (2004) ^{20*}	3	3 (100)	3–5.5 years	Basic neurological exam	
Ecker (2000) ^{23*}	1	—	6 weeks	Basic neurological exam	
<i>Mega cisterna magna</i>					
Vatansever (2013) ²⁴	6	3 (50.0)	1–2.1 years	Griffith Mental Developmental Scale (revised), Bailey Scales of Infant Development (3 rd edn)	Visuospatial perception and attention problems
Gandolfi Colleoni (2012) ^{21*}	16	2 (12.5)	2–10 years	Basic neurological exam	Case 1: Mild language disorder at 2 years 10 months Case 2: Mild language and motor disorder at 3 years (facial dysmorphism, no specific genetic diagnosis)
Patek (2012) ^{28*}	6	—	1.4–3.3 years	Basic neurological exam and parental report	
Bertucci (2011) ^{29*}	1	—	6 months	Basic neurological exam	Case 1: (cisterna magna: 12 mm during pregnancy) 23 months of age; 4–5-month general delay in all developmental aspects Case 2: (cisterna magna: 14 mm during pregnancy) 22 months of age; all developmental milestones delayed. Achieved independent walking at 20 months. The most affected aspects of development were language and communication. Currently under evaluation for autistic spectrum disorder
Dror (2009) ^{25*}	17	2 (11.8)	16–57 months	Gessell Developmental Schedules and Peabody Developmental Motor Scale	
Forzano (2007) ^{30*}	13	—	2 days to 3 months	Basic neurological exam	Delayed motor development (poor feeding and delayed walking at 29 months)
Long (2006) ^{26*}	13	1 (7.7)	4 years	Basic neurological exam	
Leitner (2004) ²⁷	9	3 (33.3)	3 months to 3 years	Telephone interview	Case 1: Delayed motor development Case 2: Delayed motor development Case 3: Delayed motor development and language deficits

Table 4 Continued

Study	Patients assessed (n)	Ab neurodev outcome (n (%))	Age at follow-up	Neurodevelopmental tool	Outcome in cases of abnormal development
<i>Blake's pouch cyst</i>					
Zhao (2013) ³¹	8	—	1–3 years	Basic neurological exam	
Paladini (2012) ^{2*}	8	—	1 month to 3.5 years	Basic neurological exam	
Gandolfi Colleoni (2012) ^{21*}	20	1 (5)	2–10 years	Basic neurological exam	Mild psychomotor disorder at 3 years, normal intellectual and language function
Bertucci (2011) ^{29*}	3	—	6 months	Basic neurological exam	
Zalel (2006) ³²	7	—	1–7.5 years	Basic neurological exam	
<i>Vermian hypoplasia</i>					
Taruı (2014) ^{33*}	12	—	Mean 6.1 years	Wechsler Preschool and Primary Scale of Intelligence (3 rd or 4 th edn), Vineland Adaptive Behaviour Scale-II, Behavior Rating Inventory of Executive Function, Child Behavior Checklist, Social Communication Questionnaire	
Patek (2012) ^{28*}	2	2 (100)	2.2–5.5 years	Basic neurological exam and parental report	Case 1: Seizures and developmental delay based on parental report Case 2: Developmental delay based on parental report
Gandolfi Colleoni (2012) ^{21*}	3	1 (33.3)	2–10 years	Basic neurological exam	NS
Bertucci (2011) ^{29*}	1	—	6 months	Basic neurological exam	NS

Only first author of each study is given. *Additional information provided by the authors. Ab neurodev, abnormal neurodevelopmental; IQ, intelligence quotient; NS, not stated.

Limitations of the study

The small sample size of the included studies, high degree of variability in the definition of the different posterior fossa anomalies and differences in age at follow-up represent the major limitations of this review. A basic neurological examination, as carried out in most of the published studies, may not be sufficient to determine the neurodevelopmental status of these children and more accurate tests investigating cognitive, affective and behavioral functions are needed in order to ascertain the actual rate of abnormal development. Furthermore, cases labeled as isolated may have had subtle undiagnosed associated chromosomal or structural anomalies³⁴. Postnatal confirmation of posterior fossa anomalies can also be challenging, with high rates of false-positive diagnoses reported in the literature⁵. The lack of a standardized protocol for postnatal assessment in most of the included studies did not enable a precise estimation of the exact number of diagnoses confirmed after birth. Moreover, confirmation of the diagnosis using postnatal imaging was not performed in some of the included cases. It is therefore plausible that limitations in study design, sample size, data extraction and outcomes observed might bias the findings of the current review.

Implications for clinical practice

Prenatal counseling when a fetus is diagnosed with a posterior fossa anomaly is challenging. Correctly defining posterior fossa anomalies is the first step in an optimal diagnostic approach^{35,36}; multiplanar assessment of the posterior fossa using axial, sagittal and coronal planes is necessary in order to define precisely these conditions, especially because anomalies with a similar appearance in the axial plane may have different appearances in other planes, and may be associated with different outcomes.

The factors already outlined, such as length of follow-up, neurodevelopmental tool adopted, age at assessment, presence of additional anomalies and choice of an appropriate control group are all relevant. The term ‘neurodevelopmental outcome’ can also be misleading and inappropriate when considering brain anomalies because it encompasses a wide spectrum of signs with different underlying disorders and pathological processes, which are not always easily measured and which represent a continuous interaction between pathological, environmental and adaptive factors.

The study by Klein *et al.*³ highlights the need for new research aimed at finding reliable prognostic imaging markers; the authors reviewed retrospectively the charts of 26 patients with a diagnosis of DWM. They found that no patient in the group with normal vermian morphology had associated brain malformations and the majority had normal outcome, while all those with a dysplastic vermian had associated brain anomalies and abnormal outcome. As all patients in the second group had associated brain anomalies, it was not possible to assess whether the presence of the normal vermian anatomy was associated independently with a better outcome³.

The feasibility of detailed evaluation of vermian anatomy during prenatal life and its independent role in predicting neurodevelopmental outcome have yet to be established¹⁹.

Isolated MCM is a relatively common finding. The rate of chromosomal abnormalities and additional CNS and extra-CNS structural anomalies that are not detected on ultrasound is low³⁷. In the current review, most of the included studies reported a normal or borderline neurodevelopmental outcome in the majority of children with isolated MCM. The pathophysiology of isolated MCM has not been elucidated completely yet and it is not clear whether expansion of the posterior fossa by fluid is a pathological development or represents a normal variant. Dror *et al.*²⁵ suggested that children with isolated MCM had lower developmental, visual motor and social performance than did controls. However, all the mean values for the neurodevelopmental measures observed were within normal range, suggesting a generally favorable outcome.

Failure of fenestration of the posterior membranous area leads to the persistence of Blake's pouch³⁸. On imaging, BPC is characterized by the presence of an upward displacement of a normal cerebellar vermis, normal fastigium, tentorium and size of the cisterna magna. Tetraventricular hydrocephaly is an associated finding commonly reported postnatally. Although none of the included studies used specific tools to assess cerebellar function, the findings of this review suggest a generally favorable outcome.

Data on the prognosis of children with isolated VH in this review are debatable. In view of the very small number of cases included, no robust evidence can be confidently extrapolated. The results from this meta-analysis are surprising and disagree with what is observed after birth, where VH, even if isolated, has been reported to be associated with developmental delay. We might speculate that the main bias is due to the definition of VH before birth – many cases labeled as hypoplasia during the prenatal period may actually correspond to a normal vermis, theoretically explaining the reason behind the favorable outcome reported in this meta-analysis. In the collective authors' experience, prenatal diagnosis of VH is affected by high rates of false-positive cases, with most of the cases found to be BPC at birth⁵.

Implications for research

The wide heterogeneity in diagnostic criteria, nomenclature and outcome definitions highlights the urgent need for prospective studies that standardize objectively the classification and prognosis of these anomalies. Future research should aim at describing objectively the different posterior fossa anomalies and correlating them with robust long-term neurodevelopmental measures.

Conclusions

Isolated DWM is associated with an increased risk of abnormal neurodevelopmental outcome, while isolated

MCM and BPC have a generally favorable outcome. In view of the very small number of patients tested and lack of an objective prenatal definition, the risk of abnormal developmental delay in cases with isolated VH needs to be further assessed. Future large prospective studies with standardized and objective protocols for diagnosis and follow-up are needed in order to ascertain the rate of abnormal neurodevelopmental outcome in children with isolated posterior fossa anomalies.

ACKNOWLEDGMENTS

We thank Prof. L. Guibaud, Prof. D. Paladini, Prof. Y. Zalel, Prof. T. Tarui, Prof. B. Benacerraf, Prof. R. Palma-Dias, Prof. R. Has, Dr E. Bertucci, Dr K. Reidy, Dr R. Ghali, Dr J. Garcia-Flores, Dr A. Borrell, Dr Y. Leitner, Dr G. Tonni, Dr A. Long, Dr K. Patek, Dr C. Spaeth, Dr M. Scheier, Dr R. Lachmann, Dr J.L. Ecker, Dr N. Kölblle, Dr T. Harper, Dr P.H. Tang, Dr Z. Ozkan and Dr R. Russo for their contribution to this systematic review in terms of support and additional data supplied.

REFERENCES

- Bolduc ME, Limperopoulos C. Neurodevelopmental outcomes in children with cerebellar malformations: a systematic review. *Dev Med Child Neurol* 2009; 51: 256–267.
- Paladini D, Quarantelli M, Pastore G, Sorrentino M, Sglavo G, Nappi C. Abnormal or delayed development of the posterior membranous area of the CNS: anatomy, ultrasound diagnosis, natural history and outcome of Blake's pouch cyst in the fetus. *Ultrasound Obstet Gynecol* 2012; 39: 279–287.
- Klein O, Pierre-Kahn A, Boddaert N, Parisot D, Brunelle F. Dandy–Walker malformation: prenatal diagnosis and prognosis. *Childs Nerv Syst* 2003; 19: 484–489.
- Guibaud L, Larroque A, Ville D, Sanlaville D, Till M, Gaucherand P, Pracros JP, des Portes V. Prenatal diagnosis of 'isolated' Dandy–Walker malformation: imaging findings and prenatal counselling. *Prenat Diagn* 2012; 32: 185–193.
- Limperopoulos C, Robertson RL Jr, Khwaja OS, Robson CD, Estroff JA, Barnewolt C, Levine D, Morash D, Nemes L, Zaccagnini L, du Plessis AJ. How accurately does current fetal imaging identify posterior fossa anomalies? *AJR Am J Roentgenol* 2008; 190: 1637–1643.
- Carroll SG, Porter H, Abdel-Fattah S, Kyle PM, Soothill PW. Correlation of prenatal ultrasound diagnosis and pathologic findings in fetal CNS abnormalities. *Ultrasound Obstet Gynecol* 2000; 16: 149–153.
- Robinson AJ. Inferior vermian hypoplasia – preconception, misconception. *Ultrasound Obstet Gynecol* 2014; 43: 123–136.
- Marlow N. Measuring neurodevelopmental outcome in neonatal trials: a continuing and increasing challenge. *Arch Dis Child Fetal Neonatal Ed* 2013; 98: F554–F558.
- Henderson LK, Craig JC, Willis NS, Tovey D, Webster AC. How to write a Cochrane systematic review. *Nephrology (Carlton)* 2010; 15: 617–624.
- NHS Centre for Reviews and Dissemination. *Systematic Reviews: CRD's Guidance for Undertaking Reviews in Healthcare*. University of York: York, UK, 2009.
- Leeflang MM, Deeks JJ, Gatsonis C, Bossuyt PM. Cochrane Diagnostic Test Accuracy Working Group. Systematic reviews of diagnostic test accuracy. *Ann Intern Med* 2008; 149: 889–897.
- PRISMA statement. <http://www.prisma-statement.org/>
- Wells GA, Shea B, O'Connell D, Peterson J, Welch V, Losos M, Tugwell P. [Newcastle–Ottawa Scale for assessing the quality of nonrandomised studies in meta-analyses.] http://www.ohri.ca/programs/clinical_epidemiology/oxford.asp
- Tortori-Donati P, Rossi A, Biancheri R. Brain malformations. In *Pediatric Neuroradiology*, Tortori-Donati P (ed). Springer: New York, 2005; 71–198.
- Manzoli L, De Vito C, Salanti G, D'Addario M, Villari P, Ioannidis JP. Meta-analysis of the immunogenicity and tolerability of pandemic influenza A 2009 (H1N1) vaccines. *PLoS One* 2011; 6: e24384.
- Hunter JP, Saratzis A, Sutton AJ, Boucher RH, Sayers RD, Bown MJ. In meta-analyses of proportion studies, funnel plots were found to be an inaccurate method of assessing publication bias. *J Clin Epidemiol* 2014; 67: 897–903.
- Egger M, Davey Smith G, Schneider M, Minder C. Bias in meta-analysis detected by a simple, graphical test. *BMJ* 1997; 315: 629–634.
- Higgins JPT, Green S (eds). *Cochrane Handbook for Systematic Reviews of Interventions Version 5.0.2* [updated September 2009]. *The Cochrane Collaboration*, 2009. Available from www.cochrane-handbook.org
- Guibaud L, Larroque A, Ville D, Sanlaville D, Till M, Gaucherand P, Pracros JP, des Portes V. Prenatal diagnosis of 'isolated' Dandy–Walker malformation: imaging findings and prenatal counselling. *Prenat Diagn* 2012; 32: 185–193.

20. Has R, Ermiş H, Yüksel A, Ibrahimoglu L, Yildirim A, Sezer HD, Başaran S. Dandy-Walker malformation: a review of 78 cases diagnosed by prenatal sonography. *Fetal Diagn Ther* 2004; **19**: 342–347.
21. Gandolfi Colleoni G, Contro E, Carletti A, Ghi T, Campobasso G, Rembouskos G, Volpe G, Pilu G, Volpe P. Prenatal diagnosis and outcome of fetal posterior fossa fluid collections. *Ultrasound Obstet Gynecol* 2012; **39**: 625–631.
22. Ozkan ZS, Gilgin H, Aygün HB, Deveci D, Simşek M, Kumru S, Yüce H. Our clinical experience about prenatal diagnosis and neonatal outcomes of fetal central nervous system anomalies. *J Matern Fetal Neonatal Med* 2011; **24**: 502–505.
23. Ecker JL, Shipp TD, Bromley B, Benacerraf B. The sonographic diagnosis of Dandy-Walker and Dandy-Walker variant: associated findings and outcomes. *Prenat Diagn* 2000; **20**: 328–332.
24. Vatanserver D, Kyriakopoulou V, Allsop JM, Fox M, Chew A, Hajnal JV, Rutherford MA. Multidimensional analysis of fetal posterior fossa in health and disease. *Cerebellum* 2013; **12**: 632–644.
25. Dror R, Malinger G, Ben-Sira L, Lev D, Pick CG, Lerman-Sagie T. Developmental outcome of children with enlargement of the cisterna magna identified in utero. *J Child Neurol* 2009; **24**: 1486–1492.
26. Long A, Moran P, Robson S. Outcome of fetal cerebral posterior fossa anomalies. *Prenat Diagn* 2006; **26**: 707–710.
27. Leitner Y, Goetz H, Gull I, Mesterman R, Weiner E, Jaffa A, Harel S. Antenatal diagnosis of central nervous system anomalies: can we predict prognosis? *J Child Neurol* 2004; **19**: 435–438.
28. Patek KJ, Kline-Fath BM, Hopkin RJ, Pilipenko VV, Crombleholme TM, Spaeth CG. Posterior fossa anomalies diagnosed with fetal MRI: associated anomalies and neurodevelopmental outcomes. *Prenat Diagn* 2012; **32**: 75–82.
29. Bertucci E, Gindes L, Mazza V, Re C, Lerner-Geva L, Achiron R. Vermian biometric parameters in the normal and abnormal fetal posterior fossa: three-dimensional sonographic study. *J Ultrasound Med* 2011; **30**: 1403–1410.
30. Forzano F, Mansour S, Ierullo A, Homfray T, Thilaganathan B. Posterior fossa malformation in fetuses: a report of 56 further cases and a review of the literature. *Prenat Diagn* 2007; **27**: 495–501.
31. Zhao D, Liu W, Cai A, Li J, Chen L, Wang B. Quantitative evaluation of the fetal cerebellar vermis using the median view on three-dimensional ultrasound. *Prenat Diagn* 2013; **33**: 153–157.
32. Zalel Y, Gilboa Y, Gabis L, Ben-Sira L, Hoffman C, Wiener Y, Achiron R. Rotation of the vermis as a cause of enlarged cisterna magna on prenatal imaging. *Ultrasound Obstet Gynecol* 2006; **27**: 490–493.
33. Tarui T, Limperopoulos C, Sullivan NR, Robertson RL, du Plessis AJ. Long-term developmental outcome of children with a fetal diagnosis of isolated inferior vermian hypoplasia. *Arch Dis Child Fetal Neonatal Ed* 2014; **99**: F54–F58.
34. Shaffer LG, Rosenfeld JA, Dabell MP, Coppinger J, Bandholz AM, Ellison JW, Ravnan JB, Torchia BS, Ballif BC, Fisher AJ. Detection rates of clinically significant genomic alterations by microarray analysis for specific anomalies detected by ultrasound. *Prenat Diagn* 2012; **32**: 986–995.
35. Guibaud L, des Portes V. Plea for an anatomical approach to abnormalities of the posterior fossa in prenatal diagnosis. *Ultrasound Obstet Gynecol* 2006; **27**: 477–481.
36. Garel C. Posterior fossa malformations: main features and limits in prenatal diagnosis. *Pediatr Radiol* 2010; **40**: 1038–1045.
37. D'Antonio F, Khalil A, Garel C, Pilu G, Rizzo G, Lerman-Sagie T, Bhide A, Thilaganathan B, Manzoli L, Papageorgiou AT. Systematic review and meta-analysis of isolated posterior fossa malformations on prenatal ultrasound imaging (part 1): nomenclature, diagnostic accuracy and associated anomalies. *Ultrasound Obstet Gynecol* 2016; **47**: 690–697.
38. Shekdar K. Posterior fossa malformations. *Semin Ultrasound CT MR* 2011; **32**: 228–241.

SUPPORTING INFORMATION ON THE INTERNET

The following supporting information may be found in the online version of this article:



Table S1 Search strategy – PRISMA 2009 checklist

Table S2 Excluded studies and reason for exclusion



RESUMEN

Objetivos El diagnóstico de anomalías aisladas de la fosa posterior en niños/as está sesgado por el hecho de que sólo se notifica al personal clínico apropiado cuando presentan síntomas, y la tasa reportada se ve a menudo afectada por la adopción de nomenclatura diferente, los criterios de diagnóstico, las medidas del resultado, la duración del seguimiento y las herramientas de desarrollo neurológico. El objetivo de esta revisión sistemática fue explorar el resultado del desarrollo neurológico de los fetos con diagnóstico prenatal de anomalías aisladas de la fosa posterior.

Métodos Se hicieron búsquedas electrónicas en MEDLINE y EMBASE, utilizando combinaciones de los términos médicos más relevantes para ‘fosa posterior’ y ‘resultado’. Se consideraron adecuados los estudios que evaluaron el resultado del desarrollo neurológico en niños/as con un diagnóstico prenatal de malformaciones aisladas de la fosa posterior. Entre las anomalías de la fosa posterior analizadas están el síndrome de Dandy-Walker (SDW), la megacisterna magna (MCM), el quiste de la Bolsa de Blake (BPC, por sus siglas en inglés) y la hipoplasia vermiana (VH, por sus siglas en inglés). Todos los resúmenes fueron revisados de forma independiente por dos de los autores. La evaluación de calidad de los estudios incluidos se realizó mediante la escala Newcastle-Ottawa para estudios de cohortes. Se utilizaron metaanálisis de proporciones para la combinación de datos, y la heterogeneidad entre estudios se examinó mediante el estadístico I^2 .

Resultados Se identificaron un total de 1640 artículos, de los cuales se evaluó la elegibilidad de 95 y se incluyó un total de 16 estudios en la revisión sistemática. La tasa global de resultado de desarrollo neurológico anormal en niños/as con un diagnóstico prenatal de SDW fue del 58,2% (IC del 95%, 21,8–90,0%), con un rango de 0–100%. En niños/as con un diagnóstico prenatal de MCM, la tasa de resultado de desarrollo neurológico anormal fue del 13,8% (IC del 95%, 7,3–21,9%), con un rango de 0–50%. No se encontró una asociación significativa entre el BPC y la presencia de retraso de desarrollo neurológico anormal, con una tasa del 4,7% (IC del 95%, 0,7–12,1%) y un rango de 0–5%. Se encontró un resultado no significativo de casos con retraso del desarrollo neurológico anormal en niños/as con un diagnóstico prenatal de VH, con una tasa del 30,7% (IC del 95%, 0,6–79,1%) y un rango de 0–100%. Aunque afectado por el escaso número de estudios

Conclusiones Los fetos diagnosticados con SWD aislado poseen un alto riesgo de resultado de desarrollo neurológico anormal, mientras que el MCM o BPC aislados tienen, en general, un resultado favorable. El riesgo de retraso en el desarrollo anormal en casos con VH aislada debe estudiarse más todavía. En vista de la gran heterogeneidad en el diseño de los estudios, el tiempo de seguimiento, las pruebas de desarrollo neurológico empleadas y el pequeño número de casos incluidos, será necesario realizar en el futuro estudios prospectivos más amplios con protocolos objetivos y estandarizados para el diagnóstico y el seguimiento, con el fin de determinar la tasa de resultados de desarrollo neurológico anormal en niños/as con anomalías aisladas de la fosa posterior.

Objetivo: Debido a que sólo los niños con síntomas atraerían la atención de los médicos clínicos, la tasa reportada de diagnóstico de anomalías aisladas de la fosa posterior en niños/as está sesgado. Además, la tasa reportada puede verse afectada por la adopción de nomenclatura diferente, los criterios de diagnóstico, las medidas del resultado, la duración del seguimiento y las herramientas de desarrollo neurológico. El objetivo de esta revisión sistemática fue explorar el resultado del desarrollo neurológico de los fetos con diagnóstico prenatal de anomalías aisladas de la fosa posterior.

Métodos: Se realizaron búsquedas electrónicas en MEDLINE y EMBASE, utilizando combinaciones de los términos médicos más relevantes para ‘fosa posterior’ y ‘resultado’. Se consideraron adecuados los estudios que evaluaron el resultado del desarrollo neurológico en niños/as con un diagnóstico prenatal de malformaciones aisladas de la fosa posterior. Entre las anomalías de la fosa posterior analizadas están el síndrome de Dandy-Walker (SDW), la megacisterna magna (MCM), el quiste de la Bolsa de Blake (BPC, por sus siglas en inglés) y la hipoplasia vermiana (VH, por sus siglas en inglés). Todos los resúmenes fueron revisados de forma independiente por dos de los autores. La evaluación de calidad de los estudios incluidos se realizó mediante la escala Newcastle-Ottawa para estudios de cohortes. Se utilizaron metaanálisis de proporciones para la combinación de datos, y la heterogeneidad entre estudios se examinó mediante el estadístico I^2 .

Resultados: Se identificaron un total de 1640 artículos, de los cuales se evaluó la elegibilidad de 95 y se incluyó un total de 16 estudios en la revisión sistemática. La tasa global de resultado de desarrollo neurológico anormal en niños/as con un diagnóstico prenatal de SDW fue del 58,2% (IC del 95%, 21,8–90,0%), con un rango de 0–100%. En niños/as con un diagnóstico prenatal de MCM, la tasa de resultado de desarrollo neurológico anormal fue del 13,8% (IC del 95%, 7,3–21,9%), con un rango de 0–50%. No se encontró una asociación significativa entre el BPC y la presencia de retraso de desarrollo neurológico anormal, con una tasa del 4,7% (IC del 95%, 0,7–12,1%) y un rango de 0–5%. Se encontró un resultado no significativo de casos con retraso del desarrollo neurológico anormal en niños/as con un diagnóstico prenatal de VH, con una tasa del 30,7% (IC del 95%, 0,6–79,1%) y un rango de 0–100%. Aunque afectado por el escaso número de estudios

Conclusiones: Los fetos diagnosticados con SWD aislado poseen un alto riesgo de resultado de desarrollo neurológico anormal, mientras que el MCM o BPC aislados tienen, en general, un resultado favorable. El riesgo de retraso en el desarrollo anormal en casos con VH aislada debe estudiarse más todavía. En vista de la gran heterogeneidad en el diseño de los estudios, el tiempo de seguimiento, las pruebas de desarrollo neurológico empleadas y el pequeño número de casos incluidos, será necesario realizar en el futuro estudios prospectivos más amplios con protocolos objetivos y estandarizados para el diagnóstico y el seguimiento, con el fin de determinar la tasa de resultados de desarrollo neurológico anormal en niños/as con anomalías aisladas de la fosa posterior.

Appearance of fetal posterior fossa at 11–14 weeks in fetuses with Dandy–Walker malformation or chromosomal anomalies

P. VOLPE*, E. CONTRO†, T. FANELLI*, B. MUTO*, G. PILU† and M. GENTILE‡

*Fetal Medicine Unit, Di Venere and Sarcone Hospitals, ASL BA, Bari, Italy; †Department of Obstetrics and Gynecology, University of Bologna, Bologna, Italy; ‡Medical Genetics Unit, Di Venere Hospital, ASL BA, Bari, Italy

KEYWORDS: chromosomal anomalies; Dandy–Walker complex; first trimester; intracranial translucency; prenatal diagnosis; posterior fossa; ultrasound

ABSTRACT

Objective To describe the sonographic appearance of fetal posterior fossa anatomy at 11–14 weeks of pregnancy and to assess the outcome of fetuses with increased intracranial translucency (IT) and/or brainstem-to-occipital bone (BSOB) diameter.

Methods Reference ranges for brainstem (BS), IT and cisterna magna (CM) measurements, BSOB diameter and the BS:BSOB ratio were obtained from the first-trimester ultrasound examination of 233 fetuses with normal postnatal outcome (control group). The intraobserver and interobserver variability of measurements were investigated using 73 stored ultrasound images. In addition, a study group of 17 fetuses with increased IT and/or BSOB diameter was selected to assess outcome.

Results No significant intraobserver or interobserver variability was found for any measurement in the control group. In the study group, IT was increased in all cases and BSOB diameter was above the 95th centile of the calculated normal range in all but two (88%) cases. In 13/17 study cases, only two of the three posterior brain spaces were recognized on ultrasound. These 13 fetuses had a larger BSOB diameter than did the four cases that showed all three posterior brain spaces, and had severe associated anomalies including Dandy–Walker malformation (DWM) and/or chromosomal anomalies.

Conclusions Visualization of the fetal posterior fossa anatomy at 11–14 weeks' gestation is feasible. Increased fluid in the posterior brain at 11–14 weeks, particularly in the case of non-visibility of the septation that divides the future fourth ventricle from the CM, is an important risk factor for cystic posterior fossa malformations,

in particular DWM, and/or chromosomal aberrations. Copyright © 2015 ISUOG. Published by John Wiley & Sons Ltd.

INTRODUCTION

The role of the first-trimester ultrasound examination has expanded from screening for aneuploidy to diagnosing fetal malformations^{1–4}. At 11–14 weeks of gestation, it is possible to visualize and measure three spaces in the posterior brain: the brainstem (BS), the fourth ventricle or intracranial translucency (IT) and the cisterna magna (CM). Such anatomical spaces are assessed routinely by ultrasound in the mid-sagittal view of the fetal face as part of the nuchal translucency (NT) scan at 11–14 weeks. Irregularities of the posterior brain spaces, including their measurements, have been proposed as markers of posterior fossa anomalies^{5–7}. The correlation between a decreased amount of fluid in the posterior brain and open spina bifida is well established^{6–12}. More recently, it has been suggested that increased fluid may indicate the presence of cystic posterior fossa anomalies such as Dandy–Walker malformation (DWM) and Blake's pouch cyst (BPC)^{13–18}. The aim of our study was to describe the outcome of fetuses with increased fluid in the posterior brain at 11–14 weeks.

PATIENTS AND METHODS

We conducted a case–control study in two referral centers for prenatal diagnosis including patients at low risk and patients referred because of an increased risk of chromosomal and/or anatomical defects. The control group included 233 fetuses with a normal ultrasound

Correspondence to: Dr P. Volpe, Fetal Medicine Unit, Di Venere Hospital, Ospedale Di Venere 1, 70100, Bari, Italy (email: paolo-volpe@libero.it)

Accepted: 16 April 2015

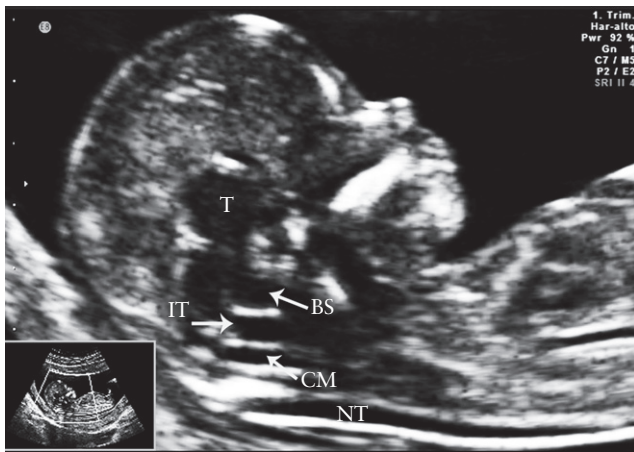


Figure 1 Mid-sagittal ultrasound image of fetal face and brain at 12 weeks' gestation, showing the three posterior brain spaces: brainstem (BS), intracranial translucency (IT) and cisterna magna (CM). The nuchal translucency (NT) and the thalamus (T) are also visible.

examination and the study group included 17 fetuses with an increased size of the fourth ventricle and/or increased brainstem-to-occipital bone (BSOB) diameter.

In each fetus, images of the mid-sagittal view of the face and brain at 11–14 weeks of gestation were obtained, following the recommendations of The Fetal Medicine Foundation (FMF). Three-dimensional volumes were also obtained and stored. In all cases, the crown–rump length (CRL) and NT were measured and the nasal bone, ductus venosus and tricuspid-valve flow were assessed. A detailed examination of the fetal anatomy for detection of major defects was performed. Maternal biochemistry (free β -human chorionic gonadotropin and pregnancy-associated plasma protein-A) was recorded when available and the estimated risk of aneuploidy was calculated using the FMF software.

All ultrasound examinations were performed trans-abdominally using a Voluson 730 Expert and E8 (GE Medical Systems, Zipf, Austria) with RAB 4–8-MHz and RM6C matrix 1–7-MHz sector probes. If the image quality was poor, an additional transvaginal ultrasound examination was performed.

Stored images were examined by two operators with extensive experience in first-trimester scanning who were unaware of the pregnancy outcomes. The operators examined the posterior brain in the mid-sagittal view by visualizing and measuring three spaces between the sphenoid and occipital bone: the BS, a hypochoic area between the posterior border of the sphenoid bone and the anterior border of the fourth ventricle; the fourth ventricle or IT, an anechoic area between the posterior border of the BS and the choroid plexus of the fourth ventricle; and the CM, another fluid-filled space between the choroid plexus of the fourth ventricle and the anterior border of the occipital bone (Figure 1). The BSOB was defined as the vertical distance between the anterior border of the fourth ventricle, anteriorly, and the occipital bone, posteriorly, representing the fourth ventricle–CM

Table 1 Intraobserver variability for brainstem (BS) diameter, brainstem-to-occipital bone (BSOB) diameter, BS : BSOB ratio, cisterna magna (CM) and intracranial translucency (IT) measurements in normal fetuses at 11–14 weeks' gestation

Measurement	Bias*	Limits of agreement	P
BS diameter (mm)	0.2	−1.01 to 1.41	0.299
BSOB diameter (mm)	−0.23	−2.46 to 2.00	0.222
BS : BSOB ratio	0.02	−0.23 to 0.26	0.245
CM width (mm)	−0.3	−1.89 to 1.29	0.1
IT (mm)	−0.03	−1.71 to 1.64	0.66

*Mean difference between paired measurements.

Table 2 Interobserver variability for brainstem (BS) diameter, brainstem-to-occipital bone (BSOB) diameter, BS : BSOB ratio, cisterna magna (CM) and intracranial translucency (IT) measurements in normal fetuses at 11–14 weeks' gestation

Measurement	Bias*	Limits of agreement	P
BS diameter (mm)	0.1	−1.1 to 1.31	0.75
BSOB diameter (mm)	−0.2	−2.40 to 2.00	0.84
BS : BSOB ratio	0.01	−0.22 to 0.25	0.79
CM width (mm)	−0.35	−1.9 to 1.20	0.86
IT (mm)	−0.05	−1.63 to 1.73	0.95

*Mean difference between paired measurements.

complex¹³. Caliper placement was performed as described previously^{7,13}.

Reference measurements for BS, IT and CM, BSOB diameter and the BS : BSOB ratio were obtained from the control group of normal fetuses. The agreement and bias of measurements by a single operator, who made two repeat measurements from the same image, and by two different operators, who produced measurements from the same image independently, were investigated using 73 ultrasound images selected randomly from the database.

To assess the outcome of the study group of fetuses with fourth-ventricle dilatation and/or an increased BSOB diameter, we first conducted a retrospective study over a period of 3 years (2009–2011) by searching the Viewpoint database (ViewPoint 5.6.8.428, ViewPoint Bildverarbeitung GmbH, Weßling, Germany) of our referral centers. Thereafter we ran a prospective evaluation from January 2013 to November 2014 that was approved by the ethics committee of our hospital. Detailed information on pregnancy outcome was obtained by medical records and interviews with the parents and their physicians.

Statistical analysis

Reference ranges according to fetal CRL for BS diameter, BSOB diameter, BS : BSOB ratio, CM and IT were obtained by regression analysis. Delta values for each parameter were calculated in relation to fetal CRL. The distribution of values was normal for all parameters in the control group, as demonstrated by a Kolmogorov–Smirnov test. An independent sample *t*-test was used to determine the significance of differences

Table 3 Outcome in 17 fetuses with posterior fossa (PF) anomaly suspected at 11–14-week ultrasound examination (US)

Case	PF spaces (n)	CRL (mm)	BSOB diameter (mm)	Associated anomalies at 11–14 weeks	High risk of aneuploidy	Karyotype	Findings at mid-trimester US	Outcome
1	2	49.8	6.2	AVSD	Yes	Trisomy 18		TOP at 14 weeks
2	2	64.3	6.1	HLHS	No	46, XY, der(5)t(5;8)(p15.33;q24.3)pat		TOP at 14 weeks
3	2	46.0	6.1	None	No	Unknown	DWM, ACC	TOP at 20 weeks
4	2	59.7	6.1	Severe cerebral ventriculomegaly	No	46, X, dup(Y) (q11.21.23)		TOP at 14 weeks
5	2	64.0	6.3	None	Yes	Trisomy 9 mosaicism	BPC, IUGR	TOP at 19 weeks
6	2	50.5	6.5	Univentricular heart, huge hygroma	Yes	46, XX		TOP at 13 weeks
7	2	54.0	6.2	None	Yes	46, XX	DWM, preauricular tags	TOP at 20 weeks
8	2	50.0	6.2	Vascular ring, micrognathia	Yes	Triploidy		TOP at 13 weeks
9	2	60.5	6.2	None	Yes	Trisomy 18		TOP at 14 weeks
10	2	55.4	6.3	None	No	Unknown	Isolated DWM	Alive
11	2	50.0	6.2	Exomphalos, BCLP	Yes	Trisomy 13		TOP at 13 weeks
12	2	68.8	6.2	None	No	Mos 92, XYYY [36]/46, XY[9]	DWM, CoA	TOP at 20 weeks
13	2	58.0	6.2	None	No	46, XY, del(5)t(5;6)(p13;q15)mat		TOP at 14 weeks
14	3	60.0	5.3	None	No	Unknown		Alive and well
15	3	52.0	5.0	None	No	Unknown		Alive and well
16	3	60.0	5.3	None	No	46, XX	BPC, interhemispheric cyst, unilateral hydronephrosis	Alive
17	3	68.0	5.0	None	No	Unknown		Alive and well

ACC, agenesis of corpus callosum; AVSD, atrioventricular septal defect; BCLP, bilateral cleft lip and palate; BPC, Blake pouch's cyst; BSOB, brainstem-to-occipital bone; CoA, aortic coarctation; CRL, crown–rump length; DWM, Dandy–Walker malformation; HLHS, hypoplastic left heart syndrome; IUGR, intrauterine growth restriction; TOP, termination of pregnancy.

in delta values for all parameters between controls and cases. Bland–Altman analysis was used to assess the intraobserver and interobserver variability for BS diameter, BSOB diameter, BS:BSOB ratio, CM and IT in the control group. Kruskal–Wallis test was used to compare the significance of the difference between the two measurements. A P -value < 0.05 was considered statistically significant. All data were analyzed with statistical software package SPSS 15.0 (SPSS, Chicago, IL, USA).

RESULTS

The median CRL at the time of the ultrasound examination was 63 (range, 45–80) mm in controls and 58 (range, 46–69) mm in the study group. Fourteen (5.6%) cases required an additional transvaginal ultrasound examination.

In the control group there was a significant increase in BS diameter ($1.6263 + 0.02101 \times \text{CRL}$ in mm; SD, 0.36; $R^2 = 0.09832$), BSOB diameter ($1.6603 + 0.04277 \times \text{CRL}$ in mm; SD, 0.5913; $R^2 = 0.1438$), CM width ($0.9883 + 0.02172 \times \text{CRL}$ in mm; SD, 0.4284; $R^2 = 0.07628$) and IT measurement ($0.6681 + 0.02092 \times \text{CRL}$ in mm; SD, 0.3759; $R^2 = 0.09051$) with increasing CRL. The ratio of BS diameter:BSOB diameter decreased with increasing

CRL ($0.81837 - 0.003757 \times \text{CRL}$ in mm; SD, 0.08517; $R^2 = 0.05881$).

The bias (mean difference) and 95% limits of agreement between paired measurements of BS and BSOB diameters, and CM and IT by the same operator and by two different operators are reported in Tables 1 and 2, respectively. Intraobserver and interobserver variability was not significant for any measurement.

In the study group (Table 3), IT was increased in all cases and BSOB diameter was above the 95th centile of the calculated normal range in all but two cases (88%; $P < 0.0001$) (Figures 2 and 3). In the remaining two cases, BSOB diameter was at the upper limit of the normal range. The mean BS:BSOB ratio was significantly lower ($P = 0.012$) than the calculated normal range in 11 (65%) cases (Figure 4). There was no significant difference in BS diameter of the two groups ($P = 0.83$), although the study-group values were in the lower segment of the reference interval.

In 13 of the study cases (Cases 1–13, Table 3), only two out of three posterior brain spaces were recognized because the border between the fourth ventricle and the CM was not visualized (Figure 5). These fetuses had larger BSOB measurements than did the remaining four cases (Cases 14–17) in which three posterior brain spaces were seen, and all had severe associated anomalies.

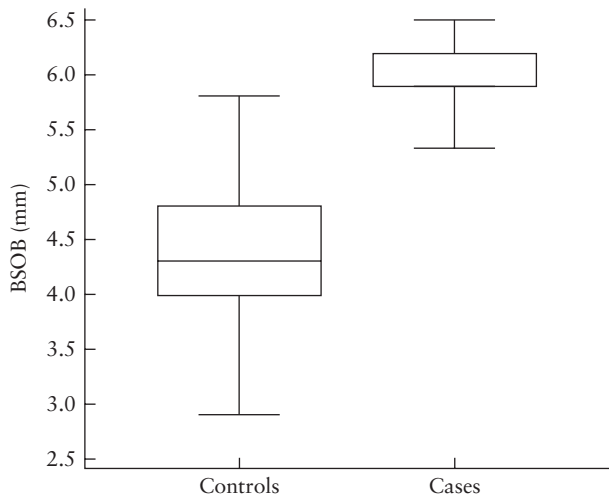


Figure 2 Brainstem-to-occipital bone (BSOB) diameter in study group of 17 fetuses with increased intracranial translucency and/or increased BSOB diameter and in 233 normal fetuses. Boxes represent median and interquartile range, and whiskers are 5th and 95th centiles.

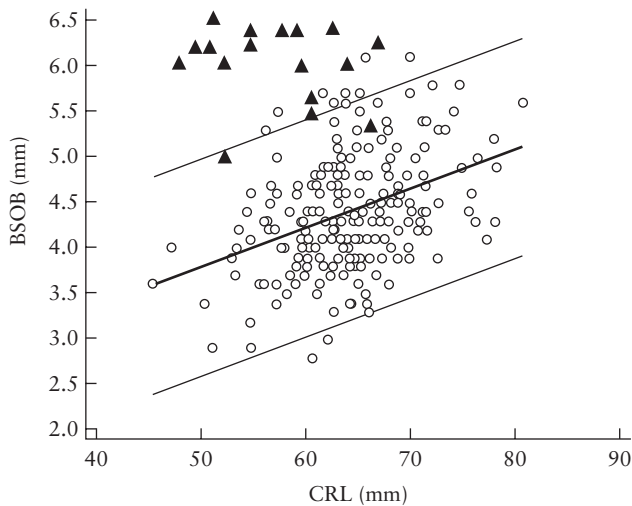


Figure 3 Measurements of brainstem-to-occipital bone (BSOB) diameter in 17 fetuses with increased intracranial translucency and/or BSOB diameter (▲) and in normal controls (○), according to crown–rump length (CRL) and plotted on the median, 5th and 95th centiles of the control group.

Chromosomal anomalies were found in nine cases, and in six cases malformations were diagnosed by ultrasound at 11–14 weeks' gestation. DWM was present in four cases (Figure 6), either alone or in combination with other abnormalities, including chromosomal aberrations and structural malformations. One fetus with mosaicism of chromosome 9 identified from chorionic villi was found to have a BPC and early severe growth restriction at 19 weeks. Overall, 12 couples requested termination of pregnancy. This was performed within the 14th week of gestation in eight cases, and it was not possible to obtain reliable postmortem conclusions at this early gestational age. In the remaining four cases that were terminated at a later gestational age, autopsy always confirmed the antenatal diagnosis. One pregnancy with a fetus affected

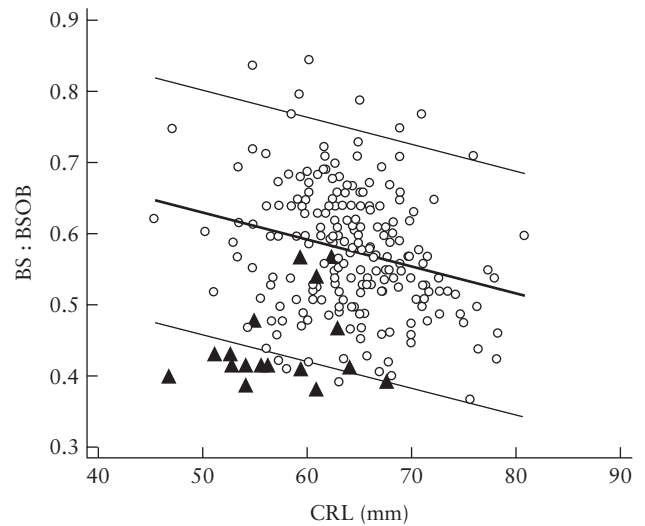


Figure 4 Measurements of brainstem (BS) to brainstem-to-occipital bone diameter (BS:BSOB) ratio in 17 fetuses with increased intracranial translucency and/or increased BSOB diameter (▲) and in normal controls (○), according to crown–rump length (CRL) and plotted on the median, 5th and 95th centiles of the control group.

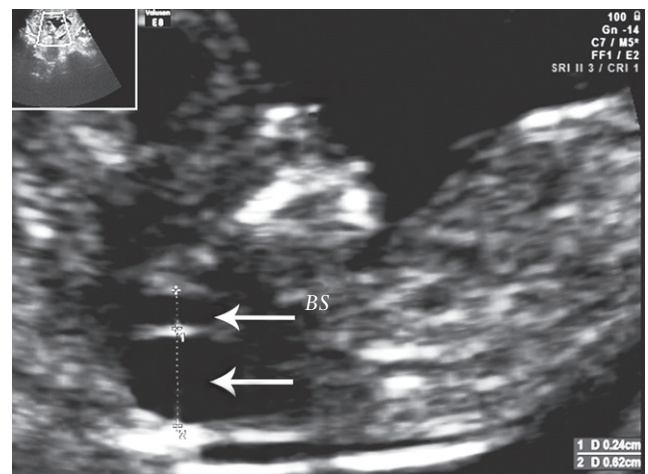


Figure 5 Mid-sagittal ultrasound image of fetal brain at 13 weeks' gestation in a case with trisomy 18 and a posterior fossa cyst (Case 9), showing only two posterior brain spaces because the border between the fourth ventricle and the cisterna magna is not visible. Measurements of brainstem (BS) diameter and brainstem-to-occipital bone diameter (lower arrow) are seen.

by isolated DWM continued to term. The infant was alive and well at the time of writing, but neurological outcome is uncertain because of the very short follow-up (4 months old).

In the four fetuses (Cases 14–17, Table 3) in which three brain spaces could be seen (Figure 7), IT was increased in all four and BSOB diameter increased in two. Only one fetus (Case 16) underwent karyotyping, with a normal result. This fetus was found at a later stage of gestation to have a BPC, an interhemispheric cyst (Figure 8) and unilateral hydronephrosis but was alive and in good condition at the time of writing, although at a rather brief follow-up (2 years old). Karyotype was not obtained

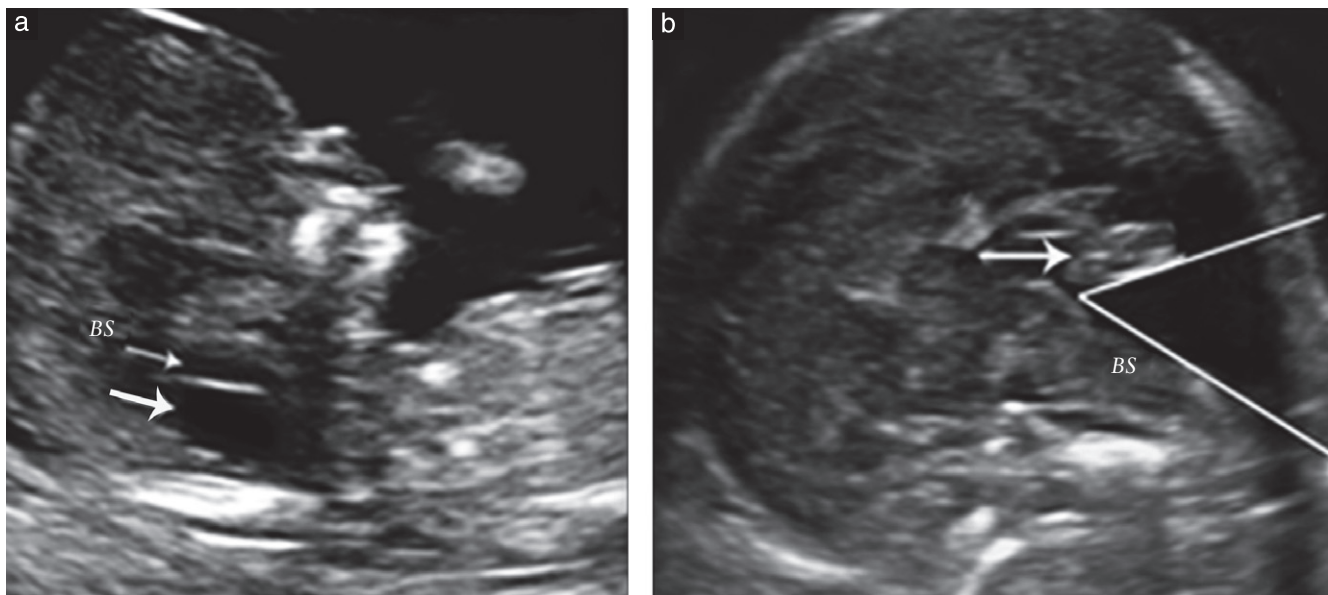


Figure 6 Mid-sagittal ultrasound images of fetal brain in a case of Dandy–Walker malformation (Case 10) at: (a) 12 weeks' gestation, visualizing only two posterior brain spaces and an enlarged brainstem (BS)-to-occipital bone diameter (lower arrow) and (b) 20 weeks' gestation, showing significant rotation of a small cerebellar vermis (BS to vermis (arrow) angle of 53°) and an enlarged posterior fossa.



Figure 7 Mid-sagittal ultrasound image of fetal brain (Case 15) at 12 weeks' gestation, showing the three posterior brain spaces: brainstem (BS), cisterna magna (CM) and intracranial translucency (IT, calipers). At 3.3 mm, IT is enlarged (>95th centile).

in the remaining three cases, but mid-trimester scans were negative for anomalies and normal infants were delivered at term.

DISCUSSION

Our results indicate that visualization and measurement of the posterior brain at 11–14 weeks' gestation using the same mid-sagittal view commonly employed for measurement of NT is feasible. This is in line with findings published previously^{6–9}. In all our cases, the examination was performed successfully, with a need for an additional transvaginal scan in only a few cases. In normal fetuses, three spaces are usually recognized, which include (from

anterior to posterior) the BS, developing fourth ventricle and CM, divided by an echogenic line that presumably represents the choroid plexus of the fourth ventricle. We obtained values of the size of these structures in a group of normal fetuses, which were consistent with those reported previously, and demonstrated that the measurements are reproducible.

It has been reported that, in fetuses with open spina bifida compared with normal fetuses, BS diameter is higher, BSOB diameter is lower and BS:BSOB ratio is substantially higher^{8–10}. Analysis of our study group indicates that, unlike in open spina bifida, a large BSOB diameter and a decreased BS:BSOB ratio, particularly in combination with the presence of only two brain spaces, is an important risk factor for either cystic posterior fossa malformations, most frequently DWM, or chromosomal aberrations. We were not able to obtain reliable postmortem conclusions in fetuses with chromosomal aberrations terminated in early gestation, but we cannot exclude that these would also have later developed a posterior fossa malformation. A minority of fetuses in the study group had three recognizable brain spaces. None of these fetuses had chromosomal aberrations, and only one was later found to have a cerebral anomaly, which was less severe than the ones described in the subgroup with only two brain spaces visualized.

Therefore, we suggest that, although the sonographic demonstration of an enlargement of the fluid spaces of the posterior fossa at 11–14 weeks' gestation does not necessarily indicate the presence of a fetal anomaly, it represents a major risk factor for cerebral malformations and a variety of chromosomal anomalies, not just aneuploidies. The risk is particularly high when the echogenic line normally dividing the future fourth

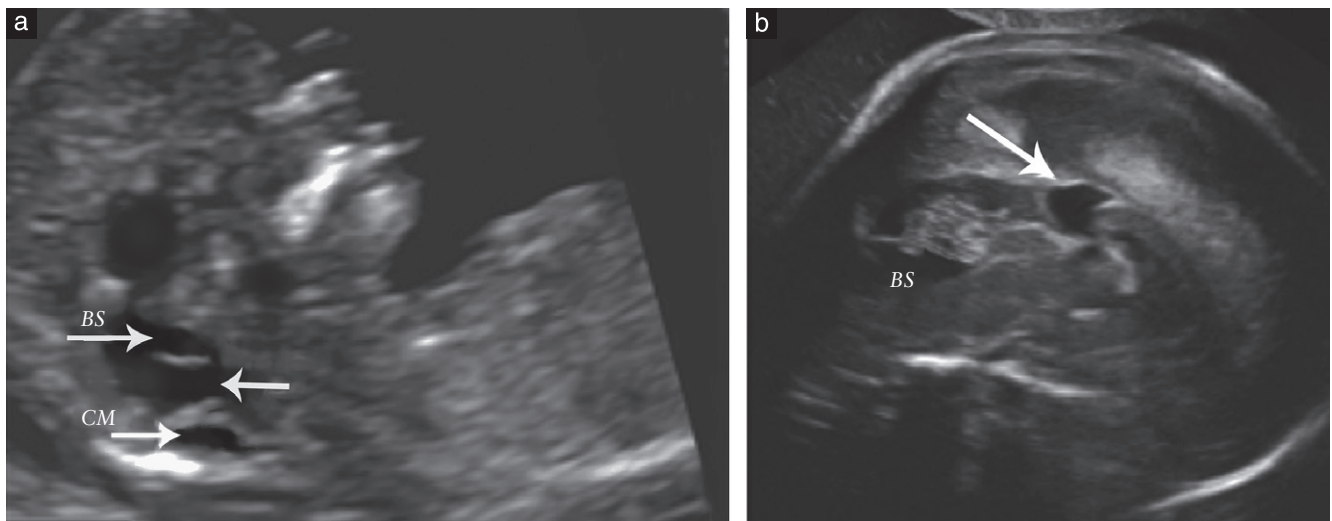


Figure 8 Mid-sagittal ultrasound image of fetal brain in a case with Blake's pouch cyst (Case 16) at: (a) 12 weeks' gestation, showing three posterior brain spaces (brainstem (BS), cisterna magna (CM) and intracranial translucency (IT)), with an enlarged IT diameter (middle arrow) and (b) 21 weeks' gestation, showing slight rotation of a normal vermis and a normal-sized posterior fossa. The arrow indicates a small interhemispheric cyst.

ventricle and CM is not seen, and only two brain spaces are visible. The combination of this finding with an increased BSOB diameter results in clearly discernible cystic dilatation of the posterior fossa that is quite obvious even in the mid-sagittal view. Conversely, the risk seems to be low when three brain spaces are seen, although the number of these cases in our study was small.

The major strengths of our study include the large number of abnormal cases, the availability of detailed follow-up information and the strong correlation between easily recognizable sonographic findings and an abnormal outcome. The main limitation is that several cases were referred from other centers and this did not allow us to assess sensitivity. However, during the period of this study we saw one case of BPC and one case of megacisterna magna but no case of DWM in fetuses that had a normal posterior fossa appearance at 11–14 weeks. Therefore, we believe that the possibility of identifying the most severe clinical presentation may be high although a normal early ultrasound scan does not exclude a cystic posterior fossa anomaly.

In conclusion, visualization of the fetal posterior fossa anatomy at 11–14 weeks is feasible. Our study confirms preliminary reports and indicates that an increased amount of fluid in the posterior brain at 11–14 weeks, particularly in the case of non-visibility of the septation dividing the future fourth ventricle from the CM, is an important risk factor for cystic posterior fossa malformations, in particular DWM, and/or chromosomal aberrations.

REFERENCES

- Grande M, Arigita M, Borobio V, Jimenez JM, Fernandez S, Borrell A. First-trimester detection of structural abnormalities and the role of aneuploidy markers. *Ultrasound Obstet Gynecol* 2012; 39: 157–163.
- Nicolaides KH. Screening for fetal aneuploidies at 11 to 13 weeks. *Prenat Diagn* 2011; 31: 7–15.
- Syngelaki A, Chelmen T, Dagklis T, Allan L, Nicolaides KH. Challenges in the diagnosis of fetal non-chromosomal abnormalities at 11–13 weeks. *Prenat Diagn* 2011; 31: 90–102.
- Volpe P, Ubaldo P, Volpe N, Campobasso G, De Robertis V, Tempesta A, Volpe G, Rembouskos G. Fetal cardiac evaluation at 11–14 weeks by experienced obstetricians in a low-risk population. *Prenat Diagn* 2011; 31: 1054–1061.
- Ferreira A, Syngelaki A, Smolin A, Vayna A, Nicolaides K. Posterior brain in fetuses with trisomy 18, trisomy 13 and triploidy at 11 to 13 weeks gestation. *Prenat Diagn* 2012; 32: 1–5.
- Chaoui R, Nicolaides KH. From nuchal translucency to intracranial translucency: towards the early detection of spina bifida. *Ultrasound Obstet Gynecol* 2010; 35: 133–138.
- Chaoui R, Benoit B, Mitkowska-Wozniak H, Heling KS, Nicolaides KH. Assessment of intracranial translucency (IT) in the detection of spina bifida at the 11–13-week scan. *Ultrasound Obstet Gynecol* 2009; 34: 249–252.
- Chaoui R, Benoit B, Heling KS, Kagan KO, Pietzsch V, Sarut Lopez A, Tekesin I, Karl K. Prospective detection of open spina bifida at 11–13 weeks by assessing intracranial translucency and posterior brain. *Ultrasound Obstet Gynecol* 2011; 38: 722–726.
- Lachmann R, Chaoui R, Moratalla J, Picciarelli G, Nicolaides KH. Posterior brain in fetuses with open spina bifida at 11 to 13 weeks. *Prenat Diagn* 2011; 31: 103–106.
- Scheier M, Lachmann R, Ľtroš M, Nicolaides KH. Three dimensional sonography of the posterior fossa in fetuses with open spina bifida at 11–13 weeks' gestation. *Ultrasound Obstet Gynecol* 2011; 38: 625–629.
- Egle D, Strobl I, Weiskopf-Schwendinger V, Grubinger E, Kraxner F, Mutz-Dehbalie IS, Straszak A, Scheier M. Appearance of the fetal posterior fossa at 11 + 3 to 13 + 6 gestational weeks on transabdominal ultrasound examination. *Ultrasound Obstet Gynecol* 2011; 38: 620–624.
- McLone DG, Dias MS. The Chiari II malformation: cause and impact. *Childs Nerv Syst* 2003; 19: 540–550.
- Lachmann R, Sinkovskaya E, Abuhamad A. Posterior brain in fetuses with Dandy-Walker malformation with complete agenesis of the cerebellar vermis at 11–13 weeks: a pilot study. *Prenat Diagn* 2012; 32: 765–769.
- Lee MY, Won HS, Hyunetal MK. One case of increased intracranial translucency during the first trimester associated with the Dandy-Walker variant. *Prenat Diagn* 2012; 32: 602–603.
- Lafouge A, Gorincour G, Desbriere R, Quarello E. Prenatal diagnosis of Blake's pouch cyst following first-trimester observation of enlarged intracranial translucency. *Ultrasound Obstet Gynecol* 2012; 40: 479–480.
- Garcia-Posada R, Eixarch E, Sanz M, Puerto B, Figueras F, Borrell A. Cisterna magna width at 11–13 weeks in the detection of posterior fossa anomalies. *Ultrasound Obstet Gynecol* 2013; 41: 515–520.
- Gandolfi Colleoni G, Contro E, Carletti A, Ghi T, Campobasso G, Rembouskos G, Volpe G, Pilu G, Volpe P. Prenatal diagnosis and outcome of fetal posterior fossa fluid collections. *Ultrasound Obstet Gynecol* 2012; 39: 625–631.
- Volpe P, Contro E, De Musso F, Ghi T, Farina A, Tempesta A, Volpe G, Rizzo N, Pilu G. Brainstem–vermis and brainstem–tentorium angles allow accurate categorization of fetal upward rotation of cerebellar vermis. *Ultrasound Obstet Gynecol* 2012; 39: 632–635.

Thick corpus callosum in the second trimester can be transient and is of uncertain significance

S. SHINAR*†, J. HAR-TOOV†, T. LERMAN-SAGIE†‡ and G. MALINGER*†

*Fetal Neurology Clinic, Ob-Gyn Ultrasound Unit, Lis Maternity Hospital, Tel Aviv, Israel; †Sackler School of Medicine, Tel Aviv University, Tel Aviv, Israel; ‡Pediatric Neurology Unit and Fetal Neurology Clinic, Wolfson Medical Center, Holon, Israel

KEYWORDS: corpus callosum; fetal anomalies; fetal MRI; prenatal diagnosis; second-trimester ultrasound

ABSTRACT

Objectives Depiction of a thick corpus callosum (CC) in utero is rare, and is generally associated with severe brain anomalies. Our aim was to describe a group of fetuses diagnosed during second-trimester ultrasound examination as having an apparently isolated thick CC, which normalized subsequently in the cases followed to term.

Methods Among 59 fetuses referred to the Ob-Gyn Ultrasound Division of Lis Maternity Hospital with suspected callosal anomalies between January 2013 and June 2014, we identified nine cases with an apparently isolated thick CC for inclusion in this retrospective cohort study. Length and body thickness of the CC were compared with previously published nomograms. Fetuses with a suspected isolated thick CC were identified and followed until delivery or termination of pregnancy (TOP). Evaluation consisted of chromosomal analysis, at least one magnetic resonance imaging (MRI) examination and repeat ultrasound examinations. Postnatal evaluation included brain ultrasound examination, MRI when indicated and neurodevelopmental assessment through validated pediatric questionnaires.

Results The nine fetuses were diagnosed with an apparently isolated thick CC at a mean gestational age of $23 + 5$ (range, 21–29) weeks. Eight exhibited a CC body thickness $\geq 2SD$ above the mean for gestational age and one exhibited only a thickened genu. Six also exhibited a relatively short CC. Two patients opted for TOP but declined autopsy. In five of the seven remaining fetuses, the CC thickness normalized during follow-up. In the remaining two, the increased CC thickness was a variant of the cingulate sulcus. The CC length remained $\leq 2SD$ in five of the six fetuses with a short CC. Fetal MRI was performed and confirmed the diagnosis in six fetuses. The karyotype was normal in all fetuses. Short-term neurodevelopmental outcome was reported as normal in all six children with complete follow-up.

Conclusions Although the number of fetuses in our study is relatively small, it seems that an apparently isolated thick CC is not necessarily associated with poor prognosis. In such cases, a definitive diagnosis should not be reached based on a single measurement and repeat follow-up examinations during the third trimester are recommended. Copyright © 2015 ISUOG. Published by John Wiley & Sons Ltd.

INTRODUCTION

The corpus callosum (CC) is the largest commissure connecting the cerebral hemispheres. By 18–20 weeks of gestation it has assumed its final shape and, usually, all its components can be visualized by ultrasound. From this time and until delivery, its length and thickness continue to increase linearly. After delivery, while the rate decreases, it continues to grow until the end of adolescence.

Increased availability and rapid improvement of imaging techniques have provided the opportunity to study *in-vivo* CC development as depicted by ultrasound^{1–3} and magnetic resonance imaging (MRI)⁴. Coinciding with the acquisition of knowledge regarding its normal development, there has been a sharp increase in the number of anomalies of the CC diagnosed *in utero*^{5,6}. There are increasing reports of complete and partial agenesis^{7,8}, as well as of callosal pathologies that are rare or have not yet been described *in utero*^{9–12}.

In 2009, we reported a series of fetuses with a thick CC. Most had associated central nervous system pathologies¹⁰. Seven of eight were diagnosed as syndromic. Only the child with an isolated thick CC and normal head circumference was developing normally at the time of writing. Here, we describe a group of fetuses whose second-trimester routine ultrasound evaluation showed an isolated thick CC, which normalized subsequently in all cases followed to term.

Correspondence to: Prof. G. Malinge, Tel-Aviv Sourasky Medical Center, Lis Maternity Hospital, Division of Ob-Gyn Ultrasound, 6 Weizmann Street, Tel Aviv 64239, Israel (e-mail: gmalinger@gmail.com)

Accepted: 13 August 2015

SUBJECTS AND METHODS

In this retrospective cohort study we retrieved from the database of the Fetal Neurology Clinic of Lis Maternity Hospital records for all fetuses with a suspected anomaly of the CC referred between January 2013 and June 2014. Those suspected of having an isolated thick CC were identified and included in this study. The study was approved by the Institutional Review Board.

The length of the CC and the thickness of the genu, body and splenium were measured by ultrasound in the mid-sagittal plane using either transabdominal or transvaginal probes, depending on fetal presentation, as described previously¹. Measurements were plotted on the nomograms published by Achiron and Achiron². The CC was regarded as thick if any of its parts deviated by $\geq 2SD$ (above 95th centile) from the reference values in the nomograms.

All of the fetuses were evaluated for chromosomal anomalies and most cases were referred for MRI during the third trimester in order to confirm the findings and to exclude other anomalies. Fetuses with a clear diagnosis of pericallosal lipoma were excluded. At least one but usually more than two follow-up examinations were performed in all cases.

Postnatal brain ultrasound examinations were performed in all cases and postnatal MRI was performed when indicated. The parents were contacted at the end of the study period to obtain a postnatal developmental evaluation, through validated standard questionnaires for infant development, in use in Israel.

RESULTS

During the study period, 59 fetuses referred with suspected callosal anomalies were examined in our center. In nine cases we identified an apparently isolated thick CC, at a mean gestational age of 23 + 5 (range, 21 + 1 to 29 + 0) weeks. Reasons for referral were: suspected callosal dysgenesis ($n=5$), an echogenic CC ($n=1$), suspected agenesis of the CC ($n=1$), deviation of the pericallosal arteries ($n=1$) and asymmetrical ventricles ($n=1$). All fetuses were appropriate in size for gestational age and there was no history of maternal disease or pregnancy complications. The growth patterns of the thickness of the body of the CC and the CC length are presented in Tables 1 and 2, respectively, and in Figure 1.

At the initial examination, eight fetuses had CC body-thickness measurements $\geq 2SD$ above the mean for

Table 1 Corpus callosal (CC) body-thickness measurements during prenatal follow-up in nine cases with an apparently isolated thick CC

	CC body thickness (mm) at:								
	20–21 weeks	22–23 weeks	24–25 weeks	26–27 weeks	28–29 weeks	30–31 weeks	32–33 weeks	34–35 weeks	36–37 weeks
5 th centile*	1.3	1.8	1.9	1.9	1.7	2.0	2.0	2.2	2.2
95 th centile*	1.9	2.2	2.3	2.3	2.2	2.8	3.4	3.3	2.55
Case 1	—	—	3.4	2.3	—	—	2.2	2.7	2.7
Case 2	2.2	2.7	—	1.8	—	1.9	—	2.3	—
Case 3	—	—	—	—	1.8	1.5	—	1.6	1.5
Case 4	—	—	—	—	2.3	1.6	—	—	—
Case 5	—	—	—	—	2.2	1.7	1.5	1.6	—
Case 6	—	2.8	—	2.8	—	—	—	2.2	—
Case 7	2.6	—	2.7	3.2	—	2.0	—	3.0	—
Case 8	2.6	—	—	—	—	—	—	—	—
Case 9	—	4.2	—	—	—	—	—	—	—

*Of normal range according to Achiron and Achiron².

Table 2 Corpus callosal (CC) length measurements during prenatal follow-up in nine cases with an apparently isolated thick CC

	CC length (mm) at:								
	20–21 weeks	22–23 weeks	24–25 weeks	26–27 weeks	28–29 weeks	30–31 weeks	32–33 weeks	34–35 weeks	36–37 weeks
5 th centile*	18.1	21.5	26.3	29.9	32.3	37.1	38.4	41.4	40.0
95 th centile*	21.2	25.7	30.6	35.9	38.6	38.4	45.6	50.4	46.8
Case 1	—	—	25.9	30.0	—	—	33.7	36.0	39.8
Case 2	20.0	28.8	—	35.0	—	41.0	—	42.0	—
Case 3	—	—	—	—	31.0	35.0	—	31.1	43.0
Case 4	—	—	—	—	30.0	30.0	—	—	—
Case 5	—	—	—	—	35.6	35.0	37.0	39.0	—
Case 6	—	17.7	—	27.0	—	—	—	36.0	—
Case 7	21.0	—	28.0	29.7	—	35.0	—	38.0	—
Case 8	23.0	—	—	—	—	—	—	—	—
Case 9	—	23.4	—	—	—	—	—	—	—

*Of normal range according to Achiron and Achiron².

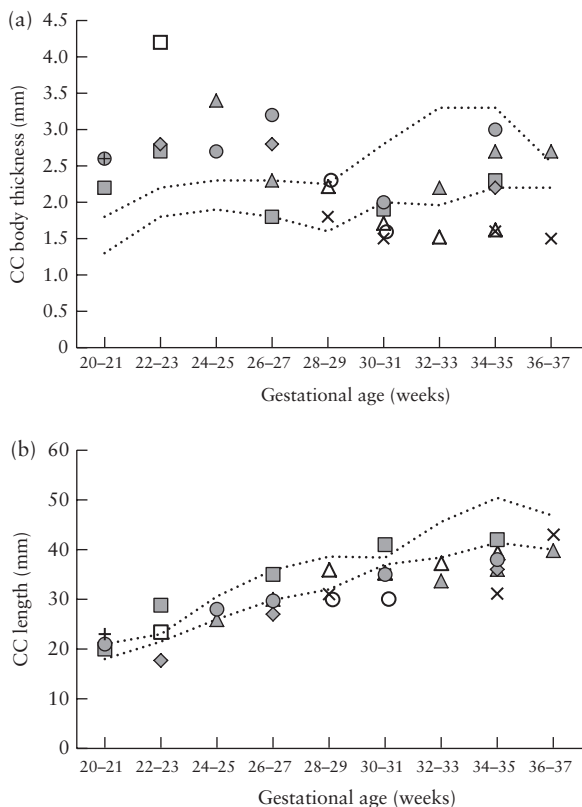


Figure 1 Corpus callosum (CC) body-thickness (a) and length (b) measurements during prenatal follow-up, plotted against reference values (.....) according to Achiron and Achiron². In Cases 8 and 9 the parents opted for termination of pregnancy during the second trimester after a single abnormal measurement. (a) In five fetuses (Cases 1, 2 and 4–6), measurements of CC body thickness were abnormal (≥ 2 SD above the norm) initially, but normalized during the third trimester; in Case 3 the only thickened part was the genu. (b) In five fetuses (Cases 1 and 4–7) the CC length was short towards the end of pregnancy, at ≥ 2 SD below the norm; in Case 2 the length was never short; in Case 3 it was short at diagnosis, but normalized by 36 weeks. Case 1, Δ ; Case 2, \square ; Case 3, \times ; Case 4, \circ ; Case 5, Δ ; Case 6, \diamond ; Case 7, \bullet ; Case 8, $+$; Case 9, \square .

their gestational age (Figure 2). Three fetuses had a thick genu; in one of them this was the only thickened part of the CC (Figure 3). The splenium was considered normal in all fetuses but in two its thickness was > 1 SD above the mean. When depicted in the coronal plane the CC was found to be thicker on one side compared with the other in three cases (Figure 3).

Six fetuses also exhibited a short CC, deviating > 2 SD below the norm, at the time of diagnosis or during follow-up examinations. Hyperechogenicity of the CC, as compared with the cingulate gyrus, was noted in all fetuses. In two of them the echogenic part was actually a cingulate gyrus variant adjacent to the anterior part of the CC (Figure 3). In one fetus the cavum septi pellucidi contained a smaller-than-expected amount of fluid, making visualization and measurements of the CC difficult. Irregularities of the lower border of the CC were present in two fetuses (Figure 4).

Associated findings included an abnormally twisted course of the pericallosal arteries ($n=2$), asymmetrical ventricles with maximum width of the atrium of the larger

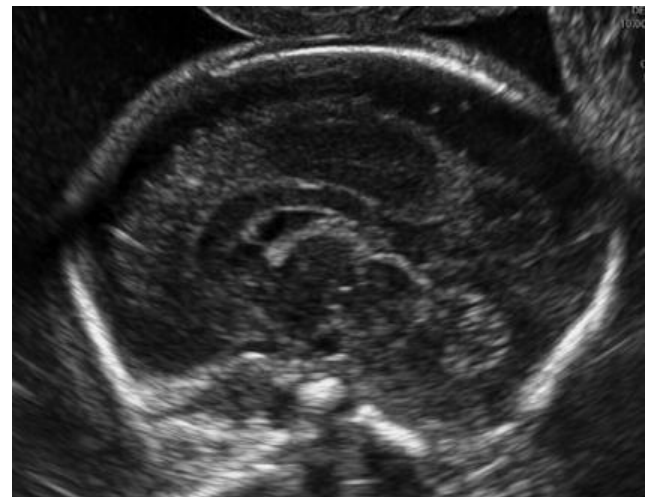


Figure 2 Ultrasound image (mid-sagittal plane) at 22 gestational weeks in Case 2, showing a thick corpus callosum body. Note that the genu is not well defined.

ventricle of 10 mm ($n=1$) and a persistent right umbilical vein ($n=1$). The head circumference was considered normal in all cases.

In four of six fetuses with complete follow-up the measurements normalized during the third trimester. In the remaining two the increased thickness of the CC was found to be related to the presence of a variant of the cingulate gyrus (Figures 3 and 5). Regarding the three without complete follow-up, the parents opted for termination of pregnancy during the second trimester in two; postmortem examination was not performed in these cases. In the other case lost to follow-up the CC normalized at 35 weeks.

The variations in the length of the CC were less pronounced than were those of the thickness and, although the CC remained short, being > 2 SD below the norm in five of six patients followed to term, it exhibited continued growth in all fetuses.

MRI was performed in six fetuses during the third trimester. In all but one (in which MRI was performed after sonographic normalization of the CC), the anomalies in the thickness of the CC were evident. Additional findings included lateral ventricular asymmetry without dilatation ($n=1$) and anterior horn asymmetry of the lateral ventricles ($n=2$).

The karyotype was normal in all nine fetuses. Chromosomal microarray was performed in two and the results were normal.

Postnatal ultrasound evaluation showed normal CC thickness in all six patients. Brain MRI was performed in two babies and showed cingulate gyrus variants (Figure 5). According to the parents' answers to the development questionnaires, adjusted for age, the children had normal development at the time of the interview (median age, 9 (range, 7–18) months). At the time of writing, two children were being followed up by a pediatric neurologist and had normal neurological and developmental examinations.

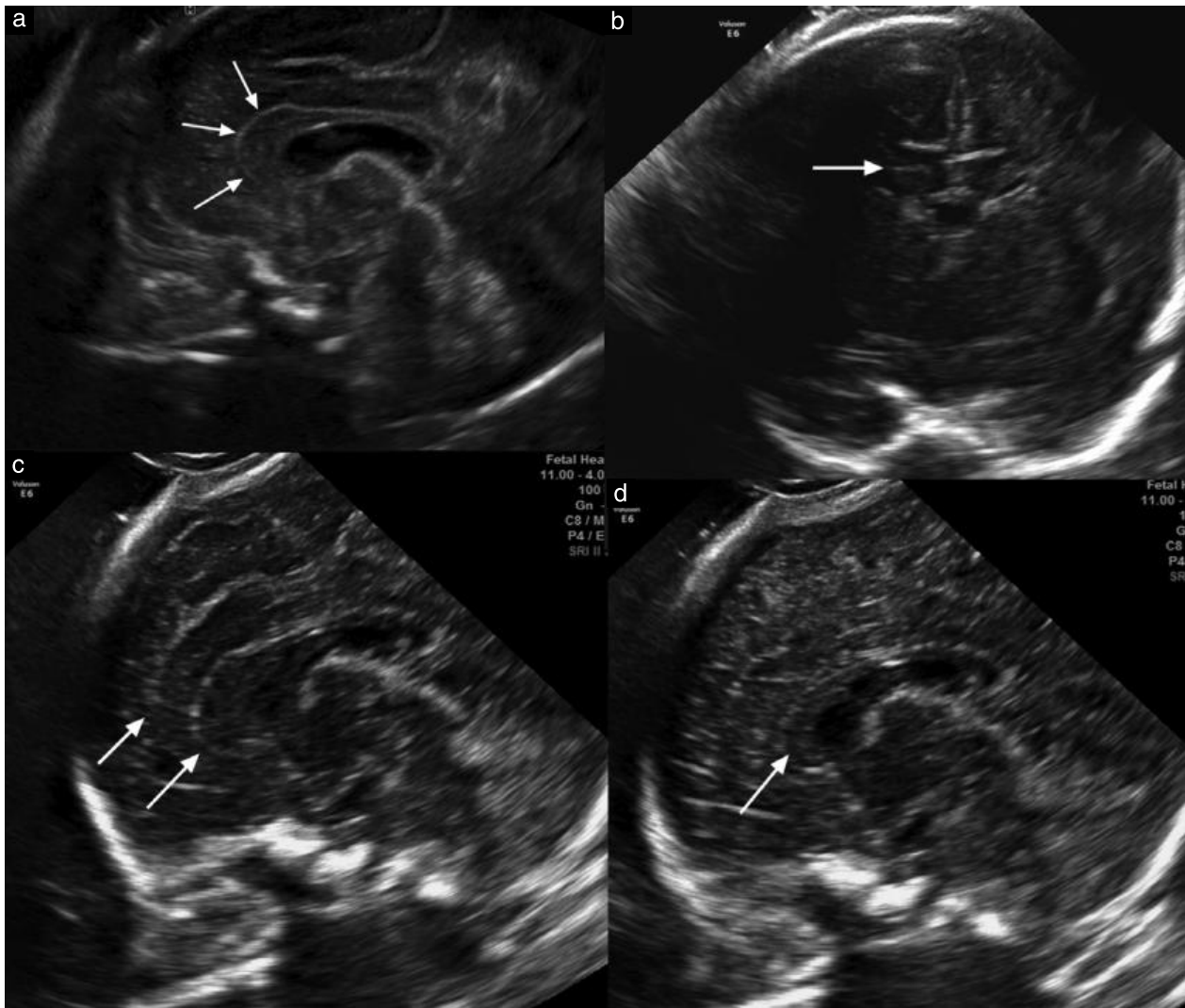


Figure 3 Ultrasound images in a fetus with thick genu (Case 3). (a) Mid-sagittal plane at 28 weeks showing thick genu (arrows). Note the difference in thickness when compared with the corpus callosum body. (b) Coronal plane at 30 weeks showing asymmetry between left and right sides of CC and presence of a sulcus (arrow) on the right. (c,d) Mid-sagittal planes at 30 weeks showing thick appearance of CC on right side of brain (c) and normal appearance on left side (d) (arrows).

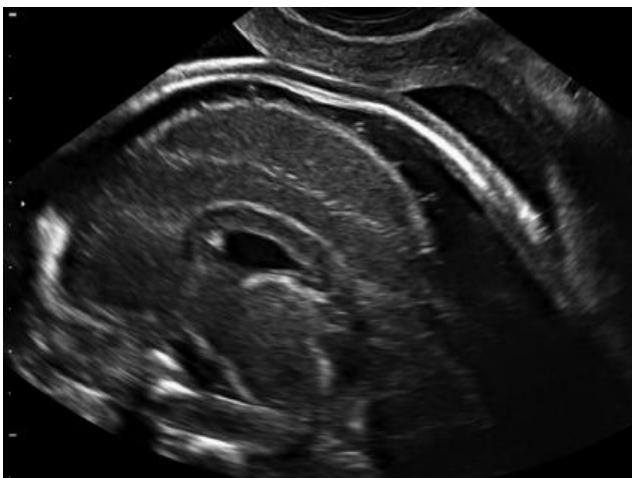


Figure 4 Ultrasound image (mid-sagittal plane) at 21 + 6 gestational weeks in Case 7, showing a thick corpus callosum with an echogenic zone protruding into the cavum septi pellucidum.

DISCUSSION

In children and adults, reports of a thick CC are rare¹³. It can be found in patients with neurofibromatosis and it has been linked to abnormalities of the white matter and macrocephaly¹⁴. A thick CC associated with microcephaly is characteristic of Cohen syndrome¹⁵. It is also found in patients with macrocephaly-capillary malformation syndrome¹⁶. Relative thickness is described in adults with schizophrenia¹⁷.

The identification of a thick CC *in utero* has been described, almost invariably in patients with associated anomalies⁹. In our previous study¹⁰ including eight fetuses with a persistent thick CC and associated anomalies, we suspected neurogenetic syndromes that would carry a poor prognosis. This finding may be supported by the fact that CC development occurs at the time of neuronal migration.

The significance and prognosis of a thick CC, when isolated, remains unknown due to the fact that there are

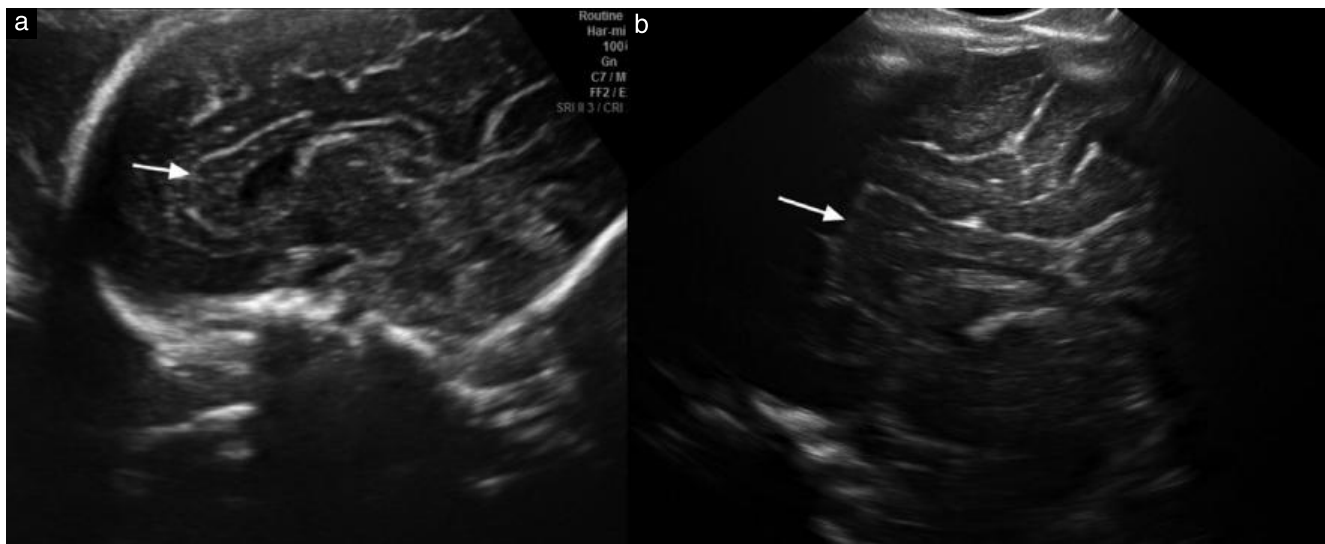


Figure 5 Prenatal (a) and postnatal (b) ultrasound images in Case 6, which had an apparently aberrant genu (arrows) due to a variant of the cingulate gyrus.

no published reports on visualization of an isolated thick CC during the second trimester. In such cases, as shown in our present series, conclusions should not be reached based on a single measurement and continued prenatal surveillance is recommended. Our patients were referred for different suspected CC or surrounding structural pathologies. Interestingly, in none of them was the CC considered thick by the referring ultrasonographer. The number of these cases with a suspected thick CC (9/59; 15.2%) is surprisingly high, three times greater than the frequency found in our previous study¹⁰. This high incidence is probably an overestimation, since many cases with clear callosal anomalies are currently diagnosed and counseled during the second-trimester scan without being referred to our unit. Another possible explanation is that, since we are aware of this pathology and its association with callosal hyperechogenicity, we currently assess the thickness of the CC in all patients referred for neurosonography.

We found that the thickness of the CC normalized during the third trimester in all the patients who were followed up, but the length remained relatively short, deviating by $\geq 2SD$ below the norm. Despite this supposed anomaly, at the time of writing, neurological development as determined by validated standard developmental questionnaires was normal in all six children who were followed to term as fetuses. We acknowledge the limitation in follow-up (parental reporting of validated neurodevelopmental questionnaires as opposed to a formal evaluation by a neurologist) and the young age of the children at the time of data acquisition. However, despite these limitations, which prevent us from drawing definitive conclusions regarding the implications of a thick/short CC, the findings cast doubt on its clinical significance.

A pericallosal lipoma should be considered as an underlying etiology¹⁸, since changes in echogenicity can occur during pregnancy in these fetuses. Pericallosal lipomas are usually isolated and carry a good prognosis,

so missing their diagnosis probably does not alter obstetric management.

We believe that in at least some cases an apparent increased thickness of the CC may be an artifact produced by either partial early obliteration of the cavum septi pellucidi or the development of cingulate variants, particularly when there is a supra cingulate gyrus (Figure 3). The significance of deviant development of the cingulate is not known.

We assume that in at least some of the cases described here, the increased thickness and normalization observed was due to remodeling of the CC during pregnancy by a continuous process of neuronal apoptosis and growth of the axons in conjunction with premyelination axonal changes. The asymmetries found in the coronal planes are more difficult to explain but are probably due to the fact that the axons do not cross the midline in a perpendicular direction, and they are therefore visualized obliquely.

According to the neurodevelopmental evaluation, the development of all six children followed to term as fetuses was normal at the time of writing. However, it is too early to reach conclusions since the children are still very young, most being below the age of language and communication development. None manifested abnormal growth, dysmorphic features or delayed motor development, so we can assume that they do not have a neurogenetic syndrome. Further formal evaluations are required to determine their neurodevelopmental status before definitive conclusions can be drawn regarding prognosis.

The significance of visualization of an abnormally thick/short CC remains unknown. We conclude that depiction of an isolated thick/short CC during the second trimester is not necessarily pathological, and can indicate late, but normal, CC development. We suggest that a prognosis should not be offered based on a single measurement of a thick CC and recommend continued prenatal surveillance in these cases.

REFERENCES

- Malinger G, Zakut H. The corpus callosum: normal fetal development as shown by transvaginal sonography. *AJR Am J Roentgenol* 1993; **161**: 1041–1043.
- Achiron R, Achiron A. Development of the human fetal corpus callosum: a high-resolution, cross-sectional sonographic study. *Ultrasound Obstet Gynecol* 2001; **18**: 343–347.
- Youssef A, Ghi T, Pilu G. How to image the fetal corpus callosum. *Ultrasound Obstet Gynecol* 2013; **42**: 718–720.
- Tilea B, Alberti C, Adamsbaum C, Armoogum P, Oury JF, Cabrol D, Sebag G, Kalifa G, Garel C. Cerebral biometry in fetal magnetic resonance imaging: new reference data. *Ultrasound Obstet Gynecol* 2009; **33**: 173–181.
- Blaicher W, Prayer D, Mittermayer C, Pollak A, Bernert G, Deutinger J, Bernaschek G. Magnetic resonance imaging in foetuses with bilateral moderate ventriculomegaly and suspected anomaly of the corpus callosum on ultrasound scan. *Ultraschall Med* 2003; **24**: 255–260.
- Paladini D, Pastore G, Cavallaro A, Massaro M, Nappi C. Agenesis of the fetal corpus callosum: sonographic signs change with advancing gestational age. *Ultrasound Obstet Gynecol* 2013; **42**: 687–690.
- Pilu G, Sandri F, Perolo A, Pittalis MC, Grisolia G, Cocchi G, Foschini MP, Salvioli GP, Bovicelli L. Sonography of fetal agenesis of the corpus callosum: a survey of 35 cases. *Ultrasound Obstet Gynecol* 1993; **3**: 318–329.
- d'Ercole C, Girard N, Cravello L, Boubli L, Potier A, Raybaud C, Blanc B. Prenatal diagnosis of fetal corpus callosum agenesis by ultrasonography and magnetic resonance imaging. *Prenatal Diagn* 1998; **18**: 247–253.
- Rypens F, Sonigo P, Aubry MC, Delezoide AL, Cessot F, Brunelle F. Prenatal MR diagnosis of a thick cc. *AJNR Am J Neuroradiol* 1996; **17**: 1918–1920.
- Lerman-Sagie T, Ben-Sira L, Achiron R, Schreiber L, Hermann G, Lev D, Kidron D, Malinger G. Thick fetal corpus callosum: an ominous sign? *Ultrasound Obstet Gynecol* 2009; **34**: 55–61.
- Hergan B, Atar OD, Poretti A, Huisman TA. Serial fetal MRI for the diagnosis of Aicardi syndrome. *Neuroradiol J* 2013; **26**: 380–384.
- Garel C, Moutard ML. Main congenital cerebral anomalies: how prenatal imaging aids counseling. *Fetal Diagn Ther* 2014; **35**: 229–239.
- Gocmen R, Oguz KK. Mega corpus callosum and caudate nuclei with bilateral hippocampal malformation. *Diagn Interv Radiol* 2008; **14**: 69–71.
- Margariti PN, Blekas K, Katzioti FG, Zikou AK, Tzoufi M, Argyropoulou MI. Magnetization transfer ratio and volumetric analysis of the brain in macrocephalic patients with neurofibromatosis type 1. *Eur Radiol* 2007; **17**: 433–438.
- Kivitie-Kallio S, Norio R. Cohen syndrome: essential features, natural history, and heterogeneity. *Am J Med Genet* 2001; **102**: 125–135.
- Conway RL, Pressman BD, Dobyns WB, Danielpour M, Lee J, Sanchez-Lara PA, Butler MG, Zackai E, Campbell L, Saitta SC, Clericuzio CL, Milunsky JM, Hoyme HE, Shieh J, Moeschler JB, Crandall B, Lauzon JL, Viskochil DH, Harding B, Graham JM Jr. Neuroimaging findings in macrocephaly-capillary malformation: a longitudinal study of 17 patients. *Am J Med Genet Part A* 2007; **143A**: 2981–3008.
- Nasrallah HA, Andreasen NC, Coffman JA, Olson SC, Dunn VD, Ehrhardt JC, Chapman SM. A controlled magnetic resonance imaging study of corpus callosum thickness in schizophrenia. *Biol Psychiatry* 1986; **21**: 274–282.
- Yilmaz N, Unal O, Kiyamaz N, Yilmaz C, Etlík O. Intracranial lipomas—a clinical study. *Clin Neurol Neurosurg* 2006; **108**: 363–368.

Vein of Galen aneurysmal malformation (VGAM) in the fetus: retrospective analysis of perinatal prognostic indicators in a two-center series of 49 cases

D. PALADINI¹, B. DELOISON², A. ROSSI³, G. E. CHALOUHI², C. GANDOLFO³, P. SONIGO⁴, S. BURATTI⁵, A. E. MILLISCHER⁴, G. TUO⁶, Y. VILLE², A. PISTORIO⁷, A. CAMA⁸ and L. J. SALOMON²

¹Fetal Medicine and Surgery Unit, Istituto Giannina Gaslini, Genoa, Italy; ²Maternité, Hôpital Universitaire Necker-Enfants Malades, Université Paris Descartes, Assistance Publique-Hôpitaux de Paris, Paris, France; ³Neuroradiology Unit, Istituto Giannina Gaslini, Genoa, Italy; ⁴Radio-Pédiatrie, Hôpital Universitaire Necker-Enfants Malades, Université Paris Descartes, Assistance Publique-Hôpitaux de Paris, Paris, France; ⁵Neonatal and Pediatric Intensive Care Unit, Department of Critical Care and Perinatal Medicine, Istituto Giannina Gaslini, Genoa, Italy; ⁶Department of Pediatric Cardiology and Cardiac Surgery, Istituto Giannina Gaslini, Genoa, Italy; ⁷Epidemiology and Biostatistics Unit, Istituto Giannina Gaslini, Genoa, Italy; ⁸Neurosurgery Unit, Istituto Giannina Gaslini, Genoa, Italy

KEYWORDS: brain anomaly; fetal echocardiography; prenatal diagnosis

ABSTRACT

Objective Vein of Galen aneurysmal malformation (VGAM) is a rare fetal anomaly, the neurological outcome of which can be good with appropriate perinatal management. However, most fetal series are too small to allow reliable statistical assessment of potential prognostic indicators. Our aim was to assess, in a two-center series of 49 cases, the prognostic value of several prenatal variables, in order to identify possible prenatal indicators of poor outcome, in terms of mortality and cerebral disability.

Methods This was a retrospective study involving 49 cases of VGAM diagnosed prenatally and managed at two centers over a 17-year period (1999–2015). All cases had undergone detailed prenatal cerebral and cardiac assessment by grayscale ultrasound, color and pulsed-wave Doppler and magnetic resonance imaging (MRI). Ultrasound and MRI examination reports and images were reviewed and outcome information was obtained from medical reports. Volume of the VGAM (on ultrasound and MRI) was calculated and development of straight-sinus dilatation, ventriculomegaly and other major brain abnormalities was noted. Cardiothoracic ratio, tricuspid regurgitation and reversed blood flow across the aortic isthmus were evaluated on fetal echocardiography. Major brain lesions were considered by definition to be associated with poor outcome in all cases. Pregnancy and fetoneonatal outcome were known in all cases. Fetoneonatal outcome and brain damage were considered as dependent variables in the statistical evaluation. Poor outcome was defined as death, late

termination of pregnancy due to association with related severe brain anomalies or severe neurological impairment.

Results At a mean follow-up time of 20 (range, 0–72) months, 36.7% of the whole series and 52.9% of the cases which did not undergo late termination were alive and free of adverse sequelae. Five (10.2%) cases showed progression of the lesion between diagnosis and delivery. On univariate analysis, dilatation of the straight sinus, VGAM volume $\geq 20\,000\text{ mm}^3$ and tricuspid regurgitation were all significantly related to poor outcome. However, on logistic regression analysis, the only variables associated significantly with poor outcome were tricuspid regurgitation and, to a lesser extent, VGAM volume $\geq 20\,000\text{ mm}^3$. The former was also the only variable associated with brain damage.

Conclusions Major brain lesions, tricuspid regurgitation and, to a lesser extent, VGAM volume $\geq 20\,000\text{ mm}^3$ are the only prenatal variables associated with poor outcome in fetal VGAM. Prenatal multidisciplinary counseling should be based on these variables. Copyright © 2016 ISUOG. Published by John Wiley & Sons Ltd.

INTRODUCTION

Vein of Galen aneurysmal malformation (VGAM) represents the most common cerebral arteriovenous malformation detected prenatally and accounts for 30% of all pediatric vascular malformations¹. This malformation results from a connection between the primitive choroidal vessels and the median prosencephalic

Correspondence to: Prof. D. Paladini, Fetal Medicine and Surgery Unit, Istituto Giannina Gaslini, Genoa, Italy (e-mail: dpaladini49@gmail.com)

Accepted: 8 August 2016

vein of Markowski between the 6th and 11th weeks of gestation. The abnormal shunt prevents involution of the embryonic vein and the subsequent development of the vein of Galen¹. The diagnosis is made prenatally, commonly in the third trimester, though earlier diagnoses have been reported^{2–5}. Fetal two- (2D) and three- (3D) dimensional ultrasound and magnetic resonance imaging (MRI) have been employed to characterize VGAM.

Modern endovascular techniques in conjunction with specialized perinatal intensive care management have enabled VGAM to become a potentially curable condition, with several affected patients achieving normal neurological development^{6,7}. Although prognostic factors detectable prenatally would be highly desirable, they are still lacking because most case series reported so far have been small, and evaluation of prognostic indices has been limited mainly to those ascertainable postnatally^{7,8}. An analysis of 21 fetal cases was reported recently by one of our two centers, together with a comprehensive review of the literature⁹. In that series, the number of cases harboring concurrent severe brain abnormalities was high, and the consequently high rate of late termination of pregnancy (TOP) limited statistical assessment of the relevance of prenatal prognostic indicators.

The aim of this study was to assess, in a two-center series of 49 cases, the prognostic value of several prenatal variables related to the malformation itself, its clinical history and the neonatal course. The primary endpoint of the analysis was to identify possible prenatal indicators of poor outcome, in terms of mortality and cerebral disabilities, with a secondary aim to identify possible factors heralding *in-utero* progression and/or association with other brain abnormalities.

METHODS

This was a retrospective study involving all cases of VGAM diagnosed prenatally which were managed at two centers over a 17-year period (1999–2015): 19 were managed at Istituto Giannina Gaslini, Genoa, Italy in the period 2008–2015, and 30 were managed at Necker Hospital, Paris, France in the period 1999–2015. Both centers act as national referral centers for VGAM, which explains the relatively high number of cases seen at each institution. Gestational age was based on measurement of crown–rump length or certain date of last menstrual period for all pregnancies. All cases underwent at least one detailed ultrasound examination (2D and, more recently, 3D) and at least one MRI prenatally (Figure 1). Ultrasound assessment included fetal neurosonography¹⁰ and echocardiography. The former, performed transabdominally and, if feasible, transvaginally, allowed a detailed grayscale and color/power Doppler evaluation of the VGAM on 2D and 3D imaging, together with a search for concurrent major brain lesions. In particular, the following parameters were recorded: orthogonal diameters of the VGAM (craniocaudal, laterolateral and anteroposterior), volume of the VGAM, calculated from the three diameters using the ellipsoid formula,

presence/absence of straight sinus dilatation (Figure 1), presence/absence of ventriculomegaly (defined as width of the ventricular atrium > 9.9 mm on an axial transventricular view of the fetal brain¹⁰) and presence/absence of other major brain abnormalities. These included (alone or in combination): ventriculomegaly, hemorrhage, necrosis, porencephaly, schizencephaly and cortical malformations (mainly micropolygyria). Fetal echocardiography was aimed at assessment of cardiac overload: after ruling out major cardiac anomalies, the cardiothoracic ratio (CTR), tricuspid regurgitation and, more recently, reversed blood flow across the aortic isthmus were evaluated. The CTR, measured as cardiac area/thoracic area on a four-chamber axial view of the fetal thorax, was considered abnormal if it was > 0.50¹¹. Tricuspid regurgitation was considered present when flow across the tricuspid valve was holosystolic (rather than occurring in early systole only) and/or if the regurgitant jet had a maximum velocity > 2 m/s¹². Blood flow in the aortic isthmus was considered abnormal if reversed diastolic flow was detected on spectral Doppler investigation^{2,13}. Prenatal MRI was similarly directed at evaluating all features of the malformation and other concurrent brain abnormalities. As a policy of both institutions, MRI was performed at the time of referral or as soon after that as was logistically feasible. In cases in which progression of the lesion was documented on ultrasound, as well as in those in which delivery took place several weeks after the diagnosis, a follow-up MRI was discussed case-by-case and performed according to local resources.

For the purposes of this study, all ultrasound and MRI examinations were reviewed, including biometric and anatomical findings based on ultrasound reports and stored images or 3D volume datasets. In five cases of the Necker series, only the MRI reports and not the images themselves were available. The VGAM volume in mm³ was calculated, for both ultrasound and MRI examinations, using the ellipsoid formula ($a \times b \times c \times 0.523$, where a, b and c are the three orthogonal diameters). For ultrasound, the three diameters were measured on grayscale images or 3D volume datasets and not on 2D or 3D color or power Doppler ones, because the relatively high priority of the color Doppler signal needed to 'fill in' the vessels would lead to overestimation of the actual diameters. The number of afferent and efferent vessels was derived only from postnatal MRI.

The categorical variables assessed pre- and postnatally included: ventriculomegaly, straight sinus dilatation, brain lesions other than VGAM, prenatal cardiothoracic ratio, reversed flow in the aortic isthmus, tricuspid regurgitation, heart failure (hydrops), neonatal embolization < 30 days of age, placement of ventriculoperitoneal shunt and need for anticonvulsant drugs. Major brain lesions evident at ultrasound or MRI were considered by definition to be associated with poor outcome in all cases. Delivery records were reviewed and pregnancy outcome data collected. Information on the outcome of liveborn infants was retrieved from pediatric, radiological and neuroradiological records, with most of the surviving

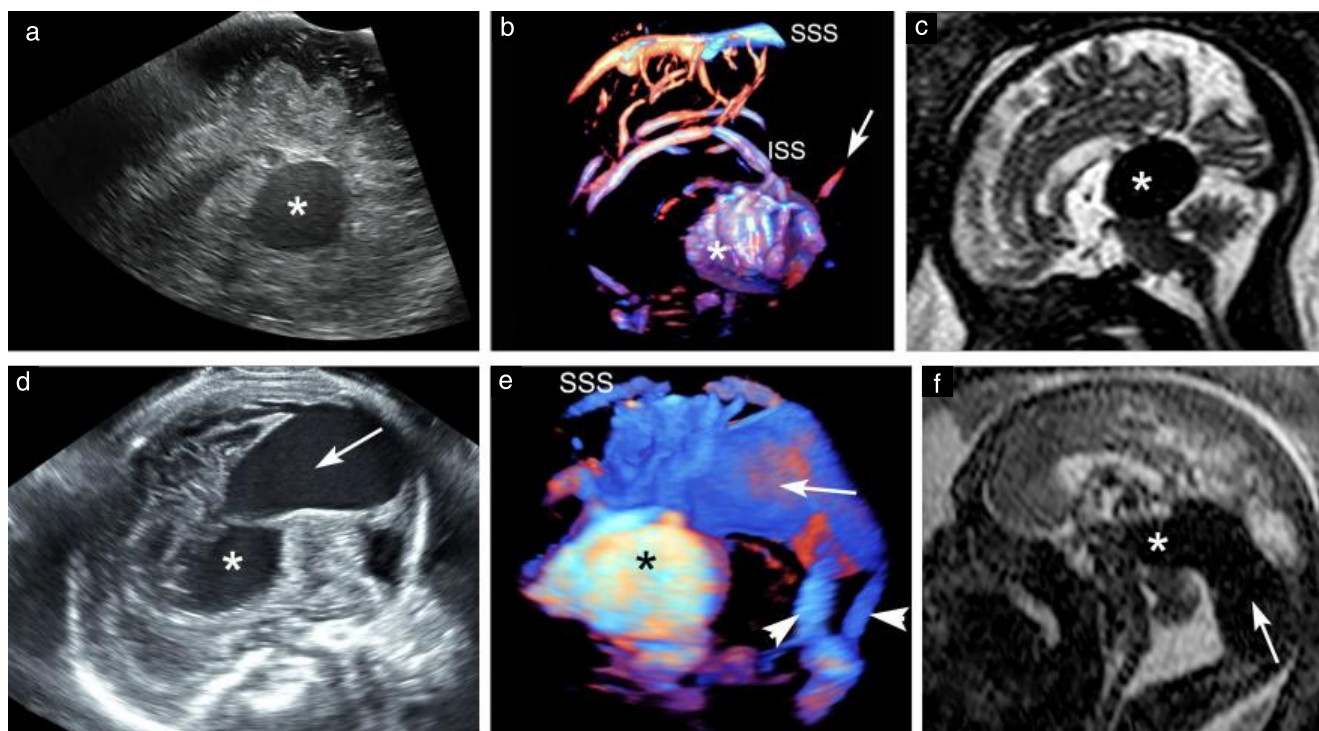


Figure 1 Prenatal imaging of vein of Galen aneurysmal malformation (VGAM) in a 36-week fetus (a,b,c) and a 35-week fetus (d,e,f), using: (a,d) three-dimensional (3D) transvaginal neurosonography (midsagittal view); (b,e) 3D power Doppler rendering; and (c,f) magnetic resonance imaging (MRI, sagittal T2-weighted imaging, 1.5 T). (a,b,c) In this case, there was only very limited dilatation of the straight sinus, evident on power Doppler rendering (arrow) and MRI (not in same slice as that shown in (c)). VGAM (*) is depicted clearly in all three modalities. (d,e,f) In this case, there was severe dilatation of the straight sinus as well as of the multiple feeder arteries and draining sinuses. The main axis of the Galen dilatation was laterolateral, which explains the apparent discrepancy between grayscale imaging (d) and power Doppler rendering (e). Both ampulla (*) and a huge dilatation of the straight sinus (arrow) were evident in all three modalities. Arrowheads in (e) indicate transverse sinuses. ISS, inferior sagittal sinus; SSS, superior sagittal sinus.

neonates being followed up at one of the two institutions. Information on cases which underwent late TOP and those which resulted in perinatal death was retrieved from medical and pathological records.

Progression was defined as development of brain damage other than the VGAM, such as hemorrhage or ventriculomegaly, in the period from diagnosis to delivery. If the new lesion was detected only after birth but the last prenatal ultrasound/MRI was normal, this was not considered as progression.

Fetoneonatal outcome and brain damage were considered as dependent variables in the statistical evaluation. Outcome was considered good if the child had normal cardiac and neurological status at the last follow-up. Poor outcome was defined as death, late TOP due to association with related severe brain anomalies, or severe neurological impairment.

As far as late TOP is concerned, this is allowed in France for pregnancies complicated by severe fetal anomalies but not in Italy, where the legal limit for TOP is 22 gestational weeks. In France, any case in which the parents opt for late TOP is discussed in a multidisciplinary committee and the procedure is then performed if approved by the committee.

The postnatal management protocol of VGAM was similar in the two centers and, due to the relatively short

(considering the rarity of the malformation) study time of 17 years, throughout the study period. After delivery, affected neonates were transferred to the neonatal intensive care unit to allow for immediate evaluation by the pediatric cardiologist and intensivist. If needed, respiratory support with positive-pressure ventilation or intubation was initiated. Cardiovascular examination, echocardiography, transcranial ultrasound and, if possible, MRI were performed on the first postnatal day. Heart failure, when present, was managed with medication. If patients could not be weaned from ventilatory support or intravenous medication or if they progressed towards multiorgan failure, early endovascular intervention was performed. In all other cases, embolization was planned at 4–6 months of age, in agreement with published evidence demonstrating poorer outcome in case of early neonatal embolization⁴.

Statistical analysis

Statistical analysis was performed with the Statistica release 9 package (StatSoft Corp., Tulsa, OK, USA) for univariate analyses and the software Stata release 7 (Stata Corporation, College Station, TX, USA) for multivariate analyses. Outcome (good *vs* poor) and brain damage (as defined above) were considered as dependent variables

in the statistical evaluation. Descriptive statistics were produced: qualitative variables were summarized in terms of absolute frequencies or percentages and quantitative variables were summarized in terms of medians and interquartile range. A comparison of frequencies was performed using chi-square or Fisher's exact test (the latter in case of expected frequencies < 5). A comparison of quantitative variables between two categories of patients (patients with good outcome *vs* those with poor outcome) was carried out using the non-parametric Mann–Whitney *U*-test (in case of skewed distributions). Before performing the logistic regression analysis, one continuous variable (VGAM volume) was categorized on the basis of receiver–operating characteristics (ROC) curve analysis. Finally, two logistic regression models were fitted in order to evaluate the role of different determinants with respect to poor outcome or brain damage. Variables that turned out to be significant at univariate analysis and those judged *a priori* to be potentially relevant from a clinical point of view were entered into the model. Odds ratios and 95% CIs were calculated and reported. The log-likelihood ratio test was used to test statistical significance. The area under the ROC curve of the best-fitting model was used as an indicator of its predictive ability. All the tests were two sided and $P < 0.05$ was considered statistically significant.

Table 1 Characteristics of study population of 49 cases of prenatally diagnosed vein of Galen aneurysmal malformation managed at two centers between 1999 and 2015

Variable	Gaslini Hospital (n = 19)	Necker Hospital (n = 30)
Maternal age (years)	33.6 ± 4.7	31.6 ± 3.4
Gestational age at diagnosis (weeks)	32 ± 2.3	33 ± 3.3
Gestational age at delivery (weeks)	37 ± 2.2	38 ± 3.2*
Birth weight (g)	2975 ± 566	3067 ± 722*
Follow-up (months)	29 ± 26	12 ± 17*
Preterm delivery < 37 weeks	8 (42)	2 (13)*
Preterm delivery < 32 weeks	1 (5)	1 (7)*
Alive at last follow-up	13 (68)	8 (53)*

Values are given as mean ± SD or *n* (%). *Excluding 15 cases which underwent late termination of pregnancy.

Table 2 Prenatal and postnatal dichotomous variables assessed in 49 cases of vein of Galen aneurysmal malformation (VGAM)

Variable	Method	Timing		Absent (n (%))	Present (n (%))	N/A (n (%))
		Pre	Post			
Ventriculomegaly	US + MRI	+	+	26 (53.1)	23 (46.9)	0 (0)
Straight sinus dilatation	US + MRI	+	+	17 (34.7)	21 (42.9)	11 (22.4)
Brain lesions other than VGAM	US	+	+	31 (63.3)	18 (36.7)	0 (0)
Prenatal cardiothoracic ratio	US	+	–	14 (28.6)	35 (71.4)	0 (0)
AI reversed flow	US	+	–	15 (30.6)	14 (28.6)	20 (40.8)
TV regurgitation	US	+	–	33 (67.3)	16 (32.7)	0 (0)
Heart failure (hydrops)	US	+	–	45 (91.8)	4 (8.2)	0 (0)
Embolization < 30 days of age	Clinical	–	+	10 (20.4)	6 (12.2)	33 (67.3)
Placement of VP shunt	Clinical	–	+	40 (81.6)	3 (6.1)	6 (12.2)
Need for anticonvulsant drugs	Clinical	–	+	47 (95.9)	2 (4.1)	0 (0)

AI, aortic isthmus; MRI, magnetic resonance imaging; N/A, not available; Post, postnatal; Pre, prenatal; TV, tricuspid valve; US, ultrasound; VP, ventriculoperitoneal.

RESULTS

Characteristics of the 49 cases of VGAM are shown in Table 1. Descriptive statistics for dichotomous and continuous variables are reported in Tables 2 and 3, respectively. With respect to fetoneonatal outcome (Table 4), 36.7% of the whole series and 52.9% of the cases which did not undergo late TOP were alive and free from adverse sequelae at a mean follow-up of 20 (range, 0–72) months. Five (10.2%) cases showed progression of the lesion between diagnosis and delivery; their characteristics are shown in Table 5. Three (6%) cases needed placement of a ventriculoperitoneal shunt to resolve post-hemorrhagic obstructive hydrocephalus, while two (4.1%) were undergoing anticonvulsant therapy at the time of writing. With respect to measurement of the VGAM volume, there was fair agreement between prenatal ultrasound and MRI values (R^2 , 0.86; Figure 2).

Predictors of poor outcome

On univariate analysis, dilatation of the straight sinus, VGAM volume $\geq 20\,000\text{ mm}^3$ (20 mL) and tricuspid regurgitation were all significantly related to poor outcome (Table 6). However, on logistic regression analysis, the only variables associated significantly with poor outcome were tricuspid regurgitation and, to a lesser extent, VGAM volume $\geq 20\,000\text{ mm}^3$ (Table 7).

Predictors of brain damage on prenatal/postnatal ultrasound or magnetic resonance imaging

The analysis was repeated with brain damage as the dependent variable, to evaluate whether any of the variables might be predictive of central nervous system lesions, such as hemorrhage, ventriculomegaly or cortical anomalies, associated with VGAM, arising *in utero* or after birth. In this case, on univariate analysis, all tested variables were associated with concurrent brain lesions (Table 8). However, on logistic regression analysis,

only the presence of tricuspid regurgitation remained associated significantly with brain damage (Table 7).

Prenatal progression of VGAM

A VGAM-related brain lesion appeared between prenatal diagnosis and delivery in five (10.2%) cases (Table 5). The numbers are too small to allow statistical analysis, but comparison of the VGAM volume in the four with this information available *vs* the remaining cases without progression showed VGAM volume to be > 40 000 mm³ in all four cases showing late-onset prenatal brain insults but in only 14.3% (4/28) of those with no progression (Figure 3). Of these four, one neonate died at 3 months and another was alive at the time of writing but underwent ventriculoperitoneal shunt placement due to hydrocephalus.

Table 3 Descriptive statistics for continuous variables in a series of 49 cases of vein of Galen aneurysmal malformation (VGAM)

Variable	n	Min	Max	Mean	SD
VGAM volume (mm ³)*	42	4423	168 911	35 794	30 590
Afferent vessels (n)†	41	1	6	3.93	1.44
Efferent vessels (n)†	41	1	2	1.12	0.33

*On prenatal magnetic resonance imaging (MRI). †On postnatal MRI. Max, maximum; Min, minimum.

Table 4 Fetoneonatal outcome in 49 cases of vein of Galen aneurysmal malformation

Outcome	n	%	% of ongoing pregnancies
Late TOP	15	30.6	—
Intrauterine fetal death	1	2.0	2.9
Neonatal death	11	22.4	32.3
Infant death	1	2.0	2.9
Alive and well*	18	36.7	52.9
Alive with sequelae*†	3	6.1	8.8

*Mean follow-up, 20 (range, 0–72) months. †One case each of: seizures in a case of hydrocephalus treated with ventriculo-peritoneal shunt; periventricular leukomalacia; spastic tetraparesis, which is currently being investigated for genetic mutations due to recurrence of cerebral arteriovenous malformation in second pregnancy (not included in present report) 5 years after index case. TOP, termination of pregnancy.

Table 5 Characteristics of the five cases of vein of Galen aneurysmal malformation (VGAM) showing progression of lesion from diagnosis to delivery

GA at diagnosis (weeks)	Straight sinus dilatation	VGAM volume (mm ³)	TR	Abnormal CTR	Heart failure	GA at progression (weeks)	New finding
31	Yes	168 910	No	Yes	No	32	Necrosis, porencephaly
32	No	52 675	No	Yes	No	36	Severe ventriculomegaly
35	N/A	33 504	No	Yes	No	37	Necrosis, porencephaly
31	N/A	N/A	No	No	No	36	Necrosis, porencephaly
31	Yes	43 345	Yes	No	No	38	Necrosis, porencephaly

CTR, cardiothoracic ratio; GA, gestational age; N/A, not available; TR, tricuspid regurgitation.

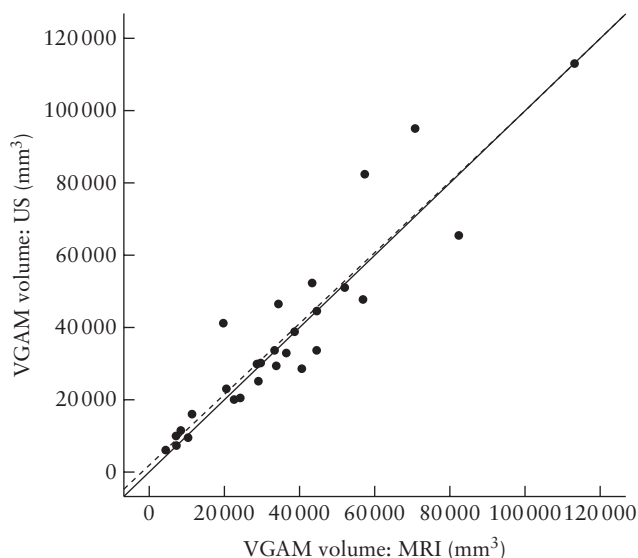


Figure 2 Vein of Galen aneurysmal malformation (VGAM) volume calculation: scatterplot showing correlation between prenatal ultrasound (US) and magnetic resonance imaging (MRI) (R^2 linear = 0.858).

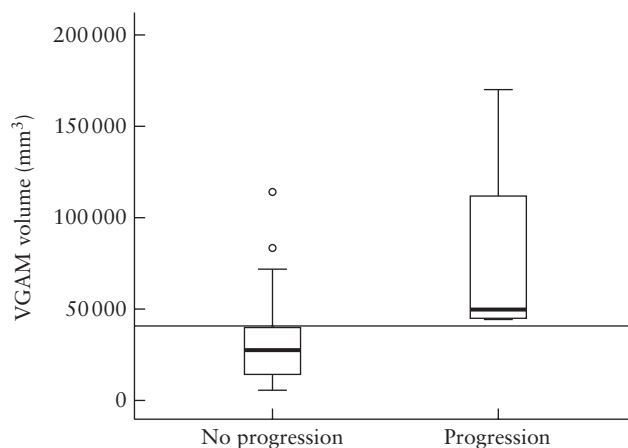


Figure 3 Box-and-whiskers plot showing relationship between vein of Galen aneurysmal malformation (VGAM) volume measured on magnetic resonance imaging and prenatal progression of lesion. Boxes and internal lines represent median and range, whiskers represent interquartile range and circles represent outliers. Reference line is at 40 000 mm³.

Table 6 Relationship according to univariate analysis between different predictors and poor outcome in a series of 49 cases of vein of Galen aneurysmal malformation (VGAM)

Variable	Missing cases (n (%))	Poor outcome	Good outcome	P
Straight sinus dilatation	11 (22.4)			< 0.0001†
Yes (n = 21)		16/21 (76.2)	5/21 (23.8)	
No (n = 17)		2/17 (11.8)	15/17 (88.2)	
Mean VGAM volume (mm ³)	7 (14.3)	33 963 (22 678–44 594)	19 216 (11 990–35 114)	0.06‡
VGAM volume ≥ 20 000 mm ³ *	7 (14.3)			0.001†
Yes (n = 29)		20/29 (69.0)	9/29 (31.0)	
No (n = 13)		2/13 (15.4)	11/13 (84.6)	
Tricuspid regurgitation	0 (0)			< 0.0001†
Yes (n = 16)		15/16 (93.8)	1/16 (6.3)	
No (n = 33)		13/33 (39.4)	20/33 (60.6)	
Aortic isthmus reversed flow	20 (40.8)			0.096†
Yes (n = 14)		8/14 (57.1)	6/14 (42.9)	
No (n = 15)		4/15 (26.7)	11/15 (73.3)	

Data are given as n/N (%) or median (interquartile range). Poor outcome defined by death, late termination due to association with related severe brain anomalies or severe neurological impairment. Good outcome defined by normal cardiac and neurological status at last neonatal/infant follow-up. *Actual value according to receiver–operating characteristics curve = 19 807.1 mm³. †Chi-square test. ‡Mann–Whitney U-test.

Table 7 Vein of Galen aneurysmal malformation (VGAM) in the fetus: best fitted logistic regression model for poor outcome (n = 22/42; 52.4%)* and brain damage (n = 13/42; 40.0%)†

	OR (95% CI)	P‡
Dependent variable: poor outcome		
VGAM vol ≥ 20 000 vs < 20 000 mm ³ §	15.5 (1.6–155.7)	0.004
TR present vs absent	33.8 (2.5–450.6)	0.0003
Dependent variable: brain damage		
VGAM vol ≥ 20 000 vs < 20 000 mm ³ §	6.2 (0.6–63.0)	0.08
TR present vs absent	9.0 (1.8–43.9)	0.001

Poor outcome defined by death, late termination due to association with related severe brain anomalies or severe neurological impairment. Brain damage defined as development of any kind of brain lesion possibly related to VGAM. *Area under location receiver–operating characteristics curve (LROC) of model: 0.86. †LROC of model: 0.82. ‡Log-likelihood ratio test. §Actual value according to ROC curve = 19 807.1 mm³. OR, odds ratio; TR, tricuspid regurgitation; vol, volume.

DISCUSSION

VGAM is a complex malformation, the natural history of which is not understood completely¹. To predict at the time of prenatal diagnosis which case will develop severe brain necrotic lesions and which will not remains challenging. Several prognostic factors have been proposed, both in the neonate^{7,8} and in the fetus^{2–5,9}, the latter based on small series⁵ or anecdotal descriptions of single cases^{2,3}. The need to identify prognostic indicators in the fetus has become more pressing over recent years for two reasons: (1) the availability of endovascular techniques in conjunction with specialized perinatal intensive care management have made VGAM a potentially curable condition^{6,7}; and (2) the earlier recognition of fetal anomalies, including late-onset ones such as VGAM, due to advancements in ultrasound technology, may enable the identification and delivery of cases that would otherwise deteriorate over the last few gestational weeks prior to term. In the latter scenario (delivery before term), it should be borne in mind

Table 8 Relationship according to univariate analysis between different predictors and brain damage in a series of 49 cases of vein of Galen aneurysmal malformation (VGAM)

	Brain damage (n/N (%))			P
	Yes	No		
Straight sinus dilatation				0.0099†
Yes (n = 21)	10/21 (47.6)	11/21 (52.4)		
No (n = 17)	1/17 (5.9)	16/17 (94.1)		
VGAM vol ≥ 20 000 mm ³ *				0.036†
Yes (n = 29)	12/29 (41.4)	17/29 (58.6)		
No (n = 13)	1/13 (7.7)	9/29 (31.0)		
Tricuspid regurgitation				0.0012‡
Yes (n = 16)	11/16 (68.8)	5/16 (31.3)		
No (n = 33)	7/33 (21.2)	26/33 (78.8)		
Aortic isthmus reversed flow				0.035†
Yes (n = 14)	6/14 (42.9)	8/14 (57.1)		
No (n = 15)	1/15 (6.7)	14/15 (93.3)		

Brain damage defined as development of any kind of brain lesion possibly related to VGAM. *Actual value according to receiver–operating characteristics curve = 19 807.1 mm³. †Fisher’s exact test. ‡Chi-square test. vol, volume.

that early neonatal embolization attempts are associated with a higher risk of death and complications^{4–14}.

The present study has the strength of including a substantial number of cases, all with prenatal diagnosis and autoptic or postnatal confirmation and follow-up, seen at two referral centers over a relatively limited period, considering the rarity of the malformation: 17 years for Necker Hospital and 8 years for Gaslini Hospital. Another advantage of this investigation is that prenatal data included detailed fetal neurosonographic, echocardiographic and MRI evaluation in all cases. A limitation of the study is that survivors with severe neurodevelopmental sequelae, neonatal deaths and late TOPs were grouped under a single variable: poor outcome. This was due to the need to reach a minimum number of events to run the statistics, but we nonetheless believe that all of these variables do indeed represent poor outcome

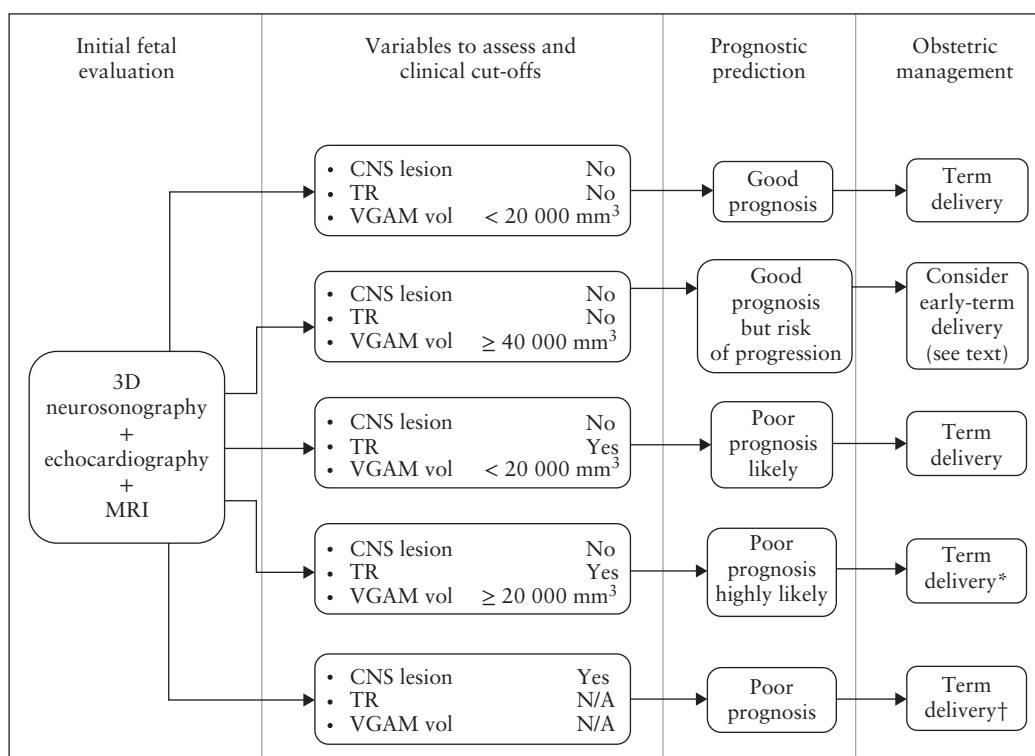


Figure 4 Flowchart summarizing obstetric management of cases of vein of Galen aneurysmal malformation (VGAM) on basis of prenatal ultrasound and magnetic resonance imaging (MRI) findings. *If VGAM volume (vol) $\geq 40\,000\text{ mm}^3$, consider early-term delivery. †If late termination of pregnancy is not performed. 3D, three-dimensional; CNS, central nervous system; N/A, not applicable; TR, tricuspid regurgitation.

for fetuses/neonates with VGAM. Another limitation concerns the fact that reversed aortic isthmus blood flow was evaluated only over the last few years, which explains why this parameter was lacking in 20/49 (40.8%) cases.

In this study, we first tried to determine if any of the prenatal variables entered in the model was significantly associated with a poor prognosis. As evident from Table 6, on univariate analysis, straight sinus dilatation, VGAM volume $\geq 20\,000\text{ mm}^3$ and tricuspid regurgitation were all associated with poor outcome, but, on logistic regression analysis, only VGAM volume $\geq 20\,000\text{ mm}^3$ and tricuspid regurgitation were significantly associated with a poor outcome (Table 7). The results were similar using brain damage, defined as development of any kind of brain lesion possibly related to VGAM, as the dependent variable (Tables 7 and 8), with tricuspid regurgitation being the only variable to remain in the logistic regression model with statistical significance.

Our results confirm that a fetus referred for VGAM should undergo detailed neurosonography, echocardiography and brain MRI. However, considering that, currently, most fetal medicine units are equipped with high-end 3D ultrasound equipment, and that 3D ultrasound provides volume calculation results comparable to those of MRI (Figure 2), it seems appropriate to base an initial prognostic evaluation on ultrasound findings. Subsequent fetal brain MRI to confirm VGAM volume and, more importantly, to diagnose recent necrotic lesions that may have escaped sonographic recognition, should then be performed. For

characterization of the malformation, its feeders and straight-sinus involvement (Figure 1), 3D color/power Doppler is a highly effective modality. However, it is not reliable for volume calculation, because, in order to obtain smooth-walled casts, it is necessary to prioritize the color Doppler signal on the background grayscale, with consequent overrepresentation of the hollow structures, i.e. aneurysm and vessels. We therefore believe that 3D color/power Doppler rendering may be used effectively to assess the general architecture of the lesion but volume calculation should be performed on the basis of 3D grayscale datasets, if available, and MRI.

Another issue to consider is the intrauterine progression of the lesion (Table 5 and Figure 3). In fact, in some cases with a relatively early third-trimester diagnosis, the lesions may progress over the weeks following diagnosis prior to delivery, with consequent significant deterioration of the prognosis. In our series, this occurred in 5/49 (10.2%) cases. Considering that some cases may still be detected late in pregnancy, it can be speculated that the risk of prenatal progression might be even higher than 10%. The small numbers prevent statistical evaluation, but visual comparison of the mean VGAM volume between four of the five cases of progression (volume data were not available for the fifth case) and the remainder of the series seems to suggest a cut-off of $40\,000\text{ mm}^3$ (40 mL) as the threshold over which the risk of progression might be higher (Figure 3).

Based on the results of this study, we have derived a diagnostic/prognostic flowchart (Figure 4). An important

caveat is that the recommendation for delivery at 37 weeks is based not on statistically proven data (only five cases in our series showed prenatal progression), but on the visual impression of Figure 3. It should also be noted that, when severe brain lesions are identified on fetal 3D neurosonography and/or MRI, late TOP can be considered in those countries in which this option is legal.

In conclusion, we have shown that, in cases of fetal VGAM, major brain abnormalities/damage, tricuspid regurgitation and, to a lesser extent, VGAM volume $\geq 20\,000\text{ mm}^3$ represent the only variables significantly associated with a poor outcome, defined as late TOP, neonatal death or severe postnatal sequelae. Tricuspid regurgitation is also associated with an increased risk of associated major brain lesions. A VGAM volume $\geq 40\,000\text{ mm}^3$ appears to indicate a higher risk of prenatal progression of the lesion, warranting planned early delivery.

REFERENCES

1. Raybaud CA, Strother CM, Hald JK. Aneurysms of the vein of Galen: embryonic considerations and anatomical features relating to the pathogenesis of the malformation. *Neuroradiology* 1989; 31: 109–128.
2. Yuval Y, Lerner A, Lipitz S, Rotstein Z, Hegesh J, Achiron R. Prenatal diagnosis of vein of Galen aneurysmal malformation: report of two cases with proposal for prognostic indices. *Prenat Diagn* 1997; 17: 972–977.
3. Campi A, Scotti G, Filippi M, Gerevini S, Strigimi F, Lasjaunias P. Antenatal diagnosis of vein of Galen aneurysmal malformation: MR study of fetal brain and postnatal follow-up. *Neuroradiology* 1996; 38: 87–90.
4. Rodesch G, Hui F, Alvarez H, Tanaka A, Lasjaunias P. Prognosis of antenatally diagnosed vein of Galen aneurysmal malformations. *Childs Nerv Syst* 1994; 10: 79–83.
5. Sepulveda W, Platt CC, Fisk NM. Prenatal diagnosis of cerebral arteriovenous malformation using color Doppler ultrasonography: case report and review of the literature. *Ultrasound Obstet Gynecol* 1995; 6: 282–286.
6. McSweeney N, Brew S, Bhate S, Cox T, Roebuck DJ, Ganesan V. Management and outcome of vein of Galen malformation. *Arch Dis Child* 2010; 95: 903–909.
7. Geibprasert S, Krings T, Armstrong D, Terbrugge KG, Raybaud CA. Predicting factors for the follow-up outcome and management decisions in vein of Galen aneurysmal malformations. *Childs Nerv Syst* 2010; 26: 35–46.
8. Berenstein A, Fifi JT, Niimi Y, Presti S, Ortiz R, Ghatan S, Rosenn B, Sorscher M, Molofsky W. Vein of Galen malformations in neonates: new management paradigms for improving outcomes. *Neurosurgery* 2012; 70: 1207–1214.
9. Deloison B, Chalouhi GE, Sonigo P, Zerah M, Millischer AE, Dumez Y, Brunelle F, Ville Y, Salomon L. Hidden mortality of prenatally diagnosed vein of Galen aneurysmal malformation: retrospective study and review of the literature. *Ultrasound Obstet Gynecol* 2012; 40: 652–658.
10. International Society of Ultrasound in Obstetrics and Gynecology (ISUOG). Sonographic examination of the fetal central nervous system: guidelines for performing the 'basic examination' and the 'fetal neurosonogram'. *Ultrasound Obstet Gynecol* 2007; 29: 109–116.
11. Chaoui R, Bollmann R, Göldner B, Heling KS, Tennstedt C. Fetal cardiomegaly: echocardiographic findings and outcome in 19 cases. *Fetal Diagn Ther* 1994; 9: 92–104.
12. Respondek ML, Kammermeier M, Ludomirsky A, Weil SR, Huhta JC. The prevalence and clinical significance of fetal tricuspid valve regurgitation with normal heart anatomy. *Am J Obstet Gynecol* 1994; 171: 1265–1270.
13. Gerards FA, Engels MA, Barkhof F, van den Dungen FA, Vermeulen RJ, van Vugt JM. Prenatal diagnosis of aneurysms of the vein of Galen (vena magna cerebri) with conventional sonography, three-dimensional sonography, and magnetic resonance imaging: report of 2 cases. *J Ultrasound Med* 2003; 22: 1363–1368.
14. Nangiana J, Lim M, Silva R, Guzman R, Chang S. Vein of Galen malformations—part II: management. *Contemp Neurosurg* 2008; 30: 1–6.



Outcome of fetuses with prenatal diagnosis of isolated severe bilateral ventriculomegaly: systematic review and meta-analysis

S. CARTA¹, A. KEALIN AGTEN, C. BELCARO and A. Bhide¹

Fetal Medicine Unit, St George's University Hospital NHS Foundation Trust, London, UK

KEYWORDS: anomaly; brain; systematic review; ultrasound; ventriculomegaly

ABSTRACT

Objective To quantify from the published literature survival and neurodevelopmental outcome of fetuses with prenatally detected isolated severe bilateral ventriculomegaly.

Methods MEDLINE, EMBASE and the Cochrane Library were searched electronically. Only cases with a prenatal diagnosis of apparently isolated severe ventriculomegaly and postnatal neurodevelopmental assessment were selected and included. Severe ventriculomegaly was defined as enlargement of the ventricular atria, with a diameter of greater than 15 mm in the transventricular plane. All cases in which the investigators were unable to detect associated structural abnormality, chromosomal abnormality or fetal infection, and in which the ventriculomegaly was therefore regarded as apparently isolated, were included. Those for which the etiology was identified prenatally were excluded, whereas those with postnatal identification of the underlying cause were not excluded, since this information was not available prenatally. The quality of the included studies was assessed using the Newcastle–Ottawa Scale (NOS) for cohort studies. Pregnancy outcomes such as termination, stillbirth, neonatal survival and developmental outcome of the baby, were recorded. The degree of disability was classified as no, mild or severe disability. Statistical assessment was performed by meta-analysis of proportions to combine data, weighting the studies using the inverse variance method and a random-effects model. Proportions and CIs were reported.

Results Eleven studies including 137 fetuses were found. Twenty-seven pregnancies underwent termination and were excluded. The remaining 110 fetuses with apparently isolated severe ventriculomegaly for which continuation

of pregnancy was intended, form the study population. Overall quality assessed using NOS for cohort studies was good. Survival was reported in 95/110 (pooled proportion 87.9% (95% CI, 75.6–96.2%)) cases. In 15/110 (pooled proportion 12.1% (95% CI, 3.8–24.4%)), either stillbirth or neonatal demise was reported. No disability was reported in 41/95 survivors (pooled proportion 42.2% (95% CI, 27.5–57.6%)). However, 17/95 showed mild/moderate disability (pooled proportion 18.6% (95% CI, 7.2–33.8%)) and 37/95 were reported to have severe disability (pooled proportion 39.6% (95% CI, 30.0–50.0%)).

Conclusions Four-fifths of fetuses with severe ventriculomegaly survive and, of these, just over two-fifths show normal neurodevelopment. The overall survivors without disability account for more than one third of the total. Given that many cases undergo termination of pregnancy and require longer follow-up in order to detect subtle abnormalities, mortality and prevalence of developmental delay may be even higher than that reported in this paper. Copyright © 2018 ISUOG. Published by John Wiley & Sons Ltd.

INTRODUCTION

Ventriculomegaly is one of the most frequently diagnosed abnormalities of the fetal central nervous system¹. It is defined as enlargement of the ventricular atria of more than 10 mm, measured in the transventricular plane at the level of the glomus of the choroid plexus, perpendicular to the ventricular cavity, with positioning of the calipers inside the echoes generated by the lateral walls². Severe ventriculomegaly is usually defined as enlargement of the ventricular atria with a diameter of greater than 15 mm in the transventricular plane, compared with mild to

Correspondence to: Dr S. Carta, Fetal Medicine Unit, Lanesborough Wing, 4th Floor, St George's Hospital, Blackshaw Road, London SW17 0QT, UK (e-mail: sisicar@live.it)

Accepted: 16 February 2018

moderate ventriculomegaly, in which the atrium measures 10 to 15 mm³. The prevalence of severe ventriculomegaly at birth is 0.3–1.5 per 1000 pregnancies^{4,5}. It is frequently challenging to identify antenatally and is worse in cases with associated abnormalities, while the prognosis depends strongly on the etiology⁶.

There are many publications on isolated mild or moderate ventriculomegaly⁷. However, data on isolated severe ventriculomegaly are scarce. Most often the literature describes cases of severe ventriculomegaly associated with extracranial abnormalities, leading to poor outcome (livebirth rate 30–40%^{4,8,9}). The high mortality rate is partly due to the inclusion of terminations of pregnancy, cephalocentesis and cases that were not actively treated postnatally¹⁰. Conversely, the pediatric surgical literature reports high survival rates and low rates of neurodevelopmental disability, with a 10-year survival rate after surgery of 60% or more, and normal intelligence in half of surviving patients¹¹. In the study of Lumenta and Skotarczak¹², normal development is reported in 62.8% of children, while 29.8% had mild developmental delay, and severe developmental delay was reported in only 7.4%. After surgery, the proportion of children with normal intelligence, measured by IQ, was reported as being between 50 and 63%, with integration into normal school for 60% of the children¹³.

In the series showing mainly poor prognosis^{4,14,15}, additional abnormalities were seen in the majority of cases. The literature on neurodevelopmental outcomes of isolated cases remains quite sparse¹⁶, negatively impacting on parental counseling and remaining for parents a source of considerable anxiety^{17,18}.

The aim of this study was to collate published data on survival and neurodevelopmental outcomes of prenatally detected cases of apparently isolated severe ventriculomegaly.

METHODS

Protocol, eligibility criteria, information sources and search

We performed a systematic review following the recommendations for systematic reviews and meta-analyses^{19,20}. The search strategy was set up using a combination of relevant medical subject heading (MeSH) terms, keywords and word variants for 'prenatal', 'diagnosis', 'ultrasound', 'severe ventriculomegaly' and 'neurodevelopment'. On 11 July and 24 August 2017, we searched MEDLINE, EMBASE and the Cochrane Library including the Cochrane Database of Systematic Reviews (CDSR), Database of Abstracts of Reviews of Effects (DARE) and The Cochrane Central Register of Controlled Trials (CENTRAL). No language restrictions were applied. We limited the search to the years 1990 and later, because the diagnostic techniques (high-resolution ultrasound, fetal magnetic resonance imaging (MRI), chromosomal microarray analysis) were not widely available before

then. No restrictions were applied in terms of study design and size, except for case series, observational studies and case reports of fewer than three cases, which were excluded to minimize publication bias. Additional relevant articles were identified by manual search in the reference lists of the included publications. The study was registered with the PROSPERO database (http://www.crd.york.ac.uk/PROSPERO/display_record.asp?ID=CRD42017048712, (registration number CRD42017048712)).

Study selection, data collection and data items

Two independent reviewers (S.C. and A.K.A.) performed the literature search and identified potentially relevant papers. The abstracts were screened independently, and relevant ones were selected for extraction of the full-text articles. Relevant data were extracted, potential inconsistencies were discussed by the authors and consensus was reached by weighing arguments. In instances in which the data of interest were not reported explicitly by the authors of the papers, we contacted them for clarification or additional details.

Study assessment and selection for inclusion were performed according to the following criteria: population, outcomes and study design. The inception cohort was assembled at the time of prenatal detection of ventriculomegaly, comprising cases for which the intention was to continue the pregnancy. Severe ventriculomegaly was defined as an atrial measurement in the transventricular plane of ≥ 15 mm. Ventriculomegaly was considered apparently isolated if the investigators were unable to detect other cranial/extracranial structural abnormality, chromosomal abnormality or fetal infection in the prenatal period. We excluded all non-isolated cases for which the etiology was identified prenatally, such as chromosomal abnormality, spina bifida, structural brain defect detected on ultrasound or MRI (e.g. encephalocele, neuronal migration defect) and congenital infections. We also excluded ventriculomegaly complicating monozygotic twin pregnancy owing to the high likelihood that this was a consequence of placental sharing.

Studies in which intrauterine treatment was performed systematically were excluded, as these might have altered the natural history of the disease and as the techniques have not yet been standardized. Studies reporting only on unilateral ventriculomegaly were also excluded *a priori*. We included cases considered apparently isolated in the prenatal period. Cases with postnatal identification of an underlying cause were not excluded, since this information had not been available prenatally. Pregnancy outcome (termination/stillbirth), neonatal survival and developmental outcome of the newborns were recorded. Cases were not eligible for inclusion if ventriculomegaly was detected only postnatally.

For assessment of the presence and degree of disability, no limitations or restrictions were placed on the diagnostic tools and/or duration of postnatal follow-up. The degree

of disability was classified as no, mild or severe disability. We reported the results obtained using the tools for the assessment of neurodevelopment used by the primary authors, seeking clarification from them when necessary. Motor disability was classified as severe when independent functioning of the individual was not deemed possible. Sensorineural disability was considered severe when the developmental assessment tool reported it as such, or when attendance at mainstream school was not deemed possible. Children who did not fit into either the severe- or the no-disability category were classified as mild/moderate cases. If information on the specific clinical finding rather than specific degree of the disability at postnatal follow-up was available, the disability class was assigned based on the reported information.

Risk of bias, summary measures and synthesis of results

The quality of the included studies was assessed using the Newcastle–Ottawa Scale (NOS) for cohort studies²¹. NOS judges each study according to the following categories: selection of the study groups, comparability of the groups and ascertainment of the outcome of interest. Selection of the study groups is performed by evaluating the representativeness of the exposed cohort, the selection of the non-exposed cohort, ascertainment of exposure and demonstration that the outcome of interest was not present at the start of the study. Comparability of the groups is assessed by evaluating the cohorts based on the design or analysis. Ascertainment of the outcome of interest includes evaluation of the assessment of the outcome parameters, and the length and adequacy of follow-up. A study can be awarded a maximum of one star for each item within the selection and outcome categories, and a maximum of two stars can be given for comparability²¹.

Statistical assessment was performed by meta-analyses of proportions to combine data. The studies were weighted by the inverse variance method for pooling. Between-study heterogeneity was explored using forest plots and was evaluated statistically using I^2 , which represents the percentage of between-study variation that is due to heterogeneity rather than to chance²². An I^2 of 0% indicates absence of heterogeneity, while values of 50% or above suggest considerable heterogeneity²³.

We used a random-effects model, since it is more conservative and the observed heterogeneity was $> 50\%$. Statistical analysis was carried out using StatsDirect 3.1.8 (StatsDirect Ltd, Altrincham, UK). We did not use either funnel plots or formal statistical tests to explore publication bias; a total of 11 studies is not an adequate number for interpreting funnel plots. Moreover, funnel plots can be misleading for exploration of publication bias, particularly when the number of studies is relatively small²⁴.



Figure 1 Flowchart summarizing selection of studies reporting on fetuses diagnosed prenatally with apparently isolated severe ventriculomegaly (VM) found by searching MEDLINE, EMBASE and the Cochrane Library. *Reasons for exclusion: all cases had associated abnormalities ($n = 2$); all cases had mild to moderate VM, but none had severe VM ($n = 1$); data collection started before 1990 ($n = 5$); no antenatal information available ($n = 1$); no postnatal follow-up information ($n = 3$); mild/moderate and severe VM were pooled together and it was not possible to connect each severe case with corresponding outcome ($n = 7$); intrauterine treatments were performed systematically ($n = 3$).

RESULTS

Study selection and characteristics

A total of 448 possible citations were identified by the initial electronic database search. After review of titles and abstracts, 417 articles did not meet the inclusion criteria and were excluded. Full-text manuscripts were retrieved for the 31 publications that potentially met the inclusion criteria. Two additional studies were identified by manual searches of reference lists^{8,15}. After analysis of the full-text manuscripts, 22 studies that did not fulfill the inclusion criteria were excluded. The remaining 11 articles were finally included in the systematic review^{8,15–17,25–31} (Figure 1).

Quality assessment of the included studies using the NOS is shown in Table S1. The included studies had an overall good quality for selection of groups and ascertainment of the outcome of interest. Common reasons for scoring low on quality assessment were cases derived from high-risk populations and lack of description of the outcome of individual cases. Follow-up varied widely in the studies, ranging from 1 month to 18 years. Several different tools for the assessment of neonatal neurodevelopmental outcome were used, ranging from self-rating questionnaires to standardized tests.

All the data from the included articles, published between 1999 and 2017, were collected over a time period spanning 1990 to 2013. Almost all the studies reported on ventriculomegaly in general, and included fetuses with severe ventriculomegaly (atrial diameter ≥ 15 mm). We extracted information about apparently isolated severe ventriculomegaly from them. Gestational age at ultrasound assessment varied from 12 weeks to term. General characteristics of the included studies are shown in Table 1.

Different developmental assessment tools were used in each study (Table S2). Karyotype was assumed to be normal if karyotyping was not performed before or after birth, provided that the phenotype after birth was normal. Data on infection screening, details of ventriculoperitoneal shunt placement and postmortem investigation were collected when available.

Four studies^{15,26–28} categorized outcome as one of two degrees of severity of delay (normal or significant abnormal, good or poor prognosis and normal or evident

Table 1 General characteristics of 11 studies reporting on fetuses diagnosed prenatally with apparently isolated severe ventriculomegaly (VM), included in systematic review

Study	Data collection period	Study design	GA at diagnosis (weeks)	Definition of severe VM	Definition of isolated VM	Follow-up (months)
Beke (1999) ²⁹	1993–1996	Retrospective cohort study	27–36	Ventricular atria width > 15 mm in transventricular US plane	No evidence of associated anomaly, aneuploidy, chromosomal abnormality, structural malformation, negative TORCH screening	3–36
Breeze (2007) ¹⁷	2001–2005	Retrospective cohort study	16–36	Ventricular atria width > 15 mm in transventricular US plane	Normal karyotype, TORCH screening and FMAIT screening (offered to all patients), detailed fetal US for anomalies by fetal medicine subspecialist, MRI (offered if potential influence on parents' decision-making process)	4–24
Gaglioti (2005) ⁸	1990–2000	Retrospective cohort study	15–36	Ventricular atria width > 15 mm in transventricular US plane	Normal detailed US evaluation of fetal anatomy, echo, karyotype, TORCH (offered to all patients)	2–144
Gezer (2015) ²⁷	2007–2009	Retrospective cohort study	17–34	Ventricular atria width > 15 mm in transventricular US and MRI planes	No associated abnormality on US and MRI investigations, no evidence of chromosomal anomaly, confirmed after birth	up to 24
Gezer (2016) ²⁸	2007–2009	Prospective cohort study	NR	Ventricular atria width > 15 mm in transventricular US and MRI planes	No evidence of chromosomal anomaly or congenital infection, normal first- and second-trimester screening	6–24
Graham (2001) ²⁵	1994–1999	Retrospective cohort study	18–22	Ventricular atria width > 15 mm in transventricular US plane	Normal karyotype and detailed anomaly scan, negative on infection screening (offered to all patients)	1–36
Kennelly (2009) ¹⁶	2000–2008	Retrospective cohort study	18–36	Ventricular atria width > 15 mm in transventricular US plane	Normal fetal anomaly US performed by fetal medicine subspecialist, echo, karyotype, TORCH screening, screening for alloimmune thrombocytopenia, fetal MRI (offered to all patients)	10–72
Letouzey (2017) ³⁰	1994–2011	Prospective cohort study	22–37	Ventricular atria width > 15 mm in transventricular US plane	Normal detailed US, MRI, karyotype, infection screening (offered to all patients)	3–216
Chu (2016) ¹⁵	2004–2013	Retrospective cohort study	18–36	Ventricular atria width > 15 mm in transventricular US plane	Normal detailed US, karyotype, TORCH screening (offered to all patients)	16–108
Bar-Yosef (2017) ³¹	2010–2013	Prospective cohort study	NR	Ventricular atria width > 15 mm in transventricular US plane	Normal detailed US, karyotype, TORCH screening (offered to all patients)	18–36
Weichert (2010) ²⁶	1993–2007	Prospective cohort study	12–38	Ventricular atria width > 15 mm in transventricular US plane	Normal detailed US, MRI, aCGH, genetic counseling, infection screening (offered to all patients)	1–151

Only first author's name given for each study. aCGH, array comparative genomic hybridization; echo, fetal echocardiography; FMAIT, fetomaternal alloimmune thrombocytopenia; GA, gestational age; MRI, magnetic resonance imaging; NR, not reported; TORCH, toxoplasmosis, other agent, rubella, cytomegalovirus, herpes; US, ultrasound examination.

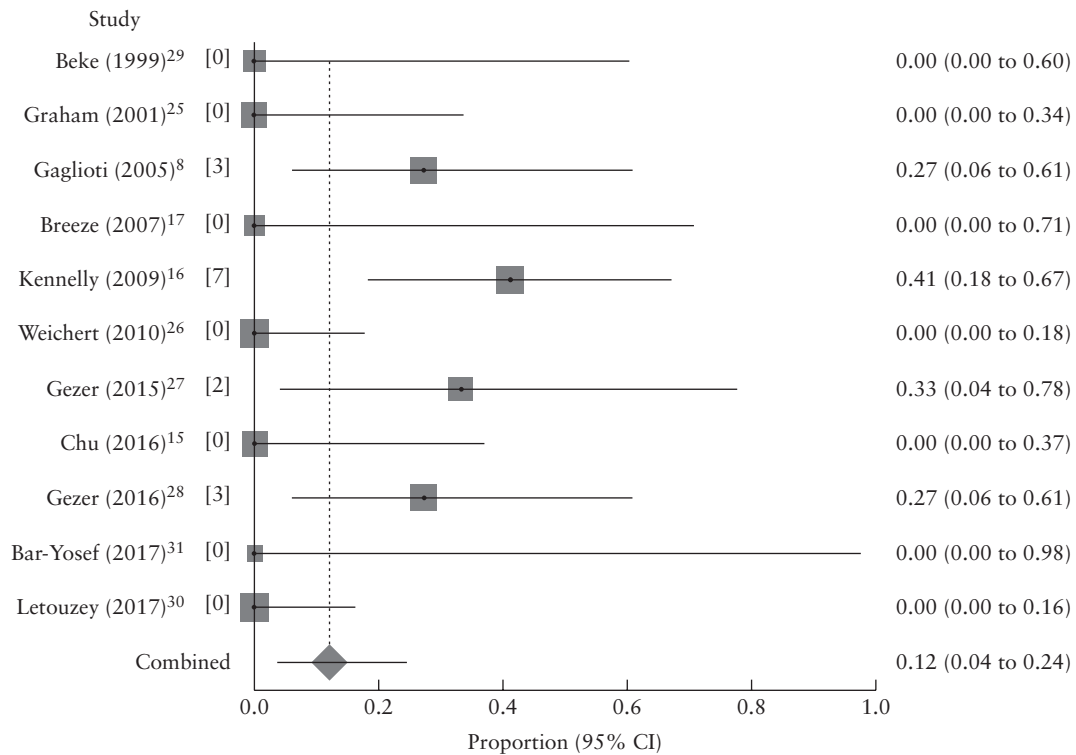


Figure 2 Forest plot (random-effects model) showing incidence of death in fetuses with isolated severe ventriculomegaly detected antenatally for each of 11 included studies and pooled for all studies. Pooled incidence was 12.1% (95% CI, 3.8–24.4%); $I^2 = 63.7\%$. Size of boxes is proportional to study sample size.

Table 2 Overview of meta-analysis of survival, disability and outcome as proportions of total number of included cases reported in 11 studies of fetuses diagnosed prenatally with apparently isolated severe ventriculomegaly

Study	Death*		Live birth/survived		Total disability		Normal		Cases included in review (n)	TOP (n)†
	n	Proportion (95% CI)	n	Proportion (95% CI)	n	Proportion (95% CI)	n	Proportion (95% CI)		
Beke (1999) ²⁹	0	0.0 (0.00–0.60)	4	1.00 (0.40–1.00)	3	0.750 (0.19–0.99)	1	0.250 (0.01–0.81)	4	0
Graham (2001) ²⁵	0	0.0 (0.00–0.34)	9	1.00 (0.66–1.00)	8	0.889 (0.52–1.00)	1	0.111 (0.00–0.48)	9	0
Gaglioti (2005) ⁸	3	0.273 (0.06–0.61)	8	0.727 (0.39–0.94)	3	0.273 (0.06–0.61)	5	0.455 (0.17–0.77)	11	13
Breeze (2007) ¹⁷	0	0.0 (0.00–0.71)	3	1.00 (0.29–1.00)	3	1.00 (0.29–1.00)	0	0.00 (0.00–0.71)	3	0
Kennelly (2009) ¹⁶	7	0.412 (0.18–0.67)	10	0.588 (0.33–0.82)	9	0.529 (0.28–0.77)	1	0.059 (0.00–0.29)	17	1
Weichert (2010) ²⁶	0	0.0 (0.00–0.18)	19	1.00 (0.82–1.00)	13	0.684 (0.43–0.87)	6	0.316 (0.13–0.57)	19	7
Gezer (2015) ²⁷	2	0.333 (0.04–0.78)	4	0.667 (0.22–0.96)	1	0.167 (0.00–0.64)	3	0.500 (0.12–0.88)	6	1
Chu (2016) ¹⁵	0	0.0 (0.00–0.37)	8	1.00 (0.63–1.00)	3	0.375 (0.09–0.76)	5	0.625 (0.24–0.91)	8	5
Gezer (2016) ²⁸	3	0.273 (0.06–0.61)	8	0.727 (0.39–0.94)	3	0.273 (0.06–0.61)	5	0.455 (0.17–0.77)	11	NR
Bar-Yosef (2017) ³¹	0	0.0 (0.00–0.98)	1	1.00 (0.03–1.00)	0	0.00 (0.00–0.98)	1	1.000 (0.03–1.00)	1	0
Letouzey (2017) ³⁰	0	0.0 (0.00–0.16)	21	1.00 (0.84–1.00)	8	0.381 (0.18–0.62)	13	0.619 (0.38–0.82)	21	NR
Total	15	0.121 (0.04–0.24)	95	0.879 (0.76–0.96)	54	0.499 (0.36–0.64)	41	0.367 (0.23–0.52)	110	27

Only first author’s name given for each study. *Intrauterine death or neonatal demise. †Cases of termination of pregnancy (TOP) were not included in systematic review. NR, not reported.

psychomotor delay). We classified ‘significant abnormal’, ‘poor prognosis’ and ‘evident psychomotor delay’ as severe disability. In one report¹⁷, the authors described the outcome with the actual clinical finding (hemiparesis, impaired visual attention) rather than with a classified degree of disability. This was recorded as severe disability after obtaining clarification from the authors. Pregnancy terminations were reported when available but excluded from the calculation of survival rate.

Synthesis of results

Significant heterogeneity was found between the included studies, with I^2 being above 50% for almost all the outcomes analyzed, hence the decision for a random-effects model. Heterogeneity was low for the proportion of severe disability among survivors, but the 95% CI was relatively wide ($I^2 = 4.2\%$ (95% CI, 0–53.2%)).

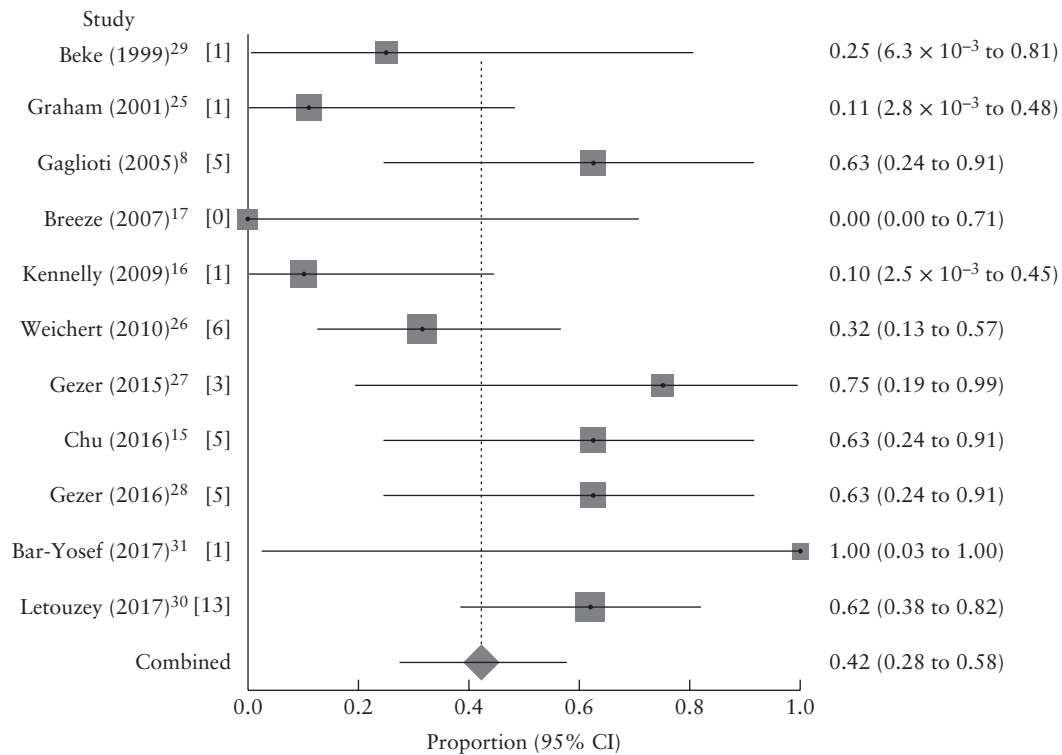


Figure 3 Forest plot (random-effects model) showing prevalence of normal neurodevelopment in surviving fetuses with isolated severe ventriculomegaly detected antenatally for each of the 11 studies (number of cases per study shown in square brackets) and pooled for all studies. Pooled prevalence was 42.2% (95% CI, 27.5–57.6%); $I^2 = 54.7\%$. Size of boxes is proportional to study sample size.

Table 3 Overview of meta-analysis of disability and outcome in surviving fetuses reported in 11 studies of fetuses diagnosed prenatally with apparently isolated severe ventriculomegaly

Study	Normal		Mild disability		Severe disability		Total disability		Survivors (n)
	n	Proportion (95% CI)	n	Proportion (95% CI)	n	Proportion (95% CI)	n	Proportion (95% CI)	
Beke (1999) ²⁹	1	0.250 (0.01–0.81)	2	0.500 (0.07–0.93)	1	0.250 (0.01–0.81)	3	0.750 (0.19–0.99)	4
Graham (2001) ²⁵	1	0.111 (0.00–0.48)	5	0.556 (0.21–0.86)	3	0.333 (0.07–0.70)	8	0.889 (0.52–1.00)	9
Gaglioti (2005) ⁸	5	0.625 (0.24–0.91)	1	0.125 (0.00–0.53)	2	0.250 (0.03–0.65)	3	0.375 (0.09–0.76)	8
Breeze (2007) ¹⁷	0	0.00 (0.00–0.71)	2	0.667 (0.09–0.99)	1	0.333 (0.01–0.91)	3	1.00 (0.29–1.00)	3
Kennelly (2009) ¹⁶	1	0.100 (0.00–0.45)	4	0.400 (0.12–0.74)	5	0.500 (0.19–0.81)	9	0.900 (0.55–1.00)	10
Weichert (2010) ²⁶	6	0.316 (0.13–0.57)	0	0.00 (0.00–0.18)	13	0.684 (0.43–0.87)	13	0.684 (0.43–0.87)	19
Gezer (2015) ²⁷	3	0.750 (0.19–0.99)	0	0.00 (0.00–0.60)	1	0.250 (0.01–0.81)	1	0.250 (0.01–0.81)	4
Chu (2016) ¹⁵	5	0.625 (0.24–0.91)	0	0.00 (0.00–0.37)	3	0.375 (0.09–0.76)	3	0.375 (0.09–0.76)	8
Gezer (2016) ²⁸	5	0.625 (0.24–0.91)	0	0.00 (0.00–0.37)	3	0.375 (0.09–0.76)	3	0.375 (0.09–0.76)	8
Bar-Yosef (2017) ³¹	1	1.00 (0.03–1.00)	0	0.00 (0.00–0.98)	0	0.00 (0.00–0.98)	0	0.00 (0.00–0.98)	1
Letouzey (2017) ³⁰	13	0.619 (0.38–0.82)	3	0.143 (0.03–0.36)	5	0.238 (0.08–0.47)	8	0.381 (0.18–0.62)	21
Total	41	0.422 (0.28–0.58)	17	0.186 (0.07–0.34)	37	0.396 (0.30–0.50)	54	0.578 (0.42–0.72)	95

Only first author's name given for each study.

Meta-analysis of proportions was performed and forest plots were used to describe the rates of death, survival and neurodevelopmental delay in isolated severe ventriculomegaly. Individual results for each of the 11 studies included in the meta-analysis are provided in terms of proportions and 95% CIs, together with pooled results for all studies, in which the size of the boxes is proportional to the study sample size.

Data for 110 fetuses with apparently isolated prenatal severe ventriculomegaly were available. Of these fetuses, 95 survived and 15 were stillborn or underwent neonatal demise.

The pooled proportion of deaths accounted for 12.1% (15/110) (95% CI, 3.8–24.4%) (Figure 2) while that of survival was 87.9% (95/110) (95% CI, 75.6–96.2%) (Table 2).

No disability was reported in 41/95 survivors (pooled proportion 42.2% (95% CI, 27.5–57.6%)) (Figure 3). However, 17/95 showed mild/moderate disability (pooled proportion 18.6% (95% CI, 7.2–33.8%)) (Figure S1) and 37/95 were reported to have severe disability (pooled proportion 39.6% (95% CI, 30.0–50.0%)) (Figure 4).

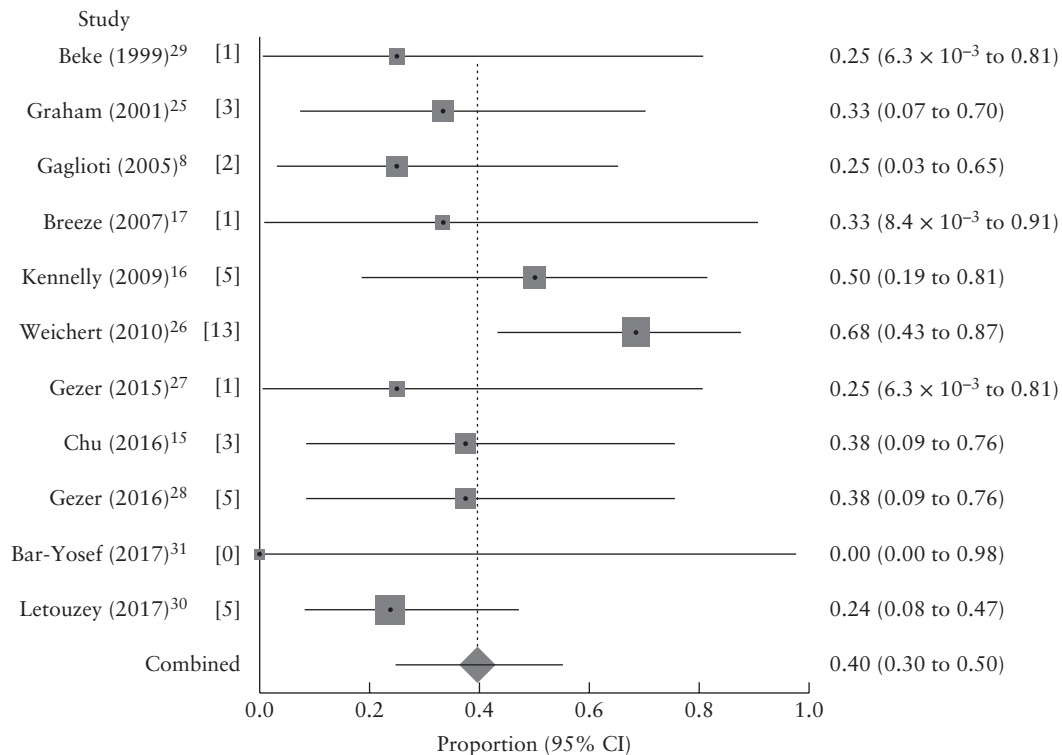


Figure 4 Forest plot (random-effects model) showing prevalence of severe disability in surviving fetuses with isolated severe ventriculomegaly detected antenatally for each of the 11 studies (number of cases per study shown in square brackets) and pooled for all studies. Pooled prevalence was 39.6% (95% CI, 30.0–50.0%); $I^2 = 4.2\%$. Size of boxes is proportional to study sample size.

An overview of individual and pooled proportions of the different outcomes is shown in Tables 2 and 3.

Additional anomalies were detected in nine (9.5%) cases postnatally only. The details of the additional anomalies are shown in Table S3. None of the infants with postnatally detected anomalies was free of disability.

DISCUSSION

Summary of evidence

We report on the outcome of children with prenatally detected apparently isolated severe ventriculomegaly. Survival without disability was seen in just over one-third of cases. Although the initial diagnosis was isolated severe ventriculomegaly, additional structural abnormalities were detected postnatally in some. The degree of information available about the postnatal diagnosis of associated abnormalities was variable. Details on number of patients affected and impact on outcomes as well as postnatal confirmation of the absence of associated abnormalities was available from only some reports (Table S2). Additional anomalies were detected postnatally in only nine (9.5%) cases, none of which was without disability.

In cases of mild ventriculomegaly, the outcome is favorable in the absence of an identifiable cause⁷. However, once the ventriculomegaly becomes severe, the outlook is unfavorable for the majority. The duration

of follow-up was variable (Table 1) and may impact on the reported degree of disability. Subtle abnormalities may not be uncovered until the child begins schooling. Therefore, the prevalence of developmental delay may be higher than that reported here.

The pediatric surgical literature reports that developmental outcome following ventriculoperitoneal shunt for obstructive hydrocephalus is normal in the large majority of cases^{12,13}. The presumed underlying cause in those patients is isolated obstruction to cerebrospinal fluid flow in cases for which the other investigations are normal. The results from the prenatal literature do not match those reported in postnatal series. The most likely reason for the disparity in the results is the selection of children undergoing a surgical procedure. Obstruction to cerebrospinal fluid flow (aqueductal stenosis) may be due to congenital or acquired reasons. The results of this study suggest that the implications of the two are vastly different, and that the outlook for acquired aqueductal stenosis may be much more favorable than that of congenital lesions. It could also be argued that children with severe ventriculomegaly who are asymptomatic after birth (hence with a good prognosis) might never present for postnatal surgery. However, it is highly unlikely that fetuses with prenatal detection of severe ventriculomegaly would not be followed up. On the other hand, pediatric surgeons do not see cases too compromised to undergo surgery in their series, in which case selection bias would work against antenatally detected cases.

Fetal MRI was not performed in every case. Many of the cases that did undergo MRI investigation were excluded from the analysis because of antenatal detection of associated abnormalities. We did not investigate those further, as this was beyond the scope of this paper. Postnatally, additional abnormalities were found on MRI in four of the 17 (23.5%) cases of mild and five of the 37 (13.5%) cases of severe developmental delay. It is difficult to say if all the abnormal findings would have been detected prenatally had fetal MRI been performed. Very often, parental opposition to intervention is a deterrent for prenatal investigation. The structural abnormalities detected after birth are potentially detectable prenatally on MRI. Therefore, we would recommend prenatal fetal MRI in cases of severe ventriculomegaly to ascertain the truly isolated cases. Similarly, not all parents chose to undergo an invasive test. Chromosomal microarray analysis is capable of detecting known pathogenic alterations in an additional 5% of cases, even when the conventional karyotyping result is normal³². This investigation has only recently become available in clinical practice and may not have been available for the series included in this review. Also, fetal MRI is able to diagnose additional brain abnormalities in 5% of cases³³, but only in the last decade has it been introduced gradually as an additional fetal central nervous system investigation. Some of the apparently isolated cases may no longer have been classified as isolated had they undergone chromosomal microarray analysis, fetal MRI or appropriate neurosonography according to the current standard guidelines (International Society of Ultrasound in Obstetrics and Gynecology guidelines)². However, these are the reports of leading centers throughout the world, and the results are a pragmatic representation of real-life situations.

Strengths and limitations

We conducted a thorough search of the literature in duplicate, according to prespecified inclusion and exclusion criteria. We excluded case reports with fewer than three cases in order to avoid publication bias. Therefore, the results of the review are robust. Apparently isolated severe ventriculomegaly is not a common condition. A considerable proportion of pregnancies are terminated, thus modifying the natural history. Both these factors are responsible for the limited number of cases on which this report is based. It is possible that cases undergoing termination might have been the ones with the most severe ventriculomegaly.

Table S2 displays the methods used to assess neurodevelopment in the included studies. Some authors referred to neuropsychiatric or pediatricians' assessment without additional details^{15,26}. Regardless of the method used to define the degree of neurodevelopmental delay, the focus of this systematic review was to identify cases with normal outcomes. The state of normality should be comparable between different studies, regardless of the method of neurodevelopmental assessment.

Implications for clinical practice and future perspectives

The prevalence of developmental delay reported in this review may overestimate the real risk, given that not all the cases of apparently isolated ventriculomegaly were truly isolated after birth, and some of them had associated abnormalities. Owing to parental choice and the retrospective nature and availability of particular investigations, not all cases underwent fetal MRI or tests to assess chromosomal imbalance.

The association between additional abnormalities and worse outcome is well known. It may be argued that developmental delay may be related to the presence of associated abnormalities rather than the ventriculomegaly itself. However, the prevalence of developmental delay remains high, even if cases of associated abnormalities are excluded. There are no data to support the assertion that developmental delay may be less frequent in 'truly isolated' severe ventriculomegaly. The data contained in this systematic review are currently the best evidence on which to base parental counseling.

In conclusion, after excluding cases of termination of pregnancy, approximately four out of five of all fetuses with an antenatal diagnosis of apparently isolated ventriculomegaly survive. There is a high (three out of five) chance of neurodevelopmental delay in this group. The overall probability of survival without disability is 41/110 (36.7% (95% CI, 23–52%)).

REFERENCES

1. Cardoza JD, Goldstein RB, Filly RA. Exclusion of fetal ventriculomegaly with a single measurement: the width of the lateral ventricular atrium. *Radiology* 1988; **169**: 711–714.
2. International Society of Ultrasound in Obstetrics & Gynecology Education Committee. Sonographic examination of the fetal central nervous system: guidelines for performing the 'basic examination' and the 'fetal neurosonogram'. *Ultrasound Obstet Gynecology* 2007; **29**: 109–116.
3. Wax JR, Bookman L, Cartin A, Pinette MG, Blackstone J. Mild fetal cerebral ventriculomegaly: diagnosis, clinical associations, and outcomes. *Obstet Gynecol Surv* 2003; **58**: 407–414.
4. Hannon T, Tennant PWG, Rankin J, Robson SC. Epidemiology, natural history, progression, and postnatal outcome of severe fetal ventriculomegaly. *Obstet Gynecol* 2012; **120**: 1345–1353.
5. Pilu G, Hobbins JC. Sonography of fetal cerebrospinal anomalies. *Prenat Diagn* 2002; **22**: 321–330.
6. D'Addario V, Pinto V, Di Cagno L, Pintucci A. Sonographic diagnosis of fetal cerebral ventriculomegaly: an update. *J Matern Fetal Neonatal Med* 2007; **20**: 7–14.
7. Pagani G, Thilaganathan B, Prefumo F. Neurodevelopmental outcome in isolated mild fetal ventriculomegaly: systematic review and meta-analysis. *Ultrasound Obstet Gynecol* 2014; **44**: 254–260.
8. Gaglioti P, Danelon D, Bontempo S, Mombrò M, Cardaropoli S, Todros T. Fetal cerebral ventriculomegaly: outcome in 176 cases. *Ultrasound Obstet Gynecol* 2005; **25**: 372–377.
9. Kirkinen P, Serlo W, Jouppila P, Ryyanen M, Martikainen A. Long-term outcome of fetal hydrocephaly. *J Child Neurol* 1996; **11**: 189–192.
10. Futagi Y, Suzuki Y, Toribe Y, Morimoto K. Neurodevelopmental outcome in children with fetal hydrocephalus. *Pediatr Neurol* 2002; **27**: 111–116.
11. Moritake K, Nagai H, Miyazaki T, Nagasako N, Yamasaki M, Sakamoto H, Miyajima M, Tamakoshi A. Analysis of a nationwide survey on treatment and outcomes of congenital hydrocephalus in Japan. *Neurol Med Chir (Tokyo)* 2007; **47**: 453–460; discussion 460–461.
12. Lumenta CB, Skotarczak U. Long-term follow-up in 233 patients with congenital hydrocephalus. *Childs Nerv Syst* 1995; **11**: 173–175.
13. Hoppe-Hirsch E, Laroussinie F, Brunet L, Sainte-Rose C, Renier D, Cinalli G, Zerah A, Pierre-Kahn A. Late outcome of the surgical treatment of hydrocephalus. *Childs Nerv Syst* 1998; **14**: 97–99.
14. Chervenak FA, Duncan C, Ment LR, Hobbins JC, McClure M, Scott D, Berkowitz RL. Outcome of fetal ventriculomegaly. *Lancet* 1984; **2**: 179–181.
15. Chu N, Zhang Y, Yan Y, Ren Y, Wang L, Zhang B. Fetal ventriculomegaly: Pregnancy outcomes and follow-ups in ten years. *Biosci Trends* 2016; **10**: 125–132.
16. Kennelly MM, Cooley SM, McParland PJ. Natural history of apparently isolated severe fetal ventriculomegaly: perinatal survival and neurodevelopmental outcome. *Prenat Diagn* 2009; **29**: 1135–1140.

17. Breeze ACG, Alexander PMA, Murdoch EM, Missfelder-Lobos HH, Hackett GA, Lees CC. Obstetric and neonatal outcomes in severe fetal ventriculomegaly. *Prenat Diagn* 2007; 27: 124–129.
18. Laskin MD, Kingdom J, Toi A, Chitayat D, Ohlsson A. Perinatal and neurodevelopmental outcome with isolated fetal ventriculomegaly: a systematic review. *J Matern Fetal Neonatal Med* 2005; 18: 289–298.
19. Henderson LK, Craig JC, Willis NS, Tovey D, Webster AC. How to write a Cochrane systematic review. *Nephrology (Carlton)* 2010; 15: 617–624.
20. Centre for Reviews and Dissemination. *Systematic reviews: CRD's guidance for undertaking reviews in health care*. Centre for Reviews and Dissemination: University of York, York, UK, 2009.
21. Wells GA, Shea B, O'Connell D, Peterson J, Welch V, Losos M, Tugwell P. The Newcastle–Ottawa Scale (NOS) for assessing the quality of nonrandomised studies in meta-analyses. *The Ottawa Hospital Research Institute: Ottawa, Canada*, 2013; 1–4.
22. Coleman SR, Mazzola RF, Guyatt G, Rennie D, Meade M. Users' guides to the medical literature: A manual for evidence-based clinical practice. *Evidence Based Med* 2008; 62: 359.
23. Higgins JP, Thompson SG, Deeks JJ, Altman DG. Measuring inconsistency in meta-analyses. *BMJ* 2003; 327: 557–560.
24. Lau J. The case of the misleading funnel plot. *BMJ* 2006; 333: 597–600.
25. Graham E, Duhl A, Ural S, Allen M, Blakemore K, Witter F. The degree of antenatal ventriculomegaly is related to pediatric neurological morbidity. *J Matern Fetal Med* 2001; 10: 258–263.
26. Weichert J, Hartge D, Krapp M, Germer U, Gembruch U, Axt-Fliedner R. Prevalence, characteristics and perinatal outcome of fetal ventriculomegaly in 29,000 pregnancies followed at a single institution. *Fetal Diagn Ther* 2010; 27: 142–148.
27. Gezer NS, Güleriyüz H, Gezer C, Koçyiğit A, Yeşilırmak D, Ekin A, Bilgin M, Ertaş IE. The prognostic role of prenatal MRI volumetric assessment in fetuses with isolated ventriculomegaly. *Turk J Pediatr* 2015; 57: 266–271.
28. Gezer NS, Gezer C, Ekin A, Yesilirmak DC, Solmaz U, Dogan A, Guleryuz H. Obstetric and neurodevelopmental outcome in fetal cerebral ventriculomegaly. *Clin Exp Obstet Gynecol* 2016; 43: 490–494.
29. Beke A, Csabay L, Rigó J Jr, Harmath A, Papp Z. Follow-up studies of newborn-babies with congenital ventriculomegaly. *J Perinat Med* 1999; 27: 495–505.
30. Letouzey M, Chadie A, Brasseur-Daudruy M, Proust F, Verspyck E, Boileau P, Marret S. Severe apparently isolated fetal ventriculomegaly and neurodevelopmental outcome. *Prenat Diagn* 2017; 37: 820–826.
31. Bar-Yosef O, Barzilay E, Doremus S, Achiron R, Katorza E. Neurodevelopmental outcome of isolated ventriculomegaly: a prospective cohort study. *Prenat Diagn* 2017; 37: 764–768.
32. Lichtenbelt KD, Knoers NV, Schuring-Blom GH. From karyotyping to array-CGH in prenatal diagnosis. *Cytogenet Genome Res* 2011; 135: 241–250.
33. Scala C, Familiari A, Pinas A, Papageorghiou AT, Bhide A, Thilaganathan B, Khalil A. Perinatal and long-term outcome in fetuses diagnosed with isolated unilateral ventriculomegaly: systematic review and meta-analysis. *Ultrasound Obstet Gynecol* 2017; 49: 450–459.

SUPPORTING INFORMATION ON THE INTERNET

The following supporting information may be found in the online version of this article:



Table S1 Quality assessment of included studies according to Newcastle–Ottawa scale

Table S2 Developmental assessment tools adopted in 11 studies included in systematic review

Table S3 Missed associated abnormalities detected postnatally via postmortem or imaging

Figure S1 Forest plot (random-effects model) showing prevalence of mild to moderate disability among surviving fetuses with antenatally detected isolated severe ventriculomegaly, individually for each of the 11 studies, and pooled for all studies. Pooled prevalence was 18.6% (95% CI, 7.2% to 33.8%; $I^2 = 64\%$). Size of the boxes is proportional to the study sample size.



This article has been selected for Journal Club.

A slide presentation, prepared by Dr Fiona Brownfoot, one of UOG's Editors for Trainees, is available online.



Desenlace de los fetos con diagnóstico prenatal de ventriculomegalia bilateral severa aislada: revisión sistemática y metaanálisis

RESUMEN

Objetivo Cuantificar, a partir de la literatura publicada, la supervivencia y el desenlace del desarrollo neurológico de aquellos fetos con ventriculomegalia bilateral severa aislada detectada antes del parto.

Métodos Se realizaron búsquedas electrónicas en MEDLINE, EMBASE y la Cochrane Library. Se seleccionaron e incluyeron únicamente aquellos casos con diagnóstico prenatal de ventriculomegalia severa aparentemente aislada y evaluación postnatal del desarrollo neurológico. La ventriculomegalia severa se definió como un agrandamiento del atrio ventricular de más de 15 mm de diámetro en el plano transventricular. Se incluyeron todos los casos en los que los investigadores no pudieron detectar anomalías estructurales asociadas, anomalías cromosómicas o infección fetal, y en los que la ventriculomegalia fue considerada como aparentemente aislada. Se excluyeron los casos en los que la etiología subyacente se identificó prenatalmente, mientras que aquellos cuya causa fue identificada postnatalmente no fueron excluidos, ya que esta información no estaba disponible antes del parto. La calidad de los estudios incluidos se evaluó mediante la escala Newcastle-Ottawa (NOS, por sus siglas en inglés) para estudios de cohortes. Se registraron los resultados del embarazo, como la interrupción del mismo, el éxitus fetal, la supervivencia neonatal y el desenlace del desarrollo del bebé. El grado de discapacidad se clasificó como ninguna, leve o severa. El método de evaluación estadístico para combinar los datos se realizó mediante un metaanálisis de proporciones, ponderando los estudios por el método del inverso de la varianza y el modelo de efectos aleatorios. Se reportaron las proporciones y los IC.

Resultados Se encontraron once estudios que incluyen datos de 137 fetos. Se excluyeron veintisiete casos en los que se decidió interrupción del embarazo. La población de estudio se compuso de los 110 fetos restantes con ventriculomegalia severa aparentemente aislada para los que se esperaba la continuación del embarazo. La calidad general evaluada mediante la NOS para estudios de cohortes fue buena. La supervivencia se reportó en 95/110 casos (proporción combinada del 87,9% (IC 95%, 75,6–96,2%)). En 15/110 casos (proporción combinada del 12,1% (IC 95%, 3,8–24,4%)) se reportó éxitus fetal o muerte neonatal. No se reportó discapacidad en 41/95 supervivientes (proporción combinada del 42,2% (IC 95%, 27,5–57,6%)). Sin embargo, 17/95 casos mostraron una discapacidad leve o moderada (proporción combinada del 18,6% (IC 95%, 7,2–33,8%)) y en 37/95 casos se reportó una discapacidad severa (proporción combinada del 39,6% (IC 95%, 30,0–50,0%)).

Conclusiones Cuatro de cada cinco fetos con ventriculomegalia severa sobreviven y, de estos, más de dos quintas partes muestran un desarrollo neurológico normal. El total de los supervivientes sin discapacidad representa más de un tercio de los casos. Dado que muchos casos sufren una interrupción del embarazo y requieren un seguimiento más prolongado para detectar anomalías sutiles, la mortalidad y la prevalencia del retraso en el desarrollo podrían ser incluso mayores que las reportadas en este artículo.

产前诊断为孤立性重度侧脑室扩张的胎儿的结局：系统评价和 meta 分析

目的：根据已发表文献，确定产前诊断为孤立性重度侧脑室扩张的胎儿的生存率和神经发育结局。

方法：计算机检索 MEDLINE、EMBASE 和 Cochrane 数据库。仅选择并纳入产前诊断为明显孤立性重度侧脑室扩张并在出生后进行神经发育评估的病例。将重度侧脑室扩张定义为脑室增宽，经脑室平面径线大于 15 mm。纳入研究人员未发现合并结构异常、染色体异常或胎儿感染、因此认为脑室扩张为明显孤立性的所有病例。排除产前明确病因的病例，但不排除出生后证实潜在病因的病例，因为该信息无法在产前获得。采用队列研究的纽卡斯尔-渥太华量表 (Newcastle-Ottawa Scale, NOS) 评估纳入研究的质量。记录妊娠结局，如终止妊娠、死产、新生儿存活率、婴儿发育结局。将伤残程度分为无、轻度或重度。通过对比例指标进行 meta 分析进行统计学分析，以合并数据，采用逆方差方法和随机效应模型对研究进行加权。报告率和 CIs。

结果：检索到 11 项研究，共 137 例胎儿。27 例终止妊娠，被排除。其余 110 例有明显孤立性重度脑室扩张、打算继续妊娠的胎儿为研究人群。根据队列研究的 NOS 评估，研究总体质量较好。110 例胎儿中存活 95 例[合并率为 87.9% (95% CI, 75.6%–96.2%)]。110 例胎儿中，死产或新生儿死亡 15 例[合并率为 12.1% (95% CI, 3.8%–24.4%)]。95 例存活胎儿中，41 例无伤残[合并率为 42.2% (95% CI, 27.5%–57.6%)]。然而 95 例胎儿中，17 例为轻/中度伤残[合并率为 18.6% (95% CI, 7.2%–33.8%)]，37 例为重度伤残[合并率为 39.6% (95% CI, 30.0%–50.0%)]。

结论：五分之四的重度脑室扩张的胎儿能够存活，其中五分之二神经发育正常。无伤残的存活胎儿占总数的三分之一。由于许多病例终止妊娠，且需要更长时间随访以发现细微异常，因此死亡率和发育延缓的患病率甚至可能高于本文结果。

Physician Alert

Zika virus intrauterine infection causes fetal brain abnormality and microcephaly: tip of the iceberg?

An unexpected upsurge in diagnosis of fetal and pediatric microcephaly has been reported in the Brazilian press recently. Cases have been diagnosed in nine Brazilian states so far. By 28 November 2015, 646 cases had been reported in Pernambuco state alone. Although reports have circulated regarding the declaration of a state of national health emergency, there is no information on the imaging and clinical findings of affected cases. Authorities are considering different theories behind the 'microcephaly outbreak', including a possible association with the emergence of Zika virus disease within the region, the first case of which was detected in May 2015¹.

Zika virus is a mosquito-borne disease closely related to yellow fever, dengue, West Nile and Japanese encephalitis viruses². It was first identified in 1947 in the Zika Valley in Uganda and causes a mild disease with fever, erythema and arthralgia. Interestingly, vertical transmission to the fetus has not been reported previously, although two cases of perinatal transmission, occurring around the time of delivery and causing mild disease in the newborns, have been described³.

We have examined recently two pregnant women from the state of Paraíba who were diagnosed with fetal microcephaly and were considered part of the 'microcephaly cluster' as both women suffered from symptoms related to Zika virus infection. Although both patients had negative blood results for Zika virus, amniocentesis and subsequent quantitative real-time polymerase chain reaction⁴, performed after ultrasound diagnosis of fetal microcephaly and analyzed at the Oswaldo Cruz Foundation, Rio de Janeiro, Brazil, was positive for Zika virus in both patients, most likely representing the first diagnoses of intrauterine transmission of the virus. The sequencing analysis identified in both cases a genotype of Asian origin.

In Case 1, fetal ultrasound examination was performed at 30.1 weeks' gestation. Head circumference (HC) was 246 mm (2.6 SD below expected value) and weight was estimated as 1179 g (21st percentile). Abdominal circumference (AC), femur length (FL) and transcranial Doppler were normal for gestational age as was the width of the lateral ventricles. Anomalies were limited to the brain and included brain atrophy with coarse calcifications involving the white matter of the frontal lobes, including the caudate, lentostriatal vessels and cerebellum. Corpus callosal and vermian dysgenesis and enlarged cisterna magna were observed (Figure 1).

In Case 2, fetal ultrasound examination was performed at 29.2 weeks' gestation. HC was 229 mm (3.1 SD below

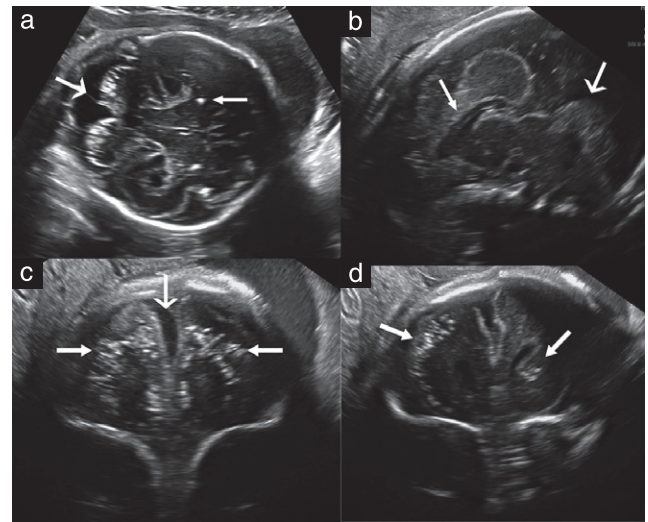


Figure 1 Case 1: (a) Transabdominal axial ultrasound image shows cerebral calcifications with failure of visualization of a normal vermis (large arrow). Calcifications are also present in the brain parenchyma (small arrow). (b) Transvaginal sagittal image shows dysgenesis of the corpus callosum (small arrow) and vermis (large arrow). (c) Coronal plane shows a wide interhemispheric fissure (large arrow) due to brain atrophy and bilateral parenchymatic coarse calcifications (small arrows). (d) Calcifications are visible in this more posterior coronal view and can be seen to involve the caudate (arrows).

expected value) and estimated fetal weight was 1018 g (19th percentile). AC was below the 3rd percentile but FL was normal. The cerebral hemispheres were markedly asymmetric with severe unilateral ventriculomegaly, displacement of the midline, thinning of the parenchyma on the dilated side, failure to visualize the corpus callosum and almost complete disappearance or failure to develop the thalami. The pons and brainstem were thin and continuous with a non-homogeneous small mass at the position of the basal ganglia. Brain calcifications were more subtle than in Case 1 and located around the lateral ventricles and fourth ventricle. Both eyes had cataracts and intraocular calcifications, and one eye was smaller than the other (Figure 2).

In the meantime, in Paraíba state, six children diagnosed with Zika virus were born to mothers who were apparently symptomatic during pregnancy, all of them with neonatal HC below the 10th percentile. Fetal neurosonograms showed two cases with cerebellar involvement and three with brain calcifications. One had severe arthrogryposis.

Intrauterine infections affecting the brain are relatively rare; cytomegalovirus (CMV), toxoplasmosis, herpes virus, syphilis and rubella are well known vectors of fetal disease. Among the Flaviviruses there have been only isolated reports linking West Nile encephalitis virus to fetal brain insults⁵.

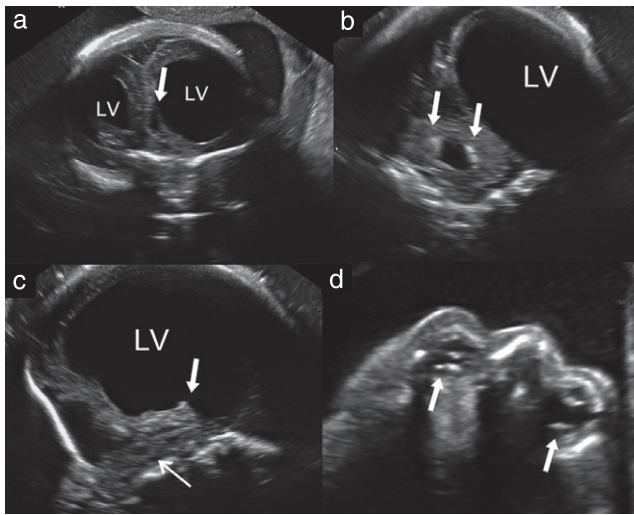


Figure 2 Case 2: (a) Anterior coronal view shows severe asymmetric ventriculomegaly with cystic formation (arrow). (b) Posterior horn of the lateral ventricle (LV) in coronal view is dilated. Note calcifications in the fourth ventricle (arrows). (c) The thalamus is absent (arrow) and the brainstem and pons are thin and difficult to visualize (sagittal view). (d) Axial view shows calcifications in both eyes (arrows). Note that the proximal eye is very small and lacks normal anatomic landmarks.

The presence of calcifications was suggestive of an intrauterine infection but severe damage of the cerebellum, brainstem and thalami is rarely associated with intrauterine infection. Both cases showed some similarities to CMV cases but with a more severe and destructive pattern and they lacked the nodules characteristic of toxoplasmosis. Interestingly, the reported case of fetal West Nile virus infection has similar characteristics⁵.

It is difficult to explain why there have been no fetal cases of Zika virus infection reported until now but this may be due to the underreporting of cases, possible early acquisition of immunity in endemic areas or due to the rarity of the disease until now. As genomic changes in the virus have been reported⁶, the possibility of a new, more virulent, strain needs to be considered. Until more cases are diagnosed and histopathological proof is obtained, the possibility of other etiologies cannot be ruled out.

As with other intrauterine infections, it is possible that the reported cases of microcephaly represent only the more severely affected children and that newborns with less severe disease, affecting not only the brain but also other organs, have not yet been diagnosed.

If patients diagnosed in other states are found to be seropositive for Zika virus, this represents a severe health threat that needs to be controlled expeditiously. The Brazilian authorities reacted rapidly by declaring a state of national health emergency. As there is no known medical treatment for this disease, a serious attempt will be needed to eradicate the mosquito and prevent the spread of the disease to other Brazilian states and across the border⁷.

A. S. Oliveira Melo†, G. Malinger*‡, R. Ximenes§, P. O. Szejnfeld¶, S. Alves Sampaio** and A. M. Bispo de Filippis**

†*Instituto de Pesquisa Professor Joaquim Amorim Neto (IPESQ), Instituto de Saúde Elpidio de Almeida (ISEA), Campina Grande, Brazil;* ‡*Division of Ultrasound in Obstetrics & Gynecology, Lis Maternity Hospital, Tel Aviv Sourasky Medical Center, Sackler Faculty of Medicine, Tel Aviv University, Tel Aviv, Israel;* §*Fetal Medicine Foundation Latinamerica – FMFLA, Centrus – Fetal Medicine, Campinas, Brazil;* ¶*FIDI - Fundação Instituto de Ensino e Pesquisa em Diagnóstico por Imagem, Departamento de Diagnóstico por Imagem -DDI- UNIFESP, Escola Paulista de Medicina, Universidade Federal de São Paulo, São Paulo, Brazil;* ***Laboratório de Flavivírus, Instituto Oswaldo Cruz – FIOCRUZ, Rio de Janeiro, Brazil*

*Correspondence.
(e-mail: gmalinger@gmail.com)

DOI: 10.1002/uog.15831

References

1. Campos GS, Bandeira AC, Sardi SI. Zika Virus Outbreak, Bahia, Brazil. *Emerg Infect Dis* 2015; 21: 1885–1886.
2. Ios S, Mallet HP, Leparc Goffart I, Gauthier V, Cardoso T, Herida M. Current Zika virus epidemiology and recent epidemics. *Medecine et maladies infectieuses* 2014; 44: 302–307.
3. Besnard M, Lastere S, Teissier A, Cao-Lormeau V, Musso D. Evidence of perinatal transmission of Zika virus, French Polynesia, December 2013 and February 2014. *Euro Surveill* 2014; 19.
4. Lanciotti RS, Kosoy OL, Laven JJ, Velez JO, Lambert AJ, Johnson AJ, Stanfield SM, Duffy MR. Genetic and serologic properties of Zika virus associated with an epidemic, Yap State, Micronesia, 2007. *Emerg Infect Dis* 2008; 8: 1232–1239.
5. Centers for Disease Control and Prevention (CDC). Intrauterine West Nile virus infection—New York, 2002. *MMWR Morb Mortal Wkly Rep* 2002; 51: 1135–1136.
6. Faye O, Freire CC, Iamarino A, Faye O, de Oliveira JV, Diallo M, Zanutto PM, Sall AA. Molecular evolution of Zika virus during its emergence in the 20(th) century. *PLoS Negl Trop Dis* 2014; 8: e2636.
7. Goenaga S, Kenney JL, Duggal NK, Delorey M, Ebel GD, Zhang B, Levis SC, Enria DA, Brault AC. Potential for Co-Infection of a Mosquito-Specific Flavivirus, Nhumirim Virus, to Block West Nile Virus Transmission in Mosquitoes. *Viruses* 2015; 7: 5801–5812.